Chemolithotrophic and chemoheterotrophic microorganisms in sediment- and rock-hosted hydrothermal systems

Dissertation
zur Erlangung des Grades eines
Doktors der Naturwissenschaften
- Dr. rer nat. –

Dem Fachbereich Biologie/ Chemie der
Universität Bremen
vorgelegt von

Matthias Winkel

Bremen
Oktober 2013

Die vorliegende Arbeit wurde in dem Zeitraum von Januar 2010 bis zum Oktober 2013 im Rahmen des Programms „International Max Planck Research School of Marine Microbiology, MarMic“ in der Abteilung Molekulare Ökologie am Max-Planck-Institut für Marine Mikrobiologie in Bremen angefertigt.

1. Gutachter: Prof. Dr. Rudolf Amann

2. Gutachter: Prof. Dr. Wolfgang Bach

Tag des Promotionskolloquiums: 19. Dezember 2013

Table of contents

Summary

Deep-sea hydrothermal vent systems are highly productive ecosystems, where reduced energy sources fuel complex communities of microorganisms, invertebrates and vertebrates. Since decades the oxidation of methane, hydrogen and inorganic sulfur compounds has been extensively studied. However, the role of inorganic nitrogen and of organic compounds as energy source has been investigated only scarcely in hydrothermal fluids, in particular at the sea floor, where hydrothermal fluids exit subsurface. The aim of my thesis was to shed light on these under-investigated topics.

In my first project I studied nitrification and the involved microbes that are associated with large, nitrate-respiring and sulfur-oxidizing bacteria (SOB) of the genus *Beggiatoa*. These SOB formed mats and covered sulfide- and ammonia-rich hydrothermal sediments in the Guaymas Basin. In these mats, nitrification rates were measured using ^{15}N-labeled ammonium. With up to 605 µmol N l^{-1} mat d^{-1} the nitrification rates were the highest measured for a deep-sea ecosystem. Diversity and quantitative PCR of the ammonia monooxygenase subunit A gene (*amoA*) indicated association of ammonia-oxidizing archaea (AOA) and bacteria (AOB) with *Beggiatoa* mats. In line with this, single cells of AOB and potentially ammonia-oxidizing thaumarchaotes were attached to narrow *Beggiatoa*-like filaments. Nitrite oxidizing bacteria were also found. Nitrifying bacteria associated with *Beggiatoa* mats that respire nitrate to ammonium (DNRA) could display a syntrophic consortium that internally cycle nitrogen and thereby reduce loss of bioavailable nitrogen. However, it is not clear whether large SOB in general respire nitrate also to dinitrogen. Therefore, I analyzed the genetic potential of the large SOB "*Candidatus* Thiomargarita nelsonii", a close relative of *Beggiatoa*. The comparison to four other *Beggiatoaceae* identified genes for both denitrification and DNRA in "*Ca*. T nelsonii" and three other *Beggiatoaceae.* This indicates that both pathways are widely distributed among large SOB and questions the hypothesis of internal N-cycling in mats of large SOB.

In my third project I investigated the microbial consumption of organic compounds that are produced in hydrothermal systems. In particular I studied acetate-assimilating heterotrophic communities in the diffuse fluids (temperature range of 4-72°C) of two rock-hosted hydrothermal systems. 16S rRNA gene-based diversity analysis and fluorescence *in situ* hybridization (FISH) showed that either *Gammaproteobacteria* or *Epsilonproteobacteria* rapidly grew during short-term (8-12 h) incubations with ^{13}C-acetate. Single cells of both groups incorporated ^{13}C-acetate as shown by nanoSIMS. *Marinobacter* spp. and a novel group among the *Nautiliales* could be heterotrophs in these systems. These are potential r-

strategists that quickly respond to the fluctuating availabilities of energy sources in hydrothermal fluids.

Zusammenfassung

Hydrothermalquellen in der Tiefsee stellen hoch-produktive Ökosysteme dar, an denen komplexe Gemeinschaften von Mikroorganismen, Wirbellosen und Wirbeltieren vorkommen. Diese Ökosysteme basieren auf chemischer Energie aus reduzierten Verbindungen. In den letzten Jahrzehnten wurde die Oxidation von Methan, Wasserstoff und anorganischen Schwefelverbindungen sowie die dafür verantwortlichen Mikroorganismen intensiv untersucht. Hingegen wurden anorganische Stickstoffverbindungen und organische Verbindungen als Energiequellen in Hydrothermalfluiden, welche am Meeresboden austreten, nur wenig erforscht. Das Ziel meiner Doktorarbeit war es, diese wenig untersuchten Themen näher zu erforschen.

In meinem ersten Projekt untersuchte ich die Nitrifikation im Guaymas Basin an Sulfid- sowie Ammonium-reichen hydrothermalen Sedimenten. An diesem Standort kommen nitrifizierende Mikroorganismen vor, die mit großen Nitrat-atmenden und Schwefel-oxidierenden Bakterien (SOB) der Gattung *Beggiatoa* assoziiert sind. Diese SOB formen charakteristische Matten. Nitrifikationsraten in diesen Matten wurden mit Hilfe von ^{15}N-markiertem Ammonium gemessen. Die gemessenen Nitrifikationsraten betrugen bis zu 605 µmol N l^{-1} Matte d^{-1} und waren die Höchsten je in Tiefsee-Ökosystemen gemessenen Raten. Die Diversität und Abundanz des Genes der Ammoniakmonooxygenase-Untereinheit A (*amoA*) deutet auf eine Assoziation von Ammoniak-oxidierenden Archaeen (AOA) und Ammoniak-oxidierenden Bakterien (AOB) mit *Beggiatoa* Matten hin. Übereinstimmend wurden einzelne Zellen von AOB und potentiellen Ammoniak-oxidierenden Thaumarchaeen auf schmalen *Beggiatoa*-ähnlichen Filamenten gefunden. Des Weiteren wurden auch Nitrit-oxidierende Bakterien gefunden. *Beggiatoa* Matten, die dissimilatorisch Nitrat zu Ammoniak (DNRA) veratmen und mit nitrifizierenden Bakterien vergesellschaft sind, könnten in einem syntrophischen Konsortium leben, welches Stickstoff in den Matten wiederverwertet und damit einen Verlust des biologisch verfügbaren Stickstoffs verhindert. Bisher ist nicht geklärt, ob große SOB das Nitrat ebenfalls zu Stickstoffgas veratmen können. Deshalb habe ich das genetische Potential des großen SOB „*Candidatus* Thiomargarita nelsonii“ untersucht, welcher eng mit *Beggiatoa* verwandt ist. Der Vergleich mit vier weiteren *Beggiatoaceae* zeigte Gene für die Denitrifikation und DNRA in „*Ca*. T. nelsonii“ und drei weiteren *Beggiatoaceae*. Dies zeigt das beide Stoffwechselwege in großen SOB verbreitet sind und stellt eine interne Wiederverwertung von Stickstoff in Matten von großen SOB in Frage.

In meinem dritten Projekt untersuchte ich den mikrobiellen Verbrauch von organischen Verbindungen die an Hydrothermalquellen produziert werden. Im Besonderen habe ich die

Acetat-Assimilierung von heterotrophen Gemeinschaften in diffusen Fluiden (Temperaturbereich von 4-72°C) von zwei hydrothermalen Systemen mit vorwiegend felsigem Untergrund erforscht. 16S rRNA-Gen-basierte Analysen der Diversität und Fluoreszenz *In Situ* Hybridisierungen (FISH) zeigten ein rasches Wachstum von entweder Gammaproteobakterien oder Epsilonproteobakterien in kurzzeitigen (8-12 h) Inkubationen mit ^{13}C-Acetat. NanoSIMS Untersuchungen zeigten Einlagerungen von ^{13}C-Acetat in einzelnen Zellen von beiden Gruppen. *Marinobacter* spp. und eine neue Gruppe unter den *Nautiliales* könnten als heterotrophe Organismen in diesen Systemen vorkommen. Es handelt sich dabei um potenzielle r-Strategen, welche schnell auf die schwankende Verfügbarkeit von Energiequellen in Hydrothermalfluiden reagieren.

List of Abbreviations

ATU - allylthiourea

amoA – ammonia monoxygenase subunit A

anammox – anaerobic ammonia oxidation

ANME – anaerobic methanotrophic archaea

AOA – ammonia-oxidizing archaea

AOB – ammonia-oxidizing bacteria

AOM – anaerobic oxidation of methane

CARD-FISH – catalyzed reporter deposition fluorescence *in situ* hybridization

DGGE – denaturating gradient gel electrophoresis

DHVEG – deep-sea hydrothermal vent euryarchaeotic group

DNRA – dissimilatory nitrate reduction to ammonia

EL-FISH – element-labeling fluorescence *in situ* hybridization

HISH-FISH – halogen *in situ* hybridization

MAR – Mid-Atlantic Ridge

MAR-FISH – microautoradiography fluorescence *in situ* hybridization

MDA – multiple displacement amplification

MGI – Marine Group I

MOR – mid-ocean ridges

nanoSIMS – nanometer-scale secondary ion mass spectrometry

nir – nitrate reductase

NOB – nitrite-oxidizing bacteria

OTU – operational taxonomic unit

q-PCR – quantitative polymerase chain reaction

PCR – polymerase chain reaction

PHA – polyhydroxyalkanoate

Redox – reduction and oxidation

rTCA – reductive tricarboxylic acid

RFLP – restriction fragment length polymorphism

SIP – stable isotope probing

SLiME – subsurface lithotrophic microbial ecosystems

SOB – sulfur-oxidizing bacteria

SRB – sulfate-reducing bacteria

Chapter I
General Introduction

1. Photo- and chemotrophic energy production

Until 1887 biologists assumed that all life depends on photosynthesis carried out by plants and algae. Photosynthesis is a light-driven process, in which inorganic carbon is reduced with electron equivalents to produce organic carbon. However, Sergei N. Winogradsky, one of the first microbial ecologists and environmental microbiologists, observed that some filamentous bacteria, later named *Beggiatoa,* use energy derived from the oxidation of hydrogen sulfide. With this energy they assimilate carbon dioxide (Winogradsky, 1887) and are the first described chemolithoautotrophic microorganisms (see Box 1). The energy gain from inorganic compounds is often referred to as chemosynthesis. His later work on iron-oxidizing bacteria and especially the isolation of nitrifying bacteria (Winogradsky, 1890) confirmed his hypothesis of chemolithoautotrophic growth (see Box 1). These findings essentially changed the perspective of life and led to a novel research area, which focuses on the understanding of these light-independent, autotrophic metabolic processes. So far, chemolithotrophy has only been reported for bacteria and archaea.

2 Metabolic processes of chemotrophic microorganisms in the environment

Most known chemotrophic bacteria and archaea studied so far are described as chemoorganoheterotrophs (see Box 1). They use a wide range of organic substrates for energy gain that range from carbohydrates, fatty acids, dicarboxylic acids, amino acids, alcohols, to more exotic substrates such as aromatic compounds (e.g. benzoate, phenol). Some heterotrophs are specialist and use only specific carbon sources such as glucose, while other heterotrophs are generalists that use a wide range of organic substrates. There are also heterotrophs that only grow optimally on complex mixes of organic carbon for example mixed amino acids (Aharon, 2010).

Inorganic compounds are used by chemolithoautotrophic microorganisms. These organisms gain energy by the oxidation of hydrogen, methane, sulfide, ammonia and iron in the presence or absence of oxygen (Table 1). Chemolithoautotrophs are widely distributed and found in sediments, soils, mammalian guts, wastewater treatment plants, marine and freshwater systems. They grow in a wide range of temperatures under hyperthermophilic (>80°C), thermophilic (45-70°C), mesophilic (20-45°C) and psychrophilic (<20°C) conditions (Durand *et al.*, 1993; Stetter, 2006; Sokolova *et al.*, 2007; Mikucki *et al.*, 2009).

It took almost hundred years to find the first ecosystem that is mainly fueled by chemosynthesis. This ecosystem was a submarine hot spring system called hydrothermal vent and was located in the deep Pacific Ocean formed by volcanism near a plate boundary

(Lonsdale, 1977; Corliss *et al.*, 1979). Here, chemosynthetic microorganisms are the basis of a complex food chain and supply chemical energy for organisms of higher trophic levels. However, this food chain is not entirely independent of light energy, since many microorganisms use oxygen and nitrate as electron acceptors that are originally derived from photosynthesis (Jørgensen and Boetius, 2007).

Table 1: Chemolithotrophic reduction and oxidation (redox) reactions mediated by microorganisms

Metabolism	**$e^-_{do.}$**	**$e^-_{acc.}$**	**Redox reaction**	**ΔG (kJ/ rxn)**	**ΔG (kJ/ e^-)**
Aerobic					
Sulfur oxidation	HS^-, S^0	O_2	$H_2S + 2O_2 \rightarrow SO_4^{2-} + 2H^+$ $S° + H_2O + 1^1/_2O_2 \rightarrow SO_4^{2-} + 2H^+$	-750 -587	-94 -98
Hydrogen oxidation	H_2	O_2	$H_2 + {}^1/_2O_2 \rightarrow H_2O$	-230	-115
Ammonia oxidation	NH_4	O_2	$NH_3 + 1^1/_2\ O_2 \rightarrow NO_2^- + H^+ + H_2O$	-275	-46
Nitrite oxidation	NO_2^-	O_2	$NO_2^- + {}^1/_2\,O_2 \rightarrow NO_3^-$	-74	-37
Methane oxidation	CH_4	O_2	$CH_4 + 2O_2 \rightarrow CO_2 + 2H_2O$	-750	-94
Iron oxidation	Fe^{2+}	O_2	$Fe^{2+} + {}^1/_4\,O_2 + H^+ \rightarrow Fe^{3+} + {}^1/_2H_2O$	-65	-65
Manganese oxidation	Mn^{2+}	O_2	$Mn^{2+} + {}^1/_2\,O_2 + H_2O \rightarrow MnO_2 + 2H^+$	-50	-25
Anaerobic					
Methane oxidation	CH_4	SO_4^{2-}	$CH_4 + SO_4^{2-} \rightarrow HCO_3^- + HS^- + H_2O$	-40	-10
Ammonia oxidation (Anammox)	NH_4^+	NO_2^-	$NH_4^+ + NO_2^- \rightarrow N_2 + 2\ H_2O$	-357	-89
Sulfate reduction	H_2	SO_4^{2-}	$2H^+ + 4H_2 + SO_4^{2-} \rightarrow H_2S + 4H_2O$	-170	-21
Methanogenesis	H_2	CO_2	$CO_2 + 4\ H_2 \rightarrow CH_4 + 2H_2O$	-130	-16
Sulfide oxidation/ Denitrification	HS^-	NO_3^-	$5H_2S + 8NO_3^- \rightarrow 5SO_4^{2-} + 4N_2 + 4H_2O + 2H^+$	-3722	-124

Data from (Strous and Jetten, 2004; Edwards *et al.*, 2005; Costa *et al.*, 2006; Op den Camp *et al.*, 2007; Aharon, 2010)

e^-_{do}: electron donor; e^-_{acc}: electron acceptor

rxn: reaction

e^-: electron

Box 1 | Energy metabolisms

Phototrophy: Phototrophy refers to the use of light as the source of energy. During this process the organisms capture photons and convert them into chemical energy in the form of ATP or reducing equivalents like NADPH. All phototrophs use electron transport chains (bacteriochlorophyll) or direct proton pumping (bacteriorhodopsin) to produce an electro-chemical gradient (proton motive force). This force is further used by ATP-synthases to produce ATP. Most phototrophs are autotrophs (photoautotrophs) fixing inorganic carbon in the form of carbon dioxide into organic carbon, which is used for structural, functional and storage cell compounds. There are other types of phototrophs, which obtain their carbon from the uptake of organic compounds and are referred to as heterotrophs (photoheterotrophs) (Madigan et al., 2010).

Chemotrophy: Organisms that gain energy through chemical conversion of substrates from their environment are called chemotrophs. When using inorganic carbon as preferred carbon source they are called chemoautotrophs. Chemoheterotrophs use mainly organic compounds as carbon and energy source (Madigan et al., 2010).

Lithotrophy: Lithotrophy defines a metabolism that uses inorganic substrates to produce reducing equivalents. An organism that uses chemical conversion of inorganic substrates and fixes carbon dioxide is called chemolithoautotroph, while an organism which uses organic instead of inorganic carbon is a chemolithoheterotroph (Madigan et al., 2010).

Organotrophy: Organotrophy defines a metabolism that uses organic substrates to produce reducing equivalents. An organism that chemically converts organic substrates and at the same time uses organic carbon assimilatory is a chemoorganoheterotroph. Organisms that fix inorganic carbon while still using organic carbon as energy source are only known for methanogens that utilize methanol (chemoorganoautotroph) (Madigan et al., 2010).

3 Hydrothermal vent systems

3.1 Discovery

The discovery of hydrothermal vents (Lonsdale, 1977) fundamentally changed the understanding of the deep seafloor (> 200 m depth), which accounts for 65% of the Earth's surface (Brown *et al.*, 1989). On the Galapagos Rift geologists did not only find submarine hot springs but also high densities of suspension-feeding mussels, clams and worms

(Lonsdale, 1977; Corliss *et al.*, 1979). Until then the deep-sea was considered as a "desert in the ocean", where only little life occurs.

In the following decades hydrothermal vents were discovered at many places at the shallow and the deep-sea seafloor (Tarasov *et al.*, 2005 and references therein). Today, 256 active hydrothermal vent fields (clusters of vent sites within several hundreds of meters (Tarasov *et al.*, 2005)) have been confirmed and another 282 are inferred to be active. A list of these vent fields are found in the InterRidge Vents Database V3.2 (Beaulieu, 2013).

Most of these hydrothermal vent fields are situated on or near tectonically active structures such as ocean spreading centers and subduction zones (Fig.1). Different types of hydrothermal systems exist depending on the tectonic setting and composition of host rock.

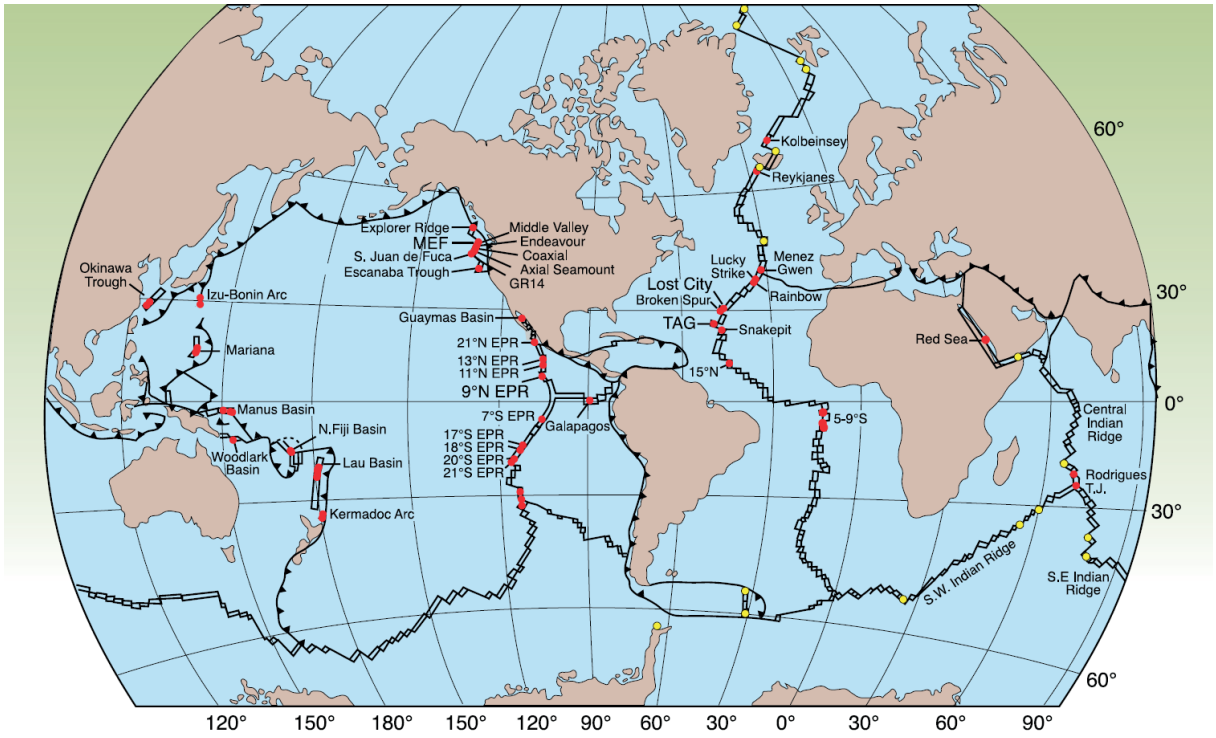

Figure 1: Hydrothermal vent fields along mid-ocean ridges, in back-arc basins, rifted arcs, and at submerged island-arc volcanoes (red), and areas of activity as indicated by mid-water chemical anomalies (yellow). EPR - East Pacific Rise, TAG - Trans Atlantic Geotraverse, MEF - Main Endeavour Field, and GR-14= Sea Cliff hydrothermal field on the northern Gorda Ridge (Tivey, 2007).

3.2 Geological formation of hydrothermal vent systems

3.2.1 Plate tectonics

The upper layer of the Earth is called lithosphere and consists of the crust and of the upper solid mantle. It is divided into an oceanic and continental part that consists of many different fragments called tectonic plates. The plates differ in the composition of the crust. While

oceanic plates have a thin (5-6 km) but dense oceanic crust, continental plates have a thick (35-50 km) and less dense continental crust. The plates are constantly moving by a process that is described as continental drift. Three types of active plate boundaries exist: the divergent (constructive), convergent (destructive) and transform (conservative) boundaries (Fig. 4). Examples for divergent plate boundaries are ocean spreading centers, where new crust is formed constantly. A heat source in the mantle below the spreading center stimulates the circulation of seawater through the permeable oceanic crust. During this circulation water-rock reactions change the chemical composition of the seawater, which then reenters the ocean as altered seawater (fluids).

3.2.2 Fluid formation by hydrothermal circulation and water-rock reactions

The circulation of seawater in the oceanic crust follows different steps of physical and chemical conversions that are influenced by the composition of the rocks and the heat source. As an initial step seawater percolates downwards through the permeable oceanic crust and reacts with the rocks. In the slightly heated layers (up to 60°C) seawater is depleted in oxygen and alkaline elements. In deeper layers the temperature rises above 150°C resulting in a precipitation of clay minerals. This leads to the removal of magnesium ions and subsequently hydroxyl ions, which results in an acidification of the fluids. The low pH causes potassium, calcium and sodium to be leached out of the rock resulting in the formation of anhydrite (calcium sulfate). The produced anhydrite removes most of the seawater sulfate, while the residual sulfate reacts at temperatures above 250°C to form metal sulfide minerals. These rock layers are defined as the recharge zone (Fig. 2). Rock layers near the heat source, where the final chemical reactions between 350 and 400°C take place, are called reaction zones (Fig. 2). Here, sulfur and metals such as zinc, copper and iron are leached from the rocks by the acidic fluids. Finally, the heated fluids rise to the seafloor caused by buoyancy in the so-called uplift zone (Fig. 2). The outflow can be focused along fissures and cracks. When hot fluids mix with cool bottom seawater minerals precipitate and from chimney-like structures. These structures

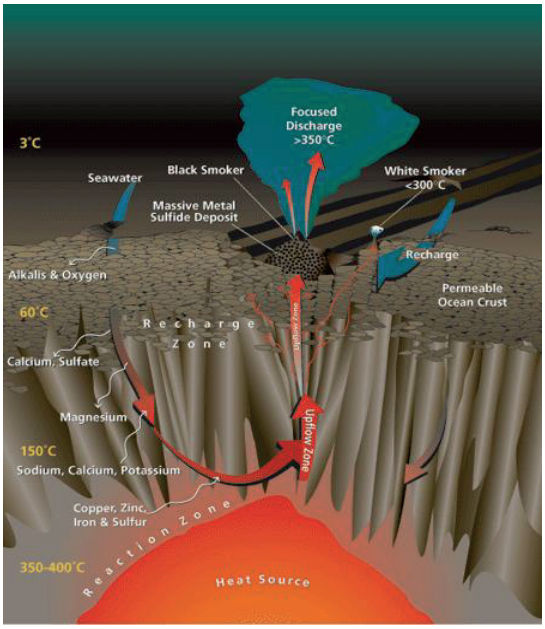

Figure 2: Hydrothermal circulation divided in the recharge zone, the reaction zone and the uplift zone. (Humphris and McCollom, 1998)

emit the black to white colored fluids into the ocean, called black or white smokers, respectively. In contrast, fluids rising diffusively through permeable ocean crust usually cool down and have temperatures under 100°C when they discharge into the ocean (Humphris and McCollom, 1998).

3.2.3 Mid-ocean ridges

Most of the ocean spreading centers, where hydrothermal circulation has led to the formation of hydrothermal vents are located at the mid-ocean ridges (MOR) (Fig. 1). MORs are a globe-spanning volcanic chain with a length of over 60.000 km and an average depth of between 2000 and 5000 m (Fig. 3) (Van Dover, 2000). At these divergent plate boundaries (Figs. 3 and 4) uprising magma from the earth mantle creates new oceanic crust by seafloor spreading. The seafloor spreading centers are classified by their spreading rates (Table 2). These rates are grouped in five different categories from ultraslow spreading to superfast spreading (Table 2). With the exception of ultraslow spreading ridges they have nearly the same crustal thickness (6-7 km) whereas the morphology of their axis is quite different. Fast and intermediate spreading ridges typically have a flat axis rise of only a few tens of meters with narrow summit calderas compared to slow spreading ridges with rift valleys that are 1-3 km deep and 5-15 km wide (Fig. 3) (Ramirez-Llodra *et al.*, 2007).

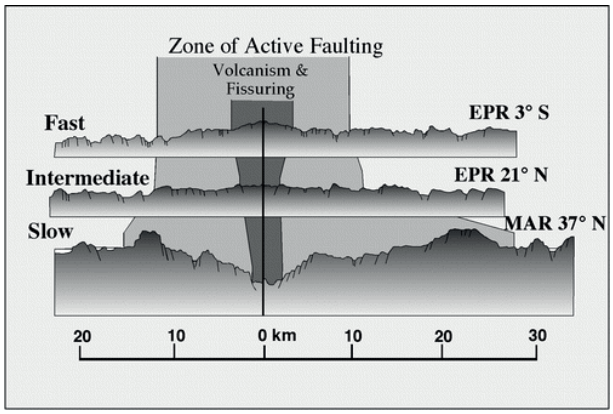

Figure 3: Across axial morphology of different spreading rates.at mid-ocean ridges. EPR – East Pacific Rise, MAR – Mid-Atlantic Ridge. Adapted from (Kelley *et al*., 2002)

Table 2: Spreading rates of different hydrothermal vent systems

category of spreading rate[1]	spreading rate [mm a^{-1}]	examples[2]
ultraslow spreading	< 20	Mohns Ridge, Lena Trough
slow spreading	20 - 50	Central Indian Ridge, Mid-Atlantic Ridge
intermediate spreading	50 - 90	East Pacific Rise 21°N, Juan de Fuca Ridge, Back-Arc Spreading Center
fast spreading	90 - 130	East Pacific Rise 8-13°N
superfast spreading	130 - 190	East Pacific Rise 27-32°S

1 categories according to (Ramirez-Llodra *et al.*, 2007);

2 (Juniper and Tunnicliffe, 1997; Van Dover, 2000; Ramirez-Llodra *et al.*, 2007; Snow and Edmonds, 2007)

In contrast, ultraslow spreading ridges, where fresh mantle peridotite (see Box 2) is exposed, show no axis rising at all (Ramirez-Llodra *et al.*, 2007; Snow and Edmonds, 2007).

MORs are separated along the axis into different spreading ridge segments, which are connected by deep transform faults (Fig. 2) that offset the spreading axis and therefore result in a typical zig-zag pattern of the MORs (Figs. 1 and 4). Moreover the morphology of intermediate-, fast-, and superfast-spreading ridges tends to be dominated by volcanism, while the morphology of slow and ultraslow-spreading ridges is dominated by tectonics (Snow and Edmonds, 2007). The Mid-Atlantic Ridge (MAR) as a typical slow spreading center (Table 2) features deep hydrothermal vent systems such as Logatchev (3050 m) to more shallow ones like Menez Gwen (840 m).

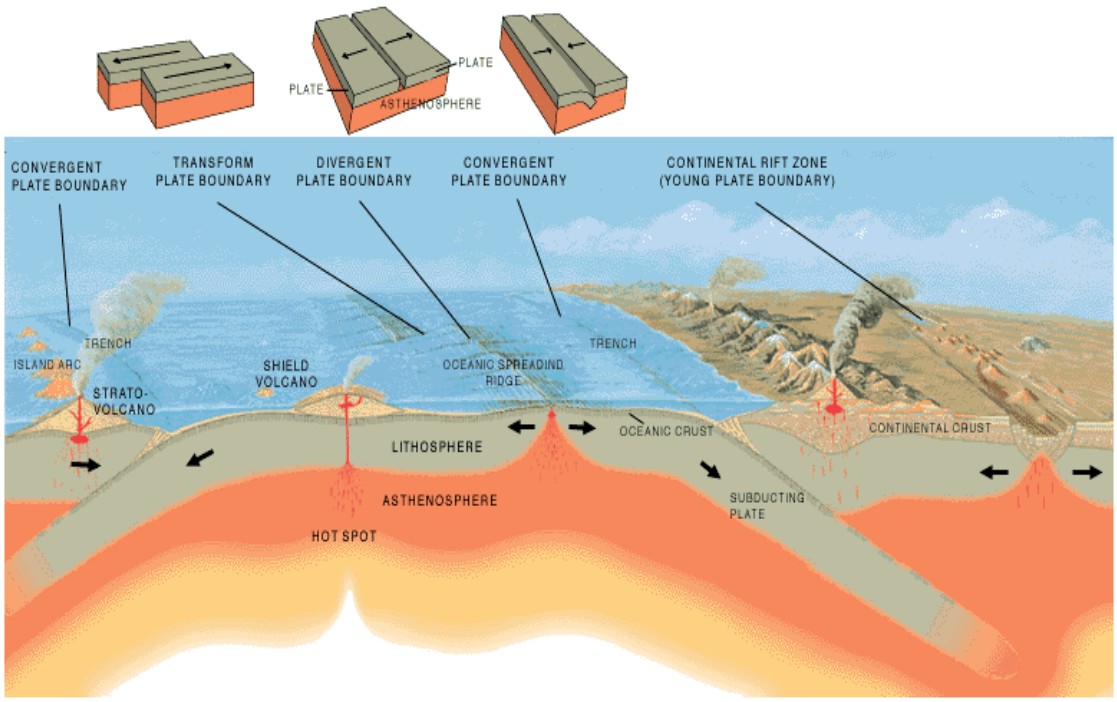

Figure 4: Plate boundaries. Divergent plate boundary - two plates move away from each other; convergent plate boundary - two plates move toward one another and a subduction zone is created; trenches are formed due to the subduction of plates; transform plate boundary - horizontal slip of tectonic plates; hot spots - unusually hot magma in mantle leads to shield volcanos.
URL: http://pubs.usgs.gov/gip/earthq1/plate.html (06.08.2013)

3.2.4 Rock-hosted and sediment-hosted MOR systems

Most of the MORs are rich in the extrusive igneous rock called mid-ocean ridge basalt (MORB). Hydrothermal systems located on such MORs are called basalt-hosted. In contrast some systems have a high fraction of peridotites (see Box 2) in the ocean crust that is scattered with minor parts of basalt and other magmatic rocks such as gabbro. These systems

are referred to as ultramafic-hosted and are often found at slow-spreading MORs (Snow and Edmonds, 2007; Tivey, 2007). The composition of the rocks plays an important role in the reaction zone of hydrothermal circulation and therefore affecting the fluid composition (Table 3). The major difference in the discharged fluids is the high concentration of hydrogen and methane in ultramafic-hosted systems. Hydrogen is mainly produced by serpentinization reactions (Charlou *et al.*, 2002) (see Box 2). Subsequently, hydrogen reacts with CO_2 to CH_4 (abiogenic methanogenesis, see Box 2). Rock-hosted systems are sometimes overlain by a thick sediment layer when located close to continental margins. The fluids of these sediment-hosted systems have a high pH and low metal content (Table 3) (German and Von Damm, 2006). Typical sediment-hosted systems are found on the western American coast, where the MOR system is influenced by the close landmasses. The Guaymas Basin is one of the best studied sediment-hosted hydrothermal systems and is located in the Gulf of California (Fig. 1). Other rock- and sediment-hosted systems are found in back-arc basins that often host felsic-rocks besides typical basaltic rocks of MORs (Tivey, 2007).

3.2.5 Back-arc basins

Back-arc basins spreading centers are formed behind subduction zones that consume the oceanic crust constantly produced at the latter (Fig. 5). At the subduction zone two plates collide, whereby one plate moves underneath the other one (Fig. 5). If both colliding plates are oceanic lithosphere, they form an island arc. The overriding plate stretches and breaks by moving towards the direction of the subducting plate (Fig. 5). In a later stage of the back-arc rifting passive upwelling of mantle material occurs and a back-arc spreading center establishes (Fig. 5). These spreading centers are similar to those at MORs often showing features such as black smokers However, the input of magmatic volatiles (e.g. SO_2) and H_2O via subduction of

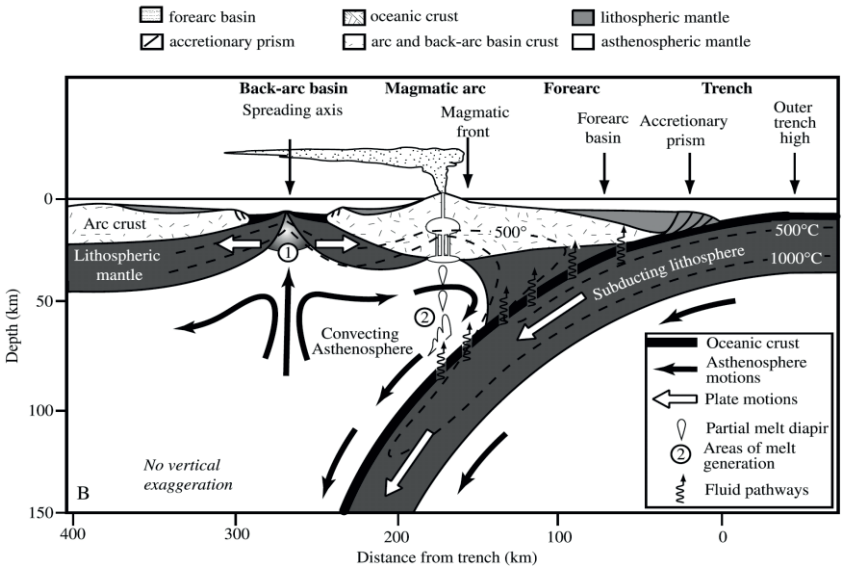

Figure 5: Schematic section of a subduction zone, showing the formation of back-arc basins (Stern, 2002).

sediments often causes a low pH (Hannington *et al.*, 2005). Most of the back-arc basins are located in the western Pacific Ocean like the Manus Basin (Fig. 1) (Hannington *et al.*, 2005).

Table 3: Composition of end-member fluids of different vent systems and seawater

chemical species	units	sea-water	Ultramafic-hosted		Basalt-hosted MOR	Sediment hosted	Back-arc basin
			high temperature	Lost City			
T	°C	2	347-365	<91	<405	100-315	278-334
pH	25°C, 1 atm	7.8	2.8-3.9	9-9.8	2.5-6.6	5.1-5.9	<1.0-5.0
H_2	mmol kg^{-1}	0	13-16	< 1-15	0.0005-38.0	<1-13	0.035-0.5
CH_4	mmol kg^{-1}	b. d.	0.13-4	1-2	0.007-2.58	2-52	0.005-0.06
H_2S	mmol kg^{-1}	0	1-2.5	< 0.064	0-110	1.1-6	2-13.1
CO_2	mmol kg^{-1}	2.36	10.1-16	< 0.8	3.6-39.9	n. d.	4.4-274
NH_4	mmol kg^{-1}	<0.01	< 0.65	n. d.	n. d.	5.6-15.6	n. d.
SO_4^{2-}	mmol kg^{-1}	28	n .d.	5.9-12.9	0	0	0
Mg	mmol kg^{-1}	53	0	9-19	0	0	0
Fe	µmol kg^{-1}	<10	2410-24000	n. d.	7-18700	0-180	13-14600
Mn	µmol kg^{-1}	< 10	330-2350	n. d.	59-3300	10-236	211-4790
Zn	µmol kg^{-1}	0.012	25-185	n. d.	0-780	0.1-40	7.6-3000
Cu	µmol kg^{-1}	0.007	15-162	n. d.	0-150	< 0.02-1.1	0.003-34

Data from (Welhan and Craig, 1983; Von Damm *et al.*, 1985a, 1985b; Lilley *et al.*, 1993; Trefry *et al.*, 1994; Ishibashi *et al.*, 1995; Kelley *et al.*, 2001; Charlou *et al.*, 2002; Douville *et al.*, 2002; German and Von Damm, 2006; Proskurowski *et al.*, 2006; McCollom and Seewald, 2007; Reeves *et al.*, 2011)

3.3 Cold-seep ecosystems

Hydrothermal vents were the first chemosynthetic ecosystems found in the ocean, while a few years later similar ecosystems, the cold seeps, that support chemosynthetic communities were discovered (Paull *et al.*, 1984). These ecosystems occur at active margins like the Peruvian Margin or at passive margins like the Golf of Mexico (Sibuet and Olu, 1998; Tunnicliffe *et al.*, 2003). In both types fluids and gases are expelled by tectonic pressure and not by heat as in hydrothermal systems. When the fluids and gases reach the seafloor they form gas-hydrate deposits, gas chimneys, brine ponds, pockmarks, mud volcanoes, hydrocarbon seeps, carbon dioxide seeps, oil and asphalt seeps (Jørgensen and Boetius, 2007; Suess, 2010). Most of the fluids from cold seeps are rich in methane, which is a result of biogenic and thermogenic methane production. Moreover, they can contain higher hydrocarbons in cases of high input from organic compounds. Similar to hydrothermal fluids seep fluids can contain elevated concentrations of hydrogen sulfide that is produced by sulfate reduction in anoxic layers. The

latter process is often coupled to the anaerobic oxidation of methane (AOM) by syntrophic consortia formed by anaerobic methanotrophic archaea (ANME) and sulfate-reducing bacteria (SRB) (Knittel and Boetius, 2009). Even though the macrofauna at seep sites and hydrothermal vents show many similar taxa that gain energy by chemosynthetic symbionts (e. g. *Bathymodiolus, Lamellibrachia, Calyptogena*) (Sibuet and Olu, 1998), the diversity of free-living microbes is remarkably different (E. Ruff personal communication). Nevertheless, similar functional groups are found in sediment-hosted hydrothermal vent systems and cold seep sediments such as the large colorless sulfur-oxdizing bacteria of the family *Beggiatoaceae* (Jannasch *et al.*, 1989; McHatton *et al.*, 1996; Boetius and Suess, 2004).

Box 2 | Geochemical processes in ultramafic-hosted systems

Serpentinization: Peridotite, which mainly consist of olivine [$(Mg,Fe)_2SiO_4$] and pyroxene [orthopyroxene (Mg,Fe)-SiO_3 and clinopyroxene $Ca(Mg,Fe)Si_2O_6$] is hydrolyzed and forms serpentine [$Mg,Fe]_3Si_2O_5(OH)_4$], magnetite [Fe_3O_4] and hydrogen. Depending on temperature and pressure the serpentinization reactions are:

Olivine at temperatures < 300°C and at 500 bar (Holm and Charlou, 2001):

1. 5 Mg_2SiO_4 (forsterite) + Fe_2SiO_4 (fayalite) + 9 H_2O → 3 $Mg_3Si_2O_5(OH)_4$ (serpentine) + $Mg(OH)_2$ (brucite) + 2 $Fe(OH)_2$ (ferrous hydroxide)
2. 3 $Fe(OH)_2$ → Fe_3O_4 (magnetite) + H_2 + 2 H_2O

Orthopyroxene at temperatures >350-400°C and at 500 bar (Allen and Seyfried Jr., 2003):

3. 3 $FeSiO_3$ (ferrosilite) + H_2O → Fe_3O_4 (magnetite) + 3 SiO_2 (Silica) + H_2
4. 12 $MgSiO_3$ (enstatite) + 2 $CaMgSi_2O_6$ (diopside) + 6 H_2O → 2 $MgSi_2O_5(OH)_4$ (serpentine) + $Mg_3Si_4O_{10}(OH)_2$ (talc) + $CaMg_5Si_8O_{22}(OH)_2$ (tremolite) + 4 Ca^{2+} + 2 H^+

Recently Bach and colleagues proposed a different form of reactions were hydrogen is produced by the reaction of Fe-rich brucite and silica formed during olivine and orthopyroxene hydrolysis (Bach et al., 2006). The net reaction is:

5. 104 $Mg_{1.8}Fe_{0.2}SiO_4$ (olivine) + 90 $Mg_{0.9}Fe_{0.1}SiO_3$ (orthopyroxene) + 208 H_2O → 72 $Mg_{2.85}Fe_{0.15}Si_2O_5(OH)_4$ (serpentine) + 30 $Mg_{2.7}Fe_{0.3}Si_2O_5(OH)_4$ (serpentine) + 4 Fe_3O_4 (magnetite) + 4 H_2

Abiogenic methanogenesis and hydrocarbon formation

During this process hydrogen formed by serpentinization of ultramafic rocks reacts with C-sources (most often CO_2) to form CH_4 (Sherwood Lollar et al., 1993). This abiogenic formation is well know by the industrial process of Fischer-Tropsch-type synthesis and is feasible under hydrothermal conditions that occur in ultramafic hydrothermal systems (Charlou et al., 2000; Sherwood Lollar et al., 2002; McCollom and Seewald, 2007; Proskurowski et al., 2008).

$CO_2 + 4\ H_2 \rightarrow CH_4 + 2H_2O$

The whole process seems to be catalyzed by iron- and chromium-bearing minerals and leads to the formation of short-chain hydrocarbons like ethane and propane (Foustoukos and Seyfried, 2004).

4. Microbial diversity at hydrothermal vent systems

4.1 Habitats for microbial life

Since the discovery of hydrothermal vents the inhabiting microorganisms and their metabolisms have been studied intensively. They live as free-living microorganisms in the different habitats or in symbiosis with invertebrate hosts and have to cope with steep gradients of temperature and chemical concentrations (Jørgensen and Boetius, 2007). Hydrothermal chimneys consist of anhydrite mineral structures that contain different metal sulfides and precipitate, when hot, reduced fluids mix with seawater (Fig. 6A). These reduced minerals are a habitat for hyperthermophilic archaea and bacteria that live in temperature gradients. Several of these hyperthermophiles were isolated from this habitat (Baross *et al.*, 1982; Jones *et al.*, 1983; Makita *et al.*, 2012) and grow optimally at >80°C (Stetter, 1999). These isolates extended the upper temperature limit of life (Cowan, 2004). To date, the record is held by two closely related archaea, by *Pyrolobus fumarii* that can grow at 113°C (Blöchl *et al.*, 1997) and by *Geogemma barossii* ('strain 121') that even showed slow growth at 121°C (Kashefi and Lovley, 2003) (Table 4). In the outflow of the chimneys metal particles precipitate due to rapidly mixing of hydrothermal fluids with seawater (Tivey, 2007). These mixing forms a plume (>99% seawater and ~ 0.01% fluids) over the hydrothermal vents system (Fig. 6B) that rises up to hundreds of meters above the seafloor and disperses over an area of hundreds of kilometers (Dick *et al.*, 2013). The resulting chemical anomaly is detectable in the water column and led to the discovery of several hydrothermal systems (Lupton and Craig, 1981; German *et al.*, 2010). In the plume, the free-living microbial community either originates from background water or from the subsurface of the hydrothermal systems (Dick *et al.*, 2013). Other vent-associated habitats are the so-called diffuse fluids, which can be of different origins including (i) the mixing of hydrothermal fluids with seawater,

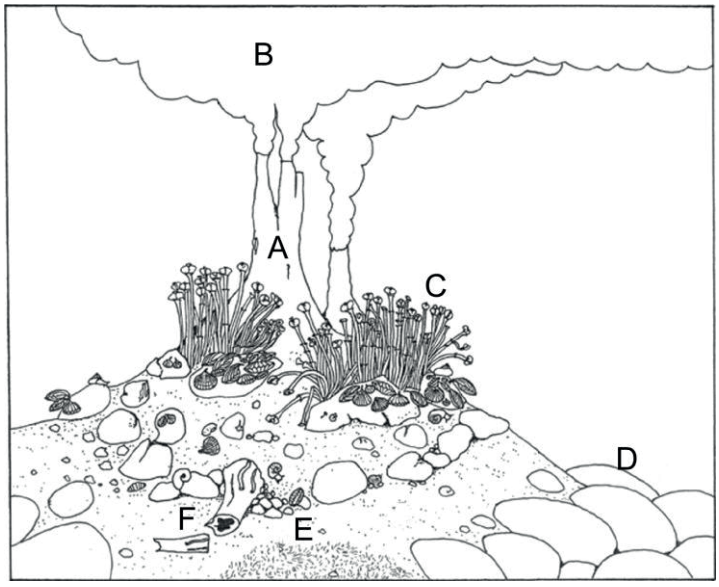

Figure 6: Hydrothermal habitats. A, hydrothermal chimney; B, hydrothermal plume; C, cluster of vestimentiferan tube worms and mussels harboring chemosynthetic symbiontic bacteria; D, rock-surface in the form of pillow lava; E, area of low temperature diffuse fluids with chemosynthetic bacteria; F, hydrothermal sediments and collapsed chimney. Modified after Little *et al*. (2004).

(ii) conductive cooling of hydrothermal fluids below the surface and (iii) conductive heating of seawater (Bemis *et al.*, 2012). Diffuse fluids are discharged through cracks and fractures at the seafloor or leak through sulfide mounds and sediments (Bemis *et al.*, 2012). Here, dense macrofaunal populations accumulate (Fig. 6C), which often harbor chemosynthetic symbiotic bacteria (Dubilier *et al.*, 2008). Moreover, biofilms form on rock-surfaces (Fig. 6D), where diffuse flows emerge in rock-hosted hydrothermal vents (Schrenk *et al.*, 2008). Similarly, bacterial mats (Fig. 6E) are found on the surface of sediment-hosted system such as the Guaymas Basin (Nelson *et al.*, 1989), where diffuse fluids seep through a thick sediment layer (Fig. 6F). In this sediment microorganisms are influenced by steep thermal gradients with increasing depth and the alteration of pore water fluid components due to hydrothermal exposure (Magenheim and Gieskes, 1992).

The last vent associated habitat, which has only recently gained more attention, is the subsurface ecosystem of MORs. The porosity of the basalt causes inflow of seawater that mixes with fluids (Alt and Bach, 2003) and circulates laterally in the upper basalt layer (Fisher and Becker, 2000). This layer is considered to harbor different chemolithoautotrophic bacteria (Bach and Edwards, 2003; Edwards *et al.*, 2005). It was shown that phylogenetically different hyperthermophilic microorganisms exist in the subsurface, which are distinct from those found in sulfidic chimneys (Summit and Baross, 2001; Reysenbach and Shock, 2002; Schrenk *et al.*, 2003; Huber *et al.*, 2002). They can be used as tracers for an active subsurface community in this habitat (Summit and Baross, 2001). Moreover, it has been proposed that these subsurface lithoautotrophic microbial ecosystems (SLiMEs) are hydrogen-driven (Takai *et al.*, 2004a; Nealson *et al.*, 2005) but also harbor chemoheterotrophic fermenters.

Table 4: Some isolated strains of chemolithoauto- and chemoorganoheterotrophic microorganisms

Organism	Isolation site and source	Growth T [°C]	$e^-_{don.}$	$e^-_{acc.}$	carbon source	reference
			Gammaproteobacteria			
*Thiomicrospira crunogena**	EPR, 21°N, Vestimentiferan tube	28–32	$S_2O_3^-$, S^0, H_2S	O_2	CO_2	(Jannasch *et al.*, 1985)*
Salinisphaera hydrothermalis	EPR, 9°N, diffuse flow	30–35	$S_2O_3^-$, COS	O_2	CO_2, n-alkanes, acetate, COS	(Crespo-Medina *et al.*, 2009)
Halothiobacillus hydrothermalis	Fiji Basin, vent chimney	35–40	$S_2O_3^-$, S^0, H_2S	O_2	CO_2, COS	(Durand *et al.*, 1993)
Thioprofundum lithotrophicum	MAR , TAG , vent chimney	30-55	$S_2O_3^-$, S^0, $S_4O_6^-$, SO_3^-	NO_3^-, O_2	CO_2	(Takai *et al.*, 2009)
Alteromonas macleodii subsp. *fijiensis*	North Fiji Basin, fluids	25-35	organic compounds	O_2	COS	(Raguénès *et al.*, 1996)
			Zetaproteobacteria			
*Mariprofundus ferrooxydans**	Loihi Seamount, iron mats on rock-surface	10-30	Fe^{2+}	O_2	CO_2	(Emerson *et al.*, 2007)
			Epsilonproteobacteria			
Sulfurovum lithotrophicum	MOT , Iheya, sediments	28–30	$S_2O_3^-$, S^0	NO_3^-, O_2	CO_2	(Inagaki *et al.*, 2004)
*Sulfurimonas autotrophica**	MOT , Hatoma Knoll, sediments	25	$S_2O_3^-$, S^0, H_2S	O_2	CO_2	(Inagaki *et al.*, 2003)
Thioreductor micantisoli	MOT , Iheya, sediments	32	H_2	NO_3^-, S^0	CO_2	(Nakagawa *et al.*, 2005a)
Nautilia nitratireducens	EPR, 9°N, chimney	55	H_2, formate, acetate, COS	NO_3^- , S^0, $S_2O_3^-$, SeO_4^-	CO_2, formate	(Pérez-Rodríguez *et al.*, 2010)
*Nautilia profundicola**	EPR, 9°N, *Alvinella*	40	H_2, formate	S^0	CO_2, formate	(Smith *et al.*, 2008)
Hydrogenimonas thermophila	CIR , Kairei Field, colonizer	55	H_2	NO_3^- , S^0, O_2	CO_2	(Takai *et al.*, 2004b)
*Nitratiruptor tergarcus**	MOT , Iheya, chimney	55	H_2	NO_3^- , S^0, O_2	CO_2	(Nakagawa *et al.*, 2005c)

Table 4 continued

*Nitratifractor salsuginis**	MOT , Iheya, chimney	37	H_2	NO_3^-, O_2	CO_2	(Nakagawa *et al.*, 2005c)
*Caminibacter mediatlanticus**	MAR , Rainbow, chimney	55	H_2	NO_3^- , S^0	CO_2	(Voordeckers *et al.*, 2005)
Lebetimonas acidiphila	Mariana Arc, colonizer	50	H_2	S^0	CO_2	(Takai *et al.*, 2005)
			Aquificales			
Persephonella marina *	EPR	73	H_2	NO_3^- , S^0, $S_2O_3^-$, O_2	CO_2	(Götz *et al.*, 2002)
Desulfurobacterium pacificum	EPR, 13°N, chimney	75	H_2	NO_3^- , S^0, $S_2O_3^-$	CO_2	(L'Haridon *et al.*, 2006)
*Desulfurobacterium thermolithotrophum**	MAR , Snake Pit, chimney	70	H_2	S^0, SO_3^-	CO_2	(L'Haridon *et al.*, 1998)
*Thermovibrio ammonificans**	EPR 9°N, chimney	75	H_2	NO_3^- , S^0	CO_2	(Vetriani *et al.*, 2004)
			Deferribacterales			
Deferribacter abyssi	MAR , Rainbow, chimney	60	H_2, COS	Fe(III), NO_3^-, S^0	CO_2, COS	(Miroshnichenko *et al.*, 2003)
*Deferribacter desulfuricans**	Izu-Bonin Arc, Suiyo Seamount, chimney	60-65	COS, (di)carb-oxylic acids	NO_3^- , S^0, AsO_4^{3-}	COS, (di)carb-oxylic acids	(Takai *et al.*, 2003)
			Thermodesulfobacteriaceae			
Thermodesulfo-bacterium hydrogeniphilum	Guaymas Basin	75	H_2	SO_4^-	CO_2	(Jeanthon *et al.*, 2002)
Thermodesulfatator atlanticus	MAR, Rainbow	65–70	H_2	SO_4^-	CO_2, COS	(Alain *et al.*, 2010)
			Deinococcus-Thermus			
Thermus thermophilus	Guaymas Basin, chimney	70-75	sugars, amino and carboxylic acids	O_2	sugars, amino and carboxylic acids	(Marteinsson *et al.*, 1999)
*Marinithermus hydrothermalis**	Izu-Bonin Arc, Suiyo Seamount, chimney	68	COS	O_2	COS	(Sako *et al.*, 2003)

Table 4 continued

			Thermotogaceae			
Marinitoga camini	MAR, Menez Gwen, chimney	55	sugars, COS	S^0	sugars, COS	(Wery *et al.*, 2001a)
*Thermosiphon melanesiensis**	Lau Basin, *Bathymodiolus* gills	70	COS	S^0	COS	(Antoine *et al.*, 1997)
			Bacteroidetes			
Rhodothermus profundi	EPR, Genesis, chimney	70	COS	O_2	COS	(Marteinsson *et al.*, 2010)
			Firmicutes			
Caloranaerobacter azorensis	MAR, Lucky Strike, chimney	65	COS	S^0	COS	(Wery *et al.*, 2001b)
			Archaea			
*Ignicoccus pacificus**	EPR, 9°, Chimney	90	H_2	S^0	CO_2	(Huber *et al.*, 2000)
*Methanothermo-coccus okinawanensis**	MOT, Ilheya, chimney	60–65	H_2, formate	CO_2	CO_2	(Takai *et al.*, 2002)
*Methanopyrus kandleri**	Guaymas Basin, chimney	100	H_2	CO_2	CO_2	(Kurr *et al.*, 1991)
*Pyrolobus fumarii**	MAR, TAG, chimney	105	H_2	NO_3^- , S^0, O_2	CO_2	(Blöchl *et al.*, 1997)
"Geogemma barosii"	JdFR	105–107; max 121	H_2	Fe(III)	CO_2	(Kashefi and Lovley, 2003)
*Archaeoglobus veneficus**	MAR , chimney	75–80	H_2, organic acids, glucose, ethanol	S^0, SO_3^-	CO_2	(Huber *et al.*, 1997)

MOT: Mid-Okinawa Trough; EPR: East Pacific Rise; CIR: Central Indian Ridge; MAR: Mid-Atlantic Ridge; JdFR: Juan de Fuca Ridge; SOT: Southern Okinawa Trough; TAG: Trans-*Atlantic Geotraverse;* COS: complex organic substrates

* Sequenced genomes are deposited in the GOLD database v.4 (Pagani *et al.*, 2011)

4.2 Phylogenetic diversity of microorganisms at hydrothermal vent sites

First microbial studies in hydrothermal systems used microscopic observations of the morphology of microorganisms including scanning-electron-microscopy and trans-electron-microscopy. Another approach was to isolate chemolithotrophic microorganisms in specific culture media (Corliss *et al.*, 1979; Jannasch and Wirsen, 1979, 1981; Tuttle *et al.*, 1983). Sulfur-oxidizers of the genera *Thiomicrospira* and *Thiobacillus* were the first isolates that confirmed chemolithotrophy as an essential metabolism in these ecosystems (Ruby and Jannasch, 1982; Jannasch *et al.*, 1985; Karl, 1995 and references therein). However, the isolation of *Hyphomicrobium* spp. gave evidence that heterotrophic organisms exist as well (Harwood *et al.*, 1982). Most of the isolated microorganisms were hyperthermophilic *Crenarchaeota* and *Euryarchaeota* from high-temperature chimneys and sediments (Jones *et al.*, 1983; Huber *et al.*, 1989; Kurr *et al.*, 1991).

With the advent of molecular approaches the microbial diversity was studied at the level of the 16S rRNA gene as phylogenetic marker. Techniques such as restriction fragment length polymorphism (RFLP) and denaturation gradient gel electrophoresis (DGGE) did not need any prior cultivation and discovered novel, uncultivated epsilonproteobacterial, gammaproteobacterial and deltaproteobacterial groups (Moyer *et al.*, 1994, 1995; Muyzer *et al.*, 1998). Sequencing of the 16S rRNA genes of these new groups showed a close relation to *Thiovulum*, *Alteromonas*, *Colwellia*, *Xanthomonas* and *Desulfovibrio* as well as to already described genera such as *Thiomicrospira*. Another breakthrough was achieved by fluorescence *in situ* hybridization (FISH) of the 16S rRNA in individual cells to identify and enumerate uncultivated microorganisms (Amann *et al.*, 1990b, 1995). The powerful combination of 16S rRNA gene sequencing and FISH, facilitated the rapid identification of microorganisms in different hydrothermal habitats such as chimneys, mats, sediments and invertebrates (Cary and Giovannoni, 1993; Harmsen *et al.*, 1997a, 1997b; Jannasch, 1995; Schauer *et al.*, 2011). Uncultivated, globally distributed groups were detected, such as the "Deep-Sea Hydrothermal Vent Euryarchaeotic Group" (DHVEG) (Takai and Horikoshi, 1999; Hoek *et al.*, 2003), several groups of *Epsilonproteobacteria, Aquificales*, *Thermotogales*, and *Thermus* spp. (Harmsen *et al.*, 1997b; Reysenbach *et al.*, 2000; Campbell *et al.*, 2001; Corre *et al.*, 2001; Longnecker and Reysenbach, 2001; Hoek *et al.*, 2003). Shortly after the first phylogenetic studies also functional genes such as the ribulose-1,5-bisphosphate carboxylase/oxygenase were targeted and provided a link between function and phylogeny at hydrothermal vents (Elsaied and Naganuma, 2001). The cultivation of the newly detected groups such as *Epsilonproteobacteria* and *Aquificales* (see Table 3) fundamentally

changed the understanding of their metabolic features. These cultures together with larger datasets have led to an emerging pattern concerning the distribution of the communities and their function in different hydrothermal vent habitats (Campbell *et al.*, 2006; Huber *et al.*, 2003). One example is the dominant *Epsilonproteobacteria*, which appeared to be early colonizers of biofilms in habitats, where temperature regimes of mesophilic to thermophilic conditions predominate (López-García *et al.*, 2003; Alain *et al.*, 2004). They are involved in sulfur- and hydrogen-oxidation coupled to carbon fixation via the reductive tricarboxylic acid (rTCA) cycle (Table 4) (Campbell *et al.*, 2006). Although *Aquificales* uses the same energy sources and carbon fixation pathways, they are only found in habitats with thermophilic conditions (Nakagawa and Takai, 2008; Hügler and Sievert, 2011). From such data first models of archaeal and bacterial successions linked to physicochemical parameters were predicted (Huber *et al.*, 2003), which was shown for the temperature-dependent (mesophilic to thermophilic) distribution of all sulfur-oxidizing bacteria (Sievert *et al.*, 2008). Moreover, the development of novel sequencing methods such as massively parallel tag sequencing of hypervariable regions on the 16S rRNA gene revealed an unexpectedly high microbial microdiversity (Huber *et al.*, 2007). A high microdiversity in phylotypes with less than 3% sequence difference points towards different niches (Whittaker, 1972) for organisms within this phylotypes that are well adapted to specific environmental conditions in a highly dynamic ecosystem.

Nevertheless, there is still a lack of knowledge about metabolic rates, substrate specificity and genes involved in metabolic pathways of theses microorganisms (Sievert and Vetriani, 2012).

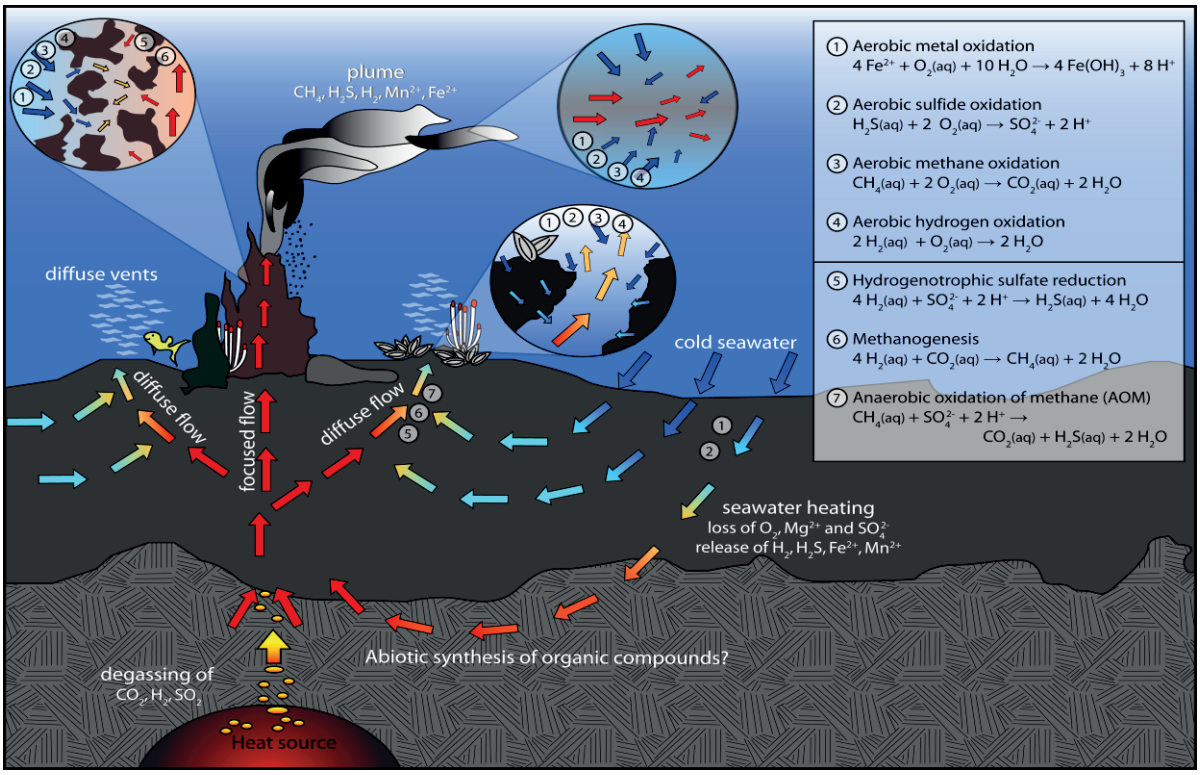

Figure 7: Geochemical-microbial interaction at hydrothermal vent systems. Upwelling hot, reducing hydrothermal fluids mix with entrained cold, oxygenated seawater in subseafloor mixing zones. The catabolic reactions for different habitat are provided in the inset. Modified after Hentscher and Bach (2012)

4.3 Energy metabolisms of hydrothermal vent microorganisms

Studying the biogeochemical element cycles in hydrothermal systems is essential to detect energy sources that fuel primary production. Early attempts in hydrothermal research showed that sulfur is used as a major energy source in this system. Many microorganisms were isolated that oxidize reduced sulfur compounds such as H_2S (sulfide), $S_2O_3^{2-}$ (thiosulfate) or S^0 (elemental sulfur) (Ruby and Jannasch, 1982; Jones *et al.*, 1983; Weiner *et al.*, 1985). Furthermore, sulfur oxidation was confirmed by *in situ* experiments, which measured dark $^{14}CO_2$ uptake with various sulfur compounds and ^{35}S oxidation (Tuttle, 1985; Wirsen *et al.*, 1986). Thermodynamic calculations supported that sulfide oxidation yields the most energy with oxygen as electron acceptor in basalt-hosted systems (Fig. 7) (McCollom, 2000; Amend *et al.*, 2011). Most known sulfur oxidizers belong to the *Gammaproteobacteria* and *Epsilonproteobacteria* that live as free-living microorganisms or in a symbiotic relationship (Sievert *et al.*, 2008). Another important energy source in hydrothermal systems is hydrogen. Modeling of catabolic energetics showed that aerobic hydrogen oxidation yields the most energy in ultramafic-hosted systems (Fig. 7) (Amend *et al.*, 2011). Hydrogen oxidizers also belong to *Gammaproteobacteria* and *Epsilonproteobacteria*, while *Aquificales*, *Thermodesulfobacteriaceae* and most hyperthermophilic *Archaea* exclusively use hydrogen

as an energy source (Table 4). Other chemolithotrophic energy processes are the aerobic oxidation of metals such as Fe^{2+} and Mn^{2+} (Amend *et al.*, 2011; Edwards *et al.*, 2005) that were confirmed by rate measurements and isolation of the corresponding microorganisms (Mandernack and Tebo, 1993; Emerson *et al.*, 2007).

Methane is the smallest organic molecule, while the oxidation of methane is referred as a lithotrophic metabolism (Fuchs and Schlegel, 2006). Measured methane oxidation rates confirmed its relevance for hydrothermal systems (de Angelis *et al.*, 1993). All described processes use oxygen as electron acceptor and are found at sites, where reduced fluids mixes with oxygen-rich seawater such as in chimney walls, diffuse flows, and hydrothermal plumes or in the upper seafloor layers (Fig. 7). In deeper anoxic layers energy is produced by methanogenesis, sulfate reduction, and by AOM (Fig. 7) (Jørgensen *et al.*, 1990; Dhillon *et al.*, 2005; Holler *et al.*, 2011)

Interestingly, the nitrogen cycle in hydrothermal vents environments is not well studied yet and processes that occur in rock- and sediment hosted systems are unclear. Moreover, the role of heterotrophic microbial communities living on organic carbon produced by chemolithoautotrophic microorganisms, waste products from organisms of higher trophic levels or abiotically produced small organic molecules have not been investigated.

5. Energy-yielding metabolisms poorly studied at hydrothermal vent systems

5.1 Nitrogen metabolisms in hydrothermal vents systems

Most of the chemolithotrophic processes that are energetically feasible (see above and Table 1) have been intensively studied in hydrothermal vent systems, whereas nitrification, one of the earliest studied chemolithotrophic processes (Winogradsky, 1890) received little attention. Nitrification is separated into two major reactions (Winogradsky, 1892b, 1892a). The first and rate limiting reaction is the aerobic oxidation of ammonia to nitrite (Fig. 8) performed by ammonia-oxidizing bacteria (AOB) and ammonia-oxidizing archaea (AOA). Currently, all AOB belong to the classes of *Betaproteobacteria* (marine, freshwater, soil) and *Gammaproteobacteria* (marine) (Arp *et al.*, 2007). More than 100 years after the first discovery of nitrifying bacteria, metagenomic analyses (Venter *et al.*, 2004; Treusch *et al.*, 2005) gave first evidence that AOA exist. The isolation of a marine AOA *Nitrosopumilus maritimus* (Könneke *et al.*, 2005) proved their existence and was further supported by the isolation of a soil AOA (Tourna *et al.*, 2011). They belong to the recently proposed phylum *Thaumarchaeota* that was placed in the superphylum "TACK" (*Thaumarchaeota, Aigarchaetoa, Crenarchaeota,* and *Korarchaeota*) (Brochier-Armanet *et al.*, 2008; Spang *et*

al., 2010; Rinke *et al.*, 2013). AOA show higher affinities to ammonium (200-fold higher than AOB) and oxygen than AOB (Martens-Habbena *et al.*, 2009). Moreover, AOA are also detected in oxygen minimum zones with oxygen concentrations < 1 µM, where they co-occur with bacteria that mediate the anaerobic ammonium oxidation (anammox) (Fig. 8) (Lam *et al.*, 2007, 2009). With these characteristics AOA are well adapted to oxic and micro-oxic conditions that typically occur in hydrothermal vent systems and are ideal candidates for a contribution to chemolithotrophic growth in various hydrothermal habitats (Table 3). Repeatedly detection of 16S rRNA genes from *Thaumarchaeota* and archaeal *amoA* in microbial mats, smoker fluids, chimneys, diffuse fluids, hydrothermal plumes, *in situ* collectors, and hydrothermally-influenced sediments (Moyer *et al.*, 1998; Takai and Horikoshi, 1999; Huber *et al.*, 2002; Nercessian *et al.*, 2003; Schrenk *et al.*, 2003; Takai *et al.*, 2004c; Nakagawa *et al.*, 2005b; Kato *et al.*, 2009; Nunoura *et al.*, 2010) showed their occurrence and points towards an impact of nitrification in hydrothermal systems. However, ammonia oxidation was only measured in the plume of sediment-hosted hydrothermal systems and linked to AOB (Lam *et al.*, 2004, 2008). Recently, metatranscriptomics also showed an involvement of AOA in another sediment-hosted system, the Guaymas Basin (Baker *et al.*, 2012). The second reaction of the nitrification, the oxidation of nitrite to nitrate (Fig. 8) is performed by nitrite-oxidizing bacteria (NOB). They belong to the classes *Alphaproteobacteria*, *Gammaproteobacteria*, *Deltaproteobacteria* (Spieck and Bock, 2005), *Betaproteobacteria* (Alawi *et al.*, 2007) and the phyla *Nitrospirae* (Ehrich *et al.*, 1995) and *Chloroflexi* (Sorokin *et al.*, 2012).

Other processes that are involved in converting inorganic nitrogen species have been confirmed in hydrothermal vent systems. Anammox that converts ammonium and nitrite to dinitrogen (Fig. 8) is performed by *Plantomycetes* (Strous *et al.*, 1999). Anammox bacteria have been detected by molecular methods in the altered sediments of the Guamyas Basin that were covered by white mats (Russ *et al.*, 2013). In the same system denitrification, the conversion of nitrate to dinitrogen as another N-loss process (Fig. 8) were measured (Bowles *et al.*, 2012) in sediments with and without *Beggiatoa* mats. The *Beggiatoa* mats were proposed as nitrogen cycling hot spots with high denitrification rates. Besides denitrification, the dissimilatory nitrate reduction to ammonium (DNRA) could be a major process performed by sulfur-oxidizing *Beggiatoa* themselves (McHatton *et al.*, 1996; Preisler *et al.*, 2007). Besides all dissimilatory processes inorganic nitrogen compounds are assimilated. The most favored form is ammonium, which is directly shuttled into the cell metabolism of heterotrophs (Kirchman and Wheeler, 1998).

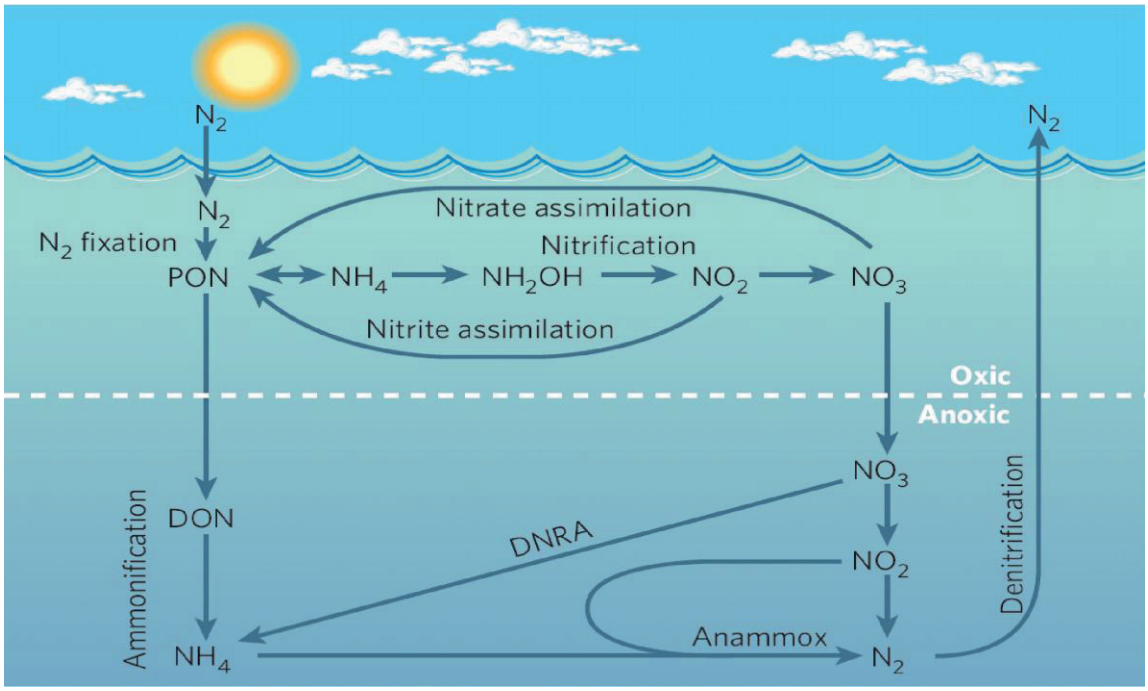

Figure 8: The marine nitrogen cycle. The cycle is divided in oxic and anoxic processes. N_2: dinitrogen; PON: particulate organic nitrogen; NH_4: ammonium; NH_2OH: hydroxylamine; NO_2^-: nitrite; NO_3^-: nitrate; DON: dissolved organic nitrogen; DNRA: dissimilatory nitrate reduction to ammonium (Arrigo, 2005).

5.2 Heterotrophy at hydrothermal vent systems

In recent years organic molecules other than methane have been detected in hydrothermal fluids (Holm and Charlou, 2001; Lang *et al.*, 2006; Konn *et al.*, 2009). Although it is widely accepted that higher organic compounds are formed (McCollom and Seewald, 2007), heterotrophic communities that degrade these compounds are unknown (Karl, 1995). Early, long-term experiments showed that organic substances are used as alternative carbon sources for chemolithoheterotrophic (Tuttle *et al.*, 1983; Tuttle, 1985) or chemoorganoheterotrophic growth (Karl *et al.*, 1989). Moreover, heterotrophic microorganisms were isolated from numerous samples of hydrothermal systems (Jeanthon and Prieur, 1990; Marteinsson *et al.*, 1995; Wery *et al.*, 2001b) (see also Table 4). Recently, hydrocarbon-degrading enzymes were detected in hydrothermal plumes (Li *et al.*, 2013; Sheik *et al.*, 2013). The origin of organic carbon compounds in hydrothermal systems is not well understood. One possibility is the abiotic formation and calculations showed that organic compounds such as carboxylic acids, hydrocarbons, amino acids could be produced under hydrothermal conditions found in vent sites (Shock, 1992; Shock and Schulte, 1998). These organic compounds were formed in simulated experiments under hydrothermal conditions (McCollom and Seewald, 2007 and reference therein) and were detected by *in situ* fluid analysis (Holm and Charlou, 2001;

Proskurowski *et al.*, 2008; Lang *et al.*, 2010; Charlou *et al.*, 2010). Other possible origins are the production and release of organic carbon by chemolithotrophic communities or higher trophical organisms and thermal degradation of organic matter (Pimenov *et al.*, 2002; Simoneit *et al.*, 2004; Lever *et al.*, 2010). All of these observations point towards a heterotrophic microbial community that lives on organic compounds that are produced in hydrothermal vent systems. Until now rates for heterotrophic growth, the substrate spectrum, phylogeny and diversity of heterotrophic communities at hydrothermal systems have not been investigated.

6. Description of sampling sites

6.1 Guaymas Basin

The Guaymas Basin, a sediment-hosted hydrothermal system in the Gulf of California, Mexico, was discovered in 1980 (Lonsdale *et al.*, 1980) and is the northern extension of the East Pacific Rise 21° N (Fig. 1 and 9) (Von Damm *et al.*, 1985b). This hydrothermal system is distinct from other MORs by the occurrence of high sedimentation rates (1 to 2 mm a^{-1}) due to high water column productivity and terrigeneous input (Lonsdale *et al.*, 1980). Consequently, the sediment layer is on average 100 m (Simoneit *et al.*, 1979) but up to 500 m thick (Teske *et al.*, 2002). The sediment largely consists of organic rich diatomaceous ooze and mineral clay (Von Damm *et al.*, 1985b). Percolation of hot fluids through the sediment leads to the alteration of chemical composition. Pyrolysis of organic material forms large amounts of petroleum-like hydrocarbons, short-chain organic acids and also releases vast amounts of ammonium of up to 16 mM (Simoneit and Lonsdale, 1982; Martens, 1990; Von Damm *et al.*, 1985b). These are the highest ammonium concentrations yet detected in hydrothermal fluids (Table 3) and would favor a nitrifying community. Areas of intense flow of diffuse fluids are indicated by

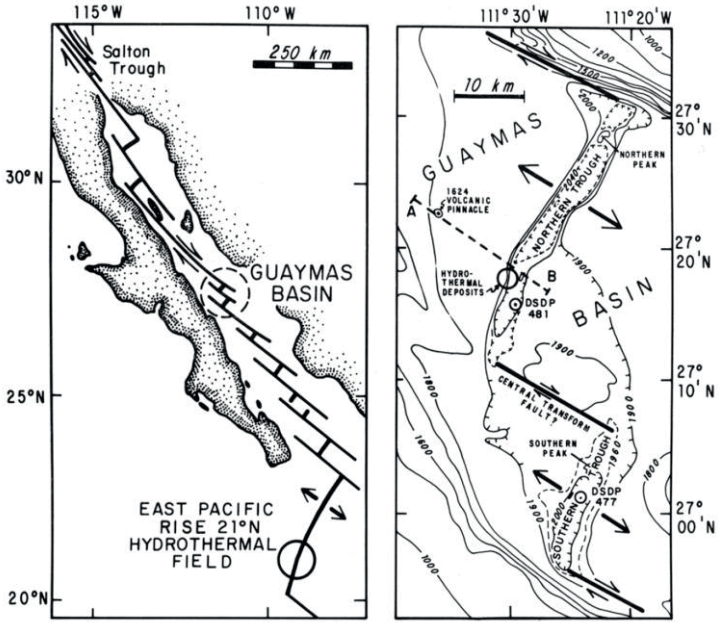

Figure 9: Geographical location and bathymetryic linie chart of the Guaymas Basin hydrothermal vent system in the Gulf of California. (Lonsdale et al., 1980)

dense populations of sulfur-oxidizing, white and orange *Beggiatoa* that form thick mats (up to 3 cm) on top of the sediments (Jannasch *et al.*, 1989). This unusually high accumulation of biomass is favored by irregular inflow of oxygenated seawater into the mats, which results in a small-scale hydrothermal circulation with the rising hydrogen sulfide- and ammonium-rich fluids (Magenheim and Gieskes, 1992; Gundersen *et al.*, 1992). The large, vacuolated cells of the filamentous, autotrophic *Beggiatoa* (Nelson *et al.*, 1989) internally store nitrate up to 130 mM (3000-fold as compared to ambient seawater), however, it is not understood, whether the source of nitrate is derived from the water column or the benthic system (McHatton *et al.*, 1996). Nitrifying communities of bacteria and archaea that converts the uprising ammonium over nitrite to nitrate could live inside the *Beggiatoa* mats and provide them with higher nitrate concentrations. *Beggiatoa* most likely respire the nitrate back to ammonium via the DNRA (McHatton *et al.*, 1996; Preisler *et al.*, 2007). The ammonium is released and a mat internal nitrogen cycle could develop between these functional communities. In anoxic niches of the mat anaerobic ammonia-oxidizing bacteria could also convert the ammonium and produced nitrite to dinitrogen, which is lost from the system. Similar associations have been demonstrated in continental margins between anammox bacteria and *Thioploca* (Prokopenko *et al.*, 2006, 2013). Both aerobic and anaerobic ammonium oxidizing communities benefit from the detoxification of the inhibitory hydrogen sulfide (Joye and Hollibaugh, 1995; Jensen *et al.*, 2008) by sulfur-oxidizing *Beggiatoa*.

.

6.2 Menez Gwen hydrothermal vent field, MAR

The Menez Gwen field (37°50'N and 31°31'W, 850 m depth) is located on the Azores Triple Junction (Fig. 10) (Charlou *et al.*, 2000). The Menez Gwen segment is dominated by a large central volcano (15 km in diameter, 700 m high), whose top is separated into two symmetrical halves that form an axial graben of 2-3 km width (Fouquet *et al.*, 1994; Parson *et al.*, 2000). At the northern end there is a young active volcano (700 m diameter, 120 m high) (Fig. 10) (Fouquet *et al.*, 1994). High proportions of hydrothermal end-member fluids were found in warm diffuse fluids that can support microbial biomass production. As described above the formation of organic carbon is more likely to occur in ultramafic-hosted system than in basalt-hosted systems (chapters 2.2.4 and 4.2) due to high serpentinization of olivine that produces hydrogen (see Box 2). Hydrogen is then further converted to small organic carbon compounds, like methane by Fisher-Tropsch-type reactions (see Box 2) (McCollom and Seewald, 2007). The detection of unusually high concentrations of methane in Menez Gwen led to the assumption that serpentinization and Fischer-Tropsch-type reactions play a

significant role in basalt-hosted hydrothermal systems, too (Charlou *et al.*, 2000). So far little is known about the microbial community of the Menez Gwen system. Earlier studies were focused on symbionts in vent mussels (Fiala-Médioni *et al.*, 2002; Duperron *et al.*, 2006; Riou *et al.*, 2010), on isolation of a novel chemolithoautotrophic bacterium (Miroshnichenko *et al.*, 2003) and on the detection of anammox bacteria associated with *Bathymodiolus azoricus* (Byrne *et al.*, 2008). Interestingly, Charlou and colleagues also detected low concentrations of unsaturated and saturated C2- and C3-hydrocarbons (Charlou *et al.*, 2000) that are in the same order of magnitude as in ultramafic-hosted systems (Charlou *et al.*, 2002).

6.3 Manus Basin

The Manus Basin is located in the Bismarck Sea and has three major spreading centers linked

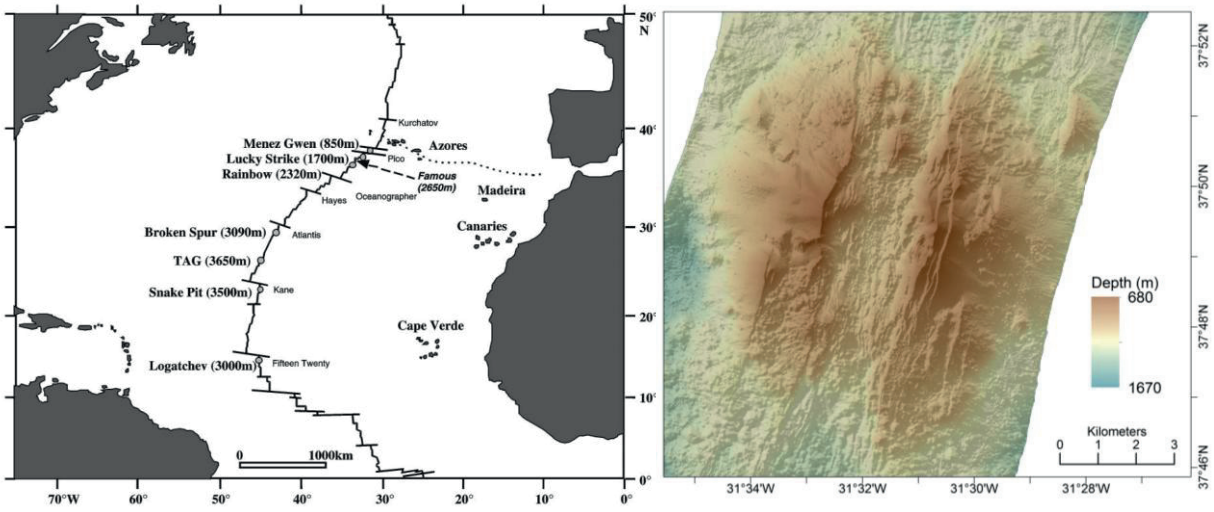

Figure 10: Left map shows the Mid-Atlantic Ridge with known hydrothermal vent systems. Right map shows the Menez Gwen volcano with the young active volcano on the north side of the ridge axis. (Desbruyères *et al*., 2001; Marcon *et al*., 2013)

with transform faults (Martinez and Taylor, 1996). The PACMANUS (Pacific Australia Canada Manus) hydrothermal vent field (Binns and Scott, 1993) mainly consist of andesite, dacite with massive sulfide deposits and has fluids with low pH (pH 2.1) (Moss and Scott, 2001). The SuSu knolls consist of dacite and massive sulfides on top of the lava (Moss and Scott, 2001). Again, the pH is low (pH 3) (Moss and Scott, 2001). So far, there is no evidence for serpentinization or a formation of organic compounds in these systems. Nevertheless, possible other sources of organic matter such as waste products of macrofauna could fuel a heterotrophic microbial community (Pimenov *et al.*, 2002).

Only since a few years the microbial communities of hydrothermal vent fields in back-arc basin have been studied (Takai *et al.*, 2006 and reference therein; Huber *et al.*, 2010; Flores

et al., 2012; Kato *et al.*, 2013). However, while back-arc basins share many features with MORs, they show a greater diversity in chemical composition (Martinez *et al.*, 2007).

7. Methods to study the activity and identity of microorganisms in hydrothermal vent systems

7.1 Cultivation-dependent techniques

Estimations showed that the majority of the microorganisms are still uncultivated (Amann *et al.*, 1995; Hugenholtz *et al.*, 1998; Whitman *et al.*, 1998). However, a pure culture of a microorganism is still the best way to explore their genetic potential and resulting physiology that can be tested and interpreted to define their specific niche in the environment. In the natural environment the microorganisms often encounter nutrient limitations, virus attacks, predation by higher organisms, and competition for substrates with other microorganisms. Therefore, it is absolute essential to also study their behavior in the natural environment.

Often the culture media contain large amounts of substrates that inhibit growth of most organisms that have an oligotrophic lifestyle (Giovannoni and Stingl, 2007). Moreover, the high substrate concentrations led to the isolation of microorganisms that are well adapted to high concentrations and not abundant (Hugenholtz, 2002). Lower substrate concentrations and dilution of microorganisms led to the cultivation of abundant and important microorganisms that previously escaped traditional cultivation methods (Connon and Giovannoni, 2002; Rappé *et al.*, 2002). Other attempts use longer incubation times for slow growing microorganisms (Davis *et al.*, 2005), co-culturing of several organisms (Ohno *et al.*, 2000) or the addition of signaling molecules that promote growth (Bruns *et al.*, 2002). However, regardless of those new approaches for culturing, the majority of microorganisms in nature still remain uncultivated.

7.2 Cultivation-independent techniques

7.2.1 Diversity analysis via ribosomal RNA and functional genes

The 16S rRNA gene is widely used as the phylogenetic marker to explore the diversity in environmental samples, however, protein-encoding genes (functional genes) are also widely studied. These can link the potential function of a microorganism with its phylogenetic identity unless horizontal gene transfer is involved. For more than 1-2 decades genes have been polymerase chain reaction (PCR) amplified, cloned and sequenced yielding a couple of hundred sequences for phylogenetic analysis. Since a few years massively parallel pyrosequencing that avoids the cloning step is nowadays widely used to access the microbial

diversity in environmental samples (Sogin *et al.*, 2006; Huber *et al.*, 2007). With primers that contain a barcode sequence the analysis of several samples in a single sequence run is possible, which drastically reduces sequencing costs. This method enables the rapid construction of datasets with several thousands of short sequence reads to compare many samples. So far, the disadvantage of the method is the read length of the sequences (up to 700 bp), which do not allow for precise phylogenetic reconstruction on taxonomic levels below order to class (Mizrahi-Man *et al.*, 2013). Nevertheless, pyrosequencing allows to quickly compare sequenced amplicons of diffuse hydrothermal fluids and analyze the relative abundance of amplified sequences in temporal and spatial scales (Perner *et al.*, 2013).

7.2.2 Fluorescence *in situ* hybridization

In the 1980s Pace and colleagues revolutionized environmental microbiology by extracting bulk DNA, amplifying and cloning the 16S rRNA gene and comparing the sequence to known 16S rRNA sequences in databases. With the rRNA approach they have overcome a pre-cultivation to determine the 16S rRNA gene of microorganisms (Lane *et al.*, 1985). When the rRNA approach was combined with PCR (Saiki *et al.*, 1988) a rapid amplification of 16S rRNA genes from bacterial communities was possible (Giovannoni *et al.*, 1990). Another breakthrough was achieved by whole-cell FISH with 16S rRNA-targeted nucleic-acid probes. FISH in combination with the rRNA approach enabled visualization and quantification of uncultured microorganisms in nature (Amann *et al.*, 1995). A scheme of the "full-cycle rRNA approach" is shown in Figure 11. One of the limitations of this method was the detection of cells with low ribosome content, which was solved by the application of probes that are labeled with the enzyme horseradish peroxidase (HRP). This enzyme radicalizes fluorescently labeled tyramides that react with cell proteins (catalyzed reporter deposition FISH, CARD-FISH). The fluorescence signal is brighter and more stable than FISH with fluorochrome-labeled probes

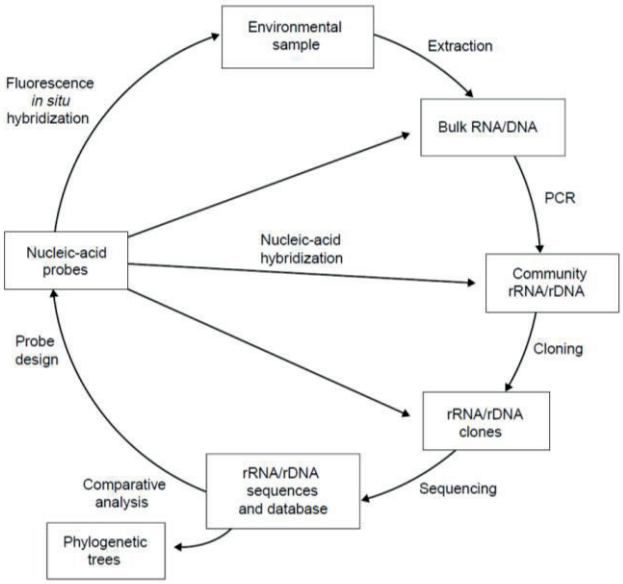

Figure 11: 'Full-cycle' rRNA approach to characterizing microorganisms in their natural settings without the need for cultivation (Hugenholtz, 2002).

(Schönhuber *et al.*, 1997; Pernthaler *et al.*, 2002). However, this method still cannot detect rare populations of less than 0.5% of the whole community (Gomez-Pereira *et al.*, 2010). Furthermore, it is not a high-throughput method, since the enumeration of signals is time consuming unless the samples can be counted automatically (Pernthaler *et al.*, 2003).

In hydrothermal systems, FISH has been used to link the *in situ* abundance of *Epsilonproteobacteria* embedded in a mucous sulfur-rich matrix that was detected with X-ray spectroscopy (Moussard *et al.*, 2006). Furthermore, (CARD)-FISH was used in combination with measurements of substrate concentrations, substrate fluxes and metabolic rates, to link possible populations to *in situ* processes such as nitrification (Lam *et al.*, 2004, 2008), AOM (Holler *et al.*, 2011; Wankel *et al.*, 2012), hydrogen oxidation (Perner *et al.*, 2010; Petersen *et al.*, 2011), sulfate reduction and sulfide oxidation (Schauer *et al.*, 2011).

7.2.3 Real-time PCR (quantitative PCR)

Another possibility to quantify microorganisms from environmental samples is the enumeration of gene copy numbers by real-time quantitative PCR (q-PCR). The PCR-amplified DNA is quantified with a fluorescent reporter dye that binds to the DNA labeled to a probe in the Taqman approach (Holland *et al.*, 1991) or intercalates into the double stranded DNA such as SYBR green I (Wittwer *et al.*, 1997). After each cycle the emitted fluorescence, which is proportional to the amplified DNA, are monitored. The amount of amplified DNA is compared to a standard of the target gene that runs in parallel (Kubista *et al.*, 2006). The method is fast and high throughput, has a wide range of quantification (7-8 log decades), a high sensitivity (< 5 copies) and is easily analyzed with high accuracy (Klein, 2002; Smith and Osborn, 2009). The q-PCR can be inhibited by high amounts of humic substances from soil or sediment. Often target genes exist in multiple operons in the genome of microorganisms, thus an absolute quantification can only be achieved by normalization (Bustin *et al.*, 2009). Results of all PCR-based methods are severely influenced by the selected nucleic acid extraction method and primers (Smith and Osborn, 2009).

7.3 Identification of active microorganisms

Several methods are available to identify microorganisms, but it is also important to understand what they actually do in nature. Therefore, rate measurements of biogeochemical processes in combination with FISH were used to indirectly link phylogenetic groups to a specific process. These rates are usually measured by stable and radioactive tracers (Reeburgh, 1983). One of those techniques excels with higher resolution and enables

identification of specific activities on single cell level by combining microautoradiography with FISH (MAR-FISH) (Ouverney and Fuhrman, 1999; Lee *et al.*, 1999). Furthermore, Raman spectroscopy identifies substances by bond vibrations and distinguishes shifts of light and heavy isotopes spectra. Combined with FISH substrate uptake into single cells is analyzed (Huang *et al.*, 2007). This method is non-destructive and combined with optical tweezers it might be possible to separate intact, active cells to sequence their genomes (Wagner, 2009). Stable isotopic probing (SIP) also uses substrates labeled with stable isotopes to follow incorporation into DNA, RNA or protein in complex communities. The heavier molecules are easily separated by gradient centrifugation of the nucleic acid extraction or by analysis of polar lipid derived fatty acids (Boschker *et al.*, 1998; Radajewski *et al.*, 2000; Manefield *et al.*, 2002). From the heavier nucleic acids the 16S rRNA genes are analyzed by the rRNA approach.

The most sensitive method that links activity to phylogeny is the combination of *in situ* hybridization techniques with nanometer-scale secondary ion mass spectrometry (nanoSIMS). NanoSIMS is a destructive method, whereby a primary ion beam (caesium beam) is scanned over the sample and expels secondary ions. These are detected by a mass spectrometer that collects up to 7 different masses simultaneously. By repeated scanning over the same area a depth profile of the cell is calculated that shows topographical information by the collection of electrons from resulting collisions. The nanoSIMS measures any stable isotope or radioisotope and has therefore a broad spectrum for applications (Musat *et al.*, 2012). Different *in situ* hybridization methods have been developed to directly quantify the target organisms, e. g. by iodine-labeled probes (Li *et al.*, 2008), halogen-containing fluorescently labeled tyramides as element labeling (EL-FISH) (Behrens *et al.*, 2008) and halogen *in situ* hybridization FISH (HISH-FISH) (Musat *et al.*, 2008). NanoSIMS can also be combined with CARD-FISH by a correlative microscopy. A major drawback of the method is the time consuming measurement and sample preparation, thus preventing a high throughput (Musat *et al.*, 2008).

7.4 Single cell genomics

Next generation sequencing enabled metagenomic studies that provides genetic information of a whole microbial community in a sample. These huge datasets often lack the possibility to assign all genes to a taxonomic group. Moreover, genes of two or more phylogenetically related organisms might be assembled into a single nucleotide sequence and thereby creating chimeric genome information (Lasken, 2012). One project to solve this problem is the GEBA

standing for "A Genomic Encyclopedia of Bacteria and Archaea" led by the Joint Genome Institute (JGI) and the Deutsche Sammlung für Mikroorganismen und Zellkulturen (DSMZ). In this project 53 bacterial and 3 archaeal genomes are sequenced from culture collections such as the DSMZ and the American Type Culture Collection (ATCC), which are used as reference genome for metagenomic studies (Wu *et al.*, 2009). Often the lack of pure cultures for many phylogenetic clades, such as proposed environmental candidate phyla (Marcy *et al.*, 2007b; Rinke *et al.*, 2013) hamper the access to their genetic material. A solution is sequencing of single cell genomes (Gilbert and Dupont, 2011) that was achieved by the development of whole genome amplification via multiple displacement amplification (MDA) to gain enough DNA. This isothermal method is used to rapidly produce micrograms of DNA from femtograms of starting material of a single bacterial cell (Lasken, 2012). In combination with single cell separation techniques such as flow cytometry (Amann *et al.*, 1990a), micromanipulation (Ishoey *et al.*, 2008; Jogler *et al.*, 2011) or microfluidic devices (Marcy *et al.*, 2007a), microorganisms of interest can be sequenced. MDA uses a special φ29 polymerase derived from a phage in combination with modified random primers. The polymerase has a strand displacement activity and synthesizes multiple copies of DNA strands (Fig. 12) (Lasken, 2007, 2012). A major problem is the chimera formation due to the strand displacement character, while other problems are the targeting of virtual every DNA so that free DNA and contaminating non-target DNA will be amplified as well (Lasken and Stockwell, 2007; Woyke *et al.*, 2011). Today, many genomes have been amplified by MDA and have given valuable insights in the genomic potential of uncultured microorganisms (Woyke *et al.*, 2009, 2010; Blainey *et al.*, 2011; Swan *et al.*, 2011; Martinez-Garcia *et al.*, 2012). These information should help to isolate uncultured microorganisms. However, the genetic information often led to the hypothesis of pathways that might be not active and therefore needs to be tested.

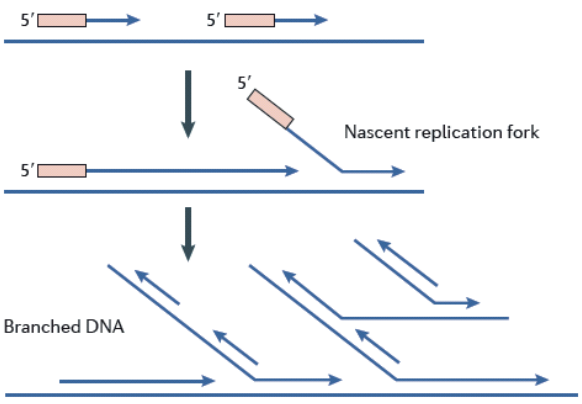

Figure 12: Principle of the multiple displacement amplification. Arrows with box represents random primer (Lasken, 2012).

8. Objectives of the thesis

Since the discovery of hydrothermal systems 30 years ago it has been shown that these fascinating ecosystems cause a high heat and mass transfer from the mantle into the ocean that

subsequently produces chemical environments for high biomass production. Chemosynthetic microorganisms that fuel many different metabolic processes have been studied as outlined in this chapter. Moreover, the fast development of new molecular techniques during these three decades allowed the identification of newly discovered taxonomic groups that are responsible for driving biogeochemical cycles in these highly dynamic ecosystems. The dynamics of substrates and other factors such as temperature influence the diversity and show distinct spatial and temporal pattern of microbial communities. However, some chemosynthetic processes that are well known from other ecosystems in the ocean have gained only little attention. Therefore, I investigated two of these insufficiently studied processes in three geographically separated hydrothermal systems (Chapter II and III). Furthermore, I analyzed the genetic and metabolic potential of a chemoautotrophic microorganism, *Candidatus* Thiomargarita nelsonii, and compared it to its relatives that play an important role at our sampling site in the Guaymas Basin (Chapter II) to get a better understanding of the general metabolic potential of the family they belong to (Chapter IV).

In more detail I tried to answer the following questions during my thesis:

1. Is nitrification a potential energy-yielding process in sediment-hosted hydrothermal systems?

Little is known about nitrification in benthic hydrothermal systems. It has been hypothesized that AOB and AOA are active in hydrothermal systems (Takai and Nakamura, 2011) and nitrification is expected to occur based on the isotopic composition of measured nitrogen species (Bourbonnais *et al.*, 2012). So far it is not clear to what extent AOB and AOA contribute to chemolithotrophy in benthic habitats of these systems. Furthermore, the activity of AOB and AOA in hydrothermal systems needs to be analyzed. What is the metabolic rate of ammonia oxidation by AOB and AOA? How diverse are AOB and AOA in hydrothermal systems?

To answer some questions I investigated the potential of nitrification in mats of large colorless sulfur-oxidizing bacteria (SOB) from the genus *Beggiatoa.* The mats grew at the surface of the sediment-covered hydrothermal system, Guaymas Basin. *Beggiatoa* are known to respire nitrate that is internally stored in their central vacuole. As described in section 5.1 mats are indicators for high fluxes of upwelling, ammonium- and sulfide-rich fluids (Magenheim and Gieskes, 1992) and might be potential nitrification spots. For testing this hypothesis we conducted challenging *in situ* microsensor measurements of oxygen, hydrogen sulfide and NO_x in combination with isotopic pairing experiments to determine nitrification

rates in *Beggiatoa* mats. Molecular analysis by q-PCR and functional gene libraries were used to analyze the diversity and abundance of bacterial and archaeal *amoA* as functional marker. Furthermore, CARD-FISH analysis targeted specific nitrifying archaea and bacteria to visualize them in the *Beggiatoa* mat and other hydrothermal vent compartments (Chapter II).

2. Which microorganisms consume organic substrates, in particular acetate in diffuse fluids from two rock-hosted hydrothermal systems?

Recently it has been recognized that hydrothermal fluids contain higher organic compounds than methane (Holm and Charlou, 2001; Lang *et al.*, 2006; Konn *et al.*, 2009; Charlou *et al.*, 2010) such as organic acids, lipids and hydrocarbons. Formate and acetate have been found in rock-hosted hydrothermal fluids (Lang *et al.*, 2010). Moreover, modelling shows that formate and acetate could occur in nM to µM concentrations in fluids from basalt-hosted systems, sufficient to fuel heterotrophic communities (W. Bach, personal communication). Although heterotrophic microorganisms have been isolated from active vent sites, little is known about their identity, abundance and *in situ* activity in hydrothermal fluids. Active heterotrophic communities that use small organic compounds have not been investigated.

Thus, the second study focused on the identification of acetate-assimilating microorganisms in diffuse fluids from two hydrothermal systems: the basalt-hosted Menez Gwen system and the felsic hydrothermal field of the Manus Basin. 16S rRNA gene diversity analysis using pyrosequencing and CARD-FISH were performed in fluids ranging from 4° to 72°C. To detect the metabolic activity on the cellular level, fluids were short-term incubated with ^{13}C-acetate and ^{15}N-ammonium for subsequent analysis of single cells by nanoSIMS in combination with FISH (Chapter III).

3. What is the genetic potential of "*Candidatus* Thiomargarita nelsonii" in particular in N-cycling and how does it compare to other *Beggiatoaceae*?

In the third part of the thesis the MDA-amplified and sequenced genome of a single *Thiomargarita nelsonii* cell has been analysed. This species belongs to the *Beggiatoaceae* (Salman *et al.*, 2011), members of which are also found in the Guaymas Basin. Comparison of the major metabolic pathways of the *Thiomargarita nelsonii* and four other *Beggiatoaceae* genomes including an orange filament from the Guaymas Basin (Chapter II) especially focused on the dissimilatory nitrate respiration during anoxic conditions (Chapter IV). The genes and pathways were annotated and analysed using bioinformatics tools.

9. References

Aharon, O. (2010). "Microbial metabolism: Importance for environmental biotechnology," in *Environmental Biotechnology* Handbook of environmental engineering., eds. L. K. Wang, V. Ivanov, and J.-H. Tay (Humana Press), 193–255.

Alain, K., Postec, A., Grinsard, E., Lesongeur, F., Prieur, D., and Godfroy, A. (2010). *Thermodesulfatator atlanticus* sp. nov., a thermophilic, chemolithoautotrophic, sulfate-reducing bacterium isolated from a Mid-Atlantic Ridge hydrothermal vent. *Int J Syst Evol Microbiol* 60, 33–38.

Alain, K., Zbinden, M., Le Bris, N., Lesongeur, F., Quérellou, J., Gaill, F., and Cambon-Bonavita, M.-A. (2004). Early steps in microbial colonization processes at deep-sea hydrothermal vents. *Environ. Microbiol.* 6, 227–241.

Alawi, M., Lipski, A., Sanders, T., Pfeiffer, E.-M., and Spieck, E. (2007). Cultivation of a novel cold-adapted nitrite oxidizing betaproteobacterium from the Siberian Arctic. *ISME J.* 1, 256.

Allen, D. E., and Seyfried Jr., W. E. (2003). Compositional controls on vent fluids from ultramafic-hosted hydrothermal systems at mid-ocean ridges: An experimental study at 400°C, 500 bars. *Geochim. Cosmochim. Acta* 67, 1531–1542.

Allen, D. E., and Seyfried Jr, W. E. (2004). Serpentinization and heat generation: constraints from Lost City and Rainbow hydrothermal systems. *Geochim. Cosmochim. Acta* 68, 1347–1354.

Alt, J. C., and Bach, W. (2003). "Alteration of oceanic crust: Subsurface rock-water interactions," in *Energy and mass transfer in marine hydrothermal systems*, eds. P. E. Halbach, V. Tunnicliffe, and J. R. Hein (Dahlem University Press).

Amann, R. I., Binder, B. J., Olson, R. J., Chisholm, S. W., Devereux, R., and Stahl, D. A. (1990a). Combination of 16S rRNA-targeted oligonucleotide probes with flow cytometry for analyzing mixed microbial populations. *Appl. Environ. Microbiol.* 56, 1919–1925.

Amann, R. I., Krumholz, L., and Stahl, D. A. (1990b). Fluorescent-oligonucleotide probing of whole cells for determinative, phylogenetic, and environmental studies in microbiology. *J. Bacteriol.* 172, 762–770.

Amann, R. I., Ludwig, W., and Schleifer, K. H. (1995). Phylogenetic identification and *in situ* detection of individual microbial cells without cultivation. *Microbiol. Rev.* 59, 143–169.

Amend, J. P., McCollom, T. M., Hentscher, M., and Bach, W. (2011). Catabolic and anabolic energy for chemolithoautotrophs in deep-sea hydrothermal systems hosted in different rock types. *Geochim. Cosmochim. Acta* 75, 5736–5748.

De Angelis, M. A., Lilley, M. D., and Baross, J. A. (1993). Methane oxidation in deep-sea hydrothermal plumes of the endeavour segment of the Juan de Fuca Ridge. *Deep Sea Res. Part Ocean. Res. Pap.* 40, 1169–1186.

Antoine, E., Cilia, V., Meunier, J. R., Guezennec, J., Lesongeur, F., and Barbier, G. (1997). *Thermosipho melanesiensis* sp. nov., a new thermophilic anaerobic bacterium belonging to the order thermotogales, isolated from deep-sea hydrothermal vents in the southwestern Pacific Ocean. *Int. J. Syst. Bacteriol.* 47, 1118–1123.

Arp, D. J., Chain, P. S. G., and Klotz, M. G. (2007). The impact of genome analyses on our understanding of ammonia-oxidizing bacteria. *Annu. Rev. Microbiol.* 61, 503–528.

Arrigo, K. R. (2005). Marine microorganisms and global nutrient cycles. *Nature* 437, 349–355.

Bach, W., and Edwards, K. J. (2003). Iron and sulfide oxidation within the basaltic ocean crust: implications for chemolithoautotrophic microbial biomass production. *Geochim. Cosmochim. Acta* 67, 3871–3887.

Bach, W., Paulick, H., Garrido, C. J., Ildefonse, B., Meurer, W. P., and Humphris, S. E. (2006). Unraveling the sequence of serpentinization reactions: petrography, mineral chemistry, and petrophysics of serpentinites from MAR 15°N (ODP Leg 209, Site 1274). *Geophys. Res. Lett.* 33, L13306

Baker, B. J., Lesniewski, R. A., and Dick, G. J. (2012). Genome-enabled transcriptomics reveals archaeal populations that drive nitrification in a deep-sea hydrothermal plume. *ISME J.* 6, 2269-2279

Baross, J. A., Lilley, M. D., and Gordon, L. I. (1982). Is the CH_4, H_2 and CO venting from submarine hydrothermal systems produced by thermophilic bacteria? *Nature* 298, 366–368.

Beaulieu, S. E. (2013). *InterRidge Global Database of Active Submarine Hydrothermal Vent Fields: prepared for InterRidge, Version 3.1*. World Wide Web electronic publication: http://vents-data.interridge.org/.

Behrens, S., Lösekann, T., Pett-Ridge, J., Weber, P. K., Ng, W.-O., Stevenson, B. S., Hutcheon, I. D., Relman, D. A., and Spormann, A. M. (2008). Linking microbial phylogeny to metabolic activity at the single-cell level by using enhanced element labeling-catalyzed reporter deposition fluorescence *in situ* hybridization (EL-FISH) and nanoSIMS. *Appl. Environ. Microbiol.* 74, 3143–3150.

Bemis, K., Lowell, R., and Farough, A. (2012). Diffuse flow on and around hydrothermal vents at mid-ocean ridges. *Oceanography* 25, 182–191.

Binns, R. A., and Scott, S. D. (1993). Actively forming polymetallic sulfide deposits associated with felsic volcanic rocks in the eastern Manus back-arc basin, Papua New Guinea. *Econ. Geol.* 88, 2226–2236.

Blainey, P. C., Mosier, A. C., Potanina, A., Francis, C. A., and Quake, S. R. (2011). Genome of a low-salinity ammonia-oxidizing archaeon determined by single-cell and metagenomic analysis. *PLoS ONE* 6, e16626.

Blöchl, E., Rachel, R., Burggraf, S., Hafenbradl, D., Jannasch, H. W., and Stetter, K. O. (1997). *Pyrolobus fumarii*, gen. and sp. nov., represents a novel group of archaea, extending the upper temperature limit for life to 113 degrees C. *Extrem. Life Extreme Cond.* 1, 14–21.

Boetius, A., and Suess, E. (2004). Hydrate Ridge: A natural laboratory for the study of microbial life fueled by methane from near-surface gas hydrates. *Chem. Geol.* 205, 291–310.

Boschker, H. T. S., Nold, S. C., Wellsbury, P., Bos, D., de Graaf, W., Pel, R., Parkes, R. J., and Cappenberg, T. E. (1998). Direct linking of microbial populations to specific biogeochemical processes by ^{13}C-labelling of biomarkers. *Nature* 392, 801–805.

Bourbonnais, A., Lehmann, M. F., Butterfield, D. A., and Juniper, S. K. (2012). Subseafloor nitrogen transformations in diffuse hydrothermal vent fluids of the Juan de Fuca Ridge evidenced by the isotopic composition of nitrate and ammonium. *Geochem. Geophys. Geosystems* 13, n/a–n/a.

Bowles, M. W., Nigro, L. M., Teske, A. P., and Joye, S. B. (2012). Denitrification and environmental factors influencing nitrate removal in Guaymas Basin hydrothermally altered sediments. *Front. Aquat. Microbiol.* 3, 377.

Brochier-Armanet, C., Boussau, B., Gribaldo, S., and Forterre, P. (2008). Mesophilic crenarchaeota: Proposal for a third archaeal phylum, the *Thaumarchaeota*. *Nat Rev Micro* 6, 245–252.

Brown, J., Colling, A., Park, D., Phillips, J., Rothery, D., and Wright, J. (1989). *The Ocean Basins: Their Structure and Evolution*, ed. G. Bearman The Open University.

Bruns, A., Cypionka, H., and Overmann, J. (2002). Cyclic AMP and acyl homoserine lactones increase the cultivation efficiency of heterotrophic bacteria from the central Baltic Sea. *Appl. Environ. Microbiol.* 68, 3978–3987.

Bustin, S. A., Benes, V., Garson, J. A., Hellemans, J., Huggett, J., Kubista, M., Mueller, R., Nolan, T., Pfaffl, M. W., Shipley, G. L., *et al.* (2009). The MIQE guidelines: minimum information for publication of quantitative real-time PCR experiments. *Clin. Chem.* 55, 611–622.

Byrne, N., Strous, M., Crepeau, V., Kartal, B., Birrien, J.-L., Schmid, M., Lesongeur, F., Schouten, S., Jaeschke, A., Jetten, M., *et al.* (2008). Presence and activity of anaerobic ammonium-oxidizing bacteria at deep-sea hydrothermal vents. *ISME J* 3, 117–123.

Campbell, B. J., Engel, A. S., Porter, M. L., and Takai, K. (2006). The versatile ϵ-proteobacteria: key players in sulphidic habitats. *Nat. Rev. Microbiol.* 4, 458–468.

Campbell, B. J., Jeanthon, C., Kostka, J. E., Luther, G. W., and Cary, S. C. (2001). Growth and phylogenetic properties of novel bacteria belonging to the epsilon subdivision of the *Proteobacteria* enriched from *Alvinella pompejana* and Deep-Sea Hydrothermal Vents. *Appl Env. Microbiol* 67, 4566–4572.

Cary, S. C., and Giovannoni, S. J. (1993). Transovarial inheritance of endosymbiotic bacteria in clams inhabiting deep-sea hydrothermal vents and cold seeps. *Proc. Natl. Acad. Sci.* 90, 5695–5699.

Charlou, J. L., Donval J.P., Douville E., Jean-Baptiste P., Radford-Knoery J., Fouquet Y., Dapoigny A., and Stievenard M. (2000). Compared geochemical signatures and the evolution of Menez Gwen (37o50'N) and Lucky Strike (37o17'N) hydrothermal fluids, south of the Azores Triple Junction on the Mid-Atlantic Ridge. *Chem. Geol.* 171, 49–75.

Charlou, J. L., Donval, J. P., Fouquet, Y., Jean-Baptiste, P., and Holm, N. (2002). Geochemistry of high H_2 and CH_4 vent fluids issuing from ultramafic rocks at the Rainbow hydrothermal field (36°14′N, MAR). *Chem. Geol.* 191, 345–359.

Charlou, J. L., Donval, J. P., Konn, C., OndréAs, H., Fouquet, Y., Jean-Baptiste, P., and Fourré, E. (2010). "High production and fluxes of H_2 and CH_4 and evidence of abiotic hydrocarbon synthesis by serpentinization in ultramafic-hosted hydrothermal systems on the Mid-Atlantic Ridge," in *Diversity of hydrothermal systems on slow spreading ocean ridges*, eds. P. A. Rona, C. W. Devey, J. Dyment, and B. J. Murton (American Geophysical Union), 265–296.

Connon, S. A., and Giovannoni, S. J. (2002). High-throughput methods for culturing microorganisms in very-low-nutrient media yield diverse new marine isolates. *Appl. Environ. Microbiol.* 68, 3878–3885.

Corliss, J. B., Dymond, J., Gordon, L. I., Edmond, J. M., von Herzen, R. P., Ballard, R. D., Green, K., Williams, D., Bainbridge, A., Crane, K., *et al.* (1979). Submarine thermal sprirngs on the Galápagos Rift. *Science* 203, 1073 –1083.

Corre, E., Reysenbach, A.-L., and Prieur, D. (2001). ε-proteobacterial diversity from a deep-sea hydrothermal vent on the Mid-Atlantic Ridge. *FEMS Microbiol. Lett.* 205, 329–335.

Costa, E., Pérez, J., and Kreft, J.-U. (2006). Why is metabolic labour divided in nitrification? *Trends Microbiol.* 14, 213–219.

Cowan, D. . (2004). The upper temperature for life – where do we draw the line? *Trends Microbiol.* 12, 58–60.

Crespo-Medina, M., Chatziefthimiou, A., Cruz-Matos, R., Pérez-Rodríguez, I., Barkay, T., Lutz, R. A., Starovoytov, V., and Vetriani, C. (2009). *Salinisphaera hydrothermalis* sp. nov., a mesophilic, halotolerant, facultatively autotrophic, thiosulfate-oxidizing gammaproteobacterium from deep-sea hydrothermal vents, and emended description of the genus Salinisphaera. *Int. J. Syst. Evol. Microbiol.* 59, 1497–1503.

Von Damm, K. ., Edmond, J. ., Grant, B., Measures, C. ., Walden, B., and Weiss, R. . (1985a). Chemistry of submarine hydrothermal solutions at 21 °N, East Pacific Rise. *Geochim. Cosmochim. Acta* 49, 2197–2220.

Von Damm, K. L., Edmond, J. M., Measures, C. I., and Grant, B. (1985b). Chemistry of submarine hydrothermal solutions at Guaymas Basin, Gulf of California. *Geochim. Cosmochim. Acta* 49, 2221–2237.

Davis, K. E. R., Joseph, S. J., and Janssen, P. H. (2005). Effects of growth medium, inoculum size, and incubation time on culturability and isolation of soil bacteria. *Appl. Environ. Microbiol.* 71, 826–834.

Desbruyères, D., Biscoito, M., Caprais, J.-C., Colaço, A., Comtet, T., Crassous, P., Fouquet, Y., Khripounoff, A., Le Bris, N., Olu, K., *et al.* (2001). Variations in deep-sea hydrothermal vent communities on the Mid-Atlantic Ridge near the Azores plateau. *Deep Sea Res. Part Ocean. Res. Pap.* 48, 1325–1346.

Dhillon, A., Lever, M., Lloyd, K. G., Albert, D. B., Sogin, M. L., and Teske, A. (2005). Methanogen diversity evidenced by molecular characterization of methyl coenzyme M reductase A (*mcrA*) genes in hydrothermal sediments of the Guaymas Basin. *Appl. Environ. Microbiol.* 71, 4592–4601.

Dick, G. J., Anantharaman, K., Baker, B. J., Li, M., Reed, D. C., and Sheik, C. S. (2013). The microbiology of deep-sea hydrothermal vent plumes: Ecological and biogeographic linkages to seafloor and water column habitats. *Front. Extreme Microbiol.* 4, 124.

Douville, E., Charlou, J., Oelkers, E., Bienvenu, P., Jove Colon, C., Donval, J., Fouquet, Y., Prieur, D., and Appriou, P. (2002). The rainbow vent fluids (36°14′N, MAR): the influence of ultramafic rocks and phase separation on trace metal content in Mid-Atlantic Ridge hydrothermal fluids. *Chem. Geol.* 184, 37–48.

Van Dover, C. . (2000). *The Ecology of Deep-Sea Hydrothermal Vents.* Princeton: NJ: Princeton University Press.

Dubilier, N., Bergin, C., and Lott, C. (2008). Symbiotic diversity in marine animals: The art of harnessing chemosynthesis. *Nat. Rev. Microbiol.* 6, 725–740.

Duperron, S., Bergin, C., Zielinski, F., Blazejak, A., Pernthaler, A., McKiness, Z. P., DeChaine, E., Cavanaugh, C. M., and Dubilier, N. (2006). A dual symbiosis shared by two mussel species, *Bathymodiolus azoricus* and *Bathymodiolus puteoserpentis* (Bivalvia: Mytilidae), from hydrothermal vents along the northern Mid-Atlantic Ridge. *Environ. Microbiol.* 8, 1441–1447.

Durand, P., Reysenbach, A.-L., Prieur, D., and Pace, N. (1993). Isolation and characterization of *Thiobacillus hydrothermalis* sp. nov., a mesophilic obligately chemolithotrophic bacterium isolated from a deep-sea hydrothermal vent in Fiji Basin. *Arch. Microbiol.* 159, 39–44.

Edwards, K. J., Bach, W., and McCollom, T. M. (2005). Geomicrobiology in oceanography: microbe–mineral interactions at and below the seafloor. *Trends Microbiol.* 13, 449–456.

Ehrich, S., Behrens, D., Lebedeva, E., Ludwig, W., and Bock, E. (1995). A new obligately chemolithoautotrophic, nitrite-oxidizing bacterium,*Nitrospira moscoviensis* sp. nov. and its phylogenetic relationship. *Arch. Microbiol.* 164, 16–23.

Elsaied, H., and Naganuma, T. (2001). Phylogenetic diversity of ribulose-1,5-bisphosphate carboxylase/oxygenase large-subunit genes from deep-sea microorganisms. *Appl. Environ. Microbiol.* 67, 1751–1765.

Emerson, D., Rentz, J. A., Lilburn, T. G., Davis, R. E., Aldrich, H., Chan, C., and Moyer, C. L. (2007). A novel lineage of *Proteobacteria* involved in formation of marine Fe-oxidizing microbial mat communities. *PLoS ONE* 2, e667.

Fiala-Médioni, A., McKiness, Z., Dando, P., Boulegue, J., Mariotti, A., Alayse-Danet, A., Robinson, J., and Cavanaugh, C. (2002). Ultrastructural, biochemical, and

immunological characterization of two populations of the mytilid mussel *Bathymodiolus azoricus* from the Mid-Atlantic Ridge: Evidence for a dual symbiosis. *Mar. Biol.* 141, 1035–1043.

Fisher, A. T., and Becker, K. (2000). Channelized fluid flow in oceanic crust reconciles heat-flow and permeability data. *Nature* 403, 71–74.

Flores, G. E., Shakya, M., Meneghin, J., Yang, Z. K., Seewald, J. S., Geoff Wheat, C., Podar, M., and Reysenbach, A.-L. (2012). Inter-field variability in the microbial communities of hydrothermal vent deposits from a back-arc basin. *Geobiology* 10, 333–346.

Fouquet, Y., Charlou, J.-L., Costa, I., Donval, J.-P., Radford-Knoery, J., Pellé, H., Ondréas, H., Michel, S., and Tivey, M. K. (1994). A detailed study of the Lucky Strike hydrothermal site and dicovery of a new hydrothermal site: Menez Gwen; preliminary results of the DIVA1 crusie. *Inter Ridge News*.

Foustoukos, D. I., and Seyfried, W. E. (2004). Hydrocarbons in Hydrothermal Vent Fluids: The Role of Chromium-Bearing Catalysts. *Science* 304, 1002–1005.

Fuchs, G., and Schlegel, H.-G. (2006). *Allgemeine Mikrobiologie: Begründet von Hans-Günter Schlegel*. Georg Thieme Verlag.

German, C. R., Bowen, A., Coleman, M. L., Honig, D. L., Huber, J. A., Jakuba, M. V., Kinsey, J. C., Kurz, M. D., Leroy, S., McDermott, J. M., *et al.* (2010). Diverse styles of submarine venting on the ultraslow spreading Mid-Cayman Rise. *Proc. Natl. Acad. Sci.* 107, 14020–14025.

German, C. R., and Von Damm, K. L. (2006). "Hydrothermal processes" in *The Oceans and Marine Geochemistry* Treatise on geochemistry., eds. H. Elderfield, H. D. Holland, and K. K. Turekian (Elsevier).

Gilbert, J. A., and Dupont, C. L. (2011). Microbial metagenomics: Beyond the genome. *Annu. Rev. Mar. Sci.* 3, 347–371.

Giovannoni, S. J., Britschgi, T. B., Moyer, C. L., and Field, K. G. (1990). Genetic diversity in Sargasso Sea bacterioplankton. *Nature* 345, 60–63.

Giovannoni, S., and Stingl, U. (2007). The importance of culturing bacterioplankton in the "omics" age. *Nat Rev Micro* 5, 820–826.

Gomez-Pereira, P. R., Fuchs, B. M., Alonso, C., Oliver, M. J., van Beusekom, J. E. E., and Amann, R. (2010). Distinct flavobacterial communities in contrasting water masses of the North Atlantic Ocean. *ISME J* 4, 472–487.

Götz, D., Banta, A., Beveridge, T. J., Rushdi, A. I., Simoneit, B. R. T., and Reysenbach, A. L. (2002). *Persephonella marina* gen. nov., sp. nov. and *Persephonella guaymasensis* sp. nov., two novel, thermophilic, hydrogen-oxidizing microaerophiles from deep-sea hydrothermal vents. *Int. J. Syst. Evol. Microbiol.* 52, 1349–1359.

Gundersen, J. K., Jørgensen, B. B., Larsen, E., and Jannasch, H. W. (1992). Mats of giant sulphur bacteria on deep-sea sediments due to fluctuating hydrothermal flow. *Nature* 360, 454–456.

Hannington, M. D., de Ronde, C. D. J., and Petersen, S. (2005). "Sea-floor tectonics and submarine hydrothermal systems," in *Economic Geology 100th Anniversary Volume*, eds. J. W. Hedenquist, J. F. H. Thompson, R. J. Goldfarb, and J. P. Richards (Littelton, Colorado, USA: Society of Economic Geologists), 111–141

Harmsen, H., Prieur, D., and Jeanthon, C. (1997a). Distribution of microorganisms in deep-sea hydrothermal vent chimneys investigated by whole-cell hybridization and enrichment culture of thermophilic subpopulations. *Appl. Environ. Microbiol.* 63, 2876–2883.

Harmsen, H., Prieur, D., and Jeanthon, C. (1997b). Group-specific 16S rRNA-targeted oligonucleotide probes to identify thermophilic bacteria in marine hydrothermal vents. *Appl. Environ. Microbiol.* 63, 4061–4068.

Harwood, C. S., Jannasch, H. W., and Canale-Parola, E. (1982). Anaerobic spirochete from a deep-sea hydrothermal vent. *Appl. Environ. Microbiol.* 44, 234–237.

Hentscher, M., and Bach, W. (2012). Geochemically induced shifts in catabolic energy yields explain past ecological changes of diffuse vents in the East Pacific Rise 9°50'N area. *Geochem. Trans.* 13, 2.

Hoek, J., Banta, A., Hubler, F., and Reysenbach, A.-L. (2003). Microbial diversity of a sulphide spire located in the Edmond deep-sea hydrothermal vent field on the Central Indian Ridge. *Geobiology* 1, 119–127.

Holland, P. M., Abramson, R. D., Watson, R., and Gelfand, D. H. (1991). Detection of specific polymerase chain reaction product by utilizing the 5'→3' exonuclease activity of *Thermus aquaticus* DNA polymerase. *Proc. Natl. Acad. Sci.* 88, 7276–7280.

Holler, T., Widdel, F., Knittel, K., Amann, R., Kellermann, M. Y., Hinrichs, K.-U., Teske, A., Boetius, A., and Wegener, G. (2011). Thermophilic anaerobic oxidation of methane by marine microbial consortia. *ISME J*. 5, 1946-1956.

Holm, N. G., and Charlou, J. L. (2001). Initial indications of abiotic formation of hydrocarbons in the Rainbow ultramafic hydrothermal system, Mid-Atlantic Ridge. *Earth Planet. Sci. Lett.* 191, 1–8.

Huang, W. E., Stoecker, K., Griffiths, R., Newbold, L., Daims, H., Whiteley, A. S., and Wagner, M. (2007). Raman-FISH: Combining stable-isotope Raman spectroscopy and fluorescence *in situ* hybridization for the single cell analysis of identity and function. *Environ. Microbiol.* 9, 1878–1889.

Huber, H., Burggraf, S., Mayer, T., Wyschkony, I., Rachel, R., and Stetter, K. O. (2000). *Ignicoccus* gen. nov., a novel genus of hyperthermophilic, chemolithoautotrophic *Archaea*, represented by two new species, *Ignicoccus islandicus* sp nov and *Ignicoccus pacificus* sp nov. and *Ignicoccus pacificus* sp. nov. *Int. J. Syst. Evol. Microbiol.* 50, 2093–2100.

Huber, H., Jannasch, H., Rachel, R., Fuchs, T., and Stetter, K. O. (1997). *Archaeoglobus veneficus* sp. nov., a novel facultative chemolithoautotrophic hyperthermophilic sulfite reducer, isolated from abyssal black smokers. *Syst. Appl. Microbiol.* 20, 374–380.

Huber, J. A., Butterfield, D. A., and Baross, J. A. (2003). Bacterial diversity in a subseafloor habitat following a deep-sea volcanic eruption. *FEMS Microbiol. Ecol.* 43, 393–409.

Huber, J. A., Butterfield, D. A., and Baross, J. A. (2002). Temporal changes in archaeal diversity and chemistry in a mid-ocean ridge subseafloor habitat. *Appl Env. Microbiol* 68, 1585–1594.

Huber, J. A., Cantin, H. V., Huse, S. M., Mark Welch, D. B., Sogin, M. L., and Butterfield, D. A. (2010). Isolated communities of *Epsilonproteobacteria* in hydrothermal vent fluids of the Mariana Arc seamounts. *FEMS Microbiol. Ecol.* 73, 538–549.

Huber, J. A., Mark Welch, D. B., Morrison, H. G., Huse, S. M., Neal, P. R., Butterfield, D. A., and Sogin, M. L. (2007). Microbial population structures in the deep marine biosphere. *Science* 318, 97 –100.

Huber, R., Kurr, M., Jannasch, H. W., and Stetter, K. O. (1989). A novel group of abyssal methanogenic archaebacteria (*Methanopyrus*) growing at 110 °C. *Nature* 342, 833–834.

Hugenholtz, P. (2002). Exploring prokaryotic diversity in the genomic era. *Genome Biol.* 3, reviews0003.

Hugenholtz, P., Goebel, B. M., and Pace, N. R. (1998). Impact of culture-independent studies on the emerging phylogenetic view of bacterial diversity. *J. Bacteriol.* 180, 4765–4774.

Hügler, M., and Sievert, S. M. (2011). Beyond the Calvin cycle: Autotrophic carbon fixation in the ocean. *Annu. Rev. Mar. Sci.* 3, 261–289.

Humphris, S., and McCollom, T. M. (1998). The cauldron beneath the seafloor - Percolating through volcanic subsurface rocks, seawater is chemically transformed into hydrothermal fluid. *Oceanus* 41.

Inagaki, F., Takai, K., Kobayashi, H., Nealson, K. H., and Horikoshi, K. (2003). *Sulfurimonas autotrophica* gen. nov., sp. nov., a novel sulfur-oxidizing ε-proteobacterium isolated from hydrothermal sediments in the Mid-Okinawa Trough. *Int. J. Syst. Evol. Microbiol.* 53, 1801–1805.

Inagaki, F., Takai, K., Nealson, K. H., and Horikoshi, K. (2004). *Sulfurovum lithotrophicum* gen. nov., sp. nov., a novel sulfur-oxidizing chemolithoautotroph within the ε-*Proteobacteria* isolated from Okinawa Trough hydrothermal sediments. *Int. J. Syst. Evol. Microbiol.* 54, 1477–1482.

Ishibashi, J.-I., Urabe, T., and Taylor, B. (1995). "Hydrothermal activity related to arc-backarc magmatism in the western Pacific," in *Backarc Basins: Tectonics and Magmatism* (New York, N.Y.: Plenum).

Ishoey, T., Woyke, T., Stepanauskas, R., Novotny, M., and Lasken, R. S. (2008). Genomic sequencing of single microbial cells from environmental samples. *Curr. Opin. Microbiol.* 11, 198–204.

Jannasch, H. W. (1995). "Microbial Interactions with Hydrothermal Fluids," in *Seafloor hydrothermal systems: Physical, chemical, biological, and geological interactions*, eds. S. E. Humphris, R. A. Zierenberg, L. S. Mullineaux, and R. E. Thomson (American Geophysical Union), 273–296.

Jannasch, H. W., Nelson, D. C., and Wirsen, C. O. (1989). Massive natural occurrence of unusually large bacteria (*Beggiatoa* sp.) at a hydrothermal deep-sea vent site. *Nature* 342, 834–836.

Jannasch, H. W., and Wirsen, C. O. (1979). Chemosynthetic primary production at East Pacific sea floor spreading centers. *BioScience* 29, 592–598.

Jannasch, H. W., and Wirsen, C. O. (1981). Morphological survey of microbial mats near deep-sea thermal vents. *Appl. Environ. Microbiol.* 41, 528–538.

Jannasch, H. W., Wirsen, C. O., Nelson, D. C., and Robertson, L. A. (1985). *Thiomicrospira crunogena* sp. nov., a colorless, sulfur-oxidizing bacterium from a deep-sea hydrothermal vent. *Int. J. Syst. Bacteriol.* 35, 422–424.

Jeanthon, C., L'Haridon, S., Cueff, V., Banta, A., Reysenbach, A.-L., and Prieur, D. (2002). *Thermodesulfobacterium hydrogeniphilum* sp. nov., a thermophilic, chemolithoautotrophic, sulfate-reducing bacterium isolated from a deep-sea hydrothermal vent at Guaymas Basin, and emendation of the genus *Thermodesulfobacterium*. *Int. J. Syst. Evol. Microbiol.* 52, 765–772.

Jeanthon, C., and Prieur, D. (1990). Susceptibility to heavy metals and characterization of heterotrophic bacteria isolated from two hydrothermal vent polychaete annelids, *Alvinella pompejana* and *Alvinella caudata*. *Appl. Environ. Microbiol.* 56, 3308–3314.

Jensen, M. M., Kuypers, M. M. M., Lavik, G., and Thamdrup, B. (2008). Rates and regulation of anaerobic ammonium oxidation and denitrification in the Black Sea. *Limnol. Ocean.* 53, 23–36.

Jogler, C., Wanner, G., Kolinko, S., Niebler, M., Amann, R., Petersen, N., Kube, M., Reinhardt, R., and Schüler, D. (2011). Conservation of proteobacterial magnetosome genes and structures in an uncultivated member of the deep-branching *Nitrospira* phylum. *Proc. Natl. Acad. Sci.* 108, 1134 –1139.

Jones, W. J., Leigh, J. A., Mayer, F., Woese, C. R., and Wolfe, R. S. (1983). *Methanococcus jannaschii* sp. nov., an extremely thermophilic methanogen from a submarine hydrothermal vent. *Arch. Microbiol.* 136, 254–261.

Jørgensen, B. B., and Boetius, A. (2007). Feast and famine - Microbial life in the deep-sea bed. *Nat Rev Micro* 5, 770–781.

Jørgensen, B. B., Zawacki, L. X., and Jannasch, H. W. (1990). Thermophilic bacterial sulfate reduction in deep-sea sediments at the Guaymas Basin hydrothermal vent site (Gulf of California). *Deep Sea Res. Part Ocean. Res. Pap.* 37, 695–710.

Joye, S. B., and Hollibaugh, J. T. (1995). Influence of sulfide inhibition of nitrification on nitrogen regeneration in sediments. *Science* 270, 623–625.

Juniper, S. K., and Tunnicliffe, V. (1997). Crustal accretion and the hot vent ecosystem. *Philos. Trans. R. Soc. Lond. Ser. Math. Phys. Eng. Sci.* 355, 459–474.

Karl, D. M. (1995). "Ecology of free-living, hydrothermal vent microbial communities," in *Microbiology of Deep-Sea Hydrothermal Vents*, ed. D. M. Karl (CRC Press).

Karl, D. M., Brittain, A. M., and Tilbrook, B. D. (1989). Hydrothermal and microbial processes at Loihi Seamount, a mid-plate hot-spot volcano. *Deep Sea Res. Part Ocean. Res. Pap.* 36, 1655–1673.

Kashefi, K., and Lovley, D. R. (2003). Extending the upper temperature limit for life. *Science* 301, 934–934.

Kato, S., Kobayashi, C., Kakegawa, T., and Yamagishi, A. (2009). Microbial communities in iron-silica-rich microbial mats at deep-sea hydrothermal fields of the Southern Mariana Trough. *Environ. Microbiol.* 11, 2094–2111.

Kato, S., Yamanaka, T., and Yamagishi, A. (2013). Characteristics of microbial communities in crustal fluids in a deep-sea hydrothermal field of the Suiyo Seamount. *Front. Extreme Microbiol.* 4, 85.

Kelley, D. S., Karson, J. A., Blackman, D. K., Früh-Green, G. L., Butterfield, D. A., Lilley, M. D., Olson, E. J., Schrenk, M. O., Roe, K. K., Lebon, G. T., *et al.* (2001). An off-axis hydrothermal vent field near the Mid-Atlantic Ridge at 30° N. *Nature* 412, 145–149.

Kelley, D. S., Baross, J. A., and Delaney, J. R. (2002). Volcanoes, Fluids, and Life at Mid-Ocean Ridge Spreading Centers. *Annu. Rev. Earth Planet. Sci.* 30, 385–491.

Kirchman, D. L., and Wheeler, P. A. (1998). Uptake of ammonium and nitrate by heterotrophic bacteria and phytoplankton in the sub-Arctic Pacific. *Deep Sea Res. Part Ocean. Res. Pap.* 45, 347–365.

Klein, D. (2002). Quantification using real-time PCR technology: applications and limitations. *Trends Mol. Med.* 8, 257–260.

Knittel, K., and Boetius, A. (2009). Anaerobic oxidation of methane: Progress with an unknown process. *Annu. Rev. Microbiol.* 63, 311–334.

Konn, C., Charlou, J. L., Donval, J. P., Holm, N. G., Dehairs, F., and Bouillon, S. (2009). Hydrocarbons and oxidized organic compounds in hydrothermal fluids from Rainbow and Lost City ultramafic-hosted vents. *Chem. Geol.* 258, 299–314.

Könneke, M., Bernhard, A. E., de la Torre, J. R., Walker, C. B., Waterbury, J. B., and Stahl, D. A. (2005). Isolation of an autotrophic ammonia-oxidizing marine archaeon. *Nature* 437, 543–546.

Kubista, M., Andrade, J. M., Bengtsson, M., Forootan, A., Jonák, J., Lind, K., Sindelka, R., Sjöback, R., Sjögreen, B., Strömbom, L., *et al.* (2006). The real-time polymerase chain reaction. *Mol. Aspects Med.* 27, 95–125.

Kurr, M., Huber, R., König, H., Jannasch, H. W., Fricke, H., Trincone, A., Kristjansson, J. K., and Stetter, K. O. (1991). *Methanopyrus kandleri*, gen. and sp. nov. represents a novel group of hyperthermophilic methanogens, growing at 110°C. *Arch. Microbiol.* 156, 239–247.

L'Haridon, S., Cilia, V., Messner, P., Raguénès, G., Gambacorta, A., Sleytr, U. B., Prieur, D., and Jeanthon, C. (1998). *Desulfurobacterium thermolithotrophum* gen. nov., sp. nov., a novel autotrophic, sulphur-reducing bacterium isolated from a deep-sea hydrothermal vent. *Int. J. Syst. Bacteriol.* 48, 701–711.

L'Haridon, S., Reysenbach, A.-L., Tindall, B. J., Schönheit, P., Banta, A., Johnsen, U., Schumann, P., Gambacorta, A., Stackebrandt, E., and Jeanthon, C. (2006). *Desulfurobacterium atlanticum* sp. nov., *Desulfurobacterium pacificum* sp. nov. and *Thermovibrio guaymasensis* sp. nov., three thermophilic members of the *Desulfurobacteriaceae* fam. nov., a deep branching lineage within the *Bacteria*. *Int. J. Syst. Evol. Microbiol.* 56, 2843–2852.

Lam, P., Cowen, J. P., and Jones, R. D. (2004). Autotrophic ammonia oxidation in a deep-sea hydrothermal plume. *FEMS Microbiol. Ecol.* 47, 191–206.

Lam, P., Cowen, J. P., Popp, B. N., and Jones, R. D. (2008). Microbial ammonia oxidation and enhanced nitrogen cycling in the Endeavour hydrothermal plume. *Geochim. Cosmochim. Acta* 72, 2268–2286.

Lam, P., Jensen, M. M., Lavik, G., McGinnis, D. F., Müller, B., Schubert, C. J., Amann, R., Thamdrup, B., and Kuypers, M. M. M. (2007). Linking crenarchaeal and bacterial nitrification to anammox in the Black Sea. *Proc. Natl. Acad. Sci.* 104, 7104–7109.

Lam, P., Lavik, G., Jensen, M. M., van de Vossenberg, J., Schmid, M., Woebken, D., Gutierrez, D., Amann, R., Jetten, M. S. M., and Kuypers, M. M. M. (2009). Revising the nitrogen cycle in the Peruvian oxygen minimum zone. *Proc. Natl. Acad. Sci.* 106, 4752–4757.

Lane, D. J., Pace, B., Olsen, G. J., Stahl, D. A., Sogin, M. L., and Pace, N. R. (1985). Rapid determination of 16S ribosomal RNA sequences for phylogenetic analyses. *Proc. Natl. Acad. Sci.* 82, 6955–6959.

Lang, S. Q., Butterfield, D. A., Lilley, M. D., Paul Johnson, H., and Hedges, J. I. (2006). Dissolved organic carbon in ridge-axis and ridge-flank hydrothermal systems. *Geochim. Cosmochim. Acta* 70, 3830–3842.

Lang, S. Q., Butterfield, D. A., Schulte, M., Kelley, D. S., and Lilley, M. D. (2010). Elevated concentrations of formate, acetate and dissolved organic carbon found at the Lost City hydrothermal field. *Geochim. Cosmochim. Acta* 74, 941–952.

Lasken, R. S. (2012). Genomic sequencing of uncultured microorganisms from single cells. *Nat. Rev. Microbiol.* 10, 631–640.

Lasken, R. S. (2007). Single-cell genomic sequencing using multiple displacement amplification. *Curr. Opin. Microbiol.* 10, 510–516.

Lasken, R., and Stockwell, T. (2007). Mechanism of chimera formation during the multiple displacement amplification reaction. *BMC Biotechnol.* 7, 19.

Lee, N., Nielsen, P. H., Andreasen, K. H., Juretschko, S., Nielsen, J. L., Schleifer, K.-H., and Wagner, M. (1999). Combination of fluorescent *in situ* hybridization and microautoradiography - a new tool for structure-function analyses in microbial ecology. *Appl Env. Microbiol* 65, 1289–1297.

Lever, M., Heuer, V., Morono, Y., Masui, N., Schmidt, F., Alperin, M., Inagaki, F., Hinrichs, K.-U., and Teske, A. (2010). Acetogenesis in deep subseafloor sediments of the Juan de Fuca Ridge flank: A synthesis of geochemical, thermodynamic, and gene-based evidence. *Geomicrobiol. J.* 27, 183–211.

Li, M., Jain, S., Baker, B. J., Taylor, C., and Dick, G. J. (2013). Novel hydrocarbon monooxygenase genes in the metatranscriptome of a natural deep-sea hydrocarbon plume. *Environ. Microbiol.*, n/a–n/a.

Li, T., Wu, T.-D., Mazéas, L., Toffin, L., Guerquin-Kern, J.-L., Leblon, G., and Bouchez, T. (2008). Simultaneous analysis of microbial identity and function using NanoSIMS. *Environ. Microbiol.* 10, 580–588.

Lilley, M. D., Butterfield, D. A., Olson, E. J., Lupton, J. E., Macko, S. A., and McDuff, R. E. (1993). Anomalous CH_4 and NH_4^+ concentrations at an unsedimented mid-ocean-ridge hydrothermal system. *Nature* 364, 45–47.

Little, C. T. S., Danelian, T., Herrington, R. J., and Haymon, R. M. (2004). Early Jurassic hydrothermal vent community from the Franciscan complex, California. *J. Paleontol.* 78, 542–559.

Longnecker, K., and Reysenbach, A.-L. (2001). Expansion of the geographic distribution of a novel lineage of ε-Proteobacteria to a hydrothermal vent site on the Southern East Pacific Rise. *FEMS Microbiol. Ecol.* 35, 287–293.

Lonsdale, P. (1977). Clustering of suspension-feeding macrobenthos near abyssal hydrothermal vents at oceanic spreading centers. *Deep Sea Res.* 24, 857–863.

Lonsdale, P. F., Bischoff, J. L., Burns, V. M., Kastner, M., and Sweeney, R. E. (1980). A high-temperature hydrothermal deposit on the seabed at a gulf of California spreading center. *Earth Planet. Sci. Lett.* 49, 8–20.

López-García, P., Duperron, S., Philippot, P., Foriel, J., Susini, J., and Moreira, D. (2003). Bacterial diversity in hydrothermal sediment and epsilonproteobacterial dominance in experimental microcolonizers at the Mid-Atlantic Ridge. *Environ. Microbiol.* 5, 961–976.

Lupton, J. E., and Craig, H. (1981). A Major Helium-3 Source at 15°S on the East Pacific Rise. *Science* 214, 13–18.

Madigan, M. T., Martinko, J. M., Stahl, D. A., and Clark, D. P. (2010). *Brock biology of microorganisms*. 13th ed. San Francisco: Prentice Hall.

Magenheim, A. J., and Gieskes, J. M. (1992). Hydrothermal discharge and alteration in near-surface sediments from the Guaymas Basin, Gulf of California. *Geochim. Cosmochim. Acta* 56, 2329–2338.

Makita, H., Nakagawa, S., Miyazaki, M., Nakamura, K., Inagaki, F., and Takai, K. (2012). *Thiofractor thiocaminus* gen. nov., sp. nov., a novel hydrogen-oxidizing, sulfur-reducing epsilonproteobacterium isolated from a deep-sea hydrothermal vent chimney in the Nikko Seamount field of the northern Mariana Arc. *Arch. Microbiol.* 194, 785–794.

Mandernack, K. W., and Tebo, B. M. (1993). Manganese scavenging and oxidation at hydrothermal vents and in vent plumes. *Geochim. Cosmochim. Acta* 57, 3907–3923.

Manefield, M., Whiteley, A. S., Griffiths, R. I., and Bailey, M. J. (2002). RNA stable isotope probing, a novel means of linking microbial community function to phylogeny. *Appl. Environ. Microbiol.* 68, 5367–5373.

Marcon, Y., Sahling, H., Borowski, C., dos Santos Ferreira, C., Thal, J., and Bohrmann, G. (2013). Megafaunal distribution and assessment of total methane and sulfide consumption by mussel beds at Menez Gwen hydrothermal vent, based on geo-referenced photomosaics. *Deep Sea Res. Part Ocean. Res. Pap.* 75, 93–109.

Marcy, Y., Ishoey, T., Lasken, R. S., Stockwell, T. B., Walenz, B. P., Halpern, A. L., Beeson, K. Y., Goldberg, S. M. D., and Quake, S. R. (2007a). Nanoliter reactors improve multiple displacement amplification of genomes from single cells. *PLoS Genet* 3, e155.

Marcy, Y., Ouverney, C., Bik, E. M., Lösekann, T., Ivanova, N., Martin, H. G., Szeto, E., Platt, D., Hugenholtz, P., Relman, D. A., *et al.* (2007b). Dissecting biological "dark matter" with single-cell genetic analysis of rare and uncultivated TM7 microbes from the human mouth. *Proc. Natl. Acad. Sci.* 104, 11889–11894.

Marteinsson, V., Birrien, J.-L., Kristjánsson, J. K., and Prieur, D. (1995). First isolation of thermophilic aerobic non-sporulating heterotrophic bacteria from deep-sea hydrothermal vents. *FEMS Microbiol. Ecol.* 18, 163–174.

Marteinsson, V. T., Birrien, J.-L., Raguénès, G., Costa, M. S. da, and Prieur, D. (1999). Isolation and characterization of *Thermus thermophilus* Gy1211 from a deep-sea hydrothermal vent. *Extremophiles* 3, 247–251.

Marteinsson, V. T., Bjornsdottir, S. H., Bienvenu, N., Kristjansson, J. K., and Birrien, J.-L. (2010). *Rhodothermus profundi* sp. nov., a thermophilic bacterium isolated from a deep-sea hydrothermal vent in the Pacific Ocean. *Int. J. Syst. Evol. Microbiol.* 60, 2729–2734.

Martens, C. S. (1990). Generation of short chain acid anions in hydrothermally altered sediments of the Guaymas Basin, Gulf of California. *Appl. Geochem.* 5, 71–76.

Martens-Habbena, W., Berube, P. M., Urakawa, H., de la Torre, J. R., and Stahl, D. A. (2009). Ammonia oxidation kinetics determine niche separation of nitrifying *Archaea* and *Bacteria*. *Nature* 461, 976–979.

Martinez, F., Okino, K., Ohara, Y., Reysenbach, A.-L., and Goffredi, S. (2007). Back-arc basins. *Oceanography* 20, 116–127.

Martinez, F., and Taylor, B. (1996). Backarc spreading, rifting, and microplate rotation, between transform faults in the Manus Basin. *Mar. Geophys. Res.* 18, 203–224.

Martinez-Garcia, M., Swan, B. K., Poulton, N. J., Gomez, M. L., Masland, D., Sieracki, M. E., and Stepanauskas, R. (2012). High-throughput single-cell sequencing identifies photoheterotrophs and chemoautotrophs in freshwater bacterioplankton. *ISME J.* 6, 113–123.

McCollom, T. M. (2000). Geochemical constraints on primary productivity in submarine hydrothermal vent plumes. *Deep Sea Res. Part Ocean. Res. Pap.* 47, 85–101.

McCollom, T. M., and Seewald, J. S. (2007). Abiotic Synthesis of Organic Compounds in Deep-Sea Hydrothermal Environments. *Chem. Rev.* 107, 382–401.

McHatton, S. C., Barry, J. P., Jannasch, H. W., and Nelson, D. C. (1996). High nitrate concentrations in vacuolate, autotrophic marine *Beggiatoa* spp. *Appl. Environ. Microbiol.* 62, 954–958.

Mikucki, J. A., Pearson, A., Johnston, D. T., Turchyn, A. V., Farquhar, J., Schrag, D. P., Anbar, A. D., Priscu, J. C., and Lee, P. A. (2009). A contemporary microbially maintained subglacial ferrous "Ocean." *Science* 324, 397–400.

Miroshnichenko, M. L., Slobodkin, A. I., Kostrikina, N. A., L'Haridon, S., Nercessian, O., Spring, S., Stackebrandt, E., Bonch-Osmolovskaya, E. A., and Jeanthon, C. (2003). *Deferribacter abyssi* sp. nov., an anaerobic thermophile from deep-sea hydrothermal vents of the Mid-Atlantic Ridge. *Int. J. Syst. Evol. Microbiol.* 53, 1637–1641.

Mizrahi-Man, O., Davenport, E. R., and Gilad, Y. (2013). Taxonomic classification of bacterial 16S rRNA genes using short sequencing reads: Evaluation of effective study designs. *PLoS ONE* 8, e53608.

Moss, R., and Scott, S. D. (2001). Geochemistry and mineralogy of gold-rich hydrothermal precipitates from the Eastern Manus Basin, Papua New Guinea. *Can. Miner.* 39, 957–978.

Moussard, H., Corre, E., Cambon-Bonavita, M.-A., Fouquet, Y., and Jeanthon, C. (2006). Novel uncultured *Epsilonproteobacteria* dominate a filamentous sulphur mat from the 13°N hydrothermal vent field, East Pacific Rise. *FEMS Microbiol. Ecol.* 58, 449–463.

Moyer, C. L., Dobbs, F. C., and Karl, D. M. (1994). Estimation of diversity and community structure through restriction fragment length polymorphism distribution analysis of bacterial 16S rRNA genes from a microbial mat at an active, hydrothermal vent system, Loihi Seamount, Hawaii. *Appl. Environ. Microbiol.* 60, 871–879.

Moyer, C. L., Dobbs, F. C., and Karl, D. M. (1995). Phylogenetic diversity of the bacterial community from a microbial mat at an active, hydrothermal vent system, Loihi Seamount, Hawaii. *Appl. Environ. Microbiol.* 61, 1555–1562.

Moyer, C. L., Tiedje, J. M., Dobbs, F. C., and Karl, D. M. (1998). Diversity of deep-sea hydrothermal vent *Archaea* from Loihi Seamount, Hawaii. *Deep Sea Res. Part II Top. Stud. Ocean.* 45, 303–317.

Musat, N., Foster, R., Vagner, T., Adam, B., and Kuypers, M. M. M. (2012). Detecting metabolic activities in single cells, with emphasis on nanoSIMS. *FEMS Microbiol. Rev.* 26, 486–511.

Musat, N., Halm, H., Winterholler, B., Hoppe, P., Peduzzi, S., Hillion, F., Horreard, F., Amann, R., Jørgensen, B. B., and Kuypers, M. M. M. (2008). A single-cell view on the ecophysiology of anaerobic phototrophic bacteria. *Proc. Natl. Acad. Sci.* 105, 17861 –17866.

Muyzer, G., Brinkhoff, T., Nübel, U., Santegoeds, C., Schäfer, H., and Wawer, C. (1998). "Denaturing gradient gel electrophoresis (DGGE) in microbial ecology," in *Molecular microbial ecology manual* (Kluwer Academic Publishers), 3.4.4/1–3.4.4/27.

Nakagawa, S., Inagaki, F., Takai, K., Horikoshi, K., and Sako, Y. (2005a). *Thioreductor micantisoli* gen. nov., sp. nov., a novel mesophilic, sulfur-reducing chemolithoautotroph within the *ε-Proteobacteria* isolated from hydrothermal sediments in the Mid-Okinawa Trough. *Int. J. Syst. Evol. Microbiol.* 55, 599–605.

Nakagawa, S., and Takai, K. (2008). Deep-sea vent chemoautotrophs: diversity, biochemistry and ecological significance. *FEMS Microbiol. Ecol.* 65, 1–14.

Nakagawa, S., Takai, K., Inagaki, F., Chiba, H., Ishibashi, J., Kataoka, S., Hirayama, H., Nunoura, T., Horikoshi, K., and Sako, Y. (2005b). Variability in microbial community and venting chemistry in a sediment-hosted backarc hydrothermal system: Impacts of subseafloor phase-separation. *FEMS Microbiol. Ecol.* 54, 141–155.

Nakagawa, S., Takai, K., Inagaki, F., Horikoshi, K., and Sako, Y. (2005c). *Nitratiruptor tergarcus* gen. nov., sp. nov. and *Nitratifractor salsuginis* gen. nov., sp. nov., nitrate-reducing chemolithoautotrophs of the *ε-Proteobacteria* isolated from a deep-sea hydrothermal system in the Mid-Okinawa Trough. *Int. J. Syst. Evol. Microbiol.* 55, 925–933.

Nealson, K. H., Inagaki, F., and Takai, K. (2005). Hydrogen-driven subsurface lithoautotrophic microbial ecosystems (SLiMEs): Do they exist and why should we care? *Trends Microbiol.* 13, 405–410.

Nelson, D. C., Wirsen, C. O., and Jannasch, H. W. (1989). Characterization of large, autotrophic *Beggiatoa* spp. abundant at hydrothermal vents of the Guaymas Basin. *Appl. Environ. Microbiol.* 55, 2909–2917.

Nercessian, O., Reysenbach, A.-L., Prieur, D., and Jeanthon, C. (2003). Archaeal diversity associated with in situ samplers deployed on hydrothermal vents on the East Pacific Rise (13°N). *Environ. Microbiol.* 5, 492–502.

Nunoura, T., Oida, H., Nakaseama, M., Kosaka, A., Ohkubo, S. B., Kikuchi, T., Kazama, H., Hosoi-Tanabe, S., Nakamura, K., Kinoshita, M., *et al.* (2010). Archaeal diversity and distribution along thermal and geochemical gradients in hydrothermal sediments at the Yonaguni Knoll IV hydrothermal field in the Southern Okinawa Trough. *Appl Env. Microbiol* 76, 1198–1211.

Ohno, M., Shiratori, H., Park, M. J., Saitoh, Y., Kumon, Y., Yamashita, N., Hirata, A., Nishida, H., Ueda, K., and Beppu, T. (2000). *Symbiobacterium thermophilum* gen. nov., sp. nov., a symbiotic thermophile that depends on co-culture with a *Bacillus* strain for growth. *Int. J. Syst. Evol. Microbiol.* 50, 1829–1832.

Op den Camp, H. J. M., Jetten, M. S. M., and Strous, M. (2007). "Anammox," in *Biology of the Nitrogen Cycle*, eds. H. Bothe, S. Ferguson, and W. E. Newton (Elsevier).

Ouverney, C. C., and Fuhrman, J. A. (1999). Combined microautoradiography-16S rRNA probe technique for determination of radioisotope uptake by specific microbial cell types *in situ*. *Appl Env. Microbiol* 65, 1746–1752.

Pagani, I., Liolios, K., Jansson, J., Chen, I.-M. A., Smirnova, T., Nosrat, B., Markowitz, V. M., and Kyrpides, N. C. (2011). The Genomes OnLine Database (GOLD) v.4: status

of genomic and metagenomic projects and their associated metadata. *Nucleic Acids Res.* 40, D571–D579.

Parson, L., Gràcia, E., Coller, D., German, C., and Needham, D. (2000). Second-order segmentation; the relationship between volcanism and tectonism at the MAR, 38°N–35°40′N. *Earth Planet. Sci. Lett.* 178, 231–251.

Paull, C. K., Hecker, B., Commeau, R., Freeman-Lynde, R. P., Neumann, C., Corso, W. P., Golubic, S., Hook, J. E., Sikes, E., and Curray, J. (1984). Biological communities at the Florida escarpment resemble hydrothermal vent taxa. *Science* 226, 965–967.

Pérez-Rodríguez, I., Ricci, J., Voordeckers, J. W., Starovoytov, V., and Vetriani, C. (2010). *Nautilia nitratireducens* sp. nov., a thermophilic, anaerobic, chemosynthetic, nitrate-ammonifying bacterium isolated from a deep-sea hydrothermal vent. *Int. J. Syst. Evol. Microbiol.* 60, 1182–1186.

Perner, M., Gonnella, G., Hourdez, S., Böhnke, S., Kurtz, S., and Girguis, P. (2013). *In situ* chemistry and microbial community compositions in five deep-sea hydrothermal fluid samples from Irina II in the Logatchev field. *Environ. Microbiol.* 15, 1551–1560.

Perner, M., Petersen, J. M., Zielinski, F., Gennerich, H.-H., and Seifert, R. (2010). Geochemical constraints on the diversity and activity of H_2-oxidizing microorganisms in diffuse hydrothermal fluids from a basalt- and an ultramafic-hosted vent. *FEMS Microbiol. Ecol.* 74, 55–71.

Pernthaler, A., Pernthaler, J., and Amann, R. (2002). Fluorescence *in situ* hybridization and catalyzed reporter deposition for the identification of marine bacteria. *Appl. Environ. Microbiol.* 68, 3094–3101.

Pernthaler, J., Pernthaler, A., and Amann, R. (2003). Automated enumeration of groups of marine picoplankton after fluorescence *in situ* hybridization. *Appl. Environ. Microbiol.* 69, 2631–2637.

Petersen, J. M., Zielinski, F. U., Pape, T., Seifert, R., Moraru, C., Amann, R., Hourdez, S., Girguis, P. R., Wankel, S. D., Barbe, V., *et al.* (2011). Hydrogen is an energy source for hydrothermal vent symbioses. *Nature* 476, 176–180.

Pimenov, N. V., Kalyuzhnaya, M. G., Khmelenina, V. N., Mityushina, L. L., and Trotsenko, Y. A. (2002). Utilization of methane and carbon dioxide by symbiotrophic bacteria in gills of *Mytilidae* (*Bathymodiolus*) from the Rainbow and Logachev hydrothermal fields on the Mid-Atlantic Ridge. *Microbiology* 71, 587–594.

Preisler, A., de Beer, D., Lichtschlag, A., Lavik, G., Boetius, A., and Jørgensen, B. B. (2007). Biological and chemical sulfide oxidation in a *Beggiatoa* inhabited marine sediment. *ISME J.* 1, 341.

Prokopenko, M. G., Hammond, D. E., Berelson, W. M., Bernhard, J. M., Stott, L., and Douglas, R. (2006). Nitrogen cycling in the sediments of Santa Barbara basin and Eastern Subtropical North Pacific: Nitrogen isotopes, diagenesis and possible chemosymbiosis between two lithotrophs (*Thioploca* and Anammox)--"riding on a glider." *Earth Planet. Sci. Lett.* 242, 186–204.

Prokopenko, M. G., Hirst, M. B., De Brabandere, L., Lawrence, D. J. P., Berelson, W. M., Granger, J., Chang, B. X., Dawson, S., Crane Iii, E. J., Chong, L., *et al.* (2013). Nitrogen losses in anoxic marine sediments driven by *Thioploca*-anammox bacterial consortia. *Nature* 500, 194–198.

Proskurowski, G., Lilley, M. D., Kelley, D. S., and Olson, E. J. (2006). Low temperature volatile production at the Lost City hydrothermal field, evidence from a hydrogen stable isotope geothermometer. *Chem. Geol.* 229, 331–343.

Proskurowski, G., Lilley, M. D., Seewald, J. S., Früh-Green, G. L., Olson, E. J., Lupton, J. E., Sylva, S. P., and Kelley, D. S. (2008). Abiogenic hydrocarbon production at Lost City hydrothermal field. *Science* 319, 604–607.

Radajewski, S., Ineson, P., Parekh, N. R., and Murrell, J. C. (2000). Stable-isotope probing as a tool in microbial ecology. *Nature* 403, 646–649.

Raguénès, G., Pignet, P., Gauthier, G., Peres, A., Christen, R., Rougeaux, H., Barbier, G., and Guezennec, J. (1996). Description of a new polymer-secreting bacterium from a deep-sea hydrothermal vent, *Alteromonas macleodii* subsp. *fijiensis*, and preliminary characterization of the polymer. *Appl. Environ. Microbiol.* 62, 67–73.

Ramirez-Llodra, E., Shank, T., and German, C. (2007). Biodiversity and biogeography of hydrothermal vent species: thirty years of discovery and investigations. *Oceanography* 20, 30–41.

Rappé, M. S., Connon, S. A., Vergin, K. L., and Giovannoni, S. J. (2002). Cultivation of the ubiquitous SAR11 marine bacterioplankton clade. *Nature* 418, 630–633.

Reeburgh, W. S. (1983). Rates of biogeochemical processes in anoxic sediments. *Annu. Rev. Earth Planet. Sci.* 11, 269–298.

Reeves, E. P., Seewald, J. S., Saccocia, P., Bach, W., Craddock, P. R., Shanks, W. C., Sylva, S. P., Walsh, E., Pichler, T., and Rosner, M. (2011). Geochemistry of hydrothermal fluids from the PACMANUS, Northeast Pual and Vienna Woods hydrothermal fields, Manus Basin, Papua New Guinea. *Geochim. Cosmochim. Acta* 75, 1088–1123.

Reysenbach, A.-L., Longnecker, K., and Kirshtein, J. (2000). Novel bacterial and archaeal lineages from an *in situ* growth chamber deployed at a Mid-Atlantic Ridge hydrothermal vent. *Appl. Environ. Microbiol.* 66, 3798–3806.

Reysenbach, A.-L., and Shock, E. (2002). Merging genomes with geochemistry in hydrothermal ecosystems. *Science* 296, 1077–1082.

Rinke, C., Schwientek, P., Sczyrba, A., Ivanova, N. N., Anderson, I. J., Cheng, J.-F., Darling, A., Malfatti, S., Swan, B. K., Gies, E. A., *et al.* (2013). Insights into the phylogeny and coding potential of microbial dark matter. *Nature* 499, 431–437.

Riou, V., Duperron, S., Halary, S., Dehairs, F., Bouillon, S., Martins, I., Colaço, A., and Serrão Santos, R. (2010). Variation in physiological indicators in *Bathymodiolus azoricus* (Bivalvia: Mytilidae) at the Menez Gwen Mid-Atlantic Ridge deep-sea hydrothermal vent site within a year. *Mar. Environ. Res.* 70, 264–271.

Ruby, E. G., and Jannasch, H. W. (1982). Physiological characteristics of *Thiomicrospira* sp. Strain L-12 isolated from deep-sea hydrothermal vents. *J. Bacteriol.* 149, 161–165.

Russ, L., Kartal, B., Camp, H. J. M. op den, Sollai, M., Godfroy, A., Damsté, J. S. S., and Jetten, M. S. M. (2013). Presence and diversity of anammox bacteria in cold hydrocarbon-rich seeps and hydrothermal vent sediments of the Guaymas Basin. *Front. Extreme Microbiol.* 4, 219.

Saiki, R. K., Gelfand, D. H., Stoffel, S., Scharf, S. J., Higuchi, R., Horn, G. T., Mullis, K. B., and Erlich, H. A. (1988). Primer-directed enzymatic amplification of DNA with a thermostable DNA polymerase. *Science* 239, 487–491.

Sako, Y., Nakagawa, S., Takai, K., and Horikoshi, K. (2003). *Marinithermus hydrothermalis* gen. nov., sp. nov., a strictly aerobic, thermophilic bacterium from a deep-sea hydrothermal vent chimney. *Int. J. Syst. Evol. Microbiol.* 53, 59–65.

Salman, V., Amann, R., Girnth, A.-C., Polerecky, L., Bailey, J. V., Høgslund, S., Jessen, G., Pantoja, S., and Schulz-Vogt, H. N. (2011). A single-cell sequencing approach to the classification of large, vacuolated sulfur bacteria. *Syst. Appl. Microbiol.* 34, 243–259.

Schauer, R., Røy, H., Augustin, N., Gennerich, H., Peters, M., Wenzhoefer, F., Amann, R., and Meyerdierks, A. (2011). Bacterial sulfur cycling shapes microbial communities in surface sediments of an ultramafic hydrothermal vent field. *Environ. Microbiol.* 13, 2633–2648.

Schönhuber, W., Fuchs, B., Juretschko, S., and Amann, R. (1997). Improved sensitivity of whole-cell hybridization by the combination of horseradish peroxidase-labeled

oligonucleotides and tyramide signal amplification. *Appl. Environ. Microbiol.* 63, 3268–3273.

Schrenk, M. O., Holden, J. F., and Baross, J. A. (2008). "Networks in the context of sulfide hosted microbial ecosystems," in *Magma to Microbe: Modeling Hydrothermal Processes at Ocean Spreading Centers*, eds. R. P. Lowell, J. S. Seewald, A. Metaxas, and M. R. Perfit (American Geophysical Union), 233–258

Schrenk, M. O., Kelley, D. S., Delaney, J. R., and Baross, J. A. (2003). Incidence and diversity of microorganisms within the walls of an active deep-sea sulfide chimney. *Appl. Environ. Microbiol.* 69, 3580–3592.

Sheik, C. S., Jain, S., and Dick, G. J. (2013). Metabolic flexibility of enigmatic SAR324 revealed through metagenomics and metatranscriptomics. *Environ. Microbiol.*, n/a–n/a.

Sherwood Lollar, B., Frape, S. K., Weise, S. M., Fritz, P., Macko, S. A., and Welhan, J. A. (1993). Abiogenic methanogenesis in crystalline rocks. *Geochim. Cosmochim. Acta* 57, 5087–5097.

Sherwood Lollar, B., Westgate, T. D., Ward, J. A., Slater, G. F., and Lacrampe-Couloume, G. (2002). Abiogenic formation of alkanes in the Earth's crust as a minor source for global hydrocarbon reservoirs. *Nature* 416, 522–524.

Shock, E. L. (1992). Chapter 5 Chemical environments of submarine hydrothermal systems. *Orig. Life Evol. Biosph.* 22, 67–107.

Shock, E. L., and Schulte, M. D. (1998). Organic synthesis during fluid mixing in hydrothermal systems. *J. Geophys. Res. Planets* 103, 28513–28527.

Sibuet, M., and Olu, K. (1998). Biogeography, biodiversity and fluid dependence of deep-sea cold-seep communities at active and passive margins. *Deep Sea Res. Part II Top. Stud. Ocean.* 45, 517–567.

Sievert, S. M., Hügler, M., Taylor, C. D., and Wirsen, C. O. (2008). "Sulfur Oxidation at Deep-Sea Hydrothermal Vents," in *Microbial Sulfur Metabolism*, eds. D. C. Dahl and D. C. G. Friedrich (Springer Berlin Heidelberg), 238–258

Sievert, S., and Vetriani, C. (2012). Chemoautotrophy at deep-sea vents: Past, present, and future. *Oceanography* 25, 218–233.

Simoneit, B. R. T., Lein, A. Y., Peresypkin, V. I., and Osipov, G. A. (2004). Composition and origin of hydrothermal petroleum and associated lipids in the sulfide deposits of the Rainbow field (Mid-Atlantic Ridge at 36°N). *Geochim. Cosmochim. Acta* 68, 2275–2294.

Simoneit, B. R. T., and Lonsdale, P. F. (1982). Hydrothermal petroleum in mineralized mounds at the seabed of Guaymas Basin. *Nature* 295, 198–202.

Simoneit, B. R. T., Mazurek, M. A., Brenner, S., Crisp, P. T., and Kaplan, I. R. (1979). Organic geochemistry of recent sediments from Guaymas Basin, Gulf of California. *Deep Sea Res. Part Ocean. Res. Pap.* 26, 879–891.

Smith, C. J., and Osborn, A. M. (2009). Advantages and limitations of quantitative PCR (Q-PCR)-based approaches in microbial ecology. *FEMS Microbiol. Ecol.* 67, 6–20.

Smith, J. L., Campbell, B. J., Hanson, T. E., Zhang, C. L., and Cary, S. C. (2008). *Nautilia profundicola* sp. nov., a thermophilic, sulfur-reducing epsilonproteobacterium from deep-sea hydrothermal vents. *Int. J. Syst. Evol. Microbiol.* 58, 1598–1602.

Snow, J., and Edmonds, H. (2007). Ultraslow-spreading ridges: Rapid paradigm changes. *Oceanography* 20, 90–101.

Sogin, M. L., Morrison, H. G., Huber, J. A., Welch, D. M., Huse, S. M., Neal, P. R., Arrieta, J. M., and Herndl, G. J. (2006). Microbial diversity in the deep sea and the underexplored "rare biosphere." *Proc. Natl. Acad. Sci.* 103, 12115–12120.

Sokolova, T., Hanel, J., Onyenwoke, R. U., Reysenbach, A.-L., Banta, A., Geyer, R., González, J. M., Whitman, W. B., and Wiegel, J. (2007). Novel chemolithotrophic,

thermophilic, anaerobic bacteria *Thermolithobacter ferrireducens* gen. nov., sp. nov. and *Thermolithobacter carboxydivorans* sp. nov. *Extremophiles* 11, 145–157.

Sorokin, D. Y., Lücker, S., Vejmelkova, D., Kostrikina, N. A., Kleerebezem, R., Rijpstra, W. I. C., Damsté, J. S. S., Paslier, D. L., Muyzer, G., Wagner, M., *et al.* (2012). Nitrification expanded: discovery, physiology and genomics of a nitrite-oxidizing bacterium from the phylum Chloroflexi. *ISME J.* 6, 2245-2256

Spang, A., Hatzenpichler, R., Brochier-Armanet, C., Rattei, T., Tischler, P., Spieck, E., Streit, W., Stahl, D. A., Wagner, M., and Schleper, C. (2010). Distinct gene set in two different lineages of ammonia-oxidizing archaea supports the phylum *Thaumarchaeota*. *Trends Microbiol.* 18, 331–340.

Spieck, E., and Bock, E. (2005). "The lithoautotrophic nitrite-oxidizing *Bacteria*," in *Bergey's Manual® of Systematic Bacteriology*, eds. D. J. Brenner, N. R. Krieg, J. T. Staley, and G. M. Garrity, 149–153

Stern, R. J. (2002). Subduction zones. *Rev. Geophys.* 40, 3–1–3–38.

Stetter, K. O. (1999). Extremophiles and their adaptation to hot environments. *FEBS Lett.* 452, 22–25.

Stetter, K. O. (2006). Hyperthermophiles in the history of life. *Philos. Trans. R. Soc. B Biol. Sci.* 361, 1837–1843.

Strous, M., Fuerst, J. A., Kramer, E. H. M., Logemann, S., Muyzer, G., van de Pas-Schoonen, K. T., Webb, R., Kuenen, J. G., and Jetten, M. S. M. (1999). Missing lithotroph identified as new planctomycete. *Nature* 400, 446–449.

Strous, M., and Jetten, M. S. M. (2004). Anaerobic Oxidation of Methane and Ammonium. *Annu. Rev. Microbiol.* 58, 99–117.

Suess, E. (2010). "Marine cold seeps," in *Handbook of Hydrocarbon and Lipid Microbiology*, ed. K. N. Timmis (Springer Berlin Heidelberg), 185–203

Summit, M., and Baross, J. A. (2001). A novel microbial habitat in the mid-ocean ridge subseafloor. *Proc. Natl. Acad. Sci.* 98, 2158–2163.

Swan, B. K., Martinez-Garcia, M., Preston, C. M., Sczyrba, A., Woyke, T., Lamy, D., Reinthaler, T., Poulton, N. J., Masland, E. D. P., Gomez, M. L., *et al.* (2011). Potential for chemolithoautotrophy among ubiquitous Bacteria lineages in the dark ocean. *Science* 333, 1296 –1300.

Takai, K., Gamo, T., Tsunogai, U., Nakayama, N., Hirayama, H., Nealson, K. H., and Horikoshi, K. (2004a). Geochemical and microbiological evidence for a hydrogen-based, hyperthermophilic subsurface lithoautotrophic microbial ecosystem (HyperSLiME) beneath an active deep-sea hydrothermal field. *Extremophiles* 8, 269–282.

Takai, K., Hirayama, H., Nakagawa, T., Suzuki, Y., Nealson, K. H., and Horikoshi, K. (2005). *Lebetimonas acidiphila* gen. nov., sp. nov., a novel thermophilic, acidophilic, hydrogen-oxidizing chemolithoautotroph within the "*Epsilonproteobacteria*", isolated from a deep-sea hydrothermal fumarole in the Mariana Arc. *Int. J. Syst. Evol. Microbiol.* 55, 183–189.

Takai, K., and Horikoshi, K. (1999). Genetic diversity of archaea in deep-sea hydrothermal vent environments. *Genetics* 152, 1285–1297.

Takai, K., Inoue, A., and Horikoshi, K. (2002). *Methanothermococcus okinawensis* sp. nov., a thermophilic, methane-producing archaeon isolated from a Western Pacific deep-sea hydrothermal vent system. *Int. J. Syst. Evol. Microbiol.* 52, 1089–1095.

Takai, K., Kobayashi, H., Nealson, K. H., and Horikoshi, K. (2003). *Deferribacter desulfuricans* sp. nov., a novel sulfur-, nitrate- and arsenate-reducing thermophile isolated from a deep-sea hydrothermal vent. *Int. J. Syst. Evol. Microbiol.* 53, 839–846.

Takai, K., Miyazaki, M., Hirayama, H., Nakagawa, S., Querellou, J., and Godfroy, A. (2009). Isolation and physiological characterization of two novel, piezophilic, thermophilic

chemolithoautotrophs from a deep-sea hydrothermal vent chimney. *Environ. Microbiol.* 11, 1983–1997.

Takai, K., Nakagawa, S., Reysenbach, A.-L., and Hoek, J. (2006). "Microbial ecology of mid-ocean ridges and back-arc basins," in *Geophysical Monograph Series*, eds. D. M. Christie, C. R. Fisher, S.-M. Lee, and S. Givens (Washington, D. C.: American Geophysical Union), 185–213.

Takai, K., and Nakamura, K. (2011). Archaeal diversity and community development in deep-sea hydrothermal vents. *Curr. Opin. Microbiol.* 14, 282–291.

Takai, K., Nealson, K. H., and Horikoshi, K. (2004b). *Hydrogenimonas thermophila* gen. nov., sp. nov., a novel thermophilic, hydrogen-oxidizing chemolithoautotroph within the *ε-Proteobacteria*, isolated from a black smoker in a Central Indian Ridge hydrothermal field. *Int. J. Syst. Evol. Microbiol.* 54, 25–32.

Takai, K., Oida, H., Suzuki, Y., Hirayama, H., Nakagawa, S., Nunoura, T., Inagaki, F., Nealson, K. H., and Horikoshi, K. (2004c). Spatial distribution of Marine Crenarchaeota Group I in the vicinity of deep-sea hydrothermal systems. *Appl. Environ. Microbiol.* 70, 2404–2413.

Tarasov, V. G., Gebruk, A. V., Mironov, A. N., and Moskalev, L. I. (2005). Deep-sea and shallow-water hydrothermal vent communities: Two different phenomena? *Chem. Geol.* 224, 5–39.

Teske, A., Hinrichs, K.-U., Edgcomb, V., de Vera Gomez, A., Kysela, D., Sylva, S. P., Sogin, M. L., and Jannasch, H. W. (2002). Microbial diversity of hydrothermal sediments in the Guaymas Basin: Evidence for anaerobic methanotrophic communities. *Appl Env. Microbiol* 68, 1994–2007.

Tivey, M. K. (2007). Generation of seafloor hydrothermal vent fluids and associated mineral deposits. *Oceanography* 20, 50–65.

Tourna, M., Stieglmeier, M., Spang, A., Könneke, M., Schintlmeister, A., Urich, T., Engel, M., Schloter, M., Wagner, M., Richter, A., *et al.* (2011). Nitrososphaera viennensis, an ammonia oxidizing archaeon from soil. *Proc. Natl. Acad. Sci.* 108, 8420-8425.

Trefry, J. H., Butterfield, D. B., Metz, S., Massoth, G. J., Trocine, R. P., and Feely, R. A. (1994). Trace metals in hydrothermal solutions from Cleft segment on the southern Juan de Fuca Ridge. *J. Geophys. Res. Solid Earth* 99, 4925–4935.

Treusch, A. H., Leininger, S., Kletzin, A., Schuster, S. C., Klenk, H.-P., and Schleper, C. (2005). Novel genes for nitrite reductase and Amo-related proteins indicate a role of uncultivated mesophilic crenarchaeota in nitrogen cycling. *Environ. Microbiol.* 7, 1985–1995.

Tunnicliffe, V., Juniper, S. K., and Sibuet, M. (2003). "Reducing environments of the deepsea floor," in *Ecosystems of the Deep Oceans*, ed. P. A. Tyler (Elsevier).

Tuttle, A. J. (1985). The role of sulfur-oxidizing bacteria at deep-sea hydrothermal vents. *Bull. Biol. Soc. Wash.* 6, 335–343.

Tuttle, J. H., Wirsen, C. O., and Jannasch, H. W. (1983). Microbial activities in the emitted hydrothermal waters of the Galápagos rift vents. *Mar. Biol.* 73, 293–299.

Venter, J. C., Remington, K., Heidelberg, J. F., Halpern, A. L., Rusch, D., Eisen, J. A., Wu, D., Paulsen, I., Nelson, K. E., Nelson, W., *et al.* (2004). Environmental genome shotgun sequencing of the Sargasso Sea. *Science* 304, 66–74.

Vetriani, C., Speck, M. D., Ellor, S. V., Lutz, R. A., and Starovoytov, V. (2004). *Thermovibrio ammonificans* sp. nov., a thermophilic, chemolithotrophic, nitrate-ammonifying bacterium from deep-sea hydrothermal vents. *Int. J. Syst. Evol. Microbiol.* 54, 175–181.

Voordeckers, J. W., Starovoytov, V., and Vetriani, C. (2005). *Caminibacter mediatlanticus* sp. nov., a thermophilic, chemolithoautotrophic, nitrate-ammonifying bacterium

isolated from a deep-sea hydrothermal vent on the Mid-Atlantic Ridge. *Int. J. Syst. Evol. Microbiol.* 55, 773–779.

Wagner, M. (2009). Single-cell ecophysiology of microbes as revealed by Raman microspectroscopy or secondary ion mass spectrometry imaging. *Annu. Rev. Microbiol.* 63, 411–429.

Wankel, S. D., Adams, M. M., Johnston, D. T., Hansel, C. M., Joye, S. B., and Girguis, P. R. (2012). Anaerobic methane oxidation in metalliferous hydrothermal sediments: influence on carbon flux and decoupling from sulfate reduction. *Environ. Microbiol.* 14, 2726–2740.

Weiner, R. M., Devine, R. A., Powell, D. M., Dagasan, L., and Moore, R. L. (1985). *Hyphomonas oceanitis* sp.nov., *Hyphomonas hirschiana* sp. nov., and *Hyphomonas jannaschiana* sp. nov. *Int. J. Syst. Bacteriol.* 35, 237–243.

Welhan, J., and Craig, H. (1983). "Methane, hydogen and helium in hydrothermal fluids at 21° N on the East Pacific Rise," in *Hydrothermal processes at seafloor spreading centers* NATO conference series. IV, Marine sciences., eds. P. Rona, K. Bostroem, L. Laubier, and K. Smith (New York, N.Y.: Plenum Press).

Wery, N., Lesongeur, F., Pignet, P., Derennes, V., Cambon-Bonavita, M. A., Godfroy, A., and Barbier, G. (2001a). *Marinitoga camini* gen. nov., sp. nov., a rod-shaped bacterium belonging to the order *Thermotogales*, isolated from a deep-sea hydrothermal vent. *Int. J. Syst. Evol. Microbiol.* 51, 495–504.

Wery, N., Moricet, J. M., Cueff, V., Jean, J., Pignet, P., Lesongeur, F., Cambon-Bonavita, M. A., and Barbier, G. (2001b). *Caloranaerobacter azorensis* gen. nov., sp. nov., an anaerobic thermophilic bacterium isolated from a deep-sea hydrothermal vent. *Int. J. Syst. Evol. Microbiol.* 51, 1789–1796.

Whitman, W. B., Coleman, D. C., and Wiebe, W. J. (1998). Prokaryotes: The unseen majority. *Proc. Natl. Acad. Sci.* 95, 6578–6583.

Whittaker, R. H. (1972). Evolution and measurement of species diversity. *Taxon* 21, 213–251.

Winogradsky, S. N. (1892a). Contributions á la morphologie des organisms de la nitrification. *Arch. Sci. Biol.* 1, 88–137.

Winogradsky, S. N. (1892b). Recherches sur les organismes de la Nitrification. *Ann Inst Pasteur* 4, 213–231, 251–257 and 760–771.

Winogradsky, S. N. (1890). Sur les organisms de la nitrification. *Ceomptes Rendus Académie Sci.* 110, 1013–1016.

Winogradsky, S. N. (1887). Über Schwefelbakterien. *Bot. Ztg.* 45, 489–507.

Wirsen, C. O., Tuttle, J. H., and Jannasch, H. W. (1986). Activities of sulfur-oxidizing bacteria at the 21°N East Pacific Rise vent site. *Mar. Biol.* 92, 449–456.

Wittwer, C. T., Herrmann, M. G., Moss, A. A., and Rasmussen, R. P. (1997). Continuous fluorescence monitoring of rapid cycle DNA amplification. *BioTechniques* 22, 130–131, 134–138.

Woyke, T., Sczyrba, A., Lee, J., Rinke, C., Tighe, D., Clingenpeel, S., Malmstrom, R., Stepanauskas, R., and Cheng, J.-F. (2011). Decontamination of MDA reagents for single cell whole genome amplification. *PLoS ONE* 6, e26161.

Woyke, T., Tighe, D., Mavromatis, K., Clum, A., Copeland, A., Schackwitz, W., Lapidus, A., Wu, D., McCutcheon, J. P., McDonald, B. R., *et al.* (2010). One Bacterial Cell, One Complete Genome. *PLoS ONE* 5, e10314.

Woyke, T., Xie, G., Copeland, A., González, J. M., Han, C., Kiss, H., Saw, J. H., Senin, P., Yang, C., Chatterji, S., *et al.* (2009). Assembling the marine metagenome, one cell at a time. *PLoS ONE* 4, e5299.

Wu, D., Hugenholtz, P., Mavromatis, K., Pukall, R., Dalin, E., Ivanova, N. N., Kunin, V., Goodwin, L., Wu, M., Tindall, B. J., *et al.* (2009). A phylogeny-driven genomic encyclopaedia of *Bacteria* and *Archaea*. *Nature* 462, 1056–1060.

9. List of publications

Contributions to the manuscripts represented in this thesis:

Chapter II

Close association of active nitrifiers with *Beggiatoa* mats covering deep-sea hydrothermal sediments

Matthias Winkel, Dirk de Beer, Gaute Lavik, Jörg Peplies and Marc Mussmann

(submitted to Environmental Microbiology)

M. W.: developed the concept, constructed amoA gene libraries of all samples and analyzed the amoA dataset, performed quantitative PCR of amoA gene, performed CARD-FISH experiments, measured nitrification rates and analyzed data, measured ammonium and nitrate concentrations, conceived and wrote the manuscript; D. de B.: performed in situ microsensor measurments, conceived and edited the manuscript: G. L.: analyzed data of nitrification rates, conceived and edited the manuscript; J. P.: analyzed 454 pyrosequencing dataset; M.M. developed the concept, constructed 454 pyrosequencing library, performed isotopic pairing shipboard experiments, took samples, conceived and wrote the manuscript

Chapter III

Identification and activity of acetate-assimilating microorganisms in diffuse hydrothermal fluids

Matthias Winkel[§], Petra Pjevac[§], Manuel Kleiner, Sten Littman, Anke Meyerdirks and Marc Mussmann

(in preparation for FEMS Microbiology Ecology)

M. W.: developed the concept, took samples, performed stable isotope shipboard experiments, performed CARD-FISH experiments, measured ammonium concentrations, conducted and evaluated nanoSIMS experiments, post-analyzed nanoSIMS dataset, analyzed 454 dataset , conceived and wrote the manuscript; P. P.: developed the concept, took samples, performed stable isotope shipboard experiments, performed CARD-FISH experiments, constructed 454 pyrosequencing libraries and analyzed dataset, conceived

and wrote the manuscript; M. K.: conducted nanoSIMS analysis, conceived and edited the manuscript; S. L.: conducted nanoSIMS analysis, conceived and edited the manuscript; A. K.: took samples, constructed 454 pyrosequencing library, conceived and edited the manuscript; M. M.: developed the concept, conceived and edited the manuscript

[§] these authors contribute equal to the study

Chapter IV

A single cell genome of "*Candidatus* Thiomargarita nelsonii" and comparison to large sulfur-oxidizing bacteria

Matthias Winkel, Salman Verena, Tanja Woyke, Heide Schulz-Vogt, Michael Richter and Marc Mussmann

(In preparation)

M. W.: developed the concept, performed multiple displacement amplification on single cells, performed gene amplification; post-analyzed automatic annotated genome dataset, reconstructed metabolic pathways, conceived and wrote the manuscript; S. V.: provided samples and analytical tools, conceived and edited the manuscript; T. W.: sequenced the genome and assembled sequencing reads; H. S.-V.: provided samples; M. R.: annotated the genome, conceived and edited the manuscript; M. M.: developed the concept, conceived and edited the manuscript

Additional manuscript I contributed to:

Colonization of freshwater biofilms by nitrifying bacteria from activated sludge

Marc Mußmann, Miquel Ribot, Daniel von Schiller, Stephanie N. Merbt, Clemens Augspurger, Clemens Karwautz, Matthias Winkel, Tom J. Battin, Eugènia Martí, and Holger Daims

(FEMS microbiology ecology (2011) 85: 104-115)

M. W.: constructed amoA gene libraries

A cruise report I contributed to:

The preparation of a research cruise is quite elaborate and the success depends to a great extent on its participants, i.e. the shipboard scientific party, their will to communicate and collaborate. Therefore, the whole shipboard scientific party is appreciated as co-authors on the following report although not every single person has necessarily contributed data to the manuscript.

Interdisciplinary geological, chemical and biological studies at the Menez Gwen hydrothermal vent field Mid-Atlantic Ridge, at 37°50' N.

Nicole Dubilier, Christian Borowski, Hauke Büttner, Ana Colaço, Leonardo Contreira, Christian dos Santos Ferreira, Dennis Fink, Phillip Franke, Philipp Hach, Michael Hentscher, Stephane Hourdez, Julia Köhler, Frank Lartaud, Nadine LeBris, Silvia Lino, Christian Lott, Anh Hong Mai, Yann Marcon, Anke Meyerdierks, Sven Petersen, Xavier Prieto Mollar, Volker Ratmeyer, Eoghan Reeves, Ralf Rehage, Michael Reuter, Christian Reuter, Heide Schulz, Thorsten Truscheit, Charles Vidoudez, Tomas Wilkop, Matthias Winkel, Matthias Zabel, Marcel Zarrouk

(Cruise No. 82, Leg 3, 06.09. – 11.10.2010, Ponta Delgada (Portugal) – Las Palmas (Spain))

(In preparation for Leitstelle Deutsche Forschungsschiffe Institut für Meereskunde der Universität Hamburg)

Chapter II

Close association of active nitrifiers with *Beggiatoa* mats covering deep-sea hydrothermal sediments

Close association of active nitrifiers with *Beggiatoa* mats covering deep-sea hydrothermal sediments

Matthias Winkel[1], Dirk de Beer[1], Gaute Lavik[1], Jörg Peplies[2] and Marc Mußmann[1*],

[1]Max Planck Institute for Marine Microbiology, Celsiusstrasse 1, 28359 Bremen, Germany

[2] Ribocon GmbH, Fahrenheitstrasse 1, 28359 Bremen, Germany

*Corresponding author: mmussman@mpi-bremen.de, Tel. (+49) 4212028936, Fax (+49) 4212028790

Key words: hydrothermal vent, nitrification, ammonia oxidation, nitrite oxidation, syntrophy, Guaymas Basin

Abstract

Hydrothermal sediments in the Guaymas Basin are covered by microbial mats that are dominated by nitrate-respiring and sulfide-oxidizing *Beggiatoa*. The presence of these mats strongly correlates with sulfide- and ammonium-rich fluids venting from the subsurface. Since ammonium and oxygen form opposed gradients at the sediment surface, we hypothesized that nitrification is an active process in these *Beggiatoa* mats. Using biogeochemical and molecular methods we measured nitrification and determined the diversity and abundance of nitrifiers. Nitrification rates ranged from 74 to 605 μmol N l^{-1} mat d^{-1}, which exceeded those previously measured in hydrothermal plumes and other deep-sea habitats. Diversity and abundance analyses of archaeal and bacterial *amoA* genes, archaeal 16S rRNA pyrotags and fluorescence *in situ* hybridization (FISH) confirmed that ammonia- and nitrite-oxidizing microorganisms were associated with *Beggiatoa* mats. Intriguingly, we observed cells of bacterial and potential thaumarchaeotal ammonia-oxidizers attached to narrow, *Beggiatoa*-like filaments. Such a close spatial coupling of nitrification and nitrate respiration in mats of large sulfur bacteria is novel and may facilitate mat-internal cycling of nitrogen, thereby reducing loss of bioavailable nitrogen in deep-sea sediments.

Introduction

Deep-sea hydrothermal fluids usually contain reduced electron donors such as sulfide, hydrogen, and metal ions that fuel microbial chemoautotrophy (Jannasch and Mottl, 1985). In contrast, the significance of ammonium for chemoautotrophy at hydrothermal vent systems is largely unknown. Ammonium concentration in end-member fluids range from 0.07 to 7 mM in some basaltic and ultramafic (Lilley *et al.,* 1993; Orcutt *et al.,* 2011; Bourbonnais *et al.,* 2012a) and up to 16 mM in sedimented hydrothermal vent systems (Von Damm *et al.,* 1985; Nunoura *et al.,* 2010). When mixing with sea water at the seafloor, ammonium ascends the water column in buoyant hydrothermal plumes and stimulates the aerobic oxidation of ammonia by bacteria (Lam *et al.,* 2004; Lam *et al.,* 2008) or archaea (Baker *et al.,* 2012; Lesniewski *et al.,* 2012). Since hydrothermal fluids can contain significant amounts of ammonium, it has been proposed to be an important energy source not only in the hydrothermal plumes but also in the direct vicinity of hydrothermal vents (Nakagawa and Takai, 2008). However, nitrification, the oxidation of ammonia to nitrite and further to nitrate, is largely unexplored at hydrothermal vents. Isotope composition in hydrothermal fluids from the Juan de Fuca Ridge suggested that nitrate could be regenerated from nitrification by subsurface microbial communities (Bourbonnais *et al.,* 2012b). Furthermore, the detection of genes from bacterial nitrifiers in hydrothermally influenced sediments and chimneys (Davis *et al.,* 2009; Kato *et al.,* 2009; Wang *et al.,* 2009; Nunoura *et al.,* 2010) indicated a genetic potential for nitrification. Nevertheless, there is no study that determined the nitrification potential and the involved microorganisms in benthic compartments of hydrothermal systems.

The end-member fluids of the sediment-covered hydrothermal system of the Guaymas Basin, Gulf of California, contain up to 16 mM ammonium (Von Damm *et al.,* 1985). These fluids mix with sea water below the sediment surface and cool down before entering the water column, which allows the formation of conspicuous microbial mats up to several cm thick. These mats are dominated by filamentous, sulfide-oxidizing *Beggiatoa*. Their horizontal

distribution is tightly coupled to subsurface processes (Lloyd *et al.,* 2010) and indicates intense venting of sulfide- and ammonium-rich fluids in the Guaymas Basin system (Jannasch *et al.*, 1989; Gundersen *et al.*, 1992; Magenheim and Gieskes, 1992; McKay *et al.*, 2012). Mats of large sulfur bacteria are generally considered as hot spots of nitrogen cycling (Prokopenko *et al.*, 2006; Teske and Nelson, 2006; Bowles *et al.*, 2012), but nitrification in these mats has not yet been explored. In particular, the vacuolated *Beggiatoa* accumulate nitrate by internally storing it up to 160 mM, which is 4,000-fold compared to ambient concentration (McHatton *et al.,* 1996). When oxygen is depleted, the stored nitrate is respired to oxidize sulfide, an inhibitor of nitrification (Joye and Hollibaugh, 1995). Therefore, we hypothesized that the *Beggiatoa* mats in the Guaymas Basin provide favorable conditions for nitrification (McHatton *et al.,* 1996), since they detoxify sulfide and are located in the mixing zone of oxic sea water and cooled, ammonium-rich fluids venting from the subsurface. Using molecular and biogeochemical methods we studied, whether active nitrification occurs in *Beggiatoa* mats at sea floor of the Guaymas Basin. To detect nitrification zones within an undisturbed *Beggiatoa* mat we profiled oxygen and NO_x using microsensors *in situ*. In addition, in shipboard slurry experiments we determined nitrification rates from added $^{15}NH_4^+$ in *Beggiatoa* mats. To identify nitrifying microorganisms we applied an array of molecular tools including diversity analyses of genes encoding ammonia monooxygenase subunit A (*amoA*) and 16S rRNA, quantitative PCR (qPCR) of *amoA* genes and fluorescence *in situ* hybridization (FISH) of single cells.

Results

O_2, NO_x, nitrate and ammonium measurements

During *Alvin* dive 4564 we used microsensors to determine *in situ* gradients of oxygen, sulfide, N_2O and NO_x in an intact *Beggiatoa* mat (BM1). At the mat surface oxygen penetrated to approximately 2 mm depth, but just as in earlier studies in the Guaymas Basin by Gundersen *et al.* (1992), we also observed temporary pulses of up to 9 µM oxygen in 6 to 8 mm depth (Fig. 1). Concentration of NO_x ranged from 20-30 µM in the diffusion boundary layer and increased to approximately 50 µM in 7 mm depth. Below 1 cm depth the nitrate biosensor was not functional anymore due to inhibition by the high sulfide concentration. From the NO_x flux we calculated an *in situ* nitrification rate of 605 µmol nitrate l^{-1} mat d^{-1} assuming steady state, diffusionally controlled transport and a porosity of 1.0 (Gieseke and de Beer, 2004). Since commonly nitrite concentrations are very low in natural samples, we also assumed that all NO_x was present as nitrate. In support of this, nitrite could previously not be detected in Guaymas Basin sediments and *Beggiatoa* mats by Bowles *et al.* (2012). N_2O was not measurable below the detection limit of 1 µM. Total sulfide concentration was at 15 mM in 15 mm depth and rapidly decreased towards the mat surface until it decreased below detection limit in 1-2 mm depth (Fig. 1). In the upper 15 mm the temperature remained at 2.5 to 2.8 °C and pH increased from 7.8 in 0-10 mm depth to 8.0 in 15 mm depth (not shown).

In addition, we determined nitrate and ammonium concentration in and above several *Beggiatoa* mats and in sediment pore waters taken from underneath mats at different locations (Table S2). It has to be noted that sediment stratification and pore water values might have been changed by outgassing of methane during the ascent of the submersible. Nitrate concentration in 18 different bottom sea water samples ranged from 6 to 54 µM, with one exception, where the concentration reached 111 µM. Nitrate concentration in *Beggiatoa* mats and in pore waters from the upper 5 cm of *Beggiatoa*-covered sediment ranged from 20 to 48

μM and was in the range of NO_x determined by microsensor measurements indicating that most NO_x was present as nitrate.

Ammonium concentration in pore waters extracted from the first cm or from the upper 5 cm of *Beggiatoa*-covered sediments ranged from 0.05 to 5.3 mM (n=10). In all but one pore water sample ammonium reached more than 0.5 mM. In pore waters from cold, non-hydrothermal sediment (NHS1) also used for nitrification rate measurements (see below), we did not detect any ammonium. In bottom sea waters sampled from supernatants of 15 *Beggiatoa*-covered sediment cores and of 3 Niskin bottles ammonium ranged from 0.03 to 0.08 mM (Table S2).

Nitrification rates in *Beggiatoa* mats, sediment and sea water.

Since we could obtain only a single NO_x profile from *in situ* microsensor measurement, we additionally determined nitrification rates in ship-board slurry experiments. Samples were retrieved from three different compartments of the Guaymas Basin hydrothermal system: i) from washed and homogenized *Beggiatoa* mats (BM2a and BM3a), ii) from ammonium-free, non-hydrothermal sediments (NHS1) and iii) from bottom sea water (BSW) sampled approximately one meter above hydrothermal, mat-covered sediments. *Beggiatoa* mat BM2a was recovered in dive 4564, during which also microsensor profiles in mat BM1 (Fig. 1) were retrieved. We measured linear nitrate formation from ^{15}N-labelled ammonium chloride after incubation for up to 36h at 4°C in the dark (Fig. S1). In *Beggiatoa* mats BM2a and BM3a we determined nitrification rates of 74 to 189 μmol N l^{-1} mat d^{-1} (Fig. 2), which are equivalent to areal rates of 740 to 1,890 μmol N m^{-2} d^{-1} of a mat with a presumed thickness of one cm. These rates were 370 to 920-fold higher than those determined for bottom sea water (Fig. 2). No ^{15}N-nitrate was detected in the incubations performed with cold, non-hydrothermal sediment (NHS1) (Fig. 2). For comparison we incubated *Beggiatoa* mats BM2a and BM3a with allylthiourea (ATU) at a concentration of 100 μM. At this level

ATU completely inhibits the bacterial ammonia monooxygenase (AMO), whereas the archaeal AMO is inhibited only partially (Santoro and Casciotti, 2011) or even stimulated (Lehtovirta-Morley et al. 2013). In mat BM2a nitrification was only partially inhibited upon ATU addition (40 µmol N l^{-1} mat d^{-1}), while in mat BM3a no measureable ^{15}N-nitrate was formed at all. All values were corrected for the *in situ* concentration of ammonium.

Quantitative PCR of *amoA* genes

Since microsensor and incubation experiments indicated active nitrification in the three investigated *Beggiatoa* mats, we first aimed at quantifying candidate archaeal and bacterial ammonia-oxidizers. By quantitative PCR (qPCR) we determined the copy number of the *amoA* gene encoding the ammonia monooxygenase subunit A in subsamples from *Beggiatoa* mat BM2a and bottom sea water used for nitrification rate measurements. In addition, we determined *amoA* copy numbers in *Beggiatoa* mats recovered from cores that were sampled directly adjacent to those used for the nitrification experiment (BM2b, BM3b, Table 1). In mats BM2a, BM2b and BM3b more than 10^6 archaeal *amoA* gene copies ml^{-1} mat were detected, whereas bottom sea water contained less than 10^3 archaeal *amoA* gene copies ml^{-1}. Betaproteobacterial *amoA* (10^4-10^5 copies ml^{-1}) were also detected in all three *Beggiatoa* mats but not in the bottom sea water (Table 1). Gammaproteobacterial *amoA* could not be detected by qPCR. In addition, we determined 10^6 archaeal *amoA* gene copies ml^{-1} in bare, hydrothermally-influenced sediment HS sampled adjacent to a *Beggiatoa* mat. No bacterial *amoA* could be amplified from this sample.

AmoA diversity

To study the diversity of ammonia-oxidizers in *Beggiatoa* mats we established *amoA* gene libraries from *Beggiatoa* mats BM3b and BM4. For comparison we also studied the *amoA* gene diversity in bottom sea water (BSW), in bare, hydrothermally-influenced sediment

(HS) adjacent to a *Beggiatoa* mat and in cold, non-hydrothermal sediment (NHS2). The archaeal *amoA* gene could be amplified from all samples. We recovered 340 sequences from 5 clone libraries, which split up into 23 OTUs (based on 98% sequence identity (SI) on amino acid level). From non-hydrothermal sediment NHS2 only 2 OTUs were recovered (Figs. 3, 4). Sequences were phylogenetically classified according to subclusters defined by Pester *et al.* (2012), but we assigned subclusters to the order/family designation *Nitrosopumilales*/*Nitrosopumilaceae* instead of the genus *Nitrosopumilus*. The overall diversity was high (minimum SI of 77%), but most AmoA sequences grouped within three *Nitrosopumilaceae*-related clusters (Fig. 3). The phylogenetic affiliation and the relative clone frequencies of AmoA clusters were similar in the two *Beggiatoa* mats sampled in 2008 and 2009 and in sediment HS. However, they were clearly distinct from those in bottom sea water and non-hydrothermal sediment NHS2 (Fig. 4). Sequences from the *Nitrosopumilaceae* cluster 4 were detected in considerable frequencies (17-90% of all sequences) in all mat and sediment samples regardless of hydrothermal influence and are typically found in diverse marine sediments, but accounted for only 3% of all clones from bottom sea water (Fig. 4). Sequences of the *Nitrosopumilaceae* subclusters 2, 9.1A and 9.1C exclusively occurred in *Beggiatoa* mats and in sediment HS and accounted for approximately 17-21% of AmoA sequences in the individual libraries. Sequences of the *Nitrosopumilaceae* subcluster 9.1B mostly occurred in *Beggiatoa* mats, sediment HS and bottom sea water, but were rare in cold, non-hydrothermal sediment NHS2 (Fig. 4). Furthermore, sequences most closely related to *N. maritimus* were only recovered from bottom sea water and grouped with AmoA sequences recovered previously from the Guaymas Basin hydrothermal plume (Baker *et al.,* 2012).

Betaproteobacterial *amoA* sequences were retrieved from *Beggiatoa* mat BM4 and from cold, non hydrothermal sediment NHS2. The overall diversity of AmoA was low (3 OTUs, minimum SI 91%) and all sequences (n=186) were affiliated with sequences earlier found at sites surrounding hydrothermal vents including the Guaymas Basin (AY785972, P.

Lam, unpublished) and from coastal and deep-sea sediments (Francis et al., 2003; O'Mullan and Ward, 2005) (Fig. S2). The closest cultured relatives were members of the genus *Nitrosospira* (85-90% SI). Gammaproteobacterial *amoA* could not be amplified, probably due to primer bias of the used primers, although gammaproteobacterial AOB were detectable by FISH (Table 1).

CARD-FISH and archaeal 16S rRNA pyrotag analysis

The measured nitrification activity and the high *amoA* copy numbers in washed *Beggiatoa* mats suggested that nitrifying organisms were closely associated with filaments from the mat. To verify these findings by an alternative method we performed catalyzed reporter deposition combined with fluorescence *in situ* hybridization (CARD-FISH) on these filaments. MG-I.1a thaumarchaeotes, which include ammonia-oxidizing archaea (AOA) such as *N. maritimus,* were found on many thin filaments, whereas ammonia-oxidizing bacteria (AOB) were detected only occasionally (Table 1, Fig. 5). These filaments displayed a diameter of 2-5 µm (Fig. 5) and resembled thin *Beggiatoa* filaments (Teske and Nelson, 2006). Due to strong autofluorescent background we could not demonstrate single cells of nitrifiers directly attached to larger *Beggiatoa* filaments. This and the highly heterogeneous distribution of cells precluded an exact quantification of cells in mat samples, but we conservatively estimate that the relative abundance of MG-I.1a thaumarchaeotes exceeded those of AOB by at least 6-8 fold (Table 1). Although clearly detectable in bottom sea water and in sediment HS, the relative abundances of thaumarchaeotes, beta- and gammaproteobacterial AOB were each below 0.5% of total cell counts (Table 1). At a total cell count of 10^5 cells ml^{-1} in bottom sea water, this equals max. 5x 10^2 cells ml^{-1} for each of the three subpopulations and confirmed the low archaeal *amoA* copy numbers (Table 1).

To verify the detection of MG-I.1a thaumarchaeotes by *amoA*, we examined the general archaeal community using 16S rRNA gene pyrotags in three compartments

(*Beggiatoa* mat BM3b, sediment HS, bottom sea water) (Fig. S3). In total 14,694 sequences of >400 bp in length were analyzed. Euryarchaeota clearly dominated mat and sediment samples. The archaeal community substantially differed between *Beggiatoa* mat BM3b and bottom sea water at the 16S rRNA gene level. MG-I.1a thaumarchaeotes accounted for 3% of recovered sequences in *Beggiatoa* mat BM3b and for 55% in bottom sea water. The partial sequences displayed 90-97% sequence identity to *N. maritimus*. Only very few thaumarchaeotal sequences (<0.1%, 7 out of 8,606 sequences) were recovered from the bare, hydrothermally-influenced sediment HS. MG-I.1b thaumarchaeotes were not detected at the 16S rRNA level (Fig. S3).

We also identified nitrite oxidizers of the genera *Nitrospina, Nitrospira* and *Nitrococcus* by CARD-FISH in *Beggiatoa* mats. These were not attached to filaments and were only occasionally observed, as they were probably removed during washing of the mats. Cells of *Nitrospira* and *Nitrococcus* appeared to be more prevalent in the *Beggiatoa* mats (Table 1). No known NOB cells were detectable in the bottom sea water, although ^{15}N-nitrate was formed during the nitrification experiment (Fig. 2).

Discussion

Nitrate is an important electron acceptor and nitrogen source for microorganisms at the sea floor of the Guaymas Basin (Bowles *et al.,* 2012). In this study, we show for the first time that nitrification and nitrifying microorganisms occur in *Beggiatoa*-dominated microbial mats. These mats reliably indicate venting of sulfide- and ammonium-rich fluids from the hydrothermal sediments underneath and are thus ideally positioned to host nitrifying microorganism in the overlapping zone of oxygen and ammonium. Our study provides an important extension to the very few reports on nitrification in deep-sea (hydrothermal) habitats (Lam et al., 2004, 2008; Baker et al., 2012) and in marine microbial mats (Bonin and Michotey, 2006), as we combined biogeochemical and molecular experiments to quantify nitrification and to identify the involved microorganisms. In our polyphasic approach we did not fully explore the variability and spatial heterogeneity of nitrification and influencing parameters, but all geochemical and molecular data concordantly gave strong evidence that nitrification is an active process in *Beggiatoa* mats at the Guaymas Basin sea floor. Such a close spatial coupling of N-cycling processes likely stimulates the detoxification and oxidation of sulfide by nitrate-respiring *Beggiatoa*, when oxygen is depleted.

High measured nitrification rates in *Beggiatoa* mats

It was the aim of our study to show that nitrification principally occurs in *Beggiatoa* mats. By microsensor and isotopic tracer experiments we indeed detected nitrification in the three investigated mats. Due to the technical challenges in deploying microsensors at 2000 m depth, microsensor profiles could only be measured once. However, we believe that the recovered data are accurate for several reasons. Such irregular-shaped oxygen profiles (Fig. 1) have been reported before in *Beggiatoa* mats of the Guaymas Basin and were attributed to pulsatory flow of hydrothermal fluids mixed with sea water (Gundersen *et al.,* 1992). Moreover, nitrate concentrations measured in different *Beggiatoa* mats well matched those

measured by the microsensor *in situ*. We can not fully exclude that nitrification rates in our slurry experiments were overestimated, for example because of sulfide removal to non-inhibitory levels upon washing. However, the nitrification rates calculated from *in situ* nitrate profile in *Beggiatoa* mat BM1 (605 µmol N l^{-1} mat d^{-1}) were in the same order of magnitude as those measured in our shipboard $^{15}NH_4^+$-labeling experiments in *Beggiatoa* mats BM2a and BM3a (189 and 74 µmol N l^{-1} mat d^{-1}). More likely though, our shipboard rate measurements have underestimated the actual *in situ* rates, as i) mats were washed before shipboard experiments and ii) the applied methods did not consider the loss of nitrate by simultaneous nitrate respiration by e.g. intact *Beggiatoa* cells. Furthermore, the $^{15}NH_4^+$ pool could have been diluted by nitrate respiration and by decomposing proteins. Nonetheless, given the highly fluctuating hydrodynamic regimes in this hydrothermal system the nitrification rates may strongly vary on small temporal and spatial scales, which has to be explored in more detail by additional rate measurements.

At the most conservative estimate of 74 µmol N per liter mat d^{-1} this exceeded ammonia removal rates determined for hydrothermal plumes (Lam *et al.,* 2004; Lam *et al.,* 2008) and nitrification rates in non-hydrothermal sediment by 340- to 2000-fold. Assuming a mat thickness of approximately one cm the estimated areal nitrification rates ranged from of 0.7 to 6 mmol N m^{-2} d^{-1} and thus outnumbered a rate of 0.2 mmol N m^{-2} d^{-1} reported for a 1450 m-deep ocean margin sediment (Glud *et al.,* 2009). To our knowledge, the nitrification rates in the *Beggiatoa* mats presented here are the highest reported for deep-sea habitats and resemble those in coastal, organic-rich sediments (Rysgaard *et al.,* 1996; Lehmann *et al.,* 2004). Our data show that nitrification occurs in mats of large sulfur bacteria, for which only anaerobic ammonia oxidation (anammox) has been reported (Prokopenko *et al.,* 2006; Høgslund *et al.,* 2009). Tests for the presence of anammox-bacteria in *Beggiatoa* mats using planctomycete/*Scalindua*-specific-FISH, -16S rRNA and -*nirS* assays were all negative (not

shown), however, anammox-bacteria have recently been detected in Guaymas Basin sediments (Russ et al. 2013).

Nitrifying microorganisms in *Beggiatoa* mats

The analysis of diversity and abundance of candidate nitrifiers in actively nitrifying *Beggiatoa* mats suggested that both AOA and AOB are involved in ammonia oxidation. In *Beggiatoa* mats the archaeal AmoA diversity was high, while in the bottom sea water (this study, Fig. 3) and in the metatranscriptome of hydrothermal plume of the Guaymas Basin only few AmoA phylotypes were detected (Baker *et al.,* 2012). In *Beggiatoa* mats and sediments we identified bacterial nitrifiers, AOB and NOB, that were not found in the previous studies of the Guaymas Basin hydrothermal plume (Baker *et al.,* 2012; Lesniewski *et al.,* 2012). Thus, the community structure of nitrifying microorganisms at the sediment surface is distinct from those in the hydrothermal plume of the Guaymas Basin.

The detection of MG-I.1a thaumarchaeotes by CARD-FISH and of 16S rRNA pyrotags related to *Nitrosopumilaceae* is consistent with the high diversity and abundances of archaeal *amoA* genes in *Beggiatoa* mats. This suggested a substantial contribution of thaumarchaeotes to aerobic ammonia oxidation. In particular, the exclusive occurrence of the AmoA subclusters 2, 9.1A and 9.1C of the *Nitrosopumilaceae*-group in the two *Beggiatoa* mats and in bare, hydrothermally-influenced sediment HS but not in other compartments of the Guaymas Basin (Figs. 3, 4) indicated the existence of discrete, surface-attached populations that are specifically adapted to this habitat. AOB were also detected in all samples either by CARD-FISH or by *amoA* gene detection (Table 1). Although cell abundances, *amoA* gene copies and AmoA diversity of AOB were always lower than those of thaumarchaeotes, they were still sufficient to explain a major part of ammonia oxidation, as AOB typically exhibit 10- to up to 100-fold higher cell-specific ammonia oxidation rates than AOA (Coskuner *et al.,* 2005; Martens-Habbena *et al.,* 2009).

The spatial and temporal patterns of nitrification at the Guaymas Basin sea floor are probably quite complex, as oxygen, sulfide and ammonium concentrations strongly fluctuate (Fig. 1, Table S2) (Magenheim and Gieskes, 1992; McKay *et al.*, 2012). These factors are known to affect the distribution and activity AOA and AOB differently. While some AOA prefer lower oxygen and ammonium concentrations than AOB (Beman et al. 2008; Molina et al. 2010; Pitcher et al. 2011; Martens-Habbena *et al.*, 2009), it was proposed that they could be more sulfide-tolerant than AOB (Caffrey *et al.,* 2007; Coolen *et al.,* 2007; Erguder *et al.,* 2009). Therefore, we hypothesize that the geochemical heterogeneity is reflected in the distribution and activity of nitrifiers. A first indication for this to-be-tested hypothesis was the differential inhibition of nitrification in two *Beggiatoa* mats upon ATU treatment. In *Beggiatoa* mat BM3a nitrate formation was totally suppressed at ATU concentrations known to completely inhibit AOB (Bedard and Knowles, 1989; Ginestet *et al.*, 1998), whereas AOA are only partially inhibited (Hatzenpichler *et al.*, 2008; Santoro and Casciotti, 2011). In contrast nitrate formation in *Beggiatoa* mat BM2a was not fully impaired, which pointed to a mainly AOA-driven ammonia oxidation in this mat (Fig. 2), although AOB where detectable in considerable numbers (Table 1). However, further nitrification experiments using additional inhibitors (Taylor et al. 2013; Shen et al. 2013) and diversity analyses are essential to explore the actual distribution and niche differentiation of AOA and AOB at the Guaymas Basin sea floor.

Very little is known about the diversity of nitrite-oxidizing bacteria (NOB) in marine systems, in particular at hydrothermal vent sites and the discovery of novel NOB in phyla previously unknown for nitrite oxidation is still ongoing (Alawi *et al.,* 2007; Sorokin *et al.,* 2012). In our study, we identified NOB cells of the genera *Nitrospira*, *Nitrococcus* and *Nitrospina* by CARD-FISH, which is in agreement with the previous detection of 16S rRNA gene sequences related *Nitrospira* in Guaymas Basin chimneys (acc. no. DQ925899) and of *Nitrospira*- and *Nitrospina*–related 16S rRNA gene sequences in chimneys of the Mid-

Atlantic Ridge (Sylvan *et al.,* 2012). The formation of ^{15}N-nitrate from $^{15}NH_4^+$ strongly indicated that these NOB were active *in situ*.

Syntrophy between nitrifiers and *Beggiatoa*?

Intriguingly, we found many cells of AOB and particularly of the *Nitrosopumilus*-related MG-I.1a thaumarchaeotes physically attached to narrow, *Beggiatoa*-like filaments (Fig. 5). Together with our biogeochemical and molecular results from washed mats this finding indicated a close physical and potentially physiological interaction between nitrifiers and mat-forming filamentous bacteria. As mats of large sulfur bacteria respire nitrate mainly to ammonium (Jørgensen and Nelson, 2004; Preisler *et al.*, 2007), we propose that inorganic nitrogen is cycled between ammonium and nitrate within the *Beggiatoa* mats (Fig. 6). In such a scenario, nitrifiers supply *Beggiatoa* with nitrate, which in turn is respired to ammonium. In addition, by their gliding motility these mats optimally position in oxic-anoxic interfaces (Nelson *et al.,* 1986; Gundersen *et al.,* 1992; Preisler *et al.,* 2007), providing micro-oxic conditions that may be favorable also to nitrifiers (McHatton *et al.,* 1996). By attaching to motile filaments, nitrifiers could thereby ensure a supply with ammonia, relatively stable temperatures and may also avoid long-term burial by sedimenting particles. Furthermore, due to their negative tactic response towards high sulfide (Preisler *et al.,* 2007) and by oxidizing sulfide *Beggiatoa* may keep local sulfide levels below concentrations inhibitory to nitrification (Joye and Hollibaugh, 1995; Caffrey *et al.*, 2007), which could open a niche for nitrifiers in sulfidic habitats. Interestingly, such an association may be functionally similar to a consortium of AOA, *Nitrospina* and sulfide-oxidizing bacteria enriched from marine sulfidic sediments (Park *et al.,* 2010). In this enrichment sulfide oxidizers are also thought to suppress both oxygen and sulfide to levels favorable for growth of AOA and *Nitrospina*.

Nitrification coupled to nitrate respiration in *Beggiatoa* mats

Large filamentous sulfur bacteria such as *Beggiatoa* and *Thioploca* intracellularly accumulate nitrate and respire it under anoxic conditions (Teske and Nelson, 2006). Major parts of mats of vacuolated *Beggiatoa* usually thrive under micro-oxic to anoxic conditions (Fig. 1) (Mussmann *et al.,* 2003; Preisler *et al.,* 2007), thus nitrate respiration coupled to sulfide oxidation is important to sustain such large biomass. Most likely, the mat-internally formed nitrate is rapidly consumed by *Beggiatoa* (Fig. 6) and thereby enables the anaerobic oxidation of sulfide and allows survival of *Beggiatoa* under micro-oxic to anoxic conditions (Fig. 1). A similar effect was observed in tidal sediments, where sedimentary nitrification replenishes the intracellular nitrate pool of nitrate-respiring microalgae (Heisterkamp *et al.,* 2012).

In summary, our biogeochemical and molecular data strongly suggest that complete nitrification of ammonia to nitrate is active in *Beggiatoa* mats covering hydrothermal sediments of the Guaymas Basin. Along with the fact that *Beggiatoa* mats co-localize with emanating ammonia- and sulfide-rich fluids and are usually not found at cold, non-hydrothermal sediments the high nitrification rates suggest that these mats could be hot spots of nitrification in the deep sea. Here, the highly dynamic hydrothermal regimes determine fluctuating oxygen, sulfide and ammonium concentrations probably influence the relative contribution of archaeal and bacterial nitrifiers to total nitrification. Nitrification coupled to nitrate-respiration and N-recycling in *Beggiatoa* mats could be an important process not only at other ammonium-rich hydrothermal vent sites such as the Juan de Fuca Ridge, but also in *Beggiatoa* mats covering large areas of organic-rich coastal sediments (Jørgensen, 1977) and cold seeps (Boetius and Suess, 2004). While previous studies underscored the role of nitrate-storage and DNRA in diminishing nitrogen loss from sediment surfaces, the potential syntrophic relationship of nitrifiers and nitrate-respiring sulfur oxidizers may intensify N-cycling at sediment surfaces and may reduce the loss of bioavailable N. This phenomenon

provides a new perspective on benthic nitrogen cycling and could be particularly relevant in nitrate-limited environments.

Material and Methods

Site description and sampling

Samples were taken from a hydrothermal vent site in the Guaymas Basin, Gulf of California during the cruises AT15-40 (Dec 5-18, 2008) and AT15-56 (Nov 22–Dec 5, 2009) with R/V Atlantis. Samples were recovered in a region ranging from 27°N00.30 to 27°N00.60, and 111°W24.65 to 111°W24.35 using the submarine *DSV Alvin.* Hydrothermal sediments in the Guaymas Basin are characterized by steep temperature gradients ranging from 2.5 to 8°C at the surface to a mean of 84°C in 40 cm depth (Gundersen *et al.,* 1992; McKay *et al.,* 2012). A survey of temperature profiles in *Beggiatoa* mats and sediments during the 2009 cruise have been published by McKay *et al.* (2012).

An overview of samples and of the performed analyses is given in Table S1. Sediments covered with *Beggiatoa* mats (BM1-4) and bare, hydrothermally influenced surface sediments (HS) in the direct vicinity of a *Beggiatoa* mat were either studied by microsensors (BM1) or sampled with push cores in 2001 to 2011 m water depth (BM2-4, HS). Cores from for either FISH or qPCR analysis were sampled right next to cores used for nitrification experiments (BM2b, BM3b). Bottom sea water (BSW) for nitrification rate measurements and molecular analyses was sampled with Niskin-bottles in approximately 1 m above a *Beggiatoa* mat during *Alvin* dive 4564 in 2002 m water depth. Non-hydrothermal sediments (NHS1, NHS2) were sampled >200m away from *Beggiatoa* mats during *Alvin* dives 4567 (NHS1, nitrification experiment) and 4491 (NHS2, *amoA* gene libraries). Hydrothermally-influenced surface sediment (HS) was sampled in the direct vicinity of a *Beggiatoa* mat during *Alvin* dive 4565. Upon arrival at the water surface all samples were transferred to 4°C and further processed within a few hours.

Microsensor measurements

During *Alvin* dive 4564 high resolution *in situ* microsensor measurements were carried out in *Beggiatoa* mat BM1 with a deep-sea microprofiler as described previously (Wenzhöfer *et al.,* 2000). The submarine *DSV Alvin* was used to precisely position the microprofiler, to start the autonomous profiling routine and for the instrument retrieval. The microsensors were driven stepwise from the water phase into the sediment to a depth of up to 8 cm. On the profiler electronic unit a total of 10 microsensors were mounted: 2x pH, 2x oxygen, 2x sulfide, 1 N_2O and 1x NO_x (Revsbech and Ward, 1983; Jeroschewski *et al.*, 1996; de Beer *et al.*, 1997; Larsen *et al.*, 1997) and one temperature sensor (3 mm diameter, Pt100, UST Umweltsensorentechnik GmbH) and were calibrated on board of the ship as described previously (de Beer *et al.,* 2006). Local fluxes and net conversions were calculated from the profile of *Beggiatoa* mat BM1, assuming steady state, diffusionally controlled transport and a porosity of 1.0 (Gieseke and de Beer, 2004).

$^{15}NH_4^+$ incubation experiments

For measurements of nitrification rates subsamples of *Beggiatoa* mats BM2a and BM3a, from non-hydrothermal surface sediment (NHS1) and from bottom sea water (BSW) were used. *Beggiatoa* mats were carefully transferred to 50 ml plastic vials using wide-bore pipet tips avoiding transfer of sediment particles. Then these mats were washed twice with sterile-filtered bottom sea water to remove particles and residual interstitial water. The washed mats were homogenized in order to destroy *Beggiatoa* filaments and to minimize formation of anoxic micro-niches, which could have caused nitrate respiration during the incubation. Then 5 ml of this cell suspension were mixed with 200 ml of sterile-filtered bottom sea water, transferred to a gas-tight bag and closed with a butyl stopper leaving a oxic head space of approximately 200 ml. From non-hydrothermal background sediment NHS1 the upper 4 mm of the surface layer were sliced off. Afterwards, 1.2 ml of sediment was

resuspended in 200 ml of sterile-filtered bottom sea water. For rate measurements of bottom sea water (BSW) 200 ml were directly transferred to the incubation bags.

After 1-2 h adaptation to shipboard conditions 250 µM of ^{15}N-NH_4Cl (>99% label, Sigma) were added to all bags containing *Beggiatoa* mats and bottom sea water. For incubation of sediment 500 µM of ^{15}N-NH_4Cl were added to increase sensitivity as we expected low rates in this type of sediment. As a control for bacterial ammonia oxidation we added 100 µM of allylthiourea ATU to mats BM2a and BM3a to inhibit the ammonia monooxygenase. All bags were incubated at 4°C for up to 36 h in the dark. Right before sampling bags were vigorously shaken and in 3-9 h intervals 6 ml of the initially 200 or 205 ml were withdrawn with a syringe, immediately transferred to exetainers without leaving a headspace, fixed with 50 µl of a saturated $HgCl_2$-solution and stored upside down at 4°C until further processing.

^{15}N-Isotope mass spectrometry

To determine nitrification rates from the bag incubations we measured the amount of $^{15}NO_3^-$ generated from added $^{15}NH_4^+$. We applied the established methods described by Füssel *et al.* (2012). Before measurements, all NO_2^- was removed by reducing it to N_2O and N_2 followed by degassing (Füssel *et al.,* 2012). Then all NO_3^- was converted to NO_2^- using spongy cadmium, which was further reduced to N_2 as described above. The formed N_2 was used for stable isotope analysis in the gas chromatography isotope mass spectrometer (GC-IRMS, Fisons VG Optima). All rates were calculated from the slopes of linear regression with ^{29}N-production as a function of time (Fig. S1). Standard deviations were calculated from ANOVA tests from data regressions. The nitrification rates were corrected for the *in situ* concentration of NH_4^+ in (filtered) bottom sea water and labelled $^{15}NH_4^+$, (250 µM, 500 µM) (Table S2).

Ammonium and nitrate measurements in mats, bottom sea waters and sediments

Bottom sea water overlaying *Beggiatoa* mats was recovered from Niskin bottles and from supernatants of push cores (0-20 cm above a mat) and was 0.15 µm-filtered. Sediment pore water was sampled by using Rhizons with 0.15 µm pore size (Rhizosphere Research Products, Wageningen, The Netherlands) that were vertically inserted into the sediment. All samples were stored at -20°C until analysis. Ammonia concentrations were measured according to a modified protocol by Kandeler and Gerber (1988). Samples were mixed with 300 µl of colour reagent solution (NaOH solution (0.3 M), sodium salicylate (17%) and sodium nitroprusside dehydrate (0.14%) solution and distilled water in a 1:1:1 ratio) and 120 µl oxidation solution (0.1% dichloroisocyanuric acid sodium salt dehydrate). After incubation of 30 min absorbance was measured at 660 nm. Nitrate was measured according to Braman and Hendrix (1989) using an CLD 60 NO_x analyzer (Eco Physics, USA).

DNA extraction

For genomic DNA extractions 250 µl of *Beggiatoa* mats BM2a, BM3a, BM2b, BM3b, BM4 and of sediments HS and NHS2 were sampled using wide bore pipet tips, transferred into bead-beating tubes and stored at -20°C. For bottom sea water (BSW) 500 ml were filtered on polycarbonate filters with a pore size of 0.2 µm and stored at -20°C. DNA was extracted from biological triplicates. From BM4 and NHS2 DNA was extracted only from a single sample and used for cloning and sequencing. All DNA was extracted using the PowerSoil® DNA Isolation Kit (MO BIO Laboratories, Inc., Carlsbad, USA) according to the manufacture's manual.

***amoA* gene libraries and phylogenetic analysis**

The archaeal *amoA* gene was amplified using primers Arch-*amoA*F and Arch-*amoA*R (Francis *et al*., 2005) (Table S3). Primers *amoA*-1F and *amoA*-2R (Rotthauwe *et al*., 1997)

were applied for amplification of the betaproteobacterial *amoA* and primers A189 and A682 (Holmes *et al*., 1995) as well as amoA3F and amoA4R (Purkhold *et al*., 2000) for the gammaproteobacterial *amoA* (Table S3). All reactions were performed under the following PCR conditions: initial denaturation at 95ºC for 5 min, followed by 30 cycles of denaturation at 95ºC for 30 s, primer annealing for 30 to 120 s, and extension at 72 ºC for 1 min followed by a final extension at 72°C for 10 min. Annealing temperatures were as follows: 53°C for archaeal and betaproteobacterial *amoA* primers, 48°C or 56°C for gammaproteobacterial *amoA* primers (Table S3). Primers were synthesized by Biomers (Ulm, Germany). PCR products were gel-purified and cloned using the TOPO TA cloning kit (Invitrogen, Karlsruhe, Germany). Randomly chosen clones were sequenced using an ABI PRISM3100 Genetic Analyser (Applied Biosystems, Darmstadt, Germany) or by GATC Biotech (Konstanz, Germany).

For phylogenetic analyses of archaeal and bacterial AmoA sequences the ARB program package was used (Ludwig *et al.,* 2004). After manual refinement of the sequence alignment maximum parsimony, distance-matrix (ARB Neighbour-Joining with the JTT correction factor) and maximum-likelihood calculations (Phylip-ML) were calculated considering 216 amino acid positions (archaeal AmoA) and a consensus tree was generated. Operational taxonomic units (OTUs) were defined at a threshold level of 98% using the *mothur* software package (Schloss *et al.,* 2009). The bacterial AmoA was phylogenetically analyzed considering 134 amino acid positions (Phylip-ML).

Quantitative PCR of archaeal and bacterial *amoA* genes

Quantification of *amoA* genes was conducted on DNA from three independent biological replicate samples. qPCR assays were performed in 96-well plates using a thermocycler IQ™5 (Bio-Rad, Hercules, USA). For calibration of the *amoA* gene assay archael *amoA* standards were generated from cloned sequences recovered from mat BM4 by

PCR amplification from plasmids using vector based primers. Standards were serially diluted to concentrations ranging from 10^8 to 10^2 copies μl^{-1}. DNA concentrations of standards were determined using a DNA spectrophotometer NanoDrop®ND-1000 (Wilmington, USA). Standards and the environmental samples were run in biological and technical triplicates. qPCR assays were repeated in three independent assays to check for reproducibility. Environmental DNA was diluted serially to determine template DNA concentrations without inhibiting the qPCR reaction. We applied primers and cycling parameters as described for *amoA* gene clone library generation, except that up to 50 cycles were performed. Fluorescence was recorded at 78°C to avoid detection of primer-dimers (Lam *et al.,* 2007). The qPCR assay contained 1x Power SYBR Green Master Mix (Applied Biosystems, USA), 500 pM of primers, 10 nm fluorescein (BioRad) and 5 µl of DNA template in a 25 µl reaction volume. The qPCR product sizes were checked with post real-time-PCR melting curves and agarose gel electrophoresis. All qPCR products displayed fragment sizes identical to those generated from archaeal or bacterial *amoA* clones. The R^2 values ranged from 0.99 to 1.00 and PCR efficiencies from 95% to 103%, respectively.

Archaeal 16S rRNA gene pyrotag analysis

Archaeal 16S rRNA gene fragments were amplified from DNA extracted from *Beggiatoa* mat BM3b, from bottom sea water (BSW) and from hydrothermally influenced sediment HS. We applied a 454 amplicon-pyrotag approach using primers 340f and 1000R (Table S3) using 30 PCR cycles in triplicate reactions. Triplicates were pooled and purified. DNA pools were then normalized according to DNA concentrations and were sequenced by GATC Biotech (Konstanz, Germany) using Roche's 454 FLX Titanium technology (Roche/454 Life Sciences, Branford). After separation of datasets according to sequence origin only sequences with a minimum read length of 400 bp and less than 2% of ambiguities and homopolymers were considered for calculations. After quality checks a total of 14,694

sequences were recovered that were analyzed as described by Klindworth *et al.* (2012) and classified according to the taxonomy of the SILVA SSURef 108 NR dataset (http://www.arb-silva.de/projects/ssu-ref-nr/) (Pruesse *et al.,* 2007).

16S rRNA-targeted CARD-FISH

For CARD-FISH *Beggiatoa* mats and sediments were fixed for up to 18 h at 4°C in 1.8% formaldehyde (Fluka, Taufkirchen, Germany) dissolved in sterile-filtered sea water. Samples were washed twice in 1x PBS and stored in PBS/ethanol (1:1, vol/vol) at -20°C. Bottom sea water was mixed with formaldehyde stock solution (37%) at a final concentration of 1.8% and fixed for up to 12 h at 4°C. Then 10 ml were filtered on polycarbonate membranes (0.2 µm pore size; 47 mm diameter; Millipore, Eschborn, Germany). Suspensions of *Beggiatoa* mats including intact filaments were filtered onto 0.2 µm polycarbonate membranes. Sediments were processed as described earlier and CARD-FISH on all samples was performed according to Ishii *et al.* (2004) using a $Alexa_{488}$-labelled tyramide. Archaeal cells were permeabilized using proteinase K according to Teira *et al.* (2004). Filter sections were embedded with a mix of Citifluor:VECTASHIELD [4:1] (VECTASHIELD® Mounting Medium H-1000, Vector Laboratories, Burlingame, CA, USA and Citifluor, London, UK) containing DAPI (4',6'-diamidino-2-phenylindole) at a final concentration of 1 µg ml^{-1}. Preparations were examined under an Axioplan II epifluorescence microscope (Zeiss, Jena, Germany).

Nucleotide sequence accession numbers

Nucleotide sequences (*amoA*) are available in the GenBank, EMBL and DDBJ databases under the accession numbers KC977572 - KC977911. The archaeal pyrotag sequences (16S rRNA gene) are available in the Sequence Read Archive under the accession number PRJEB4521.

Acknowledgements:

We thank the R/VAtlantis Crew and the *DSV Alvin* dive team. In particular, we are grateful to chief scientist Andreas Teske for giving the opportunity to attend both cruises. Captain AD Colburn is greatly acknowledged for his medical expertise. We thank Jessica Füssel and Tim Kalvelage for support in measuring nitrification rates and Elizabeth K. Robertson, Maria C. Suciu and Katrin Schmidt for their technical assistance. Many thanks also to Roland Hatzenpichler for helpful comments. Rudolf Amann is greatly acknowledged for excellent general support. This research was supported by the Cluster of Excellence MARUM and by the Max Planck Society.

References

Alawi, M., Lipski, A., Sanders, T., Pfeiffer, E.-M., and Spieck, E. (2007) Cultivation of a novel cold-adapted nitrite oxidizing betaproteobacterium from the Siberian Arctic. *ISME J* **1:** 256–264.

Baker, B.J., Lesniewski, R.A., and Dick, G.J. (2012) Genome-enabled transcriptomics reveals archaeal populations that drive nitrification in a deep-sea hydrothermal plume. *ISME J* **6:** 2269-2279.

Bedard, C., and Knowles, R. (1989) Physiology, biochemistry, and specific inhibitors of CH_4, NH_4^+, and CO oxidation by methanotrophs and nitrifiers. *Microbiol Rev* **53:** 68-84.

Beman, J.M., Popp, B.N., and Francis, C.A. (2008) Molecular and biogeochemical evidence for ammonia oxidation by marine Crenarchaeota in the Gulf of California. *ISME J* **2:** 429-441.

Boetius, A., and Suess, E. (2004) Hydrate Ridge: a natural laboratory for the study of microbial life fueled by methane from near-surface gas hydrates. *Chem Geol* **205:** 291-310.

Bonin; P.C. and Michotey, V.D. (2006) Nitrogen budget in a microbial mat in the Camargue (southern France). Mar Ecol Prog Series **322:** 75-84.

Bourbonnais, A., Juniper, S.K., Butterfield, D.A., Devol, A.H., Kuypers, M.M.M., Lavik, G., Hallam, S.J., Wenk, C.B., Chang, B.X., Murdock, S.A., and Lehmann, M.F. (2012a) Activity and abundance of denitrifying bacteria in the subsurface biosphere of diffuse hydrothermal vents of the Juan de Fuca Ridge. *Biogeosciences* **9:** 4661-4678.

Bourbonnais, A., Lehmann, M.F., Butterfield, D.A., and Juniper, S.K. (2012b) Subseafloor nitrogen transformations in diffuse hydrothermal vent fluids of the Juan de Fuca Ridge evidenced by the isotopic composition of nitrate and ammonium. *Geochem Geophy Geosy* **13**. doi: 10.1029/2011GC003863.

Bowles, M.W., Nigro, L.M., Teske, A.P., and Joye, S.B. (2012) Denitrification and environmental factors influencing nitrate removal in Guaymas Basin hydrothermally altered sediments. *Front Aquat Microbiol* **3**. doi: 10.3389/fmicb.2012.00377

Braman, R.S., and Hendrix, S.A. (1989) Nanogram nitrite and nitrate determination in environmental and biological materials by vanadium(III) reduction with chemiluminescence detection. *Anal Chem* **61:** 2715-2718.

Caffrey, J.M., Bano, N., Kalanetra, K., and Hollibaugh, J.T. (2007) Ammonia oxidation and ammonia-oxidizing bacteria and archaea from estuaries with differing histories of hypoxia. *ISME J* **1:** 660-662.

Coolen, M.J.L., Abbas, B., van Bleijswijk, J., Hopmans, E.C., Kuypers, M.M.M., Wakeham, S.G., and Damste, J.S.S. (2007) Putative ammonia-oxidizing Crenarchaeota in suboxic waters of the Black Sea: a basin-wide ecological study using 16S ribosomal and functional genes and membrane lipids. *Environ Microbiol* **9:** 1001-1016.

Coskuner, G., Ballinger, S.J., Davenport, R.J., Pickering, R.L., Solera, R., Head, I.M., and Curtis, T.P. (2005) Agreement between theory and measurement in quantification of ammonia-oxidizing bacteria. *Appl Environ Microbiol* **71:** 6325-6334.

Davis, R.E., Stakes, D.S., Wheat, C.G., and Moyer, C.L. (2009) Bacterial variability within an iron-silica-manganese-rich hydrothermal mound located off-axis at the Cleft Segment, Juan de Fuca Ridge. *Geomicrobiol J* **26:** 570-580.

de Beer, D., Glud, A., Epping, E., and Kühl, M. (1997) A fast responding CO_2 microelectrode for profiling sediments, microbial mats, and biofilms. *Limnol Oceanogr* **42:** 1590-1600.

de Beer, D., Sauter, E., Niemann, H., Kaul, N., Foucher, J.P., Witte, U., Schluter, M., and Boetius, A. (2006) In situ fluxes and zonation of microbial activity in surface sediments of the Hakon Mosby Mud Volcano. *Limnol Oceanogr* **51:** 1315-1331.

Erguder, T.H., Boon, N., Wittebolle, L., Marzorati, M., and Verstraete, W. (2009) Environmental factors shaping the ecological niches of ammonia-oxidizing archaea. *FEMS Microbiol Rev* **33:** 855-869.

Francis, C.A., O'Mullan, G.D., and Ward, B.B. (2003) Diversity of ammonia monoxygenase *amoA* genes across environmental gradients in Chesapeake Bay sediments. *Geobiology* **1:** 129-140.

Francis, C.A., Roberts, K.J., Beman, J.M., Santoro, A.E., and Oakley, B.B. (2005) Ubiquity and diversity of ammonia-oxidizing archaea in water columns and sediments of the ocean. *Proc Natl Acad Sci* **102:** 14683-14688.

Füssel, J., Lam, P., Lavik, G., Jensen, M.M., Holtappels, M., Gunter, M., and Kuypers, M.M.M. (2012) Nitrite oxidation in the Namibian oxygen minimum zone. *ISME J* **6:** 1200-1209.

Gieseke, A., and de Beer, D. (2004) Use of microelectrodes to measure in situ microbial activities in biofilms, sediments, and microbial mats. In *Molecular Microbial Ecology Manual*. Akkermans A.D.L., van Elsas D. (eds). Dordrecht (The Netherlands). Kluwer, pp. 1581-1612.

Ginestet, P., Audic, J.M., Urbain, V., and Block, J.C. (1998) Estimation of nitrifying bacterial activities by measuring oxygen uptake in the presence of the metabolic inhibitors allylthiourea and azide. *Appl Environ Microbiol* **64:** 2266-2268.

Glud, R.N., Thamdrup, B., Stahl, H., Wenzhöfer, F., Glud, A., Nomaki, H., Oguri, K., Revsbech, N.P., and Kitazato, H. (2009) Nitrogen cycling in a deep ocean margin sediment (Sagami Bay, Japan). *Limnol Oceanogr* **54:** 723-734.

Gundersen, J.K., Jørgensen, B.B., Larsen, E., and Jannasch, H.W. (1992) Mats of giant sulphur bacteria on deep-sea sediments due to fluctuating hydrothermal flow. *Nature* **360:** 454-456.

Hatzenpichler, R., Lebecleva, E.V., Spieck, E., Stoecker, K., Richter, A., Daims, H., and Wagner, M. (2008) A moderately thermophilic ammonia-oxidizing crenarchaeote from a hot spring. *Proc Natl Acad Sci U S A* **105:** 2134-2139.

Hatzenpichler, R. (2012) Diversity, physiology and niche differentiation of ammonia-oxidizing archaea. *Appl Environ Microbiol* **78:** 7501-7510

Heisterkamp, I.M., Kamp, A., Schramm, A.T., de Beer, D., and Stief, P. (2012) Indirect control of the intracellular nitrate pool of intertidal sediment by the polychaete *Hediste diversicolor*. *MEPS* **445:** 181-192.

Høgslund, S., Revsbech, N.P., Kuenen, J.G., Jorgensen, B.B., Gallardo, V.A., van de Vossenberg, J.V., Nielsen, J.L., Holmkvist, L., Arning, E.T., and Nielsen, L.P. (2009) Physiology and behaviour of marine Thioploca. *The ISME Journal* **3:** 647-657.

Holmes, A.J., Costello, A., Lidstrom, M.E., and Murrell, J.C. (1995) Evidence that participate methane monooxygenase and ammonia monooxygenase may be evolutionarily related. *FEMS Microbiol Let* **132:** 203-208.

Ishii, K., Mussmann, M., MacGregor, B.J., and Amann, R. (2004) An improved fluorescence in situ hybridization protocol for the identification of bacteria and archaea in marine sediments. *FEMS Microbiol Ecol* **50:** 203-212.

Jannasch, H.W., and Mottl, M.J. (1985) Geomicrobiology of deep-sea hydrothermal vents. *Science* **229:** 717-725.

Jannasch, H.W., Nelson, D.C., and Wirsen, C.O. (1989) Massive natural occurrence of unusually large bacteria (*Beggiatoa* sp.) at a hydrothermal deep-Sea vent site. *Nature* **342:** 834-836.

Jeroschewski, P., Steuckart, C., and Kühl, M. (1996) An amperometric microsensor for the determination of H_2S in aquatic environments. *Anal Chem* **68:** 4351-4357.

Jørgensen, B.B. (1977) Distribution of colourless sulfur bacteria (*Beggiatoa* spp.) in a coastal marine sediment. *Mar Biol* **41:** 19-28.
Jørgensen, B.B., and Nelson, D.C. (2004) Sulfide oxidation in marine sediments: geochemistry meets microbiology. In *Sulfur Biogeochemistry – Past and Present*. Amend J.P., Edwards K.J., Lyons T.W. (eds). Boulder, Colorado: Geological Society of America, pp. 63-81.
Joye, S.B., and Hollibaugh, J.T. (1995) Influence of sulfide inhibition of nitrification on nitrogen regeneration in sediments. *Science* **270:** 623-625.
Kandeler, E., and Gerber, H. (1988) Short-term assay of soil urease activity using colorimetric determination of ammonium. *Biol Fertil Soils* **6:** 68-72.
Kato, S., Kobayashi, C., Kakegawa, T., and Yamagishi, A. (2009) Microbial communities in iron-silica-rich microbial mats at deep-sea hydrothermal fields of the Southern Mariana Trough. *Environ Microbiol* **11:** 2094-2111.
Klindworth, A., Pruesse, E., Schweer, T., Peplies, J., Quast, C., Horn, M., and Glöckner, F.O. (2012) Evaluation of general 16S ribosomal RNA gene PCR primers for classical and next-generation sequencing-based diversity studies. *Nucleic Acids Res* **41**. doi:10.1093/nar/gks808.
Lam, P., Cowen, J.P., and Jones, R.D. (2004) Autotrophic ammonia oxidation in a deep-sea hydrothermal plume. *FEMS Microbiol Ecol* **47:** 191-206.
Lam, P., Jensen, M.M., Lavik, G., McGinnis, D.F., Muller, B., Schubert, C.J., Amann, R., Thamdrup, B., and Kuypers, M.M.M. (2007) Linking crenarchaeal and bacterial nitrification to anammox in the Black Sea. *Proc Natl Acad Sci U S A* **104:** 7104-7109.
Lam, P., Cowen, J.P., Popp, B.N., and Jones, R.D. (2008) Microbial ammonia oxidation and enhanced nitrogen cycling in the Endeavour hydrothermal plume. *Geochim Cosmochim Acta* **72:** 2268-2286.
Larsen, L.H., Kjaer, T., and Revsbech, N.P. (1997) A microscale NO_3^- biosensor for environmental applications. *Anal Chem* **69:** 3527-3531.
Lehmann, M.F., Sigman, D.M., and Berelson, W.M. (2004) Coupling the $^{15}N/^{14}N$ and $^{18}O/^{16}O$ of nitrate as a constraint on benthic nitrogen cycling. *Mar Chem* **88:** 1-20.
Lehtovitra-Morley, L.E., Verhamme, D.T., Nicol, G.W., and Prosser, J.I. (2013) Effect of nitrification inhibitors on the growth and activity of *Nitrosotalea devanaterra* culture and soil. *Soil Biol Biochem* **62:** 129-133.
Lesniewski, R.A., Anantharaman, K., and Dick, G.J. (2012) Metatranscriptomic insights into the geomicrobiology of deep-sea hydrothermal plumes. *ISME J* **6:** 2269–2279.
Lilley, M.D., Butterfield, D.A., Olson, E.J., Lupton, J.E., Macko, S.A., and McDuff, R.E. (1993) Anomalous CH_4 and NH_4^+ concentrations at an unsedimented mid-ocean ridge hydrothermal system. *Nature* **364:** 45-47.
Lloyd, K.G., Albert, D.B., Biddle, J.F., Chanton, J.P., Pizarro, O., and Teske, A. (2010) Spatial structure and activity of sedimentary microbial communities underlying a *Beggiatoa* spp. mat in a Gulf of Mexico hydrocarbon seep. *PLoS ONE* **5**. e8738.
Ludwig, W., Strunk, O., Westram, R., Richter, L., Meier, H., Yadhukumar, Buchner, A., Lai, T., Steppi, S., Jobb, G., Förster, W., Brettske, I., Gerber, S., Ginhart, A.W., Gross, O., Grumann, S., Hermann, S., Jost, R., König, A., Liss, T., Lussmann, R., May, M., Nonhoff, B., Reichel, B., Strehlow, R., Stamatakis, A., Stuckmann, N., Vilbig, A., Lenke, M., Ludwig, T., Bode, A., and Schleifer, K.H. (2004) ARB: a software environment for sequence data. *Nucleic Acids Res* **32:** 1363-1371.
Magenheim, A.J., and Gieskes, J.M. (1992) Hydrothermal discharge and alteration in near-surface sediments from the Guaymas Basin, Gulf of California. *Geochim Cosmochim Acta* **56:** 2329-2338.

Martens-Habbena, W., Berube, P.M., Urakawa, H., de la Torre, J.R., and Stahl, D.A. (2009) Ammonia oxidation kinetics determine niche separation of nitrifying Archaea and Bacteria. *Nature* **461:** 976-979.

McHatton, S.C., Barry, J.P., Jannasch, H.W., and Nelson, D.C. (1996) High nitrate concentrations in vacuolate, autotrophic marine *Beggiatoa* spp. *Appl Environ Microbiol* **62:** 954-958.

McKay, L.J., MacGregor, B.J., Biddle, J.F., Albert, D.B., Mendlovitz, H.P., Hoer, D.R., Lipp, J.S., Lloyd, K.G., and Teske, A.P. (2012) Spatial heterogeneity and underlying geochemistry of phylogenetically diverse orange and white *Beggiatoa* mats in Guaymas Basin hydrothermal sediments. *Deep Sea Res Part I* **67:** 21-31.

Molina, V., Belmar, L., and Ulloa, O. (2010) High diversity of ammonia-oxidizing archaea in permanent and seasonal oxygen-deficient waters of the eastern South Pacific. *Environ Microbial* **12:** 2450-2465.

Mussmann, M., Schulz, H.N., Strotmann, B., Kjaer, T., Nielsen, L.P., Rossello-Mora, R.A., Amann, R.I., and Jørgensen, B.B. (2003) Phylogeny and distribution of nitrate-storing *Beggiatoa* spp. in coastal marine sediments. *Environ Microbiol* **5:** 523-533.

Nakagawa, S., and Takai, K. (2008) Deep-sea vent chemoautotrophs: diversity, biochemistry and ecological significance. *FEMS Microbiol Ecol* **65:** 1-14.

Nelson, D.C., Revsbech, N.P., and Jorgensen, B.B. (1986) Microoxic-anoxic niche of *Beggiatoa* spp. - microelectrode survey of marine and fresh-water strains. *Appl Environ Microbiol* **52:** 161-168.

Nunoura, T., Oida, H., Nakaseama, M., Kosaka, A., Ohkubo, S.B., Kikuchi, T., Kazama, H., Hosoi-Tanabe, S., Nakamura, K., Kinoshita, M., Hirayama, H., Inagaki, F., Tsunogai, U., Ishibashi, J., and Takai, K. (2010) Archaeal diversity and distribution along thermal and geochemical gradients in hydrothermal sediments at the Yonaguni Knoll IV hydrothermal field in the southern Okinawa Trough. *Appl Environ Microbiol* **76:** 1198-1211.

O'Mullan, G.D. and Ward, B.B. (2005) Relationship of temporal and spatial variabilities of ammonia-oxidizing bacteria to nitrification rates in Monterey Bay, California. *Appl Environ Microb* **71:** 697-705.

Orcutt, B.N., Sylvan, J.B., Knab, N.J., and Edwards, K.J. (2011) Microbial ecology of the dark ocean above, at, and below the seafloor. *Microbiol Mol Biol Rev* **75:** 361-422.

Park, B.J., Park, S.J., Yoon, D.N., Schouten, S., Damste, J.S.S., and Rhee, S.K. (2010) Cultivation of autotrophic ammonia-oxidizing archaea from marine sediments in coculture with sulfur-oxidizing bacteria. *Appl Environ Microbiol* **76:** 7575-7587.

Pester, M., Rattei, T., Flechl, S., Gröngröft, A., Richter, A., Overmann, J., Reinhold-Hurek, B., Loy, A., and Wagner, M. (2012) *amoA*-based consensus phylogeny of ammonia-oxidizing archaea and deep sequencing of *amoA* genes from soils of four different geographic regions. *Environ Microbiol* **14:** 525-539.

Pitcher, A., Villanueva, L. Hopmans, E.C., Schouten, S., Reichart, G.-J., and Damsté, J.S.S. (2011) Niche segregation of ammonia-oxidizing archaea and anammox bacteria in the Arabian Sea oxygen minimum zone. *ISME J* **5:** 1896-1904.

Preisler, A., de Beer, D., Lichtschlag, A., Lavik, G., Boetius, A., and Jorgensen, B.B. (2007) Biological and chemical sulfide oxidation in a *Beggiatoa* inhabited marine sediment. *ISME J* **1:** 341-353.

Prokopenko, M.G., Hammond, D.E., Berelson, W.M., Bernhard, J.M., Stott, L., and Douglas, R. (2006) Nitrogen cycling in the sediments of Santa Barbara Basin and Eastern Subtropical North Pacific: Nitrogen isotopes, diagenesis and possible chemosymbiosis between two lithotrophs (*Thioploca* and Anammox) - "riding on a glider". *Earth Planet Sci Lett* **242:** 186-204.

Pruesse, E., Quast, C., Knittel, K., Fuchs, B.M., Ludwig, W., Peplies, J., and Glöckner, F.O. (2007) SILVA: a comprehensive online resource for quality checked and aligned ribosomal RNA sequence data compatible with ARB. *Nucleic Acids Res* **35:** 7188-7196.

Purkhold, U., Pommering-Röser, A., Juretschko, S., Schmid, M.C., Koops, H.P., and Wagner, M. (2000) Phylogeny of all recognized species of ammonia oxidizers based on comparative 16S rRNA and *amoA* sequence analysis: implications for molecular diversity surveys. *Appl Environ Microbiol* **66:** 5368-5382.

Revsbech, N.P., and Ward, D.M. (1983) Oxygen microelectrode that is insensitive to medium chemical composition: use in an acid microbial mat dominated by *Cyanidium caldarium*. *Appl Environ Microbiol* **45:** 755-759.

Rotthauwe, J.H., Witzel, K.P., Liesack, W. (1997) The ammonia monooxygenase structural gene *amoA* as a functional marker: molecular fine-scale analysis of natural ammonia-oxidizing populations. *Appl Environ Microbiol* **63:** 4704-4712.

Russ, L., Kartal, B., Op den Camp, H.J.M., Sollai, M., Godfroy, A., Damsté, J.S.S., and Jetten, M.S.M. (2013) Presence and diversity of anammox bacteria in cold hydrocarbon-rich seeps and hydrothermal vent sediments of the Guaymas Basin. *Front Microbiol* **4:** 219.

Rysgaard, S., Risgaard-Petersen, N., and Sloth, N.P. (1996) Nitrification, denitrification, and nitrate ammonification in sediments of two coastal lagoons in Southern France. *Hydrobiologia* **329:** 133-141.

Santoro, A.E., and Casciotti, K.L. (2011) Enrichment and characterization of ammonia-oxidizing archaea from the open ocean: phylogeny, physiology and stable isotope fractionation. *ISME J* **5:** 1796-1808.

Schloss, P.D., Westcott, S.L., Ryabin, T., Hall, J.R., Hartmann, M., Hollister, E.B., Lesniewski, R.A., Oakley, B.B., Parks, D.H., Robinson, C.J., Sahl, J.W., Stres, B., Thallinger, G.G., Van Horn, D.J., and Weber, C.F. (2009) Introducing mothur: open-source, platform-independent, community-supported software for describing and comparing microbial communities. *Appl Environ Microbiol* **75:** 7537-7541.

Shen, T., Stiegelmeier, M., Jiulan, D., Urich, T., and Schleper C. (2013) Responses of the terrestrial ammonia-oxidizing archaeon *Ca.* Nitrososphaera viennensis and the ammonia-oxidizing bacterium *Nitrosospira multiformis* to nitrification inhibitors. *FEMS Microbiol Lett* **340:** 121-129.

Sorokin, D.Y., Lucker, S., Vejmelkova, D., Kostrikina, N.A., Kleerebezem, R., Rijpstra, W.I.C., Damste, J.S.S., Le Paslier, D., Muyzer, G., Wagner, M., van Loosdrecht, M.C.M., and Daims, H. (2012) Nitrification expanded: discovery, physiology and genomics of a nitrite-oxidizing bacterium from the phylum *Chloroflexi*. *ISME J* **6:** 2245–2256.

Sylvan, J.B., Toner, B.M., and Edwards, K.J. (2012) Life and death of deep-sea vents: bacterial diversity and ecosystem succession on inactive hydrothermal sulfides. *Mbio* **3**. e00279.

Taylor, A.E., Vajrala, N., Giguere, A. T., Gitelman, A.I., Arp, D.J., Myrold, D.D., Sayavedra-Soto, L. and Bottomley, P.J. (2013) Use of aliphatic n-alkynes to discriminate soil nitrification activities of ammonia-oxidizing thaumarchaea and bacteria, *Appl Environ Microbiol* Published ahead of print doi: 10.1128/AEM.01928-13.

Teira, E., Reinthaler, T., Pernthaler, A., Pernthaler, J., and Herndl, G.J. (2004) Combining catalyzed reporter deposition-fluorescence in situ hybridization and microautoradiography to detect substrate utilization by bacteria and archaea in the deep ocean. *Appl Environ Microbiol* **70:** 4411-4414.

Teske, A., and Nelson, D.C. (2006) The genera *Beggiatoa* and *Thioploca*. In *The Prokaryotes*. Dworkin M., Falkow S., Rosenberg E., Schleifer K.-H., Stackebrandt E. (eds). New York: Springer pp. 784-810.

Von Damm, K.L., Edmond, J.M., Measures, C.I., and Grant, B. (1985) Chemistry of submarine hydrothermal solutions at Guaymas Basin, Gulf of California. *Geochim Cosmochim Acta* **49:** 2221–2237.

Wang, S.F., Xiao, X., Jiang, L.J., Peng, X.T., Zhou, H.Y., Meng, J., and Wang, F.P. (2009) Diversity and abundance of ammonia-oxidizing archaea in hydrothermal vent chimneys of the Juan de Fuca Ridge. *Appl Environ Microbiol* **75:** 4216-4220.

Wenzhöfer, F., Holby, O., Glud, R.N., Nielsen, H.K., and Gundersen, J.K. (2000) *In situ* microsensor studies of a shallow water hydrothermal vent at Milos, Greece. *Mar Chem* **69:** 43-54.

Table 1: Copy numbers of archaeal and betaproteobacterial *amoA* genes and semi-quantitative results of 16S rRNA-targeted CARD-FISH. Details of the applied probes and primers are given in Table S3.

	archaeal *amoA*	**bacterial[1] *amoA***	**relative cell abundance (% of total cell counts)**					
sample	copies/ml [x 10^6]	copies/ml [x 10^4]	thaumarchaeotes (MGI-554)	Beta-AOB (NSO1225/NSO190)	Gamma-AOB (Nscoc128)	*Nitrospira* (Ntspa662)	*Nitrococcus* (Ntcoc84)	*Nitrospina* (Ntspn693)
Beggiatoa mat (BM2a)	1.1	35	>8	-	≤0.5%	≤0.5%	≤0.5%	-
Beggiatoa mat (BM2b)	3.4 ±0.5	3.4 ±0.2	>8	>1	≤0.5%	≤0.5%	≤0.5%	≤0.5%
Beggiatoa mat (BM3a)	n.d.	n.d.	>6	>1	≤0.5%	-	≤0.5%	≤0.5%
Beggiatoa mat (BM3b)	3.4 ±1.2	4.9 ±0.3	n.d.	n.d.	n.d.	n.d.	n.d.	n.d.
hydrothermal sediment (HS1)	2.5 ±0.5	-	≤0.5%	≤0.5%	-	≤0.5%	-	≤0.5%
bottom sea water (BSW)	0.0005 ±0.4	-	≤0.5%	≤0.5%	≤0.5%	-	-	-

[1], only betaproteobacterial *amoA*, gammaproteobacterial *amoA* could not be amplified
-, not detectable
n.d., not determined

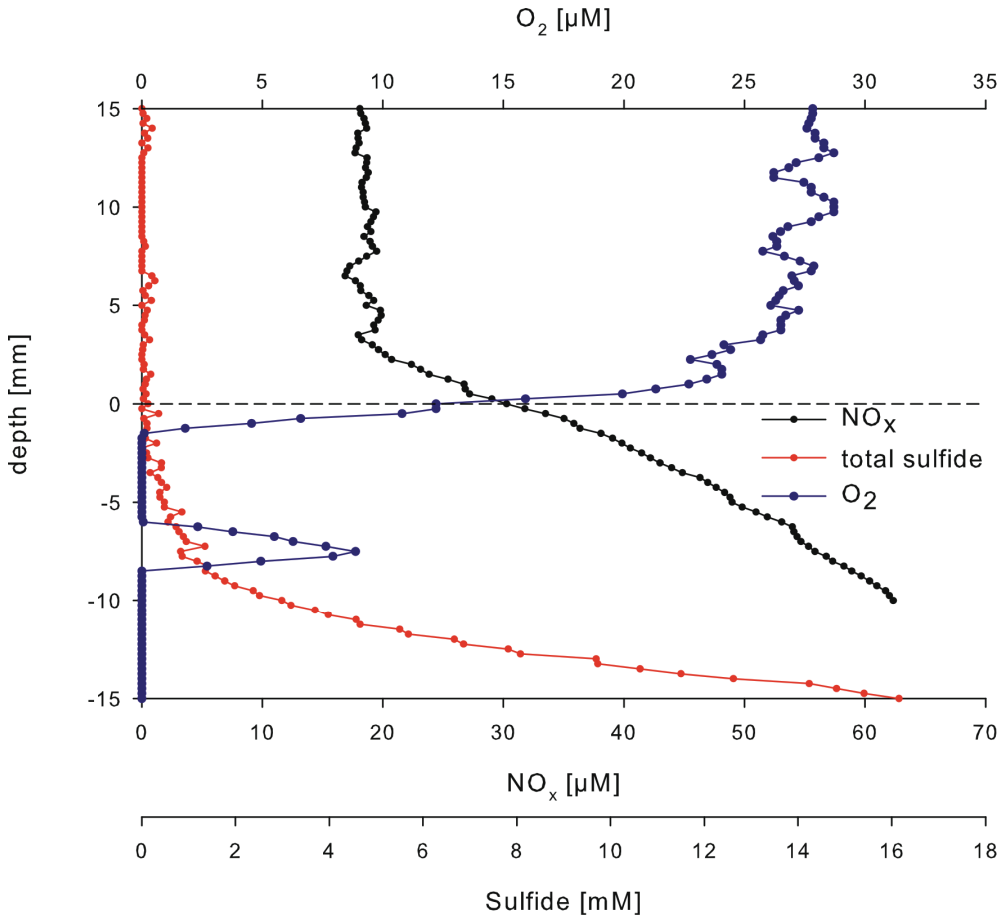

Figure 1: *In situ* microsensor profiles of O2, NO_x and sulfide in *Beggiatoa* mat BM1 at the sediment surface of the Guaymas Basin hydrothermal system (*Alvin* dive 4564). Dashed line indicates the approximate upper border of the *Beggiatoa* mat.

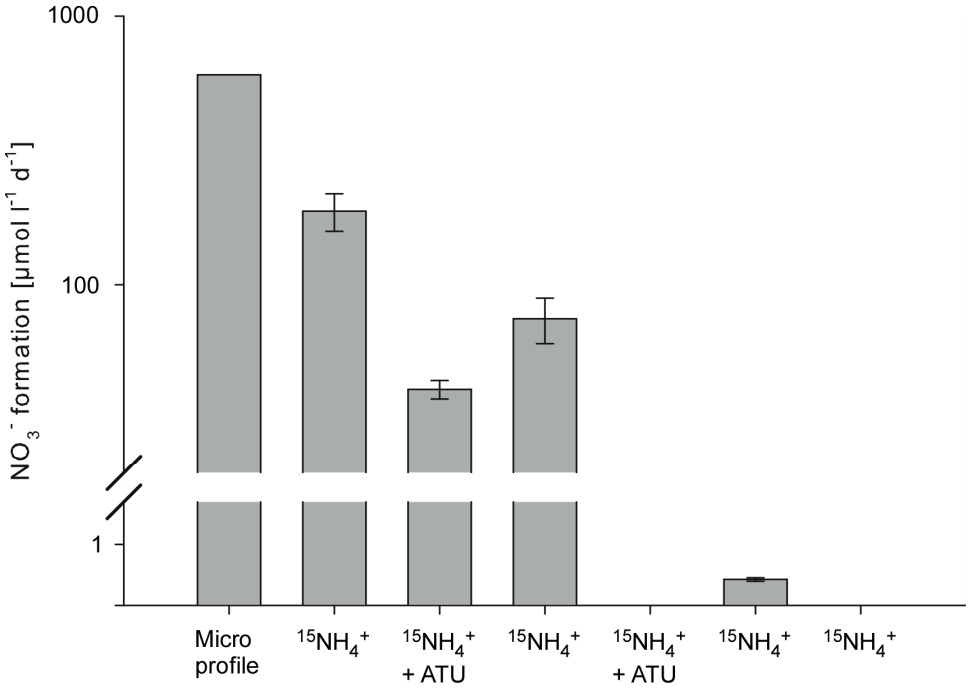

Figure 2: Nitrification rates in three compartments of the Guaymas Basin hydrothermal system. BM1, *Beggiatoa* mat; BM2a, *Beggiatoa* mat; BM3a, *Beggiatoa* mat; BSW, bottom sea water; NHS1, non-hydrothermal sediment. Samples were incubated for up to 36h at 4°C. Note that the nitrification rate in *Beggiatoa* mat BM1 was calculated from the NO_x profile (Fig. 1).

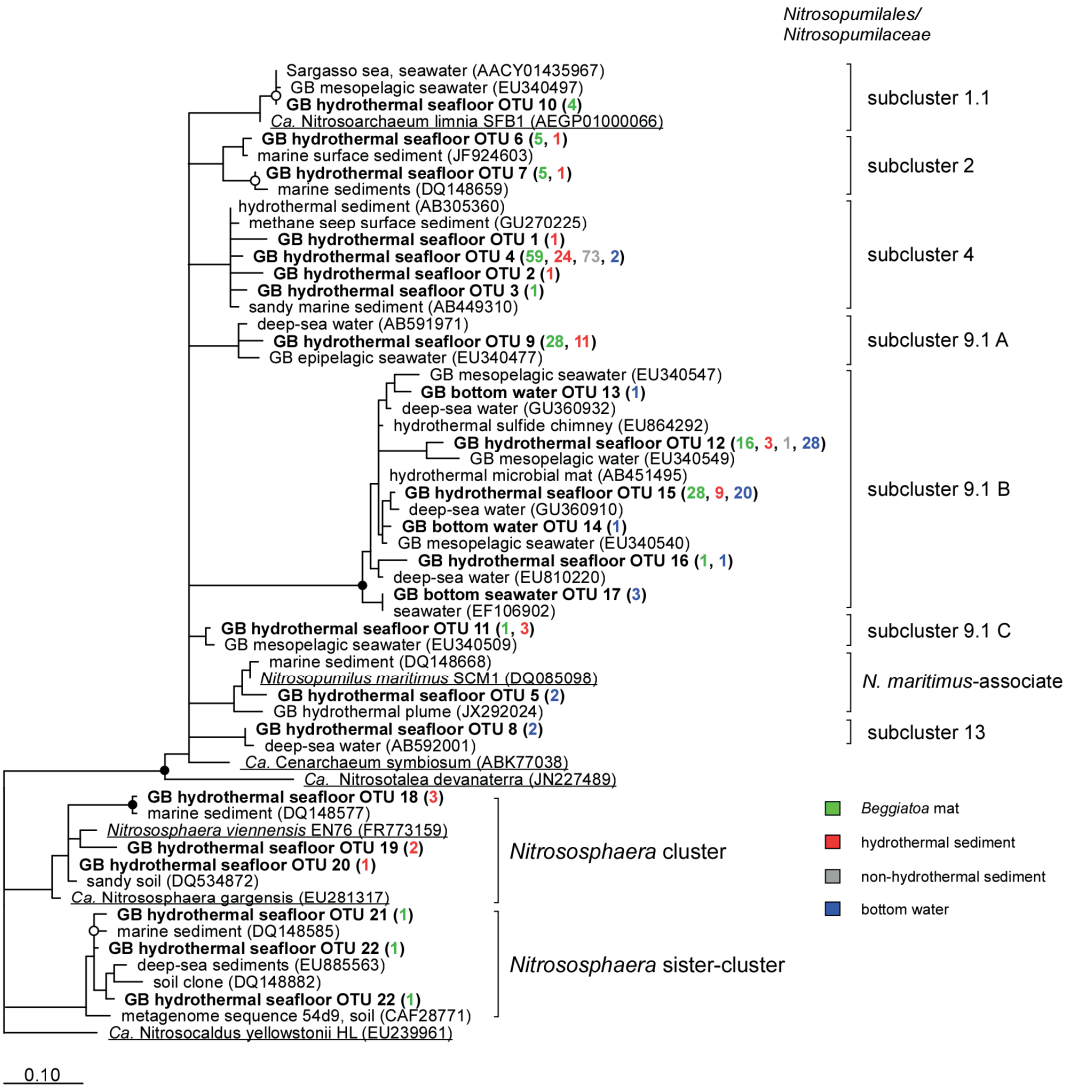

Figure 3: Consensus tree of archaeal AmoA sequences from four compartments of the Guaymas Basin hydrothermal system. Subclusters were defined according to Pester *et al*. (2012) but we assigned subclusters to the order/family designation *Nitrosopumilus/Nitrosopumilaceae* instead of the genus *Nitrosopumilus*. Open circles indicate > 70% bootstrap support, closed circles indicate > 90% bootstrap support (RAxML). Scale bar corresponds to 10% sequence changes.

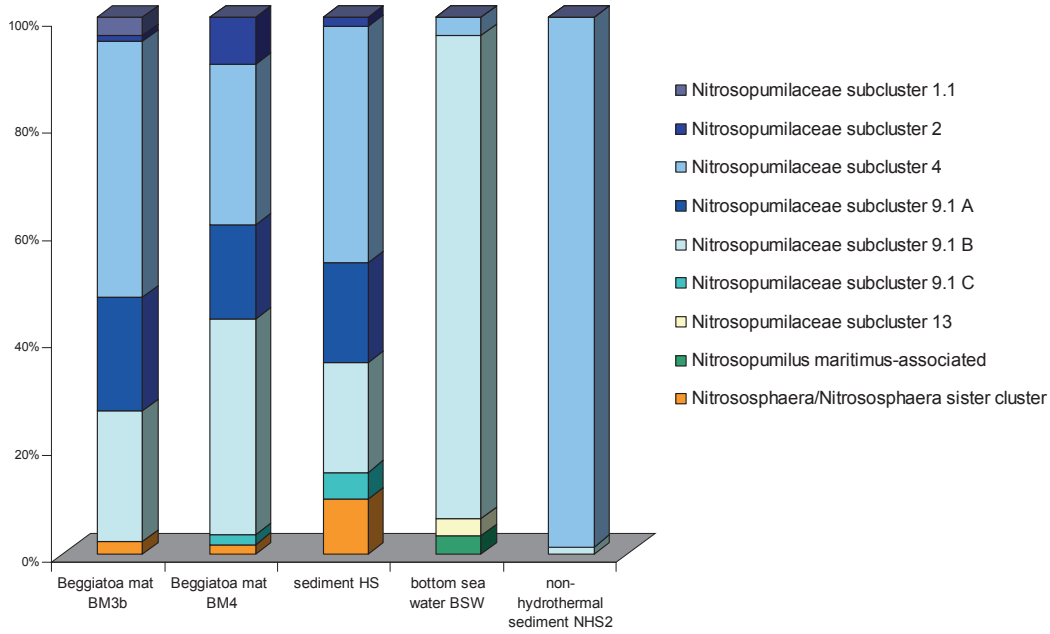

Figure 4: Phylogenetic distribution of in total 340 archaeal AmoA sequences in *Beggiatoa* mats (BM3b and BM4), bare, hydrothermally influenced sediment (HS), non-hydrothermal sediments (NHS2), and in bottom sea water (BSW) of the Guaymas Basin hydrothermal system.

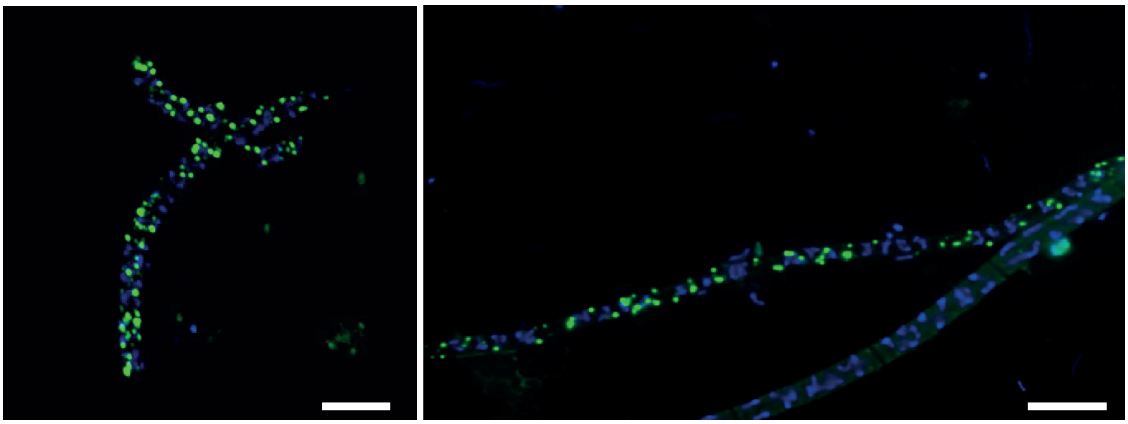

Figure 5: CARD-FISH targeting the 16S rRNA of MG-I.1a thaumarchaeotes (green fluorescence -probe MGI-554) on narrow *Beggiatoa*-like filaments stained by DAPI (blue fluorescence). Scale bars refer to 7 µm.

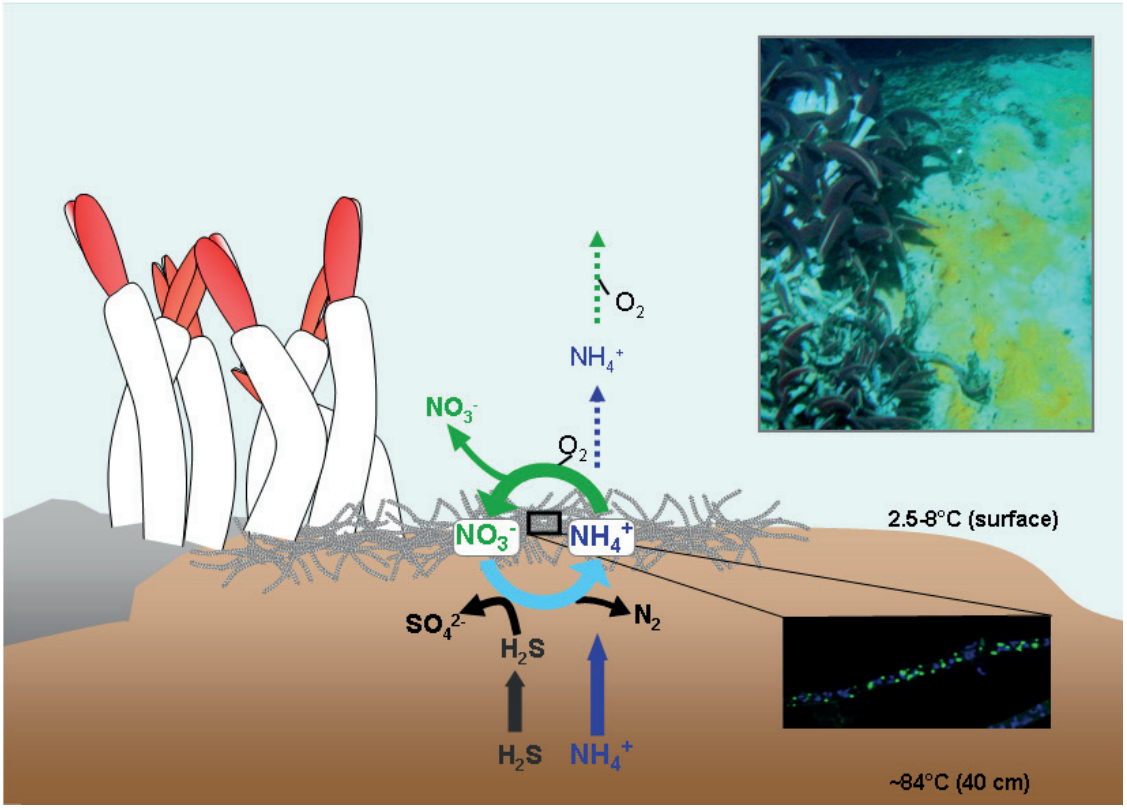

Figure 6: Model of possible N-cycling in a *Riftia-Beggiatoa* mound at a hydrothermal vent of the Guaymas Basin.

Supporting Information

Tables

Table S1. Samples collected for nitrification rate measurements and molecular analyses

	Alvin **dive-core**	**depth [m]**	**N_{ox} rate**	**FISH**	***amoA*** **gene libraries**		***amoA*** **qPCR**		**archaeal pyrotags**
					AOA	AOB[a]	AEA	AOB	
Beggiatoa mat BM2a	4564-24	2003	+	+			+		
Beggiatoa mat BM2b	4564-21	2003		+			+	+	
Beggiatoa mat BM3a	4568-25	2010	+	+					
Beggiatoa mat BM3b	4568-6	2010		+	+		+	+	+
Beggiatoa mat BM4	4487-6	2010		+	+	+			
Bottom sea water BSW	4564	2002	+	+	+		+		+
Hydrothermally influenced sediment HS	4565-5	2001		+	+		+	+	+
Non-hydrothermal sediment NHS1	4567-20	2011	+						
Non-hydrothermal sediment NHS2	4491-31	2006			+	+			

[a] AOB, ammonia-oxidizing bacteria (only betaproteobacterial *amoA*)

Table S2: Nitrate and ammonium concentrations in different compartments of the Guaymas Basin hydrothermal system.

Sample	***Alvin* dive-core**	**NO_3^- (µM)**	**NH_4^+ (µM)**	**T (°C) at surface**
***Beggiatoa* mats (0-1 cm) and sediment underneath**	4563-13, 0-1 cm	42.0	2239.3	3.6
	4564-24, 0-1 cm (BM2)	43.2	390.9	57-59
	4568-6, 0-1 cm (BM3)	42.0	1587.6	3.4
	4562-17, 0-5 cm	47.9	4751.8	8-24
	4562-10, 0-5 cm	9.8	5309.1	3.9-24.7
	4562-10, 8-12 cm	11.5	6612.5	23.9-34.5
	4562-17, 10-15 cm	3.6	6792.6	36.8-48.9
	4563-13, 5-10 cm	3.9	4443.1	5.2-7.7
	4568-25, 0-5 cm	-	944.5	3.5-16.7
	4568-5, 0-5 cm	19.5	52.7	3.2-13.1
	4569-21, 0-5 cm	-	618.6	15-23
	4572-15, 0-5 cm	31.7	524.3	3-4.3
	4572-16, 0-5 cm	-	1167.4	19
background sediment	4567-3, 0-5 cm	14.8	267.1	3.2
background sediment NHS2	4567-20, 0-5 cm	3.5	0.0	3.2
bottom sea water (supernatant of cores, 0-~30cm above sea floor)	4562-10	24.8	105.8	3.9
	4562-13	18.5	118.2	3.2
	4562-13	12.8	370.3	3.2
	4564-21	16.1	111.0	-
	4564-24	111.4	168.6	-
	4565-1	6.7	678.0	3.3
	4567-20	11.2	68.8	3.2
	4567-3	14.4	68.8	3.2
	4568-14	13.7	121.3	5.3
	4568-25	14.7	61.6	3.5
	4568-5	19.0	70.9	3.2
	4569-21	9.0	82.2	15.1
	4570-1	11.5	114.1	-
	4572-13	11.5	113.0	3.2
	4572-20	20.2	67.8	-
bottom sea water (~1 m above sea floor)	4563 Niskin bottle 5	42.5	34.8	3
	4563 Niskin bottle 4	43.9	34.8	3
	4564 Niskin bottle 5	54.6	78.1	3

Table S3: Probes and primers used in this study

Probe/primer	target molecule	target group	sequence 5' - 3'	T[a] [°C]	FA[b] [%]	reference
probes						
NON338	16S rRNA	negative control	ACT CCT ACG GGA GGC AGC		0-50	Wallner *et al.*, 1993
MGI-554	16S rRNA	MG-I.1a thaumarchaeotes	TTA GGC CCA ATA ATC MTC CT		20	Massana *et al.*, 1997
Nso1225	16S rRNA	betaproteobacterial ammonia-oxidizing bacteria	CGC CAT TGT ATT ACG TGT GA		35	Mobarry *et al.*, 1996
Nscoc128	16S rRNA	gammaproteobacterial ammonia-oxidizing bacteria	CCC CTC TAG AGG CCA GAT		35	Juretschko, 2000
Ntspa662	16S rRNA	genus *Nitrospira*	GGA ATT CCG CGC TCC TCT		35	Daims *et al.*, 2001
Ntspa662comp	16S rRNA	competitor to Ntspa662	GGA ATT CCG CTC TCC TCT		35	Daims *et al.*, 2001
Ntspn693	16S rRNA	*Nitrospina gracilis*	TTC CCA ATA TCA ACG CAT TT		10	Juretschko, 2000
NIT3	16S rRNA	*Nitrobacter* spp.	CCT GTG CTC CAT GCT CCG		40	Wagner *et al.*, 1996
NIT3 comp.	16S rRNA	competitor for NIT3	CCT GTG CTC CAG GCT CCG		40	Wagner *et al.*, 1996
Ntcoc84	16S rRNA	*Nitrococcus mobilis*	TCG CCA GCC ACC TTT CCG		10	Juretschko, 2000
Primers						
Arch-amoAF	*amoA*	ammonia oxidizing archaea	STA ATG GTC TGG CTT AGA CG	53		Francis *et al.*, 2005
Arch-amoAR	*amoA*	ammonia oxidizing archaea	GCG GCC ATC CAT CTG TAT GT	53		Francis *et al.*, 2005
amoA-1F	*amoA*	ammonia oxidizing bacteria (*Betaproteobacteria*)	GGG GTT TCT ACT GGT GGT	53		Rotthauwe *et al.*, 1997
amoA-2R	*amoA*	ammonia oxidizing bacteria (*Betaproteobacteria*)	CCC CTC KGS AAA GCC TTC TTC	53		Rotthauwe *et al.*, 1997
A189	*amoA*	ammonia oxidizing bacteria (*Gammaproteobacteria*)	GGN GAC TGG GAC TTC TGG	56		Holmes *et al.*, 1995
A682	*amoA*	ammonia oxidizing bacteria (*Gammaproteobacteria*)	GAA SGC NGA GAA GAA SGC	56		Holmes *et al.*, 1995
amoA-3F	*amoA*	ammonia oxidizing bacteria (*Gammaproteobacteria*)	GGTGAGTGGGYTAACMG	48		Purkhold *et al.*, 2000
amoA-4R	*amoA*	ammonia oxidizing bacteria (*Gammaproteobacteria*)	GCTACCACTTTCTGG	48		Purkhold *et al.*, 2000
340F	16S rRNA gene	most *Archaea*	CCCTAYGGGGYGCASCAG	57		Gantner *et al.* 2011
1000R	16S rRNA gene	most *Archaea*	GGCCATGCACYWCYTCTC	57		Gantner *et al.* 2011

[a], annealing temperature during PCR; [b], formamide (FA) concentration in hybridization buffer

Figures

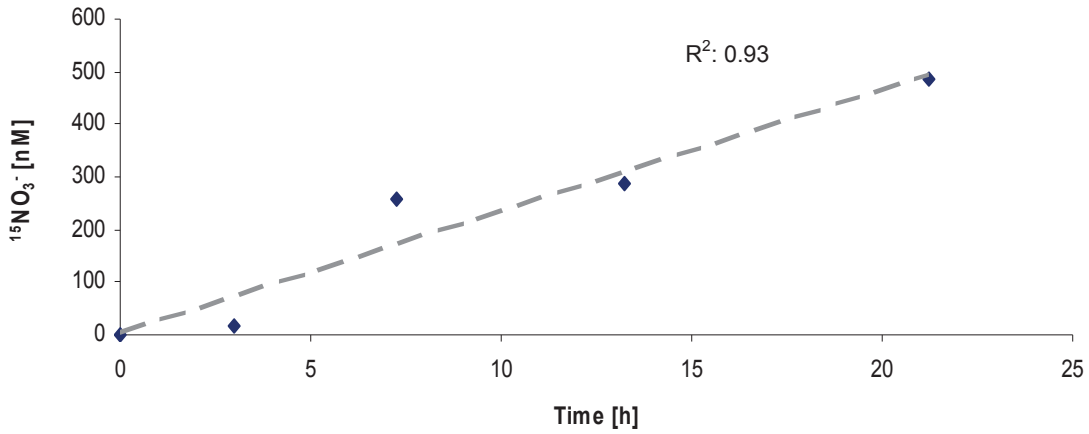

Figure S1: Exemplary graph showing the linear increase of $^{15}NO_3^-$production with time in Beggiatoa mat BM2a. The dashed line indicates the linear regression slope (R^2: 0.93) that has been used for calculating nitrification rates.

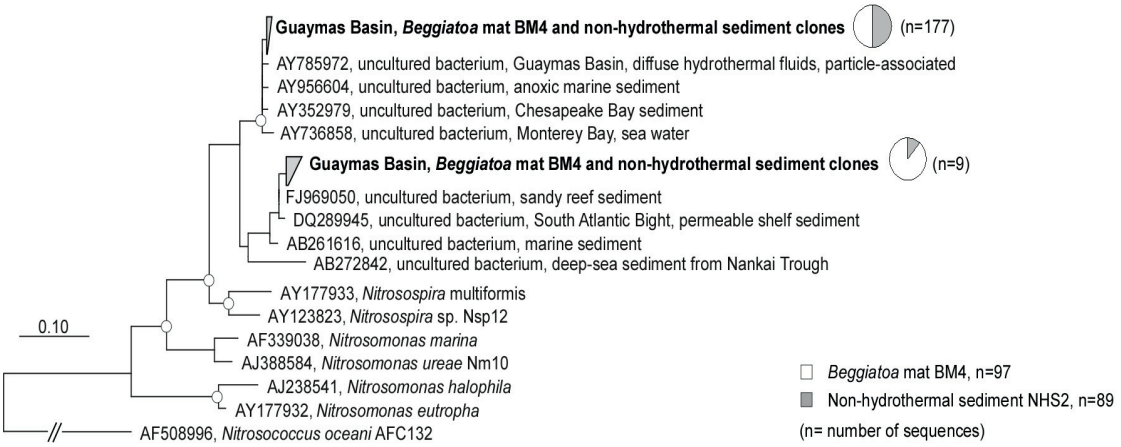

Figure S2: Neighbor-joining tree of betaproteobacterial AmoA sequences from *Beggiatoa* mat BM3a and from non-hydrothermal sediment NHS2. Open cirlces refer to >70% bootstrap support (1000 iterations). Scale bar corresponds to 10% sequence divergence.

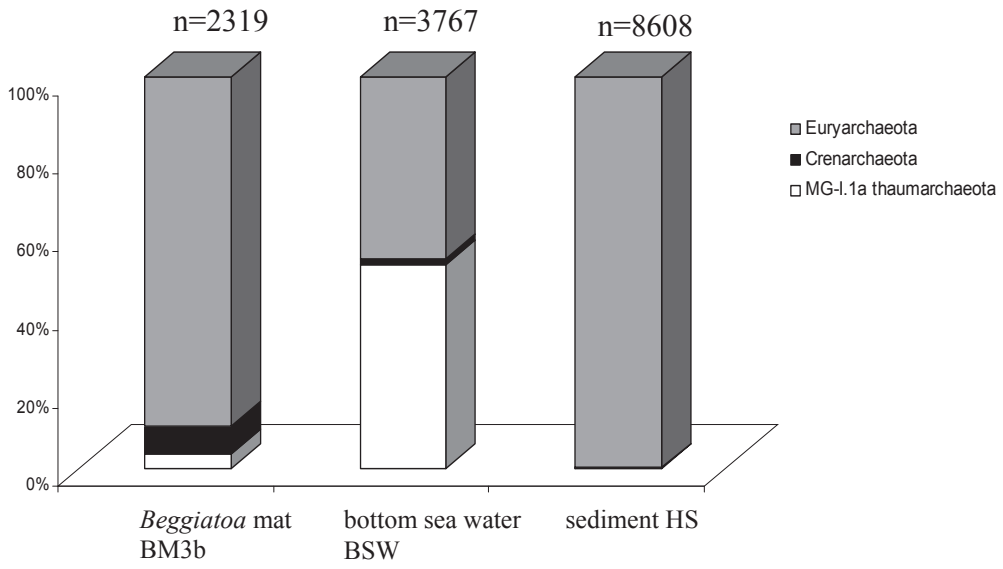

Figure S3: Phylogenetic distribution of archaeal 16S rRNA pyrotags in a *Beggiatoa* mat (BM3b), in bottom sea water (BSW) and in hydrothermally-influenced sediment (HS). n=number of sequences analyzed.

References

Daims H, Nielsen JL, Nielsen PH, Schleifer KH, Wagner M (2001). *In situ* characterization of *Nitrospira*-like nitrite-oxidizing bacteria active in wastewater treatment plants. *Appl Environ Microbiol* **67:** 5273-5284.

Francis CA, Roberts KJ, Beman JM, Santoro AE, Oakley BB (2005). Ubiquity and diversity of ammonia-oxidizing archaea in water columns and sediments of the ocean. *Proc Natl Acad Sci U S A* **102:** 14683-14688.

Gantner S, Andersson AF, Alonso-Saez L, Bertilsson S (2011). Novel primers for 16S rRNA-based archaeal community analyses in environmental samples. *J Microbiol Methods* **84:** 12-18.

Holmes AJ, Costello A, Lidstrom ME, Murrell JC (1995). Evidence that particulate methane monooxygenase and ammonia monooxygenase may be evolutionarily related. *FEMS Microbiol Lett* **132:** 203-208.

Juretschko S (2000). Mikrobielle Populationsstruktur und -dynamik in einer nitrifizierende/denitrifizierenden Belebtschlammanlage. Doctoral thesis. *Technische Universität München*

Massana R, Murray AE, Preston CM, Delong EF (1997). Vertical distribution and phylogenetic characterization of marine planktonic *Archaea* in the Santa Barbara channel. *Appl Environ Microbiol* **63:** 50-56.

Mobarry B K, Wagner M, Urbain V, Rittmann B E, Stahl D A (1996) Phylogenetic probes for analyzing abundance and spatial organization of nitrifying bacteria. *Appl Environ Microbiol* **62:** 2516-2162.

Purkhold U, Pommerening-Röser A, Juretschko S, Schmid MC, Koops HP, Wagner M (2000). Phylogeny of all recognized species of ammonia oxidizers based on comparative 16S rRNA and *amoA* sequence analysis: implications for molecular diversity surveys. *Appl Environ Microbiol* **66:** 5368-5382.

Rotthauwe J-H, Witzel K-P, Liesack W (1997). The ammonia monooxygenase structural gene *amoA* as a functional marker: molecular fine-scale analysis of natural ammonia-oxidizing populations. *Appl Environ Microbiol* **63:** 4704-4712.

Wagner M, Rath G, Koops HP, Flood J, Amann R (1996). *In situ* analysis of nitrifying bacteria in sewage treatment plants. *Water Sciand Technol* **4:** 237-244.

Wallner G, Amann R, Beisker W (1993). Optimizing fluorescent *in situ* hybridization with rRNA-targeted oligonucleotide probes for flow cytometric identification of microorganisms. *Cytometry* **14:** 136-143.

Chapter III

Identification and activity of acetate-assimilating microorganisms in diffuse hydrothermal fluids

Identification and activity of acetate-assimilating microorganisms in diffuse hydrothermal fluids

Matthias Winkel[1§], Petra Pjevac[1§], Manuel Kleiner[2], Sten Littman[3], Anke Meyerdierks[1] and Marc Mußmann[1*]

Running title:
Acetate-consuming microorganisms in two hydrothermal systems

[1] Department of Molecular Ecology, Max Planck Institute for Marine Microbiology, Bremen, Germany
[2] Department of Symbiosis, Max Planck Institute for Marine Microbiology, Germany
[3] Department of Biogeochemistry, Max Planck Institute for Marine Microbiology, Germany

§ these authors contributed equally to the study
* corresponding author:
Dr. Marc Mußmann
Department of Molecular Ecology
Max Planck Institute for Marine Microbiology
Celsiusstr. 1
Bremen, 28359, Germany
e-mail: mmussman@mpi-bremen.de

Key words:
Epsilonproteobacteria, Gammaproteobacteria, heterotrophy, 16S rRNA, nanoSIMS, stable isotopes

Abstract

In diffuse hydrothermal fluids concentrations of organic compounds such as acetate can be significant. To date knowledge about mixo- and heterotrophic microorganisms in hydrothermal systems is derived from pure cultures only. We set out to identify acetate-consuming microorganisms in diffuse fluids from two distinct hydrothermal systems using cultivation-independent approaches. For this purpose we combined a characterization of the microbial community in fluids with short-term incubations (8-12 h) using ^{13}C-labeled acetate at low concentrations (10 or 30 μM). We followed cell growth and assimilation of ^{13}C into single cells by nanoSIMS combined with fluorescence *in situ* hybridization (FISH). In 55°C fluids from the Menez Gwen system, Mid-Atlantic Ridge, a novel epsilonproteobacterial group related to *Nautiliales* accounted for nearly all acetate-assimilating cells. In contrast, in 4°C and 37°C fluids from the Manus Basin (Papua New-Guinea) *Gammaproteobacteria* dominated the ^{13}C-acetate-assimilating community, which was supported by 16S rRNA sequences related to *Marinobacter* and *Alteromonas*. We also detected yet-unidentified, weakly acetate assimilating cells in 72°C fluids (Manus Basin) that were presumably related to *Acinetobacter*. In particular in the 37°C and 55°C incubations the microbial communities differed from those in native fluids indicating rapid growth of heterotrophic organisms. The instant response suggests that acetate-consumers in diffuse fluids are r-strategists, which quickly exploit their food sources whenever available under the spatially and temporally highly fluctuating conditions at hydrothermal vents. Our data provide first insights into a largely under-investigated part of microbial carbon cycling at hydrothermal vents and reveals potential roles of known and yet-unknown heterotrophic microorganisms in these systems.

Introduction

In submarine hydrothermal systems inorganic carbon is considered the primary carbon source (Shively *et al.*, 1998; Nakagawa and Takai, 2008). Only recently it has been acknowledged that emanating hydrothermal fluids also contain non-methane organic compounds (Holm and Charlou, 2001; Lang *et al.*, 2006; Rogers and Amend, 2006; Skoog *et al.*, 2007; Konn *et al.*, 2009; Charlou *et al.*, 2010; Lang *et al.*, 2010). In hydrothermal fluids, sources of organic compounds other than methane can be diverse. Organic acids, lipids but also hydrocarbons are formed in the deep-subsurface by serpentinization and subsequent Fischer-Tropsch-type processes under elevated temperature and pressure (Shock, 1992; Shock and Schulte, 1998; McCollom *et al.*, 1999; Holm and Charlou, 2001). Furthermore, simple organic compounds are formed by thermal decomposition of biomass (McCollom and Seewald, 2007), homoacetogenesis (Drake *et al.*, 2008; Lever *et al.*, 2010) or by the vent-associated macrofauna (Pimenov *et al.*, 2002). Thus, elevated concentrations (3-35 μM) of organic compounds (e.g. formate and acetate) have been measured in venting fluids from shallow and deep-sea hydrothermal systems (Amend *et al.*, 1998; Lang *et al.*, 2010).

Early cultivation-independent studies showed that radioactively labeled organic carbon such as acetate or glucose was consumed by unknown microorganisms in hydrothermal fluids of the Galapagos Rift (Tuttle *et al.* 1983), the East Pacific Rise (Tuttle, 1985; Wirsen *et al.*, 1986), the Guaymas Basin (Karl *et al.*, 1988; Bazylinski *et al.*, 1989) and at the Loihi Seamount (Karl *et al.* 1989). Beyond these studies little is known about consumption of non-methane organic carbon in hydrothermal fluids. The current knowledge on microbial groups responsible for organic compound use is limited to cultivation-dependent studies of mostly thermophilic, phylogenetically diverse strains from *Deinococcus-Thermus*, *Thermotogae*, *Gamma- and Epsilonproteobacteria*, *Deferribacterales*, *Firmicutes* and *Archaea* (Pley, 1991; Jannasch *et al.*, 1992; Erauso *et al.*, 1993; Marteinsson *et al.*, 1995; González *et al.*, 1995; Huber *et al.*, 1995; Marteinsson *et al.*, 1996; Raguénès *et al.*, 1996, 1997; Wery *et al.*, 2001). Genomes of the vent-associated, sulfur-oxidizing *Sulfurimonas*/*Sulfurovum*-group (e.g. Campbell *et al.*, 2006; Sievert *et al.*, 2007; Yamamoto and Takai, 2011) also indicate a certain potential

for organic carbon consumption. Hence it was proposed that these thioautotrophs might use simple organic compounds like acetate as supplement (Sievert *et al.*, 2008).

Our objective was to identify non-methane organic carbon–assimilating microorganisms in diffuse hydrothermal fluids using cultivation-independent molecular and isotope-tracer experiments. In particular, we hypothesized that *in situ* abundant sulfur oxidizers such as *Epsilonproteobacteria* may use organic carbon as supplementary carbon source (Wood *et al.* 2004, Sievert *et al.* 2008). For our analysis we sampled sulfidic, diffuse fluids from two deep-sea hydrothermal systems, the Manus Basin back-arc system off the coast of Papua New-Guinea and the Menez Gwen-system at the Mid-Atlantic Ridge (MAR). These systems harbour fluids with *in situ* temperatures ranging from 4°C to 73°C (Manus Basin) and 25 to 56°C (Menez Gwen). We incubated fluids with ^{13}C-labeled acetate as model compound for organic carbon assimilation (Wright and Hobbie, 1966; Hoppe, 1978, Berg *et al.* 2013) and monitored changes in the microbial community structure by 16S rRNA gene pyrotag-sequencing, clone libraries and fluorescence *in situ* hybridisation (FISH). In contrast to previous environmental studies using ^{13}C-labelled tracers (Webster *et al.*, 2006, 2010; Miyatake *et al.*, 2009; Vandieken *et al.*, 2012; Berg *et al.*, 2013) we applied lower substrate concentrations (10 and 30 μM acetate) and shorter incubation times (8-12 h) to minimize experimentally introduced bias. Finally, we identified ^{13}C-acetate assimilating populations by combining nanometer scale secondary ion mass spectrometry (nanoSIMS) with FISH. Our approach to combine 16S rRNA gene diversity analysis, single cell identification and nanoSIMS measurements provides the first insights into the identity and activity of uncultured microorganisms consuming organic carbons other than methane in diffuse hydrothermal fluids.

Material and Methods

Site description and sampling

Diffuse fluids from the Menez Gwen hydrothermal vent field (37°50'N, 31°30'W) were sampled in September/October 2010 at 828 m depth during the cruise M82-3 on board of the R/V Meteor. Menez Gwen is a basalt-hosted hydrothermal system located southwest of the Azores on the Mid-Atlantic Ridge (MAR). We sampled diffusely venting hydrothermal fluids from "Woodys Crack" (WC), a crack in the basalt crust of

approximately 1 m length and 0.2 m width. *In situ* temperatures ranged from 25 to 56°C with a pH of ~4.9 (Table 1). Additional samples were collected from the hydrothermal plume (23 m above WC) and from bottom water above a patch of the vent mussel *Bathymodiolus azoricus* (Fig. S1) for a more detailed description of the sampling site see Marcon *et al.* (2013).

Diffuse fluids from the Manus Basin (MB) back-arc spreading centre off the coast of Papua New-Guinea were recovered in June/July 2011 during R/V Sonne cruise SO-216. Here, we sampled the felsic-hosted hydrothermal vent fields North Su (3°47'S, 152°06'W) and Fenway (3°43'S, 151°40'W). At the North Su (NS) underwater volcano rising, diffuse hydrothermal fluids were recovered from two venting fissures in the sea-floor in approximately 1200 m water depth (NS-I: 16-40°C, pH ~7.1 and NS-II: 54-73°C, pH ~3.6). From the smaller vent field Fenway (FW), located north-east of North Su in the PACMANUS area, cold but shimmering diffuse fluids were sampled above a patch of vestimentiferan tube worms in 1706 m depth (3.7°C, pH ~7.3) (Fig. S1, Table 1).

During both cruises samples were collected with the remotely controlled flow-trough system (Kiel Pumping System - KIPS) (Schmidt *et al.*, 2007) mounted on to the remotely operated underwater vehicle ROV Quest (MARUM, Bremen). A temperature probe, located next to the KIPS sampling nozzle, was used to monitor temperature during sampling. Fluid samples (volumes: 9 x 650 ml per KIPS bottle) were combined and divided into multiple subsamples for microbial community analysis, stable isotope (SI) experiments, and measurements of ammonia, nitrate and sulfide concentration. Because of the limited fluid volume (~5-5.9 l) per sampling event several ROV dives were necessary to recover sufficient material for all experiments at two sites (Table 1).

Ammonium, nitrate and sulfide concentrations

Ammonium (NH_4^+) concentrations were determined photometrically by nesslerization (Bower and Holm-Hansen, 1980). Nitrate was measured according to (Braman and Hendrix, 1989) using an CLD 60 NO_x analyzer (Eco Physics, USA). Total dissolved sulfide was determined spectrophotometrically on zinc acetate fixed samples as described in Cline, 1969. More detailed geochemical data will be published elsewhere by E. Reeves and A. Koschinsky.

16S rRNA gene-pyrotag diversity analysis in diffuse hydrothermal fluid samples

For 16S rRNA gene diversity analysis diffuse fluids from four locations (WCb, FW, NS-I, and NS-IIb, Table 1) were filtered on polyethersulfone (PES) membranes (0.22 µm pore size, Milipore, Darmstadt, Germany) attached to the KIPS system and stored at -20°C until further processing. DNA was extracted from PES membranes with the Ultra Clean Soil DNA Kit (MoBio Laboratories, Carlsbad, USA) as instructed in the manual. Bacterial 16S rRNA genes were amplified by PCR with the primers GM3 and 907RM (Muyzer *et al.*, 1998) in ten parallel reactions using the Phusion High Fidelity Polymerase (NEB, Ipswich, USA). PCR products were pooled, gel purified and 454-pyrosequenced at the Max Planck Genome Center (Cologne, Germany). Further details on PCR and sequencing are provided in the supplementary methods. Sequence reads >200 bp were analyzed with the SILVAngs bioinformatics pipeline (Quast *et al.*, 2012) as described in (Klindworth *et al.*, 2013). Details are given in the supplementary methods section. Sequencing and analysis statistics are presented in Table S1.

^{13}C-acetate and ^{15}N-ammonium incubations

Stable isotope (SI)-incubation experiments were performed onboard. Directly after retrieval fluid samples were pre-incubated at the measured *in situ* temperature for 1h. Incubations were performed in 1000 ml (WCa) or 500 ml (FW, NS-I, NS-IIa) glass bottles that were filled to 1/3 with diffuse fluids leaving 2/3 as air headspace. To WCa fluids we added sodium 1-^{13}C acetate (99 atom % ^{13}C, Sigma-Aldrich) at final concentrations of 10 µM (WC). For incubations of fluids from the Manus Basin (FW, NS-I, NS-IIa) we increased ^{13}C acetate concentrations to 30 µM to ensure sufficient labelling, since onboard *in situ* mass spectrometer measurements (XY unpublished data) indicated elevated background concentrations of acetate. To all incubations we also added ^{15}N-ammonium chloride (98 atom % ^{15}N, Sigma-Aldrich) as a general activity marker at a final concentration of 10 µM. Fluids were incubated at *in situ* temperatures for 8h (55°C, WCa and 72°C, NS-IIa), 10h (37°C, NS-I) or 12 h (4°C, FW). Incubations were stopped by addition of formaldehyde (final concentration 1%) and fixed for 1h at room temperature. From each bottle 50-100 ml fluid were filtered on a glass fiber filter (type GF, 0.7 µm pore size, Millipore, Darmstadt, Germany) for bulk SI-measurements.

The remaining volume was filtered on multiple gold-palladium coated polycarbonate membranes (type GTTP, 0.2 µm pore size, Millipore, Darmstadt, Germany) for nanoSIMS and CARD-FISH analyses. All filters were air dried and stored at -20°C. For each experimental set-up duplicate (FW, NS-I, NS-IIa) or triplicate (WCa) incubations were performed. Furthermore, formaldehyde-inactivated fluids (final concentration 1%), N_2-flushed, anoxic fluids and oxic, substrate-free fluids were run as controls.

Isotope ratio mass spectrometry (IRMS)

For bulk measurements of ^{13}C and ^{15}N, GF-filters were analyzed by gas chromatography-isotope ratio mass spectrometry (GC-IRMS). Briefly, isotope abundance in the sample was measured on released CO_2 and N_2 after flash combustion of filters in excess oxygen at 1050°C in an automated elemental analyzer (Thermo Flash EA, 1112 Series, CE Elantech, Lakewood, NJ, USA) coupled to a Delta Plus Advantage mass spectrometer (Finnigan, Thermo Fisher Scientific, Waltham, MA, USA). To remove excess label before combustion filters were acidified in an atmosphere of hydrochloric acid for 24 h.

CARD-FISH

Samples for CARD-FISH were also prepared from diffuse fluids and from the hydrothermal plume. Therefore, 100 ml fluid were directly formaldehyde-fixed on board (1% final concentration, overnight at 4°C) and filtered on polycarbonate membrane filters (type GTTP, 0.2 µm pore size, Millipore, Darmstadt, Germany). CARD-FISH was performed on membrane filters according to (Ishii *et al.*, 2004; Pernthaler *et al.*, 2002; Teira *et al.*, 2004). Details of the applied oligonucleotide probes are listed in Table S2. For simultaneous detection of multiple microbial taxa, filters were consecutively hybridized with two probes (Pernthaler *et al.*, 2004) using Alexa488 and Alexa594 fluorochromes (Invitrogen, Karlsruhe, Germany).

Marking and mapping of hybridized cells for nanoSIMS

To combine CARD-FISH identification of single cells with nanoSIMS analysis we used correlative microscopy. To this end, the position of cell assemblages identified by CARD-FISH were marked by laser micro-dissection of filter membranes (LMD model

DM6500B) (Leica, Wetzlar, Germany) using a filter set for the detection of Alexa488 (excitation maximum: 498 nm; emission maximum: 520 nm) and Alexa594 (excitation maximum: 591 nm; emission maximum: 618 nm). Fields of view with a suitable distribution of hybridized cells were marked with numbers, arrows and borders to guarantee recovery of cells during nanoSIMS analysis. Microscopic images were taken for orientation purpose during the nanoSIMS analysis and for post-processing with the Look@nanoSIMS software tool (Polerecky *et al.*, 2012).

NanoSIMS analysis

Hybridized cells within the marked areas on the filter membranes were analyzed with a nanoSIMS 50L instrument (Cameca, Gennevilliers, Cedex-France). Secondary ions $^{12}C^-$, $^{13}C^-$, $^{12}C^{14}N^-$, $^{12}C^{15}N^-$ and $^{32}S^-$ were simultaneously recorded for each individual cell using 5 electron multipliers. Samples were pre-sputtered with a Cs^+ beam of 400 to 500 pA to remove surface contaminations, to implant Cs^+ ions and to achieve a stable ion emission rate. During analysis samples were sputtered with a 0.8 to 1.8 pA Cs^+ primary ion beam focused into a spot of 50 to 100 nm diameter that was scanned over an analysis area of 5 x 5 µm to 30 x 30 µm with an image size of 256 x 256 pixel or 512 x 512 pixel and a counting time of 1 ms per pixel. The individual masses were tuned for high mass resolution (9200 MRP Cameca). Respective mass peaks were tuned directly on the sample. Depending on the fields of view (5 x 5 µm to 30 x 30 µm), between 20 to 100 planes were recorded.

The measured data were processed using the Look@NanoSIMS software (Polerecky *et al.*, 2012). The images of one field of view recorded during one measurement were drift corrected and accumulated. Regions of interest (ROI) corresponding to individual cells were defined using images of $^{12}C^-$, $^{12}C^{14}N^-$ and $^{32}S^-$. For each ROI $^{13}C/(^{13}C+^{12}C)$, $^{12}C^{15}N/(^{12}C^{15}N+^{12}C^{14}N)$ and $^{32}S/^{12}C$ ratios were calculated. Ratios with more than 10% trend (increase or decrease) with depth were excluded from further analysis.

Calculation of assimilation per biovolume

Assimilation of ^{13}C and ^{15}N per biovolumes were calculated for 164 cells from the Menez Gwen (WC), and for 125 cells from the Manus Basin (FW: 47 cells; NS-I: 72 cells; NS-

IIa: 7 cells). Most cells were rod-shaped and cell volume was calculated based on measured values of cell diameters and cell lengths by adding up the respective volumes of a sphere and a cylinder. For biovolume-to-biomass conversion we used a calibration factor of 0.38 pg C μm^{-3} known for small heterotrophic *Bacteria* (Lee and Fuhrman, 1987). The calculated biomasses were correlated with $^{13}C/^{13}C+^{12}C$ ratio and corrected for dead control bulk measurements, assuming 100%-labeling with ^{13}C acetate. The nitrogen content of cells was calculated based on a conversion factor of 3.7 for C : N ratio in heterotrophic cells (Lee and Fuhrman, 1987), correlated with $^{15}N/^{15}N+^{14}N$ ratio and corrected for dead control bulk measurements.

16S rRNA gene libraries and phylogenetic analyses

Bacterial 16S rRNA genes were amplified by filter-PCR (Kirchman *et al.*, 2001) or from filter-extracted DNA (Ultra Clean Soil DNA Kit, MoBio Laboratories, Carlsbad, USA) of formaldehyde-fixed samples collected at the end of ^{13}C-acetate incubations. Bacterial primers GM3F and GM4R, or primers GM5F and 907RM were applied (Muyzer *et al.*, 1998). After gel purification, PCR products were cloned and Sanger-sequenced. Further details are described in the Supplementary Methods.

Phylogenetic analysis was performed with the ARB software package (Ludwig *et al.*, 2004), based on a sequence alignment with the SINA (SILVA Incremental) aligner (Pruesse *et al.*, 2012), against the SILVA 16S rRNA SSU reference database, release 111 (Quast *et al.*, 2012). Phylogenetic trees were calculated with nearly full-length sequences (>1400 bp) using the maximum likelihood algorithm RAxML with 100 bootstraps (Stamatakis *et al.*, 2005) implemented in ARB. For calculation we applied a 50% conservation filter calculated with reference sequences for the considered phylogenetic group. Nucleotide substitutions were weighted according to the GTR model (Lanave *et al.*, 1984). Partial sequences were added after tree calculation using the ARB implemented maximum parsimony algorithm, without allowing changes in tree topology.

Nucleotide sequence accession numbers

Nucleotide sequences from this study were deposited in the EMBL, GeneBank and DDBJ nucleotide database with the following accession numbers: Manus Basin (…); Menez

Gwen (…). The 454-pyrotag sequences have been deposited at Sequence Read Archive with the following accession number ….

Results

Geochemistry of diffuse hydrothermal fluids

Ammonium concentrations in fluids from Woody´s Crack (WCa) in the Menez Gwen hydrothermal vent field were between 5-8 µM. Nitrate concentrations were between 16-18 µM (Table 1). In all fluids oxygen was detected (personal communication, Stéphane Hourdez). The 4°C and 37°C fluids (FW and NS-I) from the Manus Basin displayed low ammonium concentrations (<3 µM), whereas up to 30 µM ammonium were detected in the 72°C fluids (NS-IIa). In all fluid samples oxygen saturation levels were high (personal communication, Christian Breuer). Furthermore, in the low temperature fluid (FW) sulfide concentrations were close to the detection limit (~2 µM), while 14-66 µM and 113-302 µM sulfide were detected in the temperate (NS-I) and high temperature (NS-IIa) fluid (Table 1). Acetate was below detection limit (1 µM) in fluids from Menez Gwen. In fluids from Manus Basin acetate could not be measured due to interference with other soluble compounds during liquid chromatography. All samples featured the typical odor of hydrogen sulfide, while exact sulfide concentrations and other geochemical data will be published elsewhere (E. Reeves, unpublished data).

Microbial community in source fluids from Woody's' crack (Menez Gwen)

To determine the composition of the microbial community and to identify potential organic carbon consuming microorganisms in the 55°C diffuse fluid at Menez Gwen, we performed total cell counts (TCCs), CARD-FISH and 16S rRNA gene 454-pyrosequencing. TCC were $1.6 \pm 0.3 \times 10^5$ cells ml^{-1}, of which 99% were identified as *Bacteria* by CARD-FISH (Table S3). Bacterial 16S rRNA gene pyrotag-sequences (6,880 reads) were dominated by *Epsilonproteobacteria* (51%, Fig. 1), which accounted for 10% of TCC (Fig. 2 and Table S3). *Gammaproteobacteria* accounted for 10% of pyrotag sequences but made up 65% of TCC (Fig. 2 and Table S3). Besides *Gammaproteobacteria* and *Epsilonproteobacteria*, only *Alphaproteobacteria* contributed a larger number of sequences to the overall diversity (18%), while all other bacterial groups made up <5% of pyrotags (Fig. 1).

The majority (85%) of epsilonproteobacterial pyrotag sequences was related to the mesophilic, lithoautotrophic genera *Sulfurimonas*, *Sulfurovum* and *Arcobacter* within the

Campylobacterales (Fig. 1). These genera are frequently detected in sulfidic, hydrothermal environments in the deep-sea (Taylor *et al.*, 1999; Wirsen *et al.*, 2002; Campbell *et al.*, 2006; Sievert *et al.*, 2007). *Nautiliales* constituted 10% of epsilonproteobacterial pyrotags (Fig. 1). This order harbours metabolically diverse organisms including mixo- and autotrophic, thermophiles (Campbell *et al.*, 2001, 2006; Miroshnichenko *et al.*, 2002). Most of the gammaproteobacterial sequences were affiliated with sequences from *Oceanospirillales* (SUP05, *Psychromonas*) and *Alteromonadales* (SAR86).

Microbial community composition in source fluids from the Manus Basin

Despite the three diffuse fluids from the Manus Basin covered a large temperature range (4°C, 37°C, 72°C) TCCs were relatively similar ranging from 1.6 to 6.2 x 10^4 cells ml^{-1}. *Bacteria* accounted for 58-85% and Archaea for 8-11% of TCC (Table S3). Of in total 10,516 bacterial pyrotag sequences 84-91% affiliated with *Proteobacteria* (Fig. 1). In the 4°C fluids (FW), *Gammaproteobacteria* made up 57% of pyrotag sequences, whereas they contributed to only 4% of TCC. Besides numerous sequences related to the sulfur-oxidizing SUP05 clade of *Oceanospirillales* (Fig. 1), some sequences grouped with genera such as *Acinetobacter, Marinobacter* and *Alteromonas* that harbour heterotrophs (Fig. 5). *Epsilonproteobacteria* (all *Campylobacterales*) accounted for 12% of pyrotag sequences (Fig. 1) and for 4% of TCC (Table S3).

In both fluid samples from the North Su vent field (37°C, NS-I and 72°C, NS-IIb), *Epsilonproteobacteria* were the dominant sequence group (78-85%) but again accounted only for 7 to 15% of TCC (Table S3). In the 37°C fluid sample (NS-I) the majority of all epsilonproteobacterial sequences (90%) was again related to the same *Campylobacterales*, while sequences related to the *Nautiliales* represented a minor fraction (9% of epsilonproteobacterial sequences). Contrastingly, over 93% of epsilonproteobacterial sequences retrieved from the 72°C fluid (NS-IIb) were classified as *Nautiliales* (Fig. 1). *Gammaproteobacteria* were similarly abundant (5-15%) as *Epsilonproteobacteria* according to CARD-FISH (Table S3) and accounted for 4-7% of pyrotag sequences in NS-I and NS-IIb fluids. Here, gammaproteobacterial sequences

were also closely related to sequences of *Alteromonas* that have been detected in cold FW fluids and to *Acinetobacter* (Fig. 5).

Acetate-assimilation by *Epsilonproteobacteria* in Menez Gwen diffuse fluids

To identify microbial populations that actively assimilate organic carbon in fluids from Woody´s Crack (WCa), we followed assimilation of the model compound ^{13}C acetate in bulk samples and individual cells in short-term experiments at *in situ* temperature (55°C). Besides ^{13}C-acetate, we also added ^{15}N-ammonium as general activity marker. Bulk ratios of $^{13}C/^{12}C$ and $^{15}N/^{14}N$ in atom percent were higher than in the dead controls (1.7 to 2.0 fold and 25.2 to 33.1 fold, respectively) (Fig. S2 and Table S4) and indicated assimilation of ^{13}C-acetate and ^{15}N-ammonium into cell material. TCC increased by on average 2.8-fold (Table S3). Furthermore, within 8h of incubation the community significantly shifted from *Gammaproteobacteria* (65% of TCC in fluids) to an *Epsilonproteobacteria*-dominated community (88.2% ± 4.2 of TTC) (Fig. 5; Table S3).

Epsilonproteobacteria grown in ^{13}C-acetate incubations were further identified by 16S rRNA gene sequencing. Almost all retrieved epsilonproteobacterial sequences were affiliated to the family *Nautiliaceae* and formed a separate branch with 94.2% sequence identity to *Nautilia profundicola* (Fig. 5). We designated this novel sequence cluster as NautMG-group. Most gammaproteobacterial sequences recovered from this experiment affiliated with the heterotrophic genus *Alcanivorax* (Yakimov *et al.*, 1998; Fernández-Martínez *et al.*, 2003) (Fig. 5).

To quantify these *Epsilonproteobacteria* in incubations and source fluids we designed the specific oligonucleotide probe Naut842 (Fig. 5). This probe targeted 84-87% of TCC in all triplicate ^{13}C-acetate incubations (Fig. 6), indicating that the large majority of epsilonproteobacterial cells grown on ^{13}C-acetate indeed belongs to the novel NautMG-group. In the diffuse fluids (WCa) and in bottom waters above a nearby *Bathymodiolus*-mussel bed (WC-M) the NautMG-cells made up 0.8% (Table S3) and 0.3% (not shown) of TCC, respectively. No NautMG-cells were detected in the plume obtained from 23 m above Woody's Crack (WC-P; Table 1) (not shown). *Gammaproteobacteria* did not grow and even declined in cell numbers in ^{13}C-acetate incubations (Fig. 2, Table S3).

We selected two of the triplicate incubations to confirm ^{13}C-acetate consumption by the NautMG-group using nanoSIMS. To this end 157 cells were identified beforehand by correlative microscopy using CARD-FISH. Almost all analysed epsilonproteobacterial cells significantly incorporated ^{13}C and ^{15}N, whereas the few gammaproteobacterial cells found showed little or no incorporation (Fig. 3 and Fig. S4). Epsilonproteobacterial cells displayed large differences in ^{13}C- and ^{15}N- assimilation per biovolume. A major fraction of cells showed both low ^{13}C (0.2-7.0 amol μm^{-3}) and ^{15}N (0.7-18.0 amol μm^{-3}) incorporation. Another fraction of cells showed high assimilation per biovolume in ^{15}N (18.0 to 50.1 amol μm^{-3}), while they assimilated less ^{13}C (~5 amol μm^{-3}). Only a small cell fraction assimilated both high ^{15}N (18.0 to 46.3 amol μm^{-3}) and high ^{13}C (7.0 to 18.0 amol μm^{-3}) (Fig. 4). The average uptake of ^{15}N was 4.6 ± 3.8 amol μm^{-3} and the average uptake of ^{13}C was 14.5 ± 10.7 amol μm^{-3}.

Acetate-assimilation by *Gammaproteobacteria* in Manus Basin diffuse fluids

Similar incubations with ^{13}C acetate and ^{15}N ammonium were performed with diffuse fluids from three different sources at the Manus Basin hydrothermal systems (FW, NS-I, NS-IIa). In the 4°C and 37°C incubations bulk ratios of ^{12}C/^{13}C and ^{15}N/^{14}N in atom percent were higher than in corresponding dead controls indicating assimilation of the ^{13}C and ^{15}N (Fig. S2). In the 72°C incubation bulk ratios of ^{13}C/^{12}C and ^{15}N/^{14}N were not clearly higher than in controls (Fig. S2 and Table S4).

In 4°C and 37°C incubations the TCC increased up to 11- fold to a final TCC of 0.8-3.7 x 10^5 cells ml^{-1} (Table S3), while TCC in controls remained stable or changed only slightly (Table S3). In both experiments observed growth could be attributed to *Gammaproteobacteria,* which accounted for 63-87% of TCC after incubations (Table S3). This was supported by a 16S rRNA gene library of 4°C fluids that were dominated by sequences of the sea water-associated and heterotrophic genera *Alteromonas*, and *Marinobacter* (Fig. 1 and Fig. S4). Notably, both gene libraries from duplicates of the 37°C incubations were dominated by *Marinobacter hydrocarbonoclasticus* (98-99.7% sequence identity) and contained few sequences related to *Altermonas marina* (99-99.6% sequence identity). Both organisms are known to grow with acetate (Gauthier *et al.*, 1992; Yoon *et al.*, 2003).

In the 72°C incubation TCCs with up to 3.2 x 10^4 cells ml^{-1} were only slightly higher than in controls. These cells could not be further identified by FISH most likely because of an over-fixation with formaldehyde at 72°C. The 16S rRNA gene library of the nanoSIMS-analyzed replicate exclusively contained *Acinetobacter*-related sequences (*Gammaproteobacteria*) with 94-99.9% sequence identity to *Acinetobacter* species (Fig. 5). Archaeal 16S rRNA genes could not be amplified from the 72°C incubations.

The incorporation of ^{13}C and ^{15}N into single gammaproteobacterial cells was confirmed by nanoSIMS and CARD-FISH (Fig. 3). In the 4°C fluids (FW) ^{13}C acetate assimilation by gammaproteobacterial cells (n=38) was low (0.2 to 2.0 amol μm^{-3} ^{13}C and 0.1 to 6.4 amol μm^{-3} ^{15}N). The few found epsilonproteobacterial cells (n= 9) assimilated no or very little ^{13}C and ^{15}N (Fig. 3 and 4). In the 37°C incubation (NS-I) ^{13}C acetate assimilation varied strongly between individual gammaproteobacterial cells (n=65), and ranged between 0.08 to 10.2 amol μm^{-3} for ^{13}C and 0.2 to 13.8 amol μm^{-3} for ^{15}N (Fig. 4). In the 72°C incubation only very few intact cells (n=6), not further identifiable by FISH, were slightly enriched in ^{13}C and ^{15}N (Figs. S3 and S4).

Discussion

Here we show for the first time that microbial communities in diffuse hydrothermal fluids assimilate non-methane organic carbon during short-term incubations over a temperature range of 4-72°C. We combined nanoSIMS analysis of ^{13}C-acetate assimilating cells with 16S rRNA gene sequencing and FISH. The molecular methods allowed us to detect community shifts in cells with sufficient SI-labelling after incubation periods of only 8-12 h. The added acetate levels were close to those measured previously at other hydrothermal sites (Lang *et al.*, 2010) or in pelagic redoxclines (Albert *et al.*, 1995; Ho *et al.*, 2002). By using this approach we avoided extended incubation times and high substrate levels as generally applied for stable isotope-probing of acetate-assimilating microbes in environmental studies (Boschker *et al.*, 1998; Webster *et al.*, 2006, 2010; Miyatake *et al.*, 2009; Pester *et al.*, 2010; Vandieken *et al.*, 2012; Miyatake *et al.*, 2013; Berg *et al.*, 2013). Due to the dynamic nature of hydrothermal fluids (Perner *et al.*, 2013) our approach provides a snapshot of the physiological properties of particular microbes as our experimental set-up offered a rather narrow niche, leading to stimulation of very specific populations and not of the broad microbial communities.

Acetate-assimilation in diffuse fluids of the Manus Basin

In the 4°C and 37°C diffuse fluids from the Manus Basin the microbial communities clearly shifted within 8 to 12h to *Gammaproteobacteria*-dominated communities. These *Gammaproteobacteria* accounted for the majority of acetate assimilation. While in the 4°C (FW) incubation a single actively acetate-assimilating population could not be ultimately identified, both 37°C (NS-I) incubations were clearly dominated by *Marinobacter*-related organisms. Consistent with this result is the widespread distribution of marine *Marinobacter* in other diffuse fluids, in cold seawater surrounding spots of hydrothermal discharge (Huber *et al.*, 2007; Kaye *et al.*, 2011) and other samples of hydrothermal origin (Rogers *et al.*, 2003; Santelli *et al.*, 2008). Moreover, they are metabolically flexible and a number of strains use organic substrates including acetate (Kaye and Baross, 2000; Handley *et al.*, 2009). Their competitive advantage over other acetate-consuming microorganisms in our 37°C-experiments and their frequent detection

in hydrothermal habitats suggests that the *Marinobacter*-group is probably an important heterotroph at many hydrothermal sites.

Under thermophilic conditions (NSIIa, 72°C), we observed slight growth of acetate-assimilating organisms, which are not fully identified as FISH was difficult on these samples. Since sequences of the *Acinetobacter*-group were the only 16S rRNA phylotype recovered in the incubation analysed by nanoSIMS, presumably these *Gammaproteobacteria* were selectively stimulated upon acetate addition. While mesophilic *Acinetobacter*-strains have been repeatedly isolated from hydrothermal sites (Jeanthon and Prieur, 1990; La Duc *et al.*, 2007), our experiments suggest that the *Acinetobacter*-group also harbours heterotrophic thermophiles. This is consistent with previous reports on thermostable enzymes in this genus (Tani *et al.*, 2000).

A novel group of aerobic and thermophilic *Nautiliales* assimilated acetate

In contrast, the microbial community in incubations of diffuse fluids from Menez Gwen shifted to *Epsilonproteobacteria,* which were dominated by a yet undiscovered group phylogenetically affiliated with *Nautiliales*. Although these organisms were rare in the original fluids they rapidly multiplied by 291-fold within 8 h, equalling generation times of approximately 59 min. Like other *Nautiliales* the NautMG-group is thermophilic and constituted the most active, aerobic, acetate-assimilating population at 55°C, but did not grow in anoxic or acetate-free control experiments. To date only a few *Nautiliales* strains were shown to anaerobically grow with organic carbon such as formate but not yet with acetate (Campbell *et al.*, 2001; Miroshnichenko *et al.*, 2002; Smith *et al.*, 2008; Pérez-Rodríguez *et al.*, 2010). Moreover, some strains grow mixotrophically with hydrogen under anaerobic conditions (Alain *et al.*, 2002; Miroshnichenko *et al.*, 2002; Smith *et al.*, 2008; Alain *et al.*, 2009; Pérez-Rodríguez *et al.*, 2010), whereas *Nautilia lithotrophica* tolerates oxygen (Miroshnichenko *et al.*, 2004). Thus, the NautMG-group identified here is the first description of an aerobic, acetate-consuming member of the *Nautiliales*. Although we detected the NautMG-group as the only epsilonproteobacterial phylotype after the incubation, single cells displayed remarkable differences in ^{13}C and ^{15}N uptake. The most parsimonious explanation is that during the multiple division cycles the cellular ^{13}C and ^{15}N content accumulated from generation to generation resulting in incrementally

higher labelling of the daughter cells (L. Polerecky, personal communication). Interestingly, we also observed some cells with high ^{15}N but relatively low ^{13}C uptake (Fig. 5) possibly reflecting an alternative strategy of this subpopulation.

The low relative abundance of the NautMG-group in the diffuse fluids is likely not representative for the entire hydrothermal system, since cells in hydrothermal fluids commonly have very short residence times that do not allow significant growth. More likely, these meso-and thermophiles found in fluids are rather sessile organisms detached from the (hardly accessible) subsurface (Summit and Baross, 2001; Takai *et al.*, 2004) that were previously shown to harbour thermophilic *Epsilonproteobacteria* (Huber *et al.*, 2003). Furthermore, these organisms could also thrive at the crack rim or in mussel beds, where conditions are more favourable In support of this hypothesis, we found several sequences of the NautMG–group (98% sequence identity) in bottom waters above mussel beds and at other sites of the Menez Gwen system (unpublished data, D. Meier).

Rapid growth as adaptation to fluctuating conditions in hydrothermal fluids

Apparently, none of the *in situ* dominant sulfur-oxidizing clades (*Sulfurimonas*, *Sulfurovum*, SUP05) were stimulated in our sulfide-containing incubations, although even strict autotrophs may use acetate as supplementary carbon source (Wood *et al.*, 2004). Sulfide was clearly present in all incubations and was thus not a limiting factor. Presumably temperatures in our incubation experiments were not in the range preferred by these groups and/or their enzymatic machinery was tuned for only lithoautotrophic growth.

There is accumulating evidence that geochemical properties, temperature and the microbial community composition of hydrothermal diffuse fluids are highly dynamic in time and space (Perner *et al.*, 2013). Consequently, microorganisms experience quick changes in their immediate vicinity and therefore require strategies to efficiently exploit resources in a narrow time window when conditions are favourable. In such a fluctuating environment, lifestyles with short lag-phases and rapid growth, commonly known as r-strategy, are more competitive than relatively slow growth. In two incubation experiments with elevated temperatures (37°C, 55°C) we observed a quick response of different microbial populations within a couple of hours after adding acetate. These

microorganisms apparently did not require a significant lag phase to adapt to the incubation conditions, suggesting that they were already metabolically active during sampling. Therefore, we propose that the rapid growth of specific populations upon acetate addition well reflects an adaptation to the fluctuating environment of hydrothermal fluids.

In conclusion, our results complement earlier findings by Tuttle *et al.* (1983) and Karl *et al.* (1989), who observed significant assimilation of acetate in diffuse fluids by however unknown microorganisms in long-term incubations. The widespread *Marinobacter*-group and two groups (NautMG-group, thermophilic *Acinetobacter*) with previously unknown metabolic properties could be important heterotrophs at hydrothermal vents as they are capable of rapidly exploiting organic carbon when available. Further studies on different compartments with higher organic carbon content such as mussel beds are desirable to quantify the general importance of organic carbon turnover. Future SI-labelling experiments should test a wider range of temperatures, hydrostatic pressures and other organic carbon source such as formate, which is the major abiotically formed organic acid in hydrothermal fluids (McCollom and Seewald, 2001; Lang *et al.*, 2010). These could be combined with transcriptomics and proteomics to identify the involved metabolic pathways.

Acknowledgements

We acknowledge the officers and crew of the R/V Meteor and R/V Sonne as well as the the ROV team of the MARUM Quest 4000m. We thank the scientific parties of the cruises M83 leg 2 and SO216 for their wonderful support, especially the chief scientist Nicole Dubilier and Wolfgang Bach, respectively. We thank Marcus Petzold, Nicole Rödiger, Jörg Wulf, Lisa Drews, Lisa Kieweg for excellent assistance in the Molecular Ecology department, Gabriele Klockgether for technical help with ISMS measurements, Andreas Krupke for support in the nanoSIMS analysis. We are grateful to Rudolf Amann for excellent general support.

The cruise M82 with R/V Meteor was integral part in the Cluster of Excellence of the MARUM “The Ocean in the Earth System, Research Area F: Lithosphere-Biosphere

Interaction" funded by the German Research Foundation (DFG). The cruise SO216 was funded by a grant (03G0216) from the Bundesministerium für Bildung und Forschung (BMBF) awarded to Wolfgang Bach and co-PIs. This work was supported by the Max Planck Society.

References

Alain, K., Callac, N., Guégan, M., Lesongeur, F., Crassous, P., Cambon-Bonavita, M.-A., Querellou, J., and Prieur, D. (2009). *Nautilia abyssi* sp. nov., a thermophilic, chemolithoautotrophic, sulfur-reducing bacterium isolated from an East Pacific Rise hydrothermal vent. *Int. J. Syst. Evol. Microbiol.* 59, 1310–1315.

Alain, K., Querellou, J., Lesongeur, F., Pignet, P., Crassous, P., Raguénès, G., Cueff, V., and Cambon-Bonavita, M.-A. (2002). *Caminibacter hydrogeniphilus* gen. nov., sp. nov., a novel thermophilic, hydrogen-oxidizing bacterium isolated from an East Pacific Rise hydrothermal vent. *Int. J. Syst. Evol. Microbiol.* 52, 1317–1323.

Albert, D. B., Taylor, C., and Martens, C. S. (1995). Sulfate reduction rates and low molecular weight fatty acid concentrations in the water column and surficial sediments of the Black Sea. *Deep Sea Res. Part Ocean. Res. Pap.* 42, 1239–1260.

Amend, J. P., Amend, A. C., and Valenza, M. (1998). Determination of volatile fatty acids in the hot springs of Vulcano, Aeolian Islands, Italy. *Org. Geochem.* 28, 699–705.

Bazylinski, D. A., Wirsen, C. O., and Jannasch, H. W. (1989). Microbial utilization of naturally occurring hydrocarbons at the Guaymas Basin hydrothermal vent site. *Appl. Environ. Microbiol.* 55, 2832–2836.

Berg, C., Beckmann, S., Jost, G., Labrenz, M., and Jürgens, K. (2013). Acetate-utilizing bacteria at an oxic–anoxic interface in the Baltic Sea. *FEMS Microbiol. Ecol.* 85, 251–261.

Boschker, H. T. S., Nold, S. C., Wellsbury, P., Bos, D., de Graaf, W., Pel, R., Parkes, R. J., and Cappenberg, T. E. (1998). Direct linking of microbial populations to specific biogeochemical processes by ^{13}C-labelling of biomarkers. *Nature* 392, 801–805.

Bower, C. E., and Holm-Hansen, T. (1980). A salicylate–hypochlorite method for determining ammonia in seawater. *Can. J. Fish. Aquat. Sci.* 37, 794–798.

Braman, R. S., and Hendrix, S. A. (1989). Nanogram nitrite and nitrate determination in environmental and biological materials by vanadium (III) reduction with chemiluminescence detection. *Anal. Chem.* 61, 2715–2718.

Campbell, B. J., Engel, A. S., Porter, M. L., and Takai, K. (2006). The versatile □-proteobacteria: Key players in sulphidic habitats. *Nat. Rev. Microbiol.* 4, 458–468.

Campbell, B. J., Jeanthon, C., Kostka, J. E., Luther, G. W., and Cary, S. C. (2001). Growth and phylogenetic properties of novel bacteria belonging to the epsilon subdivision of the *Proteobacteria* enriched from *Alvinella pompejana* and deep-sea hydrothermal vents. *Appl Env. Microbiol* 67, 4566–4572.

Charlou, J. L., Donval, J. P., Konn, C., OndréAs, H., Fouquet, Y., Jean-Baptiste, P., and Fourré, E. (2010). "High production and fluxes of H_2 and CH_4 and evidence of abiotic hydrocarbon synthesis by serpentinization in ultramafic-hosted hydrothermal systems on the Mid-Atlantic Ridge," in *Diversity of hydrothermal systems on slow spreading ocean ridges*, eds. P. A. Rona, C. W. Devey, J. Dyment, and B. J. Murton (American Geophysical Union), 265–296.

Drake, H. L., Gößner, A. S., and Daniel, S. L. (2008). Old acetogens, new light. *Ann. N. Y. Acad. Sci.* 1125, 100–128.

La Duc, M. T., Benardini, J. N., Kempf, M. J., Newcombe, D. A., Lubarsky, M., and Venkateswaran, K. (2007). Microbial diversity of Indian Ocean hydrothermal vent plumes: Microbes tolerant of desiccation, peroxide exposure, and ultraviolet and γ -irradiation. *Astrobiology* 7, 416–431.

Erauso, G., Reysenbach, A.-L., Godfroy, A., Meunier, J.-R., Crump, B., Partensky, F., Baross, J. A., Marteinsson, V., Barbier, G., Pace, N. R., *et al.* (1993). *Pyrococcus abyssi* sp. nov., a new hyperthermophilic archaeon isolated from a deep-sea hydrothermal vent. *Arch. Microbiol.* 160, 338–349.

Fernández-Martínez, J., Pujalte, M. J., García-Martínez, J., Mata, M., Garay, E., and Rodríguez-Valera, F. (2003). Description of *Alcanivorax venustensis* sp. nov. and reclassification of *Fundibacter jadensis* DSM 12178T (Bruns and Berthe-Corti 1999) as *Alcanivorax jadensis* comb. nov., members of the emended genus *Alcanivorax*. *Int. J. Syst. Evol. Microbiol.* 53, 331–338.

Gauthier, M. J., Lafay, B., Christen, R., Fernandez, L., Acquaviva, M., Bonin, P., and Bertrand, J.-C. (1992). *Marinobacter hydrocarbonoclasticus* gen. nov., sp. nov., a new, extremely halotolerant, hydrocarbon-degrading marine bacterium. *Int. J. Syst. Bacteriol.* 42, 568–576.

González, J. M., Kato, C., and Horikoshi, K. (1995). *Thermococcus peptonophilus* sp. nov., a fast-growing, extremely thermophilic archaebacterium isolated from deep-sea hydrothermal vents. *Arch. Microbiol.* 164, 159–164.

Handley, K. M., Héry, M., and Lloyd, J. R. (2009). *Marinobacter santoriniensis* sp. nov., an arsenate-respiring and arsenite-oxidizing bacterium isolated from hydrothermal sediment. *Int. J. Syst. Evol. Microbiol.* 59, 886–892.

Ho, T.-Y., Scranton, M. I., Taylor, G. T., Varela, R., Thunell, R. C., and Muller-Karger, F. (2002). Acetate cycling in the water column of the Cariaco Basin: Seasonal and vertical variability and implication for carbon cycling. *Limnol. Ocean.* 47, 1119–1128.

Holm, N. G., and Charlou, J. L. (2001). Initial indications of abiotic formation of hydrocarbons in the Rainbow ultramafic hydrothermal system, Mid-Atlantic Ridge. *Earth Planet. Sci. Lett.* 191, 1–8.

Hoppe, H.-G. (1978). Relations between active bacteria and heterotrophic potential in the sea. *Neth. J. Sea Res.* 12, 78–IN4.

Huber, J. A., Butterfield, D. A., and Baross, J. A. (2003). Bacterial diversity in a subseafloor habitat following a deep-sea volcanic eruption. *FEMS Microbiol. Ecol.* 43, 393–409.

Huber, J. A., Mark Welch, D. B., Morrison, H. G., Huse, S. M., Neal, P. R., Butterfield, D. A., and Sogin, M. L. (2007). Microbial population structures in the deep marine biosphere. *Science* 318, 97 –100.

Huber, R., Stohr, J., Hohenhaus, S., Reinhard, R., Burggraf, S., Jannasch, H. W., and Stetter, K. O. (1995). *Thermococcus chitonophagus* sp. nov., a novel, chitin-degrading, hyperthermophilic archaeum from a deep-sea hydrothermal vent environment. *Arch. Microbiol.* 164, 255–264.

Ishii, K., Mußmann, M., MacGregor, B. J., and Amann, R. (2004). An improved fluorescence *in situ* hybridization protocol for the identification of bacteria and archaea in marine sediments. *FEMS Microbiol. Ecol.* 50, 203–213.

Jannasch, H. W., Wirsen, C. O., Molyneaux, S. J., and Langworthy, T. A. (1992). Comparative physiological studies on hyperthermophilic archaea isolated from deep-sea hot vents with emphasis on *Pyrococcus* strain GB-D. *Appl. Environ. Microbiol.* 58, 3472–3481.

Jeanthon, C., and Prieur, D. (1990). Susceptibility to heavy metals and characterization of heterotrophic bacteria isolated from two hydrothermal vent polychaete annelids, *Alvinella pompejana* and *Alvinella caudata*. *Appl. Environ. Microbiol.* 56, 3308–3314.

Karl, D. M., Brittain, A. M., and Tilbrook, B. D. (1989). Hydrothermal and microbial processes at Loihi Seamount, a mid-plate hot-spot volcano. *Deep Sea Res. Part Ocean. Res. Pap.* 36, 1655–1673.

Karl, D. M., Taylor, G. T., Novitsky, J. A., Jannasch, H. W., Wirsen, C. O., Pace, N. R., Lane, D. J., Olsen, G. J., and Giovannoni, S. J. (1988). A microbiological study of Guaymas Basin high temperature hydrothermal vents. *Deep Sea Res. Part Ocean. Res. Pap.* 35, 777–791.

Kaye, J. Z., and Baross, J. A. (2000). High incidence of halotolerant bacteria in Pacific hydrothermal-vent and pelagic environments. *FEMS Microbiol. Ecol.* 32, 249–260.

Kaye, J. Z., Sylvan, J. B., Edwards, K. J., and Baross, J. A. (2011). *Halomonas* and *Marinobacter* ecotypes from hydrothermal vent, subseafloor and deep-sea environments. *FEMS Microbiol. Ecol.* 75, 123–133.

Kirchman, D. L., Yu, L., Fuchs, B. M., and Amann, R. (2001). Structure of bacterial communities in aquatic systems as revealed by filter PCR. *Aquat. Microb. Ecol.* 26, 13–22.

Klindworth, A., Pruesse, E., Schweer, T., Peplies, J., Quast, C., Horn, M., and Glöckner, F. O. (2013). Evaluation of general 16S ribosomal RNA gene PCR primers for classical and next-generation sequencing-based diversity studies. *Nucleic Acids Res.* 41, e1–e1.

Konn, C., Charlou, J. L., Donval, J. P., Holm, N. G., Dehairs, F., and Bouillon, S. (2009). Hydrocarbons and oxidized organic compounds in hydrothermal fluids from Rainbow and Lost City ultramafic-hosted vents. *Chem. Geol.* 258, 299–314.

Lanave, C., Preparata, G., Saccone, C., and Serio, G. (1984). A new method for calculating evolutionary substitution rates. *J. Mol. Evol.* 20, 86–93.

Lang, S. Q., Butterfield, D. A., Lilley, M. D., Paul Johnson, H., and Hedges, J. I. (2006). Dissolved organic carbon in ridge-axis and ridge-flank hydrothermal systems. *Geochim. Cosmochim. Acta* 70, 3830–3842.

Lang, S. Q., Butterfield, D. A., Schulte, M., Kelley, D. S., and Lilley, M. D. (2010). Elevated concentrations of formate, acetate and dissolved organic carbon found at the Lost City hydrothermal field. *Geochim. Cosmochim. Acta* 74, 941–952.

Lee, S., and Fuhrman, J. A. (1987). Relationships between biovolume and biomass of naturally derived marine bacterioplankton. *Appl. Environ. Microbiol.* 53, 1298–1303.

Lever, M., Heuer, V., Morono, Y., Masui, N., Schmidt, F., Alperin, M., Inagaki, F., Hinrichs, K.-U., and Teske, A. (2010). Acetogenesis in deep subseafloor sediments of the Juan de Fuca ridge flank: A synthesis of geochemical, thermodynamic, and gene-based evidence. *Geomicrobiol. J.* 27, 183–211.

Marcon, Y., Sahling, H., Borowski, C., dos Santos Ferreira, C., Thal, J., and Bohrmann, G. (2013). Megafaunal distribution and assessment of total methane and sulfide consumption by mussel beds at Menez Gwen hydrothermal vent, based on geo-referenced photomosaics. *Deep Sea Res. Part Ocean. Res. Pap.* 75, 93–109.

Marteinsson, V., Birrien, J.-L., Jeanthon, C., and Prieur, D. (1996). Numerical taxonomic study of thermophilic *Bacillus* isolated from three geographically separated deep-sea hydrothermal vents. *FEMS Microbiol. Ecol.* 21, 255–266.

Marteinsson, V., Birrien, J.-L., Kristjánsson, J. K., and Prieur, D. (1995). First isolation of thermophilic aerobic non-sporulating heterotrophic bacteria from deep-sea hydrothermal vents. *FEMS Microbiol. Ecol.* 18, 163–174.

McCollom, T. M., and Seewald, J. S. (2001). A reassessment of the potential for reduction of dissolved CO_2 to hydrocarbons during serpentinization of olivine. *Geochim. Cosmochim. Acta* 65, 3769–3778.

McCollom, T. M., and Seewald, J. S. (2007). Abiotic synthesis of organic compounds in deep-sea hydrothermal environments. *Chem. Rev.* 107, 382–401.

McCollom, T., Ritter, G., and Simoneit, B. (1999). Lipid synthesis under hydrothermal conditions by Fischer-Tropsch-type reactions. *Orig Life Evol Biosph* 29, 153–166.

Miroshnichenko, M. L., Kostrikina, N. A., L'Haridon, S., Jeanthon, C., Hippe, H., Stackebrandt, E., and Bonch-Osmolovskaya, E. A. (2002). *Nautilia lithotrophica* gen. nov., sp. nov., a thermophilic sulfur-reducing epsilon-proteobacterium isolated from a deep-sea hydrothermal vent. *Int. J. Syst. Evol. Microbiol.* 52, 1299–1304.

Miroshnichenko, M. L., L'Haridon, S., Schumann, P., Spring, S., Bonch-Osmolovskaya, E. A., Jeanthon, C., and Stackebrandt, E. (2004). *Caminibacter profundus* sp. nov., a novel thermophile of *Nautiliales* ord. nov. within the class "*Epsilonproteobacteria*", isolated from a deep-sea hydrothermal vent. *Int. J. Syst. Evol. Microbiol.* 54, 41–45.

Miyatake, T., MacGregor, B. J., and Boschker, H. T. S. (2013). Depth-related differences in organic substrate utilization by major microbial groups in intertidal marine sediment. *Appl. Environ. Microbiol.* 79, 389–392.

Miyatake, T., MacGregor, B. J., and Boschker, H. T. S. (2009). Linking microbial community function to phylogeny of sulfate-reducing *Deltaproteobacteria* in marine sediments by combining stable isotope probing with magnetic-bead capture hybridization of 16S rRNA. *Appl. Environ. Microbiol.* 75, 4927–4935.

Muyzer, G., Brinkhoff, T., Nübel, U., Santegoeds, C., Schäfer, H., and Wawer, C. (1998). "Denaturing gradient gel electrophoresis (DGGE) in microbial ecology," in *Molecular microbial ecology manual* (Kluwer Academic Publishers), 3.4.4/1–3.4.4/27.

Nakagawa, S., and Takai, K. (2008). Deep-sea vent chemoautotrophs: diversity, biochemistry and ecological significance. *FEMS Microbiol. Ecol.* 65, 1–14.

Pérez-Rodríguez, I., Ricci, J., Voordeckers, J. W., Starovoytov, V., and Vetriani, C. (2010). *Nautilia nitratireducens* sp. nov., a thermophilic, anaerobic,

chemosynthetic, nitrate-ammonifying bacterium isolated from a deep-sea hydrothermal vent. *Int. J. Syst. Evol. Microbiol.* 60, 1182–1186.

Perner, M., Gonnella, G., Hourdez, S., Böhnke, S., Kurtz, S., and Girguis, P. (2013). *In situ* chemistry and microbial community compositions in five deep-sea hydrothermal fluid samples from Irina II in the Logatchev field. *Environ. Microbiol.* 15, 1551–1560.

Pernthaler, A., Pernthaler, J., and Amann, R. (2004). "Sensitive multi-color fluorescence in situ hybridization for indentification of environmental microorganisms," in *Molecular Microbial Ecology Manual* (Dodrecht, Boston, London: Kluwer Academic Publishers), 711–726.

Pernthaler, A., Pernthaler, J., Schattenhofer, M., and Amann, R. (2002). Identification of DNA-synthesizing bacterial cells in coastal North Sea plankton. *Appl Env. Microbiol* 68, 5728–5736.

Pester, M., Bittner, N., Deevong, P., Wagner, M., and Loy, A. (2010). A "rare biosphere" microorganism contributes to sulfate reduction in a peatland. *ISME J.* 4, 1591–1602.

Pimenov, N. V., Kaliuzhnaia, M. G., Khmelenina, V. N., Mitiushina, L. L., and Trotsenko, I. A. (2002). Utilization of methane and carbon dioxide by symbiotrophic bacteria in gills of *Mytilidae* (*Bathymodiolus*) from the Rainbow and Logachev hydrothermal fields on the Mid-Atlantic Ridge. *Mikrobiologiia* 71, 681–689.

Pley (1991). *Pyrodictium abyssi* sp. nov. represents a novel heterotrophic marine archaeal hyperthermophile growing at 110°C. *Syst. Appl. Microbiol.* 14, 245–253.

Polerecky, L., Adam, B., Milucka, J., Musat, N., Vagner, T., and Kuypers, M. M. M. (2012). Look@NanoSIMS – a tool for the analysis of nanoSIMS data in environmental microbiology. *Environ. Microbiol.* 14, 1009–1023.

Pruesse, E., Peplies, J., and Glöckner, F. O. (2012). SINA: Accurate high-throughput multiple sequence alignment of ribosomal RNA genes. *Bioinformatics* 28, 1823–1829.

Quast, C., Pruesse, E., Yilmaz, P., Gerken, J., Schweer, T., Yarza, P., Peplies, J., and Glöckner, F. O. (2012). The SILVA ribosomal RNA gene database project: improved data processing and web-based tools. *Nucleic Acids Res.* 41, D590–D596.

Raguénès, G., Christen, R., Guezennec, J., Pignet, P., and Barbier, G. (1997). *Vibrio diabolicus* sp. nov., a new polysaccharide-secreting organism isolated from a deep-sea hydrothermal vent Polychaete Annelid, *Alvinella pompejana*. *Int. J. Syst. Bacteriol.* 47, 989–995.

Raguénès, G., Pignet, P., Gauthier, G., Peres, A., Christen, R., Rougeaux, H., Barbier, G., and Guezennec, J. (1996). Description of a new polymer-secreting bacterium from a deep-sea hydrothermal vent, *Alteromonas macleodii* subsp. *fijiensis*, and preliminary characterization of the polymer. *Appl. Environ. Microbiol.* 62, 67–73.

Rogers, D. R., Santelli, C. M., and Edwards, K. J. (2003). Geomicrobiology of deep-sea deposits: Estimating community diversity from low-temperature seafloor rocks and minerals. *Geobiology* 1, 109–117.

Rogers, K. L., and Amend, J. P. (2006). Energetics of potential heterotrophic metabolisms in the marine hydrothermal system of Vulcano Island, Italy. *Geochim. Cosmochim. Acta* 70, 6180–6200.

Santelli, C. M., Orcutt, B. N., Banning, E., Bach, W., Moyer, C. L., Sogin, M. L., Staudigel, H., and Edwards, K. J. (2008). Abundance and diversity of microbial life in ocean crust. *Nature* 453, 653–656.

Schmidt, K., Koschinsky, A., Garbe-Schönberg, D., de Carvalho, L. M., and Seifert, R. (2007). Geochemistry of hydrothermal fluids from the ultramafic-hosted Logatchev hydrothermal field, 15°N on the Mid-Atlantic Ridge: Temporal and spatial investigation. *Chem. Geol.* 242, 1–21.

Shively, J. M., van Keulen, G., and Meijer, W. G. (1998). SOMETHING FROM ALMOST NOTHING: Carbon dioxide fixation in chemoautotrophs. *Annu. Rev. Microbiol.* 52, 191–230.

Shock, E. L. (1992). Chapter 5 chemical environments of submarine hydrothermal systems. *Orig. Life Evol. Biosph.* 22, 67–107.

Shock, E. L., and Schulte, M. D. (1998). Organic synthesis during fluid mixing in hydrothermal systems. *J. Geophys. Res. Planets* 103, 28513–28527.

Sievert, S. M., Hügler, M., Taylor, C. D., and Wirsen, C. O. (2008). "Sulfur oxidation at deep-sea hydrothermal vents," in *Microbial Sulfur Metabolism*, eds. D. C. Dahl and D. C. G. Friedrich (Springer Berlin Heidelberg), 238–258.

Sievert, S. M., Wieringa, E. B. A., Wirsen, C. O., and Taylor, C. D. (2007). Growth and mechanism of filamentous-sulfur formation by *Candidatus* Arcobacter sulfidicus in opposing oxygen-sulfide gradients. *Environ. Microbiol.* 9, 271–276.

Skoog, A., Vlahos, P., Rogers, K. L., and Amend, J. P. (2007). Concentrations, distributions, and energy yields of dissolved neutral aldoses in a shallow hydrothermal vent system of Vulcano, Italy. *Org. Geochem.* 38, 1416–1430.

Smith, J. L., Campbell, B. J., Hanson, T. E., Zhang, C. L., and Cary, S. C. (2008). *Nautilia profundicola* sp. nov., a thermophilic, sulfur-reducing epsilonproteobacterium from deep-sea hydrothermal vents. *Int. J. Syst. Evol. Microbiol.* 58, 1598–1602.

Stamatakis, A., Ludwig, T., and Meier, H. (2005). RAxML-III: a fast program for maximum likelihood-based inference of large phylogenetic trees. *Bioinformatics* 21, 456–463.

Summit, M., and Baross, J. A. (2001). A novel microbial habitat in the mid-ocean ridge subseafloor. *Proc. Natl. Acad. Sci.* 98, 2158–2163.

Takai, K., Gamo, T., Tsunogai, U., Nakayama, N., Hirayama, H., Nealson, K. H., and Horikoshi, K. (2004). Geochemical and microbiological evidence for a hydrogen-based, hyperthermophilic subsurface lithoautotrophic microbial ecosystem (HyperSLiME) beneath an active deep-sea hydrothermal field. *Extremophiles* 8, 269–282.

Tani, A., Sakai, Y., Ishige, T., and Kato, N. (2000). Thermostable NADP+-Dependent Medium-chain alcohol dehydrogenase from *Acinetobacter* sp. strain M-1: Purification and characterization and gene expression in *Escherichia coli*. *Appl. Environ. Microbiol.* 66, 5231–5235.

Taylor, C. D., Wirsen, C. O., and Gaill, F. (1999). Rapid microbial production of filamentous sulfur mats at hydrothermal vents. *Appl. Environ. Microbiol.* 65, 2253–2255.

Teira, E., Reinthaler, T., Pernthaler, A., Pernthaler, J., and Herndl, G. J. (2004). Combining catalyzed reporter deposition-fluorescence *in situ* hybridization and microautoradiography to detect substrate utilization by bacteria and archaea in the deep ocean. *Appl. Environ. Microbiol.* 70, 4411–4414.

Tuttle, A. J. (1985). The role of sulfur-oxidizing bacteria at deep-sea hydrothermal vents. *Bull. Biol. Soc. Wash.* 6, 335–343.

Tuttle, J. H., Wirsen, C. O., and Jannasch, H. W. (1983). Microbial activities in the emitted hydrothermal waters of the Galápagos rift vents. *Mar. Biol.* 73, 293–299.

Vandieken, V., Pester, M., Finke, N., Hyun, J.-H., Friedrich, M. W., Loy, A., and Thamdrup, B. (2012). Three manganese oxide-rich marine sediments harbor similar communities of acetate-oxidizing manganese-reducing bacteria. *ISME J.* 6, 2078–2090.

Webster, G., Rinna, J., Roussel, E. G., Fry, J. C., Weightman, A. J., and Parkes, R. J. (2010). Prokaryotic functional diversity in different biogeochemical depth zones in tidal sediments of the Severn Estuary, UK, revealed by stable-isotope probing. *FEMS Microbiol. Ecol.* 72, 179–197.

Webster, G., Watt, L. C., Rinna, J., Fry, J. C., Evershed, R. P., Parkes, R. J., and Weightman, A. J. (2006). A comparison of stable-isotope probing of DNA and phospholipid fatty acids to study prokaryotic functional diversity in sulfate-reducing marine sediment enrichment slurries. *Environ. Microbiol.* 8, 1575–1589.

Wery, N., Moricet, J. M., Cueff, V., Jean, J., Pignet, P., Lesongeur, F., Cambon-Bonavita, M. A., and Barbier, G. (2001). *Caloranaerobacter azorensis* gen. nov., sp. nov., an anaerobic thermophilic bacterium isolated from a deep-sea hydrothermal vent. *Int. J. Syst. Evol. Microbiol.* 51, 1789–1796.

Wirsen, C. O., Sievert, S. M., Cavanaugh, C. M., Molyneaux, S. J., Ahmad, A., Taylor, L. T., DeLong, E. F., and Taylor, C. D. (2002). Characterization of an autotrophic sulfide-oxidizing marine *Arcobacter* sp. that produces filamentous sulfur. *Appl. Environ. Microbiol.* 68, 316–325.

Wirsen, C. O., Tuttle, J. H., and Jannasch, H. W. (1986). Activities of sulfur-oxidizing bacteria at the 21°N East Pacific Rise vent site. *Mar. Biol.* 92, 449–456.

Wood, A. P., Aurikko, J. P., and Kelly, D. P. (2004). A challenge for 21st century molecular biology and biochemistry: what are the causes of obligate autotrophy and methanotrophy? *FEMS Microbiol. Rev.* 28, 335–352.

Wright, R. R., and Hobbie, J. E. (1966). Use of glucose and acetate by bacteria and algae in aquatic ecosystems. *Ecology* 47, 447–464.

Yakimov, M. M., Golyshin, P. N., Lang, S., Moore, E. R. B., Abraham, W.-R., Lünsdorf, H., and Timmis, K. N. (1998). *Alcanivorax borkumensis* gen. nov., sp. nov., a new, hydrocarbon-degrading and surfactant-producing marine bacterium. *Int. J. Syst. Bacteriol.* 48, 339–348.

Yamamoto, M., and Takai, K. (2011) Sulfur metabolisms in epsilon- and gamma-*Proteobacteria* in deep-sea hydrothermal fields. *Front. Microb. Physiol. Metab.* 2, 192.

Yoon, J.-H., Kim, I.-G., Kang, K. H., Oh, T.-K., and Park, Y.-H. (2003). *Alteromonas marina* sp. nov., isolated from sea water of the East Sea in Korea. *Int. J. Syst. Evol. Microbiol.* 53, 1625–1630.

Tables

Table 1: List of sampling sites of the cruises M82-3 and SO216 used in this study

Station	Area (Sample)	Latitude & Longitude	Depth [m]	Temperature [°C]	pH	NH_4 [µM]	NO_3^- [µM]	H_2S [µM]
Menez Gwen (Azor Ana) at Woody´s Crack (WC)								
M83-2-702	Plume above Woody´s crack (WC-P)[1]	N 37°50.671 E 31°31.150	805	9	n.d.	66.9	22.9	n.d.
M83-2-719	Woody´s Crack (WCa)[1,2]	N 37°50.673 E 31°31.154	828	46-56[4]	5.0	7.8	16.3	+[5]
M83-2-736	Woody´s Crack (WCb)[1,3]	N 37°50.673 E 31°31.158	828	25-49[4]	4.9	5.3	17.4	+[5]
M83-2-754	Woody's crack (WCc)[6]	N 37°50.673 E 31°31.154	828	49-68[4]	4.6	n.d.	n.d.	+[5]
M83-2-761	Mussel bed (WC-M) [1]	N 37°50.675 E31°31.155	828	9.3	7.0	n.d.	n.d.	n.d.
Manus Basin								
SO216-29	Fenway[1,2,3] (FW)	S 03°43.697 E 151°40.350	1706	3.7	7.2	2.6	n.d.	<5
SO216-21	North Su[1,2,3] (NS-I)	S 03°47.955 E 152°06.080	1200	16-40[4]	7.1	1.9	n.d.	14-66
SO216-19	NorthSu[3] (NS-IIa)	S 03°47.998 E152°06.051	1155	59-73[4]	3.1	30.0	n.d.	n.d.
SO216-45	North Su[1,2] (NS-IIb)	S 03°47.998 E 152°06.057	1155	54-73[4]	3.6	10.9	n.d.	113-302

[1]used for CARD-FISH analysis

[2]used for ^{13}C-acetate incubations, molecular and isotopic analysis (CARD-FISH, 16S rRNA gene libraries, IRMS, nanoSIMS)

[3]used for 16S rRNA gene pyrotag analysis

[4] temperature range during sampling

[5]samples with typical H_2S odour (detailed data will be published by E. Reeves)

[6] used for acetate-free and anoxic control experiments

n.d. – not determined

Figures

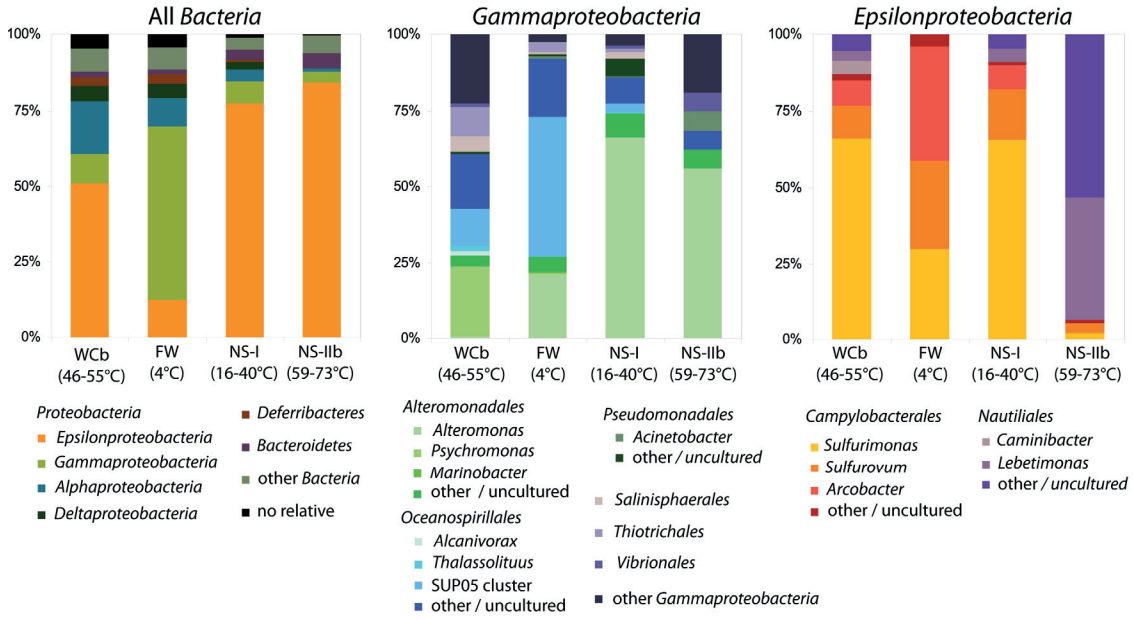

Figure 1: 16S rRNA pyrotag analysis of the bacterial community in source fluids from Woody´s Crack at Menez Gwen (WCb) and Fenway (FW), North Su-I (NS-I) and North Su–IIb (NS-IIb), at Manus Basin (MB).

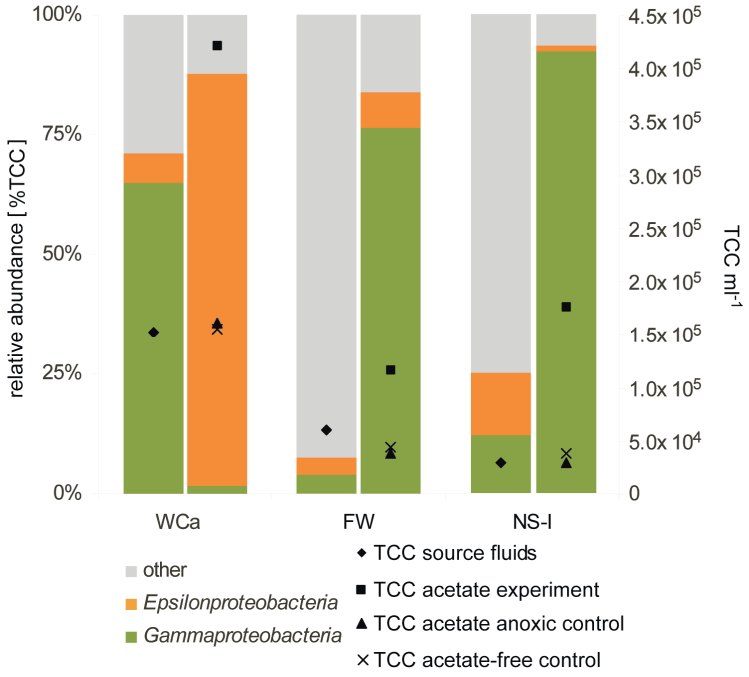

Figure 2: Relative abundances (CARD-FISH) of *Gamma-* and *Epsilonproteobacteria* and total cell counts (TCC) in source fluids and in the incubation experiments (WC, FW and NS-I). Relative abundance (bars) and TCC (symbols) are displayed as mean values calculated from replicates. Left bars: relative abundance in source fluids. Right bars: relative abundance in incubation experiments.

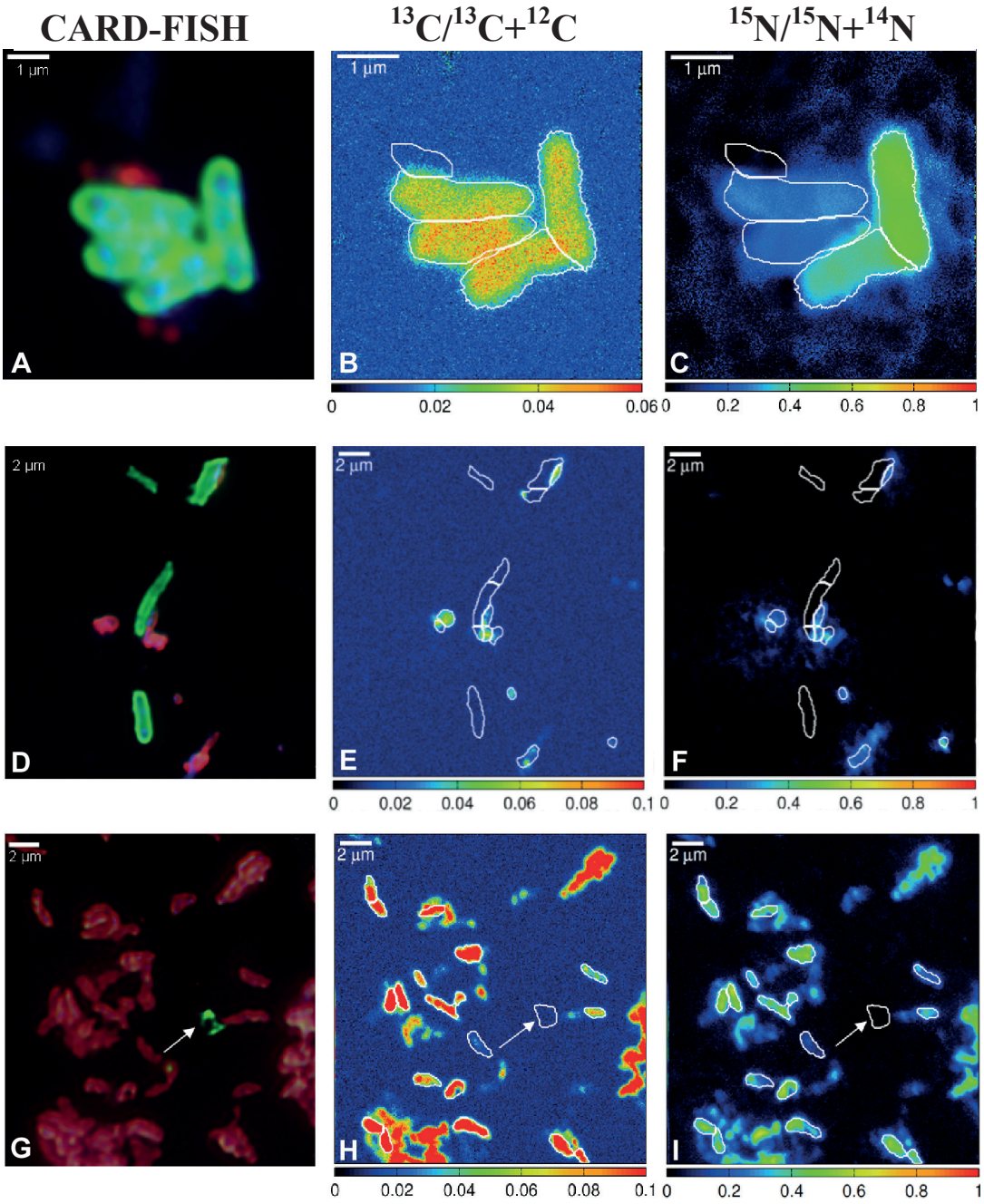

Figure 3: ^{13}C-acetate and ^{15}N-ammonium uptake by single cells in incubation experiments from Woody's crack, WCa 55°C, (Menez Gwen), Fenway, FW 4°C, and North Su, NS-I 37°C, (Manus Basin). *Epsilonproteobacteria* (green fluorescence) and *Gammaproteobacteria* (red fluorescence) (A, D and G). Upper row: WCa, middle row: NS-I and lower row: FW.

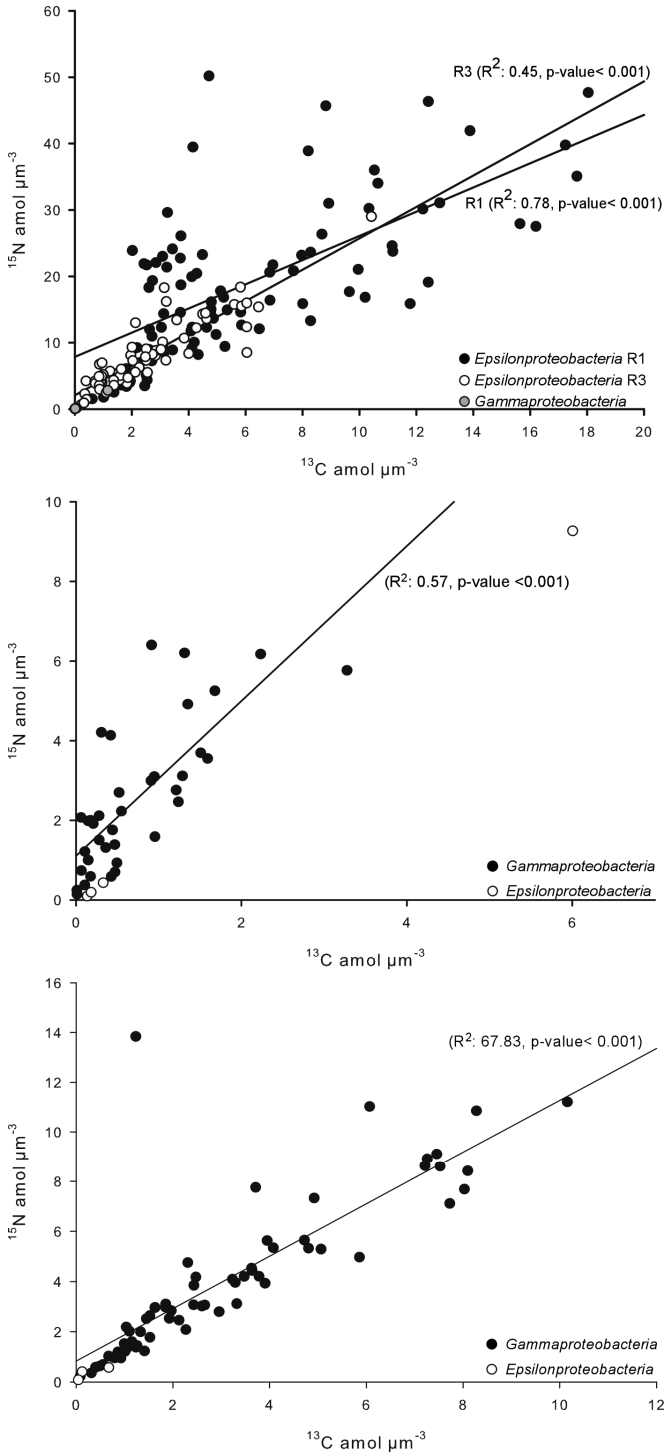

Figure 4: Assimilation of ^{13}C-acetate and ^{15}N-ammonium in amol µm^{-3} of *Gammaproteobacteria* and *Epsilonproteobacteria* in incubation experiments. Upper row: WCa, 55°C;. middle row: FW, 4°C; lower row NS-I, 37°C. The lines represent the linear regression analysis with the coefficient of determination R^2 and the p-value for the linear regression analysis. P-values with <0.05 are interpreted as significant.

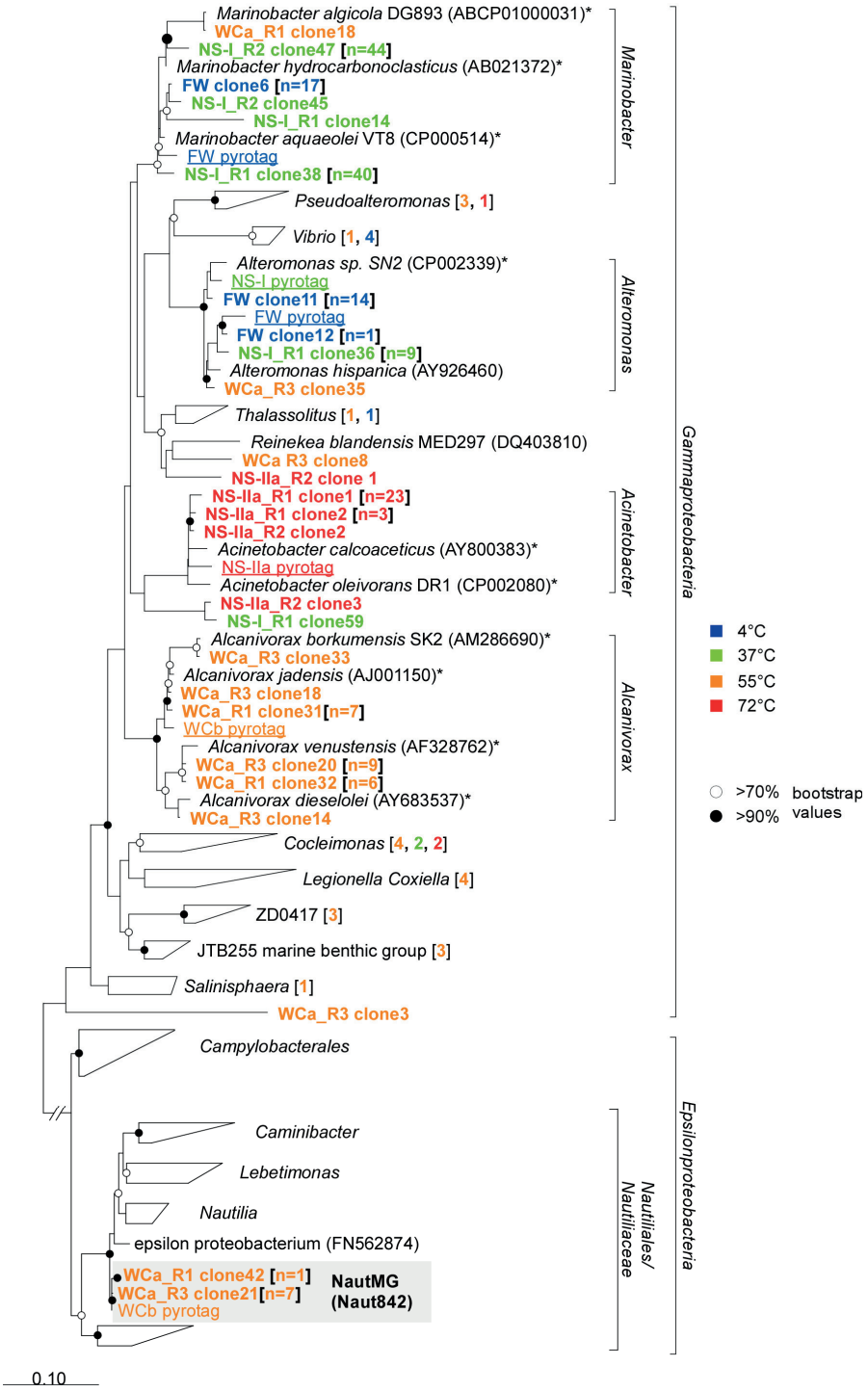

Figure 5: Phylogeny reconstruction of partial sequences of *Gammaproteobacteria* and *Epsilonproteobacteria* from source fluids of Menez Gwen and Manus Basin (pyrotags, underlined) and from 13C-acetate incubation experiments (clones). The gray rectangle indicates the Menez Gwen-specific (NautMG)-group targeted by probe Naut842. Numbers of sequences per OTU (97% cut-off) are given in parenthesis. Scale bar represents 10% estimated sequence divergence.

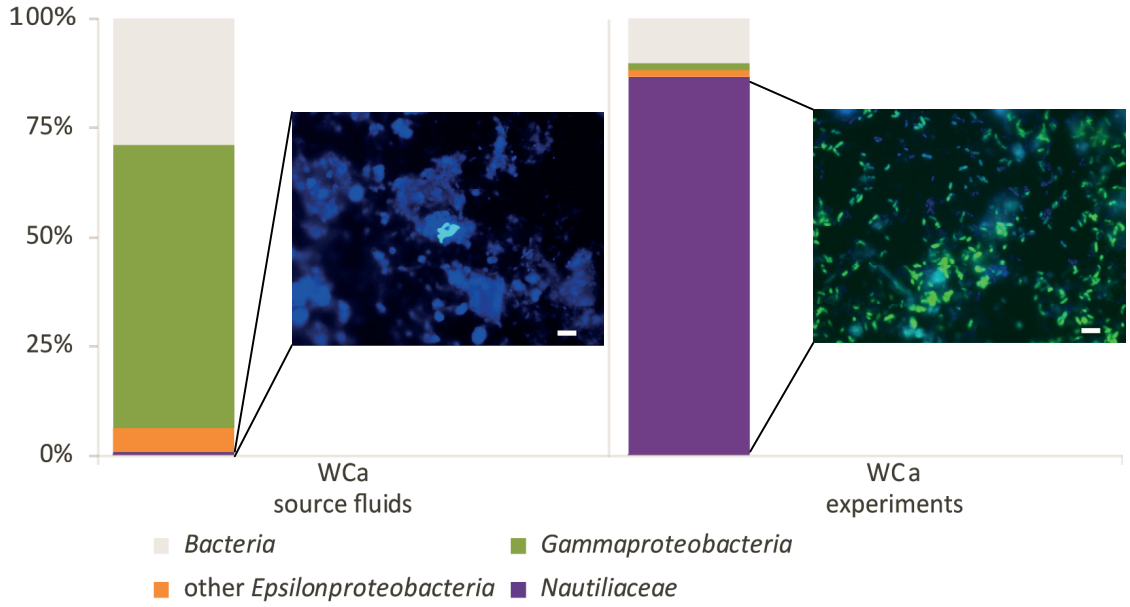

Figure 6: Relative abundance of *Gammaproteobacteria*, *Epsilonproteobacteria* and the NautMG-group in fluids of Woody's Crack (WCa) and in 13C-acetate incubation experiments. Images show cells of NautMG-group (probe Naut842) in source fluids and in 13C-acetate incubation experiments. Scale bar represents 5 µm.

Supporting Information

Construction of 16S rRNA gene libraries and phylogenetic analysis

Bacterial 16S rRNA genes for samples WCa, FW and NS-I were directly amplified from polycarbonate filters. Therefore a filter piece of 2-3 mm was put in a 100µl PCR mix, containing 1x PCR buffer (500 mM KCl, 100 mM Tris-HCl pH 8.3 at 25°C, 15 mM WC^{2+}) (5 Prime, Hamburg, Germany), 0.2 mM of each deoxynucleoside (Roche, Basel, Schweiz), 0.5 µM of each primer (Biomers, Ulm, Deutschland), 0.3 ml^{-1} BSA (Fluka, Buchs, Schweiz) and 0.01 U μl^{-1} *Taq*-polymerase (5 Prime, Hamburg, Germany). For sample NS-IIa, DNA was first extracted from polycarbonate filters with the Ultra Clean Soil DNA Kit (MoBio Laboratories, Carlsbad, USA) and 20 µl PCR reactions with 1µl DNA template and same ingredients as given above were set up. The bacteria specific 16S rRNA gene primers GM3F and GM4R (Muyzer *et al.*, 1995), as well as GM5F and 907RM (Muyzer *et al.*, 1998) were used for library construction. The thermocycler conditions were 94°C for 5 minutes (denaturation), followed by 25-40 cycles of 94°C for 1 minute (denaturation), 44°C for 1.5 minutes (annealing) and 72°C for 1 minute (elongation)and concluded a final elongation step at 72°C for 10 minutes.

All PCR products were run on a 1% LE agarose gel and stained with 1 x SYBR green I solution (Invitrogen, Karlsruhe, Germany) dissolved in 1 x TAE buffer. DNA bands of desired size were exised with a sterile scalpel, dissolved in pre-warmed PCR water and ligated directly or after gel purification with QIAquick gel extraction kit (QIAgen, Hilden, Germany) into the pCR®4-TOPO® vectors of the TOPO TA cloning kit (Invitrogen, Karlsruhe, Germany) or pGem-T-easy vector of the Promega cloning kit (Promega, Mannheim, Germany). Chemically competent *E. coli* cells, strain TOP 10, were transformed with the ligation products, as described in the manuals. Clones were screened for inserts or the right size with M13F and M13R vector primers (Yanisch-Perron *et al.*, 1985). PCRs were performed in 20 µl reactions as described above. Positive screening PCR products were cleaned with the PCR Clean Up NucleoFast96 kit from Machery& Nagel according to manufacturers' protocol. Cleaned PCR products were Sanger sequenced with the internal primer 907RM (Muyzer *et al.*, 1998) using the ABO Prism BigDye Terminator v 3.0 cycles sequencing kit and an ABI Prism 3100 Genetic Analyzer (Applied Biosystems, Darmstadt, Germany).

16S rRNA gene amplicons and 454-pyrotag sequencing of bacterial diversity in fluids

Bacterial diversity in diffuse fluid samples was analyzed by 454-pyrosequencing of 16S rRNA gene amplicons. Therefore DNA was extracted with the Ultra Clean Soil DNA Kit (MoBio Laboratories, Carlsbad, USA) from a PES filter piece of pumped fluids. Bacterial 16S rRNA genes were amplified with modified GM3 (Muyzer *et al.*, 1995) ad 907RM (Muyzer *et al.*, 1998) primers in ten parallel PCR reactions. Primer modification included the addition of individual, error-tolerant, hexamer barcodes at the 5' end of primer 907RM, and the extension of both GM3F and 907RM primers with asymmetric SfiI-restriction sites at the 5' end (for subsequent ligation of the 454-sequencing adapters). PCR's were performed with the Phusion High Fidelity Polymerase Kit (Finnzymes, New England BioLabs Inc.), following manufacturers' instructions. Therefore, 1x Phusion HF Buffer, 250 µM of each deoxynucleoside triphosphate, 0.5 µM of each primer and 0.4U of Phusion DNA polymerase were mixed and to each reaction 1 µl DNA template was added. The thermocycler conditions were set as follows: 3 min initial denaturation at 98°C, 30 cycles consisting of 10 sec denaturation at 98°C, 30 sec of annealing at 48°C and 30 sec elongation at 72°C, followed by a 10 min final elongation step at 72°C. Replicate reactions were pooled after amplification and, DNA was precipitated during a 60 min incubation on ice, after addition of 3.3 volumes of non-denaturated, absolute ethanol and 0.15 volumes of 3 M Na-Acetate (ph 5.2). Finally, DNA was pelleted by 20 min centrifuged at 10,000 g and the pellet was re-suspended in 20 µl TE buffer. Next, DNA was mixed with 2 µl loading dye and run on a 1% low-melting agarose electrophoresis gel. The gel was stained with SYBR Green I Nucleotide Stain and the DNA bands were visualized under UV light. Band of the desired size (~900 bp) were cut out with sterile scalpels. The obtained gel fragments were dissolved in 60 µl of pre-warmed (65°C) PCR water and purified with the MinElute Gel Extraction Kit (QIAgen) as instructed in the accompanying protocol. DNA concentrations were determined fluorometrically at 260nm, with the Qubit 2.0 Fluorometer and the Qubit dsDNA HS Assay KIT (life Technologies). Amplicones were pooled and shipped to the Max Planck Genome Center (Cologne, Germany). There, amplicon pools were digested for 1 hour at 50°C with a SfiI-restriction enzyme (NEB) and digested DNA was purified with the

MinElute PCR purification kit (QIAgen). In the next step, the 454 adaptors (A and B) were ligated to the fragment, by an overnight incubation with 1 U T4 DNA ligase (Roche) at 6°C. After incubation, the ligase was inactivated by 10 min heat treatment at 65°C. To remove excess adapters by size fractionation, electrophoresis on a 2% LE agarose gel was performed. Gel bands were excised and purified with the QIAquick gel extraction kit (QIAgen). Finally, emulsion PCRs were performed with the GS FLX Titanium LV emPCR Kit (Lib-L) and sequencing with the GS FLX Titanium Sequencing Kit XLR70 on a Roche 454 Genome Sequencer FLX+ instrument according to the manufacturers' protocols.

Design and testing of specific probe for the MG-specific group

We designed an oligonucleotide probe (Naut842) targeting only the 16S rRNA of the *Nautiliaceae*-phylotype defined as NautMG-group (Fig. 5) and two unlabeled helper oligonucleotides (Fuchs *et al.*, 2000). For discrimination from other *Nautiliaceae* we designed three competitor oligonucleotides (up to 3 mismatches). The competitors bind to the target site of the Naut842 oligonucleotide probe in closely related non-target organisms (Table S2). We tested the probe *in silico* with the mathFISH web-based software tool (Yilmaz *et al.*, 2011) with parameters for FISH as described in material and methods. Calculated formamide dissociation curves were used as proxy for testing the probe. A formamide series was performed on cells from the incubations to optimize stringency conditions.

Supporting Tables

Table S1: Statistics on 454-pyrosequences analyzed and used in this study

Sample	Reads retrieved	Sequences (% passed quality check)	Average length (bp)	Sequences (after quality check)		
				OTUs* (%)	Clustered** (%)	Replicates*** (%)
WCa	7524	6880	416.6	1648	4640	592
		(91.44)		(21.9)	(61.7)	(16.4)
FW	3503	3316	445.9	860	1832	624
		(94.7)		(25.9)	(55.3)	(18.8)
NS-I	7134	6739	441.6	1043	3954	1742
		(94.5)		(15.5)	(58.7)	(25.8)
NS-IIa	479	461	465.0	81	315	65
		(96.2)		(17.6)	(68.3)	(14.1)

*number of OTUs (≥98% sequence identity) in the sample

**number of unique reads in the sample assigned to OTUs (≥98% sequence identity)

***reads identical to another read within the sample

Table S2: Oligonucleotide probes applied in this study

Probe name	Target group	Sequence (3'-5')	position[a]	% FA	Reference
EUB338	**most *Bacteria***	GCTGCCTCCCGTAGGAGT	338-355	0-50	(Amann *et al.*, 1990)
EUB338 II	***Plantomycetales***	GCAGCCACCCGTAGGTGT	338-355	0-50	(Daims *et al.*, 1999)
EUB338 III	***Verrucomicrobiales***	GCTGCCACCCGTAGGTGT	338-355	0-50	(Daims *et al.*, 1999)
EUB338 IV	***Lentisphaerae***	GCAGCCTCCCGCAGGAGT	338-355	0-50	(Arnds, 2009)
NON338	**complementary to EUB338**	ACTCCTACGGGAGGCAGC	-	0-50	(Wallner *et al.*, 1993)
Gam42a	***Gammaproteobacteria***	GCCTTCCCACATCGTTT	1027-1043	35	(Manz *et al.*, 1992)
cGam42a	**competitor for Gam42a**	GCCTTCCCACTTCGTTT	1027-1043	35	(Manz *et al.*, 1992)
EPSY549	***Epsilonproteobacteria***	CAGTGATTCCGAGTAACG	549-566	35	(Lin *et al.*, 2006)
EPSY914	***Epsilonproteobacteria***	GGTCCCCGTCTATTCCTT	914-932	35	(Loy, 2003)
Naut842	**NautMg *Nautiliaceae***	CTGCGTGACTGCAGGACTGT	842-862	30	this study
Naut_helper1	**helper**	CTACTAGTGGTTGTGGGGGG	822-842	30	this study
Naut_helper2	**helper**	ATGGCTACTAGTGGTTGTGGGG	820-842	30	this study
cNaut842_1	**competitor for Naut842**	CTGCGTGACTGAAGGACTGT	842-862	30	this study
cNaut842_2	**competitor for Naut842**	CTGCGTGACTGAAGGACTAT	842-862	30	this study
cNaut842_3	**competitor for Naut842**	CTGCGTGACTGAGGGACTAT	842-862	30	this study

[a] *E. coli* numbering according to (Brosius *et al.*, 1978)

Table S3: TCC and CARD-FISH results in source fluid samples and incubation experiments as range with standard deviation for triplicates or values for duplicates

Sample	TCC [cells ml^{-1}]	x-fold change of TCC	CARD-FISH [%]				
			EUB I-IV	Arch915	Gam42a	EPSY549/914	Naut842
Menez Gwen, WC 55°C							
Source fluid (WCa)	$1.6 \pm 0.3 \times 10^5$		99	n.d	65	10	0.8
^{13}C-acetate incubation	$4.4 \pm 0.2 \times 10^5$	2.7-2.8	93.7 ± 3.6		1.5 ± 0.2	86.3 ± 2.5	84-87
Source fluid (WCb)	$1{,}26 \times 10^5$						
Anoxic control	$1{,}32 \times 10^5$	1.0					
Acetate-free control	$1{,}28 \times 10^5$	1.0					
Manus Basin, FW, 4°C							
Source fluid	$6.2 \pm 0.5 \times 10^4$		58	8	4	4	
^{13}C-acetate incubation	$0.8/ 1.6 \times 10^5$	1.3/ 2.5	99		63/ 87	1.6/ 12	
Anoxic controls	$4.0/ 4.2 \times 10^4$	0.6/ 0.7					
Acetate-free controls	$4.5/ 4.9 \times 10^4$	0.7/ 0.8					
Manus Basin, NS-I, 37°C							
Source fluid	$3.3 \pm 1.4 \times 10^4$		83/ 85	11	9/ 12	7/ 15	
^{13}C-acetate incubation	$1.8/ 3.7 \times 10^5$	5.5/ 11.3	99		78/ 108	1.1/ 1.3	
Anoxic controls	$2.9/ 3.5 \times 10^4$	0.9/ 1.1					
Acetate-free controls	$3.8/ 4.2 \times 10^4$	1.2/ 1.3					
Manus Basin, NS-IIa, 72°C							
Source fluid	$2.2 \pm 0.8 \times 10^4$		62/ 64		5/ 15	8/ 11	
^{13}C-acetate incubation	$2.9/ 3.5 \times 10^4$	1.4/ 1.6	1.0/3.8	0.5/ 0	0.6/ 0	0.2/ 0	
Anoxic controls	$1.2/ 1.5 \times 10^4$	0.6/ 0.7					
Acetate-free controls	$1.7/ 2.3 \times 10^4$	0.8/ 1.0					

Table S4: Bulk ratios of $^{13}C/^{12}C$ and $^{15}N/^{14}N$ in atom percent as determined by IRMS

Sample	$^{13}C/^{12}C$	$^{15}N/^{14}N$
WCa	**55°C – 8 h incubation**	
Replicate I[1,2]	2.20	23.58
Replicate II[2]	1.84	26.05
Replicate III[1,2]	1.84	19.83
Dead control I	1.08	0.95
Dead control II	1.08	0.63
FW	**4°C – 12 h incubation**	
Replicate I[1,2]	2.20	22.09
Replicate II[2]	1.56	9.19
Dead control	1.09	0.46
NS-I	**37°C – 10 h incubation**	
Replicate I[1,2]	2.00	11.27
Replicate II[2]	10.70	45.62
Dead control	1.08	0.49
NS-IIa	**72°C – 8 h incubation**	
Replicate I[1,2]	1.35	4.32
Replicate II[2]	1.15	2.28
Dead control	1.08	1.28

[1]used for NanoSIMS analysis

[2]used for CARD-FISH / 16S rRNA gene diversity analysis

Supporting Figures:

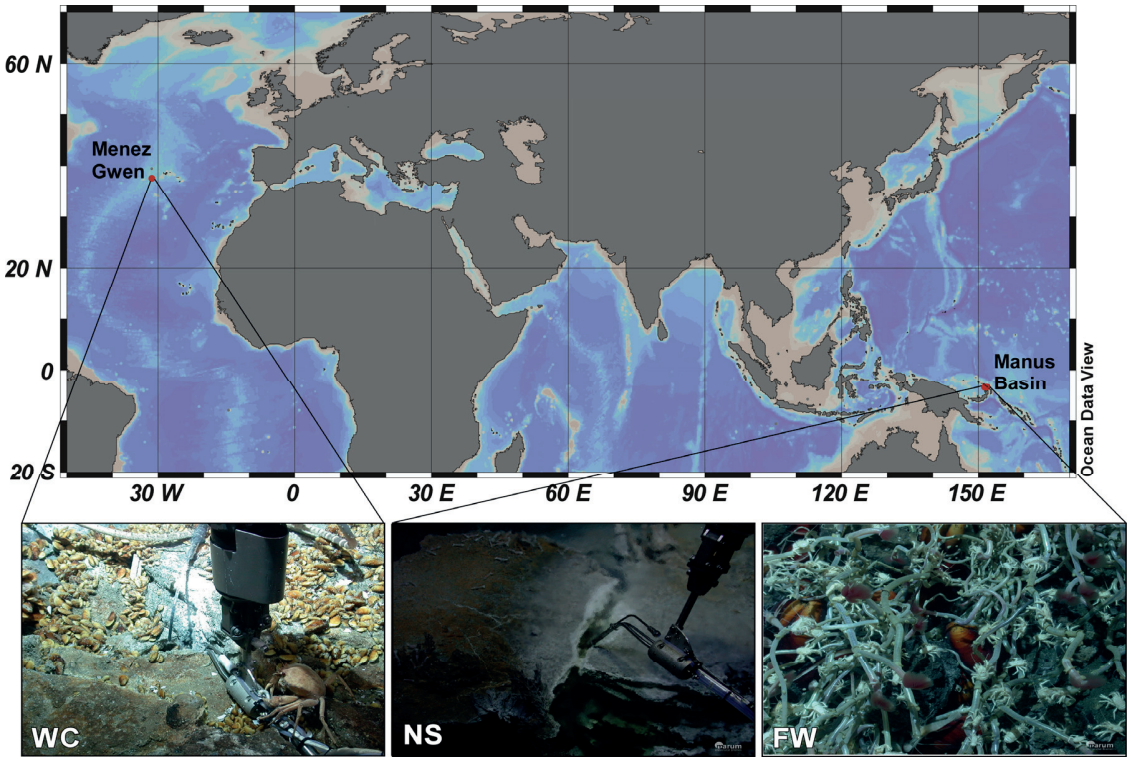

Figure S1: Study sites. The red points on the world map mark the geographical locations of the investigated hydrothermal vent systems. Images show sampling sites with surrounding fauna. Woody's crack (WC) and North Su (NS) with ROV-arm holding KIPS system and coupled temperature sensor. Fauna: mussels of the genus *Bathymodilus* and a crab at WC and mussels and tube worms at Fenway (FW).

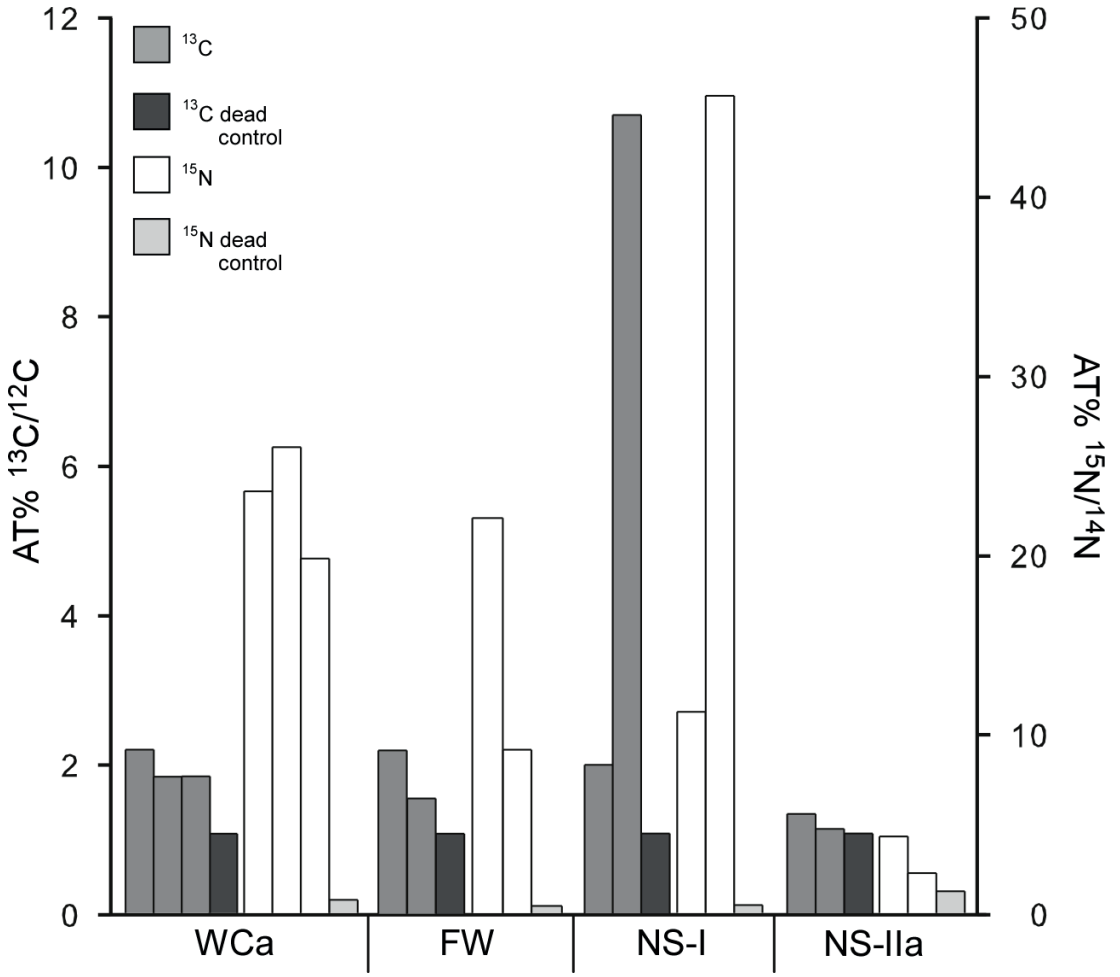

Figure S2: Bulk measurements of ^{13}C-acetate and ^{15}N-ammonia uptake. Each bar represents measurement of one replicate.

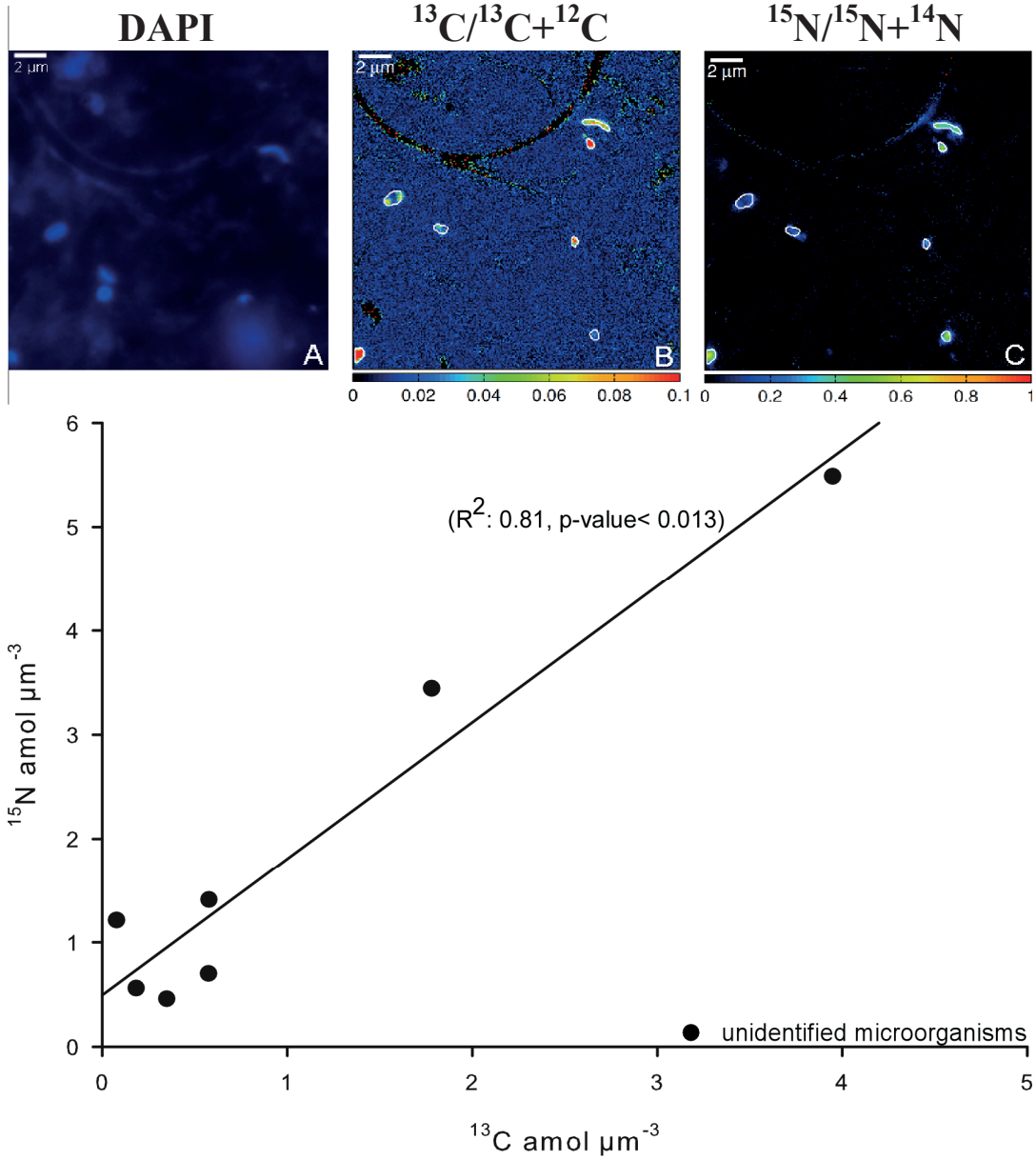

Figure S3: ^{13}C-acetate and ^{15}N-ammonium uptake by cells of NS-IIa fluids. Parallel secondary ion images of cells (B-C). DAPI detected cells that could not be assigned to a phylogenetic group (A). Plot shows assimilation rates in amol µm^{-3} after 8 h incubation.

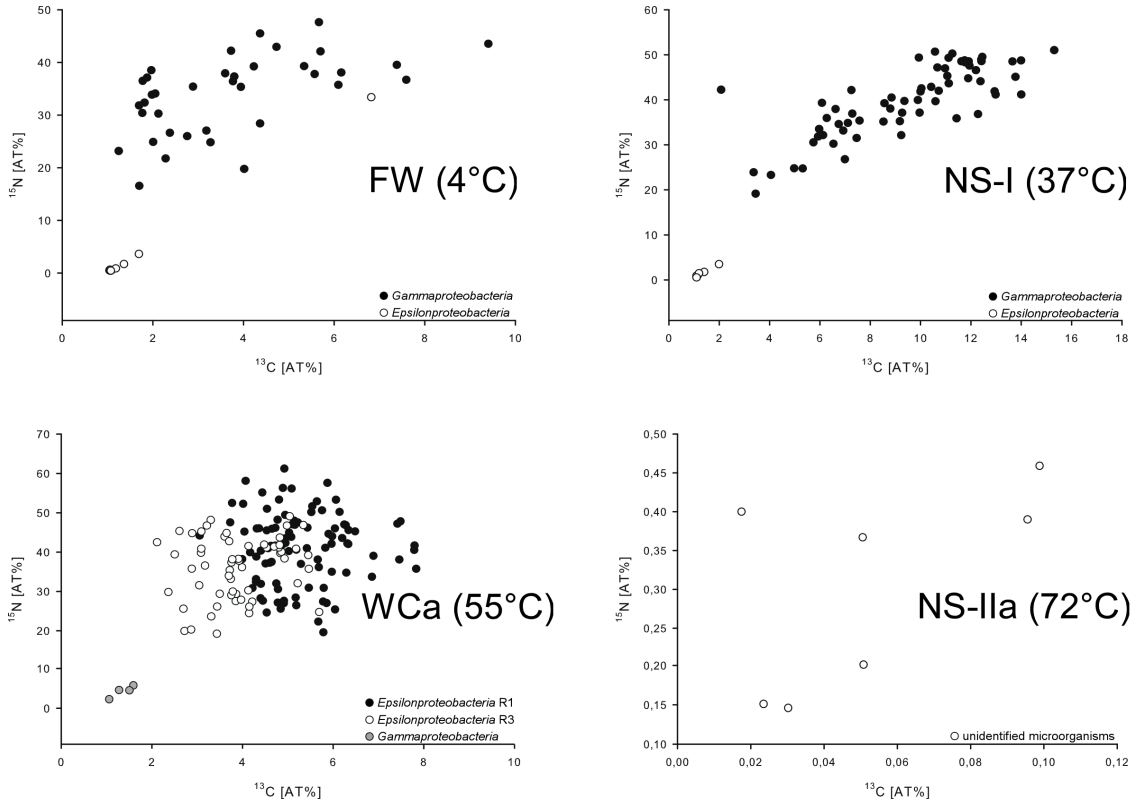

Figure S4: Atom-percent labeling of individual cells in ^{13}C-acetate/ ^{15}N-ammonium all incubation experiments.

References

Amann, R. I., Krumholz, L., and Stahl, D. A. (1990). Fluorescent-oligonucleotide probing of whole cells for determinative, phylogenetic, and environmental studies in microbiology. *J. Bacteriol.* 172, 762–770.

Arnds, J. (2009). Molecular characterization of microbial populations in methane-rich marine habitats. PhD thesis.

Brosius, J., Palmer, M. L., Kennedy, P. J., and Noller, H. F. (1978). Complete nucleotide sequence of a 16S ribosomal RNA gene from *Escherichia coli*. *Proc. Natl. Acad. Sci.* 75, 4801–4805.

Daims, H., Brühl, A., Amann, R., Schleifer, K. H., and Wagner, M. (1999). The domain-specific probe EUB338 is insufficient for the detection of all *Bacteria*: development and evaluation of a more comprehensive probe set. *Syst. Appl. Microbiol.* 22, 434–444.

Fuchs, B. M., Glöckner, F. O., Wulf, J., and Amann, R. (2000). Unlabeled helper oligonucleotides increase the *in situ* accessibility to 16S rRNA of fluorescently labeled oligonucleotide probes. *Appl Env. Microbiol* 66, 3603–3607.

Lin, X., Wakeham, S. G., Putnam, I. F., Astor, Y. M., Scranton, M. I., Chistoserdov, A. Y., and Taylor, G. T. (2006). Comparison of vertical distributions of prokaryotic assemblages in the anoxic Cariaco Basin and Black Sea by use of fluorescence *in situ* hybridization. *Appl. Environ. Microbiol.* 72, 2679–2690.

Loy, A. (2003). DNA microarray technology for biodiversity inventories of sulphate reducing prokaryotes. PhD thesis.

Manz, W., Amann, R., Ludwig, W., Wagner, M., and Schleifer, K.-H. (1992). Phylogenetic oligodeoxynucleotide probes for the major subclasses of *Proteobacteria*: Problems and solutions. *Syst. Appl. Microbiol.* 15, 593–600.

Muyzer, G., Brinkhoff, T., Nübel, U., Santegoeds, C., Schäfer, H., and Wawer, C. (1998). "Denaturing gradient gel electrophoresis (DGGE) in microbial ecology," in *Molecular microbial ecology manual* (Kluwer Academic Publishers), 3.4.4/1–3.4.4/27.

Muyzer, G., Teske, A., Wirsen, C., and Jannasch, H. (1995). Phylogenetic relationships of *Thiomicrospira* species and their identification in deep-sea hydrothermal vent samples by denaturing gradient gel electrophoresis of 16S rDNA fragments. *Arch. Microbiol.* 164, 165–172.

Wallner, G., Amann, R., and Beisker, W. (1993). Optimizing fluorescent in situ hybridization with rRNA-targeted oligonucleotide probes for flow cytometric identification of microorganisms. *Cytometry* 14, 136–143.

Yanisch-Perron, C., Vieira, J., and Messing, J. (1985). Improved M13 phage cloning vectors and host strains: Nucleotide sequences of the M13mpl8 and pUC19 vectors. *Gene* 33, 103–119.

Yilmaz, L. S., Parnerkar, S., and Noguera, D. R. (2011). mathFISH, a web tool that uses thermodynamics-based mathematical models for *in silico* evaluation of oligonucleotide probes for fluorescence *in situ* hybridization. *Appl Env. Microbiol* 77, 1118–1122.

Chapter IV

A single cell genome of "*Candidatus* Thiomargarita nelsonii" and comparison to large sulfur-oxidizing bacteria

A single cell genome of "*Candidatus* Thiomargarita nelsonii" and comparison to large sulfur-oxidizing bacteria

Contributors:
Matthias Winkel[1], Salman Verena[2,3], Tanja Woyke[4], Heide Schulz-Vogt[2,5], Michael Richter[6] and Marc Mußmann[1*]

Running title:
Single cell genome of *Candidatus* Thiomargarita nelsonii

Affiliations:
[1] Molecular Ecology Group, Department of Molecular Ecology, Max Planck Institute for Marine Microbiology, Bremen, Germany
[2] Ecophysiology Group, Department of Molecular Ecology, Max Planck Institute for Marine Microbiology, Bremen, Germany
[3] current address: Department of Marine Science, 3117L Murray Halls, CB 3300 Chapel Hill, NC 27599-3300
[4] Department of Energy Joint Genome Institute Walnut Creek, California, USA
[5] current address: Leibniz-Institut für Ostseeforschung Warnemünde, Seestrasse 15, D-18119 Rostock
[6] Ribocon GmbH, Fahrenheitstr. 1, 28359, Bremen

*corresponding author:
Dr. Marc Mußmann
Department of Molecular Ecology
Max Planck Institute for Marine Microbiology
Celsiusstr. 1
Bremen, 28359, Germany
e-mail: mmussman@mpi-bremen.de

Key words: *Candidatus* Thiomargarita nelsonii, single cell genome, SOB, cyanobacteria, multiple-displacement amplification

Abstract

Large, colorless sulfur-oxidizing bacteria of the family *Beggiatoaceae* often cover the seafloor and prevent the release of toxic hydrogen sulfide into the water column. Among them, the genus *Thiomargarita* harbors the largest known free-living bacteria with cell sizes of up to 750 µm in diameter. Besides the ability to oxidize reduced sulfur compounds, *Thiomargarita* spp. are known to store nitrate, phosphate and elemental sulfur. To date little is known about their genetic repertoire for carbon fixation, sulfur oxidation and nitrate respiration and how it compares to other *Beggiatoaceae*. Here, we present a draft single-cell genome sequence of a chain-forming "*Candidatus* Thiomargarita nelsonii" and compared it to four draft genomes of other members of the *Beggiatoaceae.* Genes for sulfur oxidation, nitrate respiration and inorganic carbon fixation confirmed a chemolithoautotrophic lifestyle. Alternative to the Calvin-Benson-Bassham cycle for CO_2 fixation widespread in *Beggiatoaceae* the genome encoded the reductive tricarboxylic acid cycle. Additionally, "*Ca*. T. nelsonii" encoded key genes of the C2-cycle that converts 2-phosphoglycolate, an inhibitor of carbon fixation. Nitrate can be respired either by dissimilatory nitrate reduction to ammonium (DNRA) or by denitrification up to dinitrogen. Additionally, energy can be gained by hydrogen oxidation and by a proposed flavin-based energy bifurcation coupled to a Na^+-translocating membrane complex (Rnf).The phylogenetic affiliation of many genes of *Thiomargarita* with (filamentous) cyanobacteria suggest massive horizontal gene transfer between large *Beggiatoaceaea* and cyanobacteria. The analysis of the genetic potential of these giant sulfur-oxidizing bacteria helps to understand the evolution and adaptation to extreme conditions in their habitats and their contribution to sulfur, carbon and nitrogen cycling.

Introduction

Large colorless sulfur-oxidizing bacteria (SOB) are globally distributed and found in sulfidic habitats like nutrient-rich sediment surfaces. Here, opposed gradients of oxygen and sulfide (Jørgensen and Revsbech, 1983; Nelson *et al.*, 1986b) favor the formation of dense populations of the genera *Beggiatoa*, *Thioploca* and *Thiomargarita* (Jørgensen, 1977; Jannasch *et al.*, 1989; Fossing *et al.*, 1995; Schulz *et al.*, 1999). Both marine and freshwater large colorless SOB have been shown to oxidize various reduced forms of sulfur (hydrogen sulfide, thiosulfate, elemental sulfur) (Teske and Nelson, 2006; Schulz, 2006). Besides reduced sulfur compounds they also use smaller organic compounds as energy sources such as acetate, lactate, and ethanol (Teske and Nelson, 2006). The majority of organisms in the family *Beggiatoaceae* has the ability to store nitrate in a central vacuole in order to use it as electron acceptor under anoxic conditions (Fossing *et al.*, 1995; McHatton *et al.*, 1996; Schulz *et al.*, 1999). Freshwater and marine *Beggiatoa* spp. as well as *Thioploca* spp. are able to dissimilatorily reduce nitrate to ammonium (Vargas and Strohl, 1985; McHatton *et al.*, 1996; Otte *et al.*, 1999; Sayama *et al.*, 2005; Preisler *et al.*, 2007). Other experiments suggested denitrification in freshwater bacteria identified as *Beggiatoa alba* (Sweerts *et al.*, 1990), however, these experiments have to be cautiously interpreted, since adhering contaminating bacteria could have performed the actual denitrification. Thermodynamic calculations of the free energy yield for both processes showed 60% more energy yield (kJ/mol) per mole sulfide for denitrification when sulfide is the limiting factor, while nitrate as limiting factor showed similar values (Jørgensen and Nelson, 2004). Large colorless SOB occur as filaments or single cells that can form chains and often forming mats on top or within the top centimeter of the sediment. The mat-forming species *Beggiatoa* and *Thioploca* can store elemental sulfur and nitrate. By their gliding motility they migrate and thereby transport electron donors and acceptors between deeper surficial layers of the sediment. In this manner these SOB may gain an competitive advantage over other sulfur oxidizers, which require simultaneous access to both electron donor and acceptor (Jørgensen and Gallardo, 1999). Filaments and single cells can also live attached to solid surfaces like rocks and snail shells (Bailey *et al.*, 2011). Although many studies have targeted their ecological niche (Nelson and Castenholz, 1981a, 1981b; Nelson *et al.*, 1982; Nelson and Castenholz, 1982; Nelson and Jannasch, 1983; Nelson *et al.*, 1986a), little is known about their genomic potential (Mußmann *et al.*, 2007; MacGregor *et al.*, 2013b).

Among the large colorless SOB the genus *Thiomargarita* is hardly studied. *Thiomargarita namibiensis* was first discovered at sediment surfaces along the Namibian

upwelling system and appeared as large single chain-forming cells that were surrounded by a mucus layer. They inhabit the upper most centimeters of the diatomaceous ooze of this organic rich upwelling system. The underlying sediments contain extremely high sulfide concentrations of up to 22 mM (Brüchert *et al.*, 2003). This enormous sulfide load causes oxygen depletion in the sediment itself as well as the overlaying water, and forces *Thiomargarita namibiensis* to use other electron acceptors than oxygen, such as nitrate. Therefore the large cells with diameters of up to 750 µm mainly consist of a large central vacuole storing 800-1000 mM nitrate (Schulz *et al.*, 1999). Being the preferred process, however, *Thiomargarita* namibiensis also oxidize reduced sulfur compounds aerobically with oxygen (Schulz and de Beer, 2002). Besides the storage of sulfur, *Thiomargarita* can also store glycogen, polyphosphate (Schulz and Schulz, 2005), whereas filamentous *Beggiatoa* species usually store polyphosphate and polyhydroxyalcanoate (Brock and Schulz-Vogt, 2011; Schwedt *et al.*, 2012). *Thiomargarita namibiensis* are non-motile and therefore depend on a resuspension of sediment to regain nitrate from the water column. Other marine sediments also contain *Thiomargarita* spp. such as the Chilean margin (Salman *et al.*, 2011), the Costa Rican margin (Kalanetra *et al.*, 2005), around methane seeps (Bailey *et al.*, 2011; Girnth *et al.*, 2011; Grünke *et al.*, 2011) and the hydrothermal system of the Guaymas Basin (Fig. S1). At some of these sites they occur in close proximity to filamentous, *Beggiatoa*-like organisms that form mats. This co-occurrence is yet proposed to result in niche separation on the microscale correlating with different sulfide and oxygen conditions in these metabolically similar microorganisms (Grünke *et al.*, 2011).

Recently, the taxonomy of large colorless SOB was revised and an amended family *Beggiatoaceae* and together with several *Candidatus* taxa were proposed, including the species "*Ca.* Thiomargarita nelsonii" and "*Ca.* Thiomargarita joergensenii" (Salman *et al.*, 2011). It was also shown that *Thiomargarita* spp. have up to four introns in their 16S rRNA gene (Salman *et al.*, 2012). *Thiomargarita* spp. are ideal organisms for whole genome sequencing, since single cells can be easily obtained and they can be distinguished from contaminating microorganisms. Several attempts to cultivate *Thiomargarita* or other large vacuolated SOB have failed so far, and genomic information of representatives from their phylogenetic group is scarce (Schulz, 2006; Mußmann *et al.*, 2007; MacGregor *et al.*, 2013a).

In the last decade, whole genome amplification and sequencing from single cells has overcome the necessity to cultivate microorganism to get detailed information about its genomic potential. Current whole genome amplification-techniques using single cells as template include multiple-displacement amplification (MDA), which allows the amplification

of micrograms of DNA (Lasken, 2012). This method in combination with next generation sequencing have been successfully applied to acquire genome information of environmentally relevant bacteria from diverse habitats (Hongoh *et al.*, 2008; Woyke *et al.*, 2009, 2010; Blainey *et al.*, 2011; Siegl *et al.*, 2011).

In this study the genome of a single cell of "*Ca.* T. nelsonii" was sequenced and the assembled draft genome was compared to other genomes of large colorless SOB of the family *Beggiatoaceae* ("*Ca.* Isobeggiatoa divolgata" (Mußmann *et al.*, 2007), *Beggiatoa alba* B18LD (DOE Joint Genome Institute , GOLD ID: Gi1563) and an orange *Beggiatoa* filament from the Guaymas basin hydrothermal vent system (J. Craig Venter Institute, Gi01404, (MacGregor *et al.*, 2013a)). Furthermore, the genome of the cultured *Beggiatoa* strain 35Flor collected from the black band disease of corals (Brock *et al.*, 2012; Schwedt *et al.*, 2012) (M. Mußmann, unpublished data) and was used for comparison. We analyzed major pathways involved in energy, sulfur, carbon, phosphorus and nitrogen metabolisms, in "*Ca*. T. nelsonii". A special focus of this analysis was the nitrogen cycle as it was still unclear, whether *Thiomargarita* performs DNRA or denitrification.

Material and methods

Samples

Sediment samples containing *Thiomargarita* cells were taken at the Benguela Upwelling System off the coast of Namibia during the cruises AHAB leg 4 with the R/V Alexander von Humboldt (2004) and M76 onboard the R/V Meteor (2008). Sediment was retrieved with a multicorer from water depth of 100-200 m across the coordinate block 19°1.01'–25°30.00'S and 12°13.75'–14°23.36' E. The upper 3 cm of the sediments, which contained most of the *Thiomargarita* cells, were stored in closed plastic containers overlaid with bottom sea-water and kept at 4°C.

Separation of single cells

Single cells with cylindrical (Fig. S1) and spherical shapes were removed from their external sheath under a stereo-microscope with at a magnification of 20x. The sheath, which surrounds the cells, was opened with two sterile needles and single cells were separated from the chain. The cells were clearly visible due to their inclusion of elemental sulfur. Cells were carefully washed in autoclaved, sterile-filtered, 0.4% low-melting agarose (NuSiva) in dissolved seawater using wide-bored pipet tips to avoid cell damage. This procedure was repeated several times to remove potentially contaminating microorganisms. Cells were transferred onto Ampligrid slides (Advalytix, Olympus, Hamburg, Germany) that contain a hydrophilic central area surrounded by a hydrophobic ring, which allows reactions in very small volumes to avoid contamination. Slides with single *Thiomargarita* cells were air-dried and directly processed or stored at -20°C.

Single cell MDA reaction

MDA reactions were prepared under a PCR hood irradiated with UV-light to avoid contaminations with free DNA, plasmids or DNA from human skin or breath. All used materials and chemicals were UV-light irradiated with the exception of the polymerase/ primer mix. MDA reactions were performed with the Illustra GenomePhi V2 DNA amplification kit (GE Healthcare, Buckinghamshire, UK) as described previously (Jogler *et al.*, 2011). MDA products were further diluted 1:100 and 1:1000 to prevent inhibitory effects of branched DNA on downstream applications. The MDA products were tested for contamination by amplifying the 16S rRNA gene with different primer combinations. Furthermore, the purity of MDA products was tested by amplification of the functional gene

adenylylsulfate reductase subunit A (*aprA*), the single copy gene recombinase for DNA repair (*recA*) and a partial intergenic transcribed spacer (ITS) region up/downstream of the 23S rRNA gene. For detailed PCR conditions see SI used oligonucleotides are listed in Table S1.

Whole genome sequencing and assembly

The genomic DNA from the MDA product was quality-checked with the "Genomic DNA QC Using Standard Gel Electrophoresis|" protocol from the DOE Joint Genome Institute (JGI) (http://my.jgi.doe.gov/general/protocols/Genomic-DNA-QC-2012.pdf). Purified genomic DNA was sent to JGI (Walnut Creek, California, USA) and sequenced using 2x 150 bp pair-end library on an Illumina HiSeq by the Illumina sequencing technology according to manufactory protocol (Bennett, 2004). After quality controlling and removing of redundant reads, the remaining reads were assembled with a combination of the Velvet (Zerbino and Birney, 2008) and Allpaths (Gnerre *et al.*, 2011) assembler.

Gene prediction, annotation and pathway construction

The ORF prediction was carried out with a combination of different tools using Glimmer3 (Delcher *et al.*, 2007), and MetaGene (Noguchi *et al.*, 2006). Ribosomal RNA gene sequences were predicted with the RNAmmer 1.2 software (Lagesen *et al.*, 2007) and transfer RNAs were identified with tRNAscan-SE (Lowe and Eddy, 1997). The annotation was performed by a refined version of GenDB v2.2 system (Meyer *et al.*, 2003) supplemented by the java-based comparative analysis and search tool JCoast version 1.7 (Richter *et al.*, 2008). For predicted ORFs retrieved observations were collected from similarity searches against sequence databases NCBI-nr, Swiss-Prot, KEGG, COG, genomesDB (releases May 2013) and protein family database Pfam (release 27), Inter-Pro (release 42) as well as signal peptide prediction by SignalP (Dyrløv Bendtsen *et al.*, 2004) and transmembrane helix-analysis by TMHMM (Krogh *et al.*, 2001). Predicted protein coding sequences were automatically annotated with MicHanThi (Quast, 2006). The MicHanThi software predicts gene functions based on similarity searches using the NCBI-nr (including Swiss-Prot) and InterPro database. Pathways were manually searched and compared to published pathways in the Kyoto Encyclopedia of Genes and Genomes (KEGG) (Kanehisa and Goto, 2000). Predicted genes and pathways were compared to automated annotations of the IMG/ ER (Markowitz *et al.*, 2012) and RAST (Aziz *et al.*, 2008) platforms.

Phylogenetic analysis

The retrieved almost full length 16S rRNA gene sequence was used for tree calculation with the ARB software package (Ludwig *et al.*, 2004). Trees were calculated with other nearly full length sequences of the ARB-Silva release 111 (Quast *et al.*, 2012) using a maximum likelihood algorithm and a 50% base frequency filter. Subsequently, partial sequences were added to the reconstructed tree by the maximum parsimony algorithm without allowing changes in the overall tree topology. A multiple protein alignment of the ribulose-1,5-bisphosphate carboxylase/ oxygenase large subunit (*rbcL*) was constructed with the integrated aligner of the ARB software tool, which was then manually adjusted. Phylogenetic tree reconstructions were performed with a maximum likelihood algorithm using the Dayhoff amino acid substitution matrix (Dayhoff *et al.*, 1978) for evolutionary distance. A base frequency and termini filter were applied considering 256 amino acid positions.

Results and discussion

Whole genome amplification

The whole genome amplification of an individual *Thiomargarita* cell gave a way to the study of the genomic potential of this uncultured bacterium. Yet, the reamplification of MDA products is prone to cause frame shifts, which likely prevented the retrieval of complete genome sequencing in this study, and hindered an accurate determination of the genome size. However, the whole genome amplification was uncontaminated as a PCR on the no 16S rRNA gene generated a product of the expected size, which is larger in "*Ca.* T. nelsonii" due to an intron of the length of 855 nt as compared to regular size 16S rRNA genes in bacteria (Salman *et al.*, 2012). The amplification of a partial 23S rRNA gene together with an intergenic spacer region confirmed the success of the whole genome amplification via MDA. For a detailed description see SI.

General genome features

The sequenced MDA product of the '*Candidatus* Thiomargarita nelsonii' cell resulted in a total of 1.1 x 10^7 number of sequence reads. After quality controlling and removing of redundant reads, 1.2 x 10^6 unique number of reads remained. The assembled reads resulted in 3,613 contigs and 5.3 Mb of unique sequence information. The contigs could not be further assembled to scaffolds due to high numbers of frame shifts that most likely resulted from the repeated reamplification the initially MDA-generated genomic DNAwhole genome amplification. The details of the draft genome and compared genomes are listed in table 1.

Phylogenetic affiliation

The genus *Thiomargarita* belongs to the family of *Beggiatoaceae* of the *Gammaproteobacteria*, and contains three species, out of which two have been recently newly proposed as *Candidatus* species (Salman *et al.*, 2011). We detected an almost complete 16S rRNA gene in the amplified genome, which showed a typical intron (S1369) at the expected position for "*Ca.* T. nelsonii" (Salman *et al.*, 2012). The 16S rRNA gene was used for phylogenetic tree calculation and affiliated with the cluster of other "*Ca.* T. nelsonii" sequences as well as the earlier amplified partial 16S rRNA genes of the same chain-forming morphotype (Salman *et al.*, 2011; Figure 1). The sequence shared 99.1-100% sequence identity of to other "*Ca.* T. nelsonii" sequences.

To further analyze the relatedness to large colorless SOB we compared the "*Ca.* T. nelsonii" dataset with the draft genome of the "*Ca.* I. divolgata" (Mußmann *et al.*, 2007) and tested for reciprocal best match (RBM) hits. The two genomes shared 471 open reading frames (ORFs) (cut off e^{-05}, 65% alignment coverage). Usually, the expected number of RBM hits is considerably higher than observed here, which might be caused by the fact that a large amount of genes in both tested genomes are only partially covered.

The genome of "*Ca.* T. nelsonii" showed several gene fragments with high sequence identity values with cyanobacteria (n=434), as was shown by previous studies with filamentous SOB (Mußmann *et al.*, 2007; MacGregor *et al.*, 2013b). For example, the genome contained the genes *xisH* and *xisI,* which are required in cyanobacteria for the heterocyst-specific rearrangement of the FdxN element as part of the nitrogenase operon (Ramaswamy *et al.*, 1997). The FdxN element is also encoded in the genome of "*Ca.* T. nelsonii" and "*Ca.* I. divolgata" (data not shown). Other examples were several ORFs that encoded for polyketide synthase type I with highest identity values to cyanobacteria entries (data not shown). These multimodular megasynthases produce macrolide, which acts as an antibacterial by inhibiting protein synthesis (Kehr *et al.*, 2011). These findings suggested substantial horizontal gene transfer between ancestors of "*Ca.* Thiomargarita nelsonii" and other large, colorless SOB with cyanobacteria (Mußmann *et al.*, 2007; MacGregor *et al.*, 2013b). This hypothesis is further supported by the observation that large colorless SOB often occur in the same environment as cyanobacteria, where they can form cohesive microbial mats (Larkin and Strohl, 1983; Garcia-Pichel *et al.*, 1994; Mattison *et al.*, 1998).

Nitrogen metabolism

Large, colorless sulfur bacteria are known to use nitrate as electron acceptor performing dissimilatory nitrate reduction to ammonia (DNRA) (Otte *et al.*, 1999; Preisler *et al.*, 2007). A contribution to dentrification is not clear, although it was reported for freshwater *Beggiatoa*, which might be due to contaminating bacteria (Sweerts *et al.*, 1990).

"Ca. T. nelsonii" encoded for two dissimilatory nitrate reductases (*nar* and *nap*) and a assimilatory nitrate reductase (*nasA*) (Fig. 2 and Table S2). The first dissimilatory nitrate reductase (*nar*) is membrane-bound and catalyzes the first step in both the DNRA and denitrification (Moreno-Vivián *et al.*, 1999). The same is true for the second dissimilatory nitrate reductase (*nap*) (Morozkina and Zvyagilskaya, 2007), which is located in the periplasm. Both dissimilatory nitrate reductases are also found in the "*Ca.* I. divolgata" (Mußmann *et al.*, 2007) as well as in the genome of the orange BOGUAY filament

(MacGregor *et al.*, 2013a), whereas the genome of *Beggiatoa alba* B18LD only encoded for the periplasmic enzyme (Fig. 2 and Table S2). The cytoplasmic assimilatory nitrate reductase (*nasA*) is also found in *Beggiatoa alba* B18LD, which also has a nitrite reductase (*nirBD*) involved in both the assimilatory and dissimilatory pathway. Together with the assimilatory nitrate reductase (*nasA*), these two enzymes are assimilate ammonium (Fig. 2 and Table 2), as was also shown for endosymbiontic SOB of the vesicomyid clams and *Bathymodiulus* sp. mussels (Kleiner *et al.*, 2012a). The nitrite reductase in combination with the cytoplasmic or periplasmic dissimilatory nitrate reductase could be used by "*Ca.* T. nelsonii" and *B. alba* B18LD to perform DNRA (Fig. 2, Table 2 and Table S2), and has been experimentally demonstrated for *B. alba* (Vargas and Strohl, 1985). In no marine *Beggiatoa*-related genomes genes for the assimilatory and dissimilatory nitrite reductases was detected, instead they encoded for a multiheme cytochrome with nitrite reductase function (MacGregor *et al.*, 2013a) which may be involved in DNRA. For a more detailed description see SI.

Genes encoding the nitrite reductase (*nirSCF*) for denitrification were also detected in the genome of "*Ca*. T. nelsonii". Furthermore, "*Ca.* T. nelsonii", "*Ca.*I. divolgata" and the orange BOGUAY filament encoded for a membrane-bound nitric oxide reductase (*nor*). Together with the earlier described periplasmic nitrate reductase and the multiheme cytochrome with nitrite reductase-function all three organisms are theoretically able to denitrify nitrate to nitrous oxide (Fig. 2 and Table S2). Thus, the analysis of the genes for DNRA or denitrification in "*Ca*. T. nelsonii" showed the potential for both processes (Fig. 2)

Interestingly, we also found genes for the nitrous oxide reductase (*nosZD*)(Table S2) in "*Ca*. T. nelsonii", which are similar to *nosZD* of *Pseudomonas aeroginosa* and *Paracoccus denitrificans* (Zumft, 1997). Accordingly, a complete denitrification to dinitrogen seems possible in "*Ca*. T. nelsonii" (Fig 2 and Table S2). The draft genome of strain *Beggiatoa* sp. 35Flor lacks all necessary genes for DNRA and denitrification, which was supported experimentally. This strain rather uses internal stored sulfur for anaerobic respiration (Schwedt *et al.*, 2012).

Besides the described assimilatory pathway for nitrate reduction to ammonia (*nasA* and *nirBD*), all analyzed genomes encoded for an ammonium transporter (*amt*) and for a glutamine synthetase (*glnA*) to directly convert ammonia and glutamate to glutamine (Fig. 2 and Table S2).

Sulfur metabolism

Large colorless SOB oxidize reduced sulfur compounds like sulfide, thiosulfate and elemental sulfur (Teske and Nelson, 2006; Schulz, 2006).

We found different genes for sulfide-oxidizing enzymes in the genome of "*Ca*. T. nelsonii" and all other genomes of large SOB (Table 2). The sulfide:quinone oxidoreductase (*sqr*) was encoded in all genomes, while an alternative enzyme, the flavocytochrome c sulfide dehydrogenase (*fccAB*) was encoded with both subunits in all genomes with the exception of the *Beggiatoa alba* B18LD (Fig. 1 and Table S3). The occurrence of two different enzymes points towards well regulated sulfide oxidation under different environmental sulfide conditions in these organisms. The produced sulfur can be stored in the form of elemental sulfur by a yet unknown process (Dahl *et al.*, 2008) and is visible as sulfur globules in all analyzed large colorless SOB (Fig. S1) (Mezzino *et al.*, 1984; Mußmann *et al.*, 2007; Salman *et al.*, 2011; Schwedt *et al.*, 2012; MacGregor *et al.*, 2013a).

We also found genes of the reductive dissimilatory sulfite reductase (DSR) pathway which oxidizes the internally stored sulfur to sulfite. The set of genes for this pathway was incomplete in comparison to the genomes "*Ca.* I. divolgata", *Beggiatoa* sp. 35Flor and the orange BOGUAY filament (Fig. 2 and Table S3). However we also detected a partial alpha subunit of the APS reductase and a gene encoding for the ATP sulfurylase, which supports the assumption that "*Ca*. T. nelsonii" is able to completely oxidize internally stored zerovalent sulfur to sulfate (Dahl *et al.*, 2008). Furthermore, we found genes involved in thiosulfate oxidation from the SOX pathway (Dahl *et al.*, 2008). For a more detailed description of the localization of genes involved in the sulfur cycle see SI.

Carbon metabolism

Glycolysis

The "*Ca*. T. nelsonii" genome encoded for a nearly complete glycolysis, while it missed the glucose-6-phosphate isomerase (Table S4). This gene was found in all other large colorless SOB, so most probably it is encoded on the missing parts of the "*Ca*. T. nelsonii" genome. Furthermore, "*Ca*. T. nelsonii" encoded for a polyphosphate glucokinase instead of the ATP glucokinase that was shown for microorganisms that accumulate polyphosphate (Tanaka *et al.*, 2003) and *Thiomargarita namibiensis* accumulates polyphosphate granules (Schulz and Schulz, 2005). All other large colorless SOB showed a complete glycolysis with "*Ca.* I. divolgata" and the orange BOGUAY filament having the same polyphosphate-

dependent glucokinase. So far no growth on sugars and other complex organic substrates was observed among cultured SOB and when growing heterotrophically almost all freshwater strains use acetate as carbon and energy source (Teske and Nelson, 2006). Other growth-stimulating substrates are intermediates of the tricarboxylic acid cycle (TCA) (Nelson and Castenholz, 1981a).

Tricarboxylic acid cycle (TCA) and glyoxylate bypass

A full TCA cycle could be identified in the genome of "*Ca*. T. nelsonii" and is also encoded in the genomes of all other large colorless SOB (Table 2 and S4). "*Ca.* I. divolgata" lacked a malate dehydrogenase (Table S4), which is again most probably located on the unsequenced part of the genome. The findings of TCA cycle genes is not so common among lithotrophic organisms such as sulfur oxidizers, because they are often obligate autotrophs (Teske and Nelson, 2006). Especially the encoding of a complete alpha ketoglutarate dehydrogenase-complex is unusual, because it was previously argued that the lack of this gene was an indicator for obligate autotrophy (Wood *et al.*, 2004).

Genes for the glyoxylate cycle that use acetate as carbon source could be confirmed by the presence of genes for malate synthase and isocitrate lyase (Walsh and Koshland, 1984) in the *Beggiatoa alba* B18LD and *Beggiatoa* sp. strain 35Flor genomes, but were missing in all other (Table 2 and S4). This confirmed earlier experimental studies with freshwater *Beggiatoa* sp. strain OH-75-B, clone 2a (Nelson and Castenholz, 1981a) and *Beggiatoa* sp. strain D-402 (Stepanova *et al.*, 2002), where both strains performed a glyoxylate bypass. Nevertheless, all organisms with the exception of the orange BOGUAY filament have genes predicted for acetyl-CoA synthethase, which catalyze the formation of acetyl-CoA from acetate, making it an additional energy source for the autotrophic marine and freshwater organisms.

Thiomargarita namibiensis is supposedly mixotrophic, i.e. it can use organic carbon such as acetate as carbon source but not as electron source, as oxygen uptake rates in the presence of external sulfide or internal sulfur remained stable over longer time periods than they did without acetate (Schulz and de Beer, 2002). Accordingly, the reverse TCA (rTCA) could be utilized by *Thiomargarita* spp. to transform organic carbon into biomass, as is argued below.

Carbon fixation pathways

Calvin-Benson-Bassham (CBB) cycle

The key enzyme of the carbon fixation in the CBB-cycle is the ribulose-1,6-bisphosphate carboxylase/oxygenase (RubiscCO), which was initially detected in marine *Beggiatoa* spp. (Nelson and Jannasch, 1983). The genomes of "*Ca*. T. nelsonii", "*Ca.*I. divolgata", and *B. alba* B18LD contained form I, while the orange BOGUAY filament and *Beggiatoa* sp. strain 35Flor have form II (Fig. 3 and Table S4). It is known that SOB express different forms of this enzyme (Kleiner *et al.*, 2012a) with distinct affinities for CO_2 and oxygen (Badger and Bek, 2008). We also identified most genes of the CBB-cycle (Hügler and Sievert, 2011) in "*Ca*. T. nelsonii" with the exception of the sedoheptulase-1,7-bisphophatase and the fructose-1,6-bisphosphatase. Instead, a 6-phosphofructokinase was found (Table S4), which has pyrophosphate binding sites similar to a pyrophosphate-dependent 6-phosphofructokinase (Reshetnikov *et al.*, 2008). This enzyme is proposed to have a tri-function while replacing the missing enzymes sedoheptulase-1,7-bisphophatase and the fructose-1,6-bisphosphatase as well as a phosphoribulosekinase (Kleiner *et al.*, 2012b). The genome of "*Ca*. T. nelsonii" also lacks a ribose-5-phosphate isomerase, which is encoded by all other large colorless SOB, but again it is likely that this enzyme is encoded in the missing parts of the genome (Table S4).

Oxygenase-activity of RubisCO and a potential glycolate cycle

Growth in *Thiomargarita* spp. is known to be stimulated by atmospheric oxygen concentrations (Schulz, 2006), thus a production of the 2-phosphoglycolate (2-PG) by the oxygenase activity of RubisCO is expected. 2-PG is an inhibitor of the CBB-cycle and has to be removeed. In higher plants this is carried out by the photorespiratory metabolism (Bauwe *et al.*, 2012), which converts the 2-PG into 3-phosphoglycerate (3-PG) and shuttles it back into the CBB-cycle. The genome of "*Ca*. T. nelsonii" encodes for an almost complete set of genes, which are known to be involved in the photorespiratory metabolism (C2-cycle) (Table S4). The only missing gene was the essential glycerate kinase of the class III (GLYK) (Table S4) producing 3-PG, however, they also encoded for genes which that can convert the photorespiratory intermediate serine via a phosphorylation to phosphoserine, and produce 3-PG in an alternative way (Fig. 4). Homologs of these genes were also detected in other large colorless SOB, with the exception of the orange BOGUAY filament, which lacks a glycolate oxidase (Fig. 4 and Table S4). For a detailed description see SI.

Reductive tricarboxylic acid (rTCA)

Until now only the sulfur-oxidizing endosymbiont "*Ca.* Endoriftia persephone" of the hydrothermal tubeworm *Riftia pachyptila* has been shown to use both the CBB- and the rTCA-cycle for CO_2 fixation under different conditions (Markert *et al.*, 2007). Homologs of the genes for a complete rTCA have been found in the genome of "*Ca*. T. nelsonii" (Table S4). The detected ATP-citrate lyase, the key enzyme for the rTCA, showed highest identities >70% to the ATP-citrate lyase of "*Ca.* E. Persephone". The same gene is found in the genome of the orange BOGUAY filament from the hydrothermal system in the Guaymas Basin (MacGregor *et al.*, 2013a). Furthermore, the genome of "*Ca*. T. nelsonii" contains genes for enzymes that are known to fix additional 2 mole CO_2 by converting produced acetyl-CoA by the ATP citrate lyase. Accordingly, "*Ca*. T. nelsonii" and the orange BOGUAY filament are the further examples of SOB, which apply two different CO_2 fixation pathways.

Energy metabolism

Oxidative phosphorylation

All five complexes of the oxidative phosphorylation were found in the genome of "*Ca*. T. nelsonii" (Table 2 and S5), and are known to be coupled to sulfide oxidation in *Beggiatoa* (Strohl *et al.*, 1986; Grabovich *et al.*, 2001). The complexes are also encoded in all other investigated genomes of large colorless SOB. Besides the ubiquinol-cytochrome c reductase complex III, we found up to two cytochrome types (cbb3 and aa3) of complex IV in the genomes of "*Ca*. T. nelsonii", similar to "*Ca,* I. divolgata" (Mußmann *et al.*, 2007). Furthermore, the "*Ca*. T. nelsonii" genome encoded for two different types of ATPase (F-type and V-type) involved in ATP synthesis via a proton and sodium ion gradient.

Possible additional energy metabolisms

Recently, in the endosymbiontic SOB of the hydrothermal vent mussel *Bathymodiolus* an uptake hydrogenase was found actively oxidizing hydrogen (Petersen *et al.*, 2011). The same hydrogenase was encoded by "*Ca*. T. nelsonii" and all other large colorless SOB. For detailed analyses see Kreutzmann *et al.* (unpublished). Accordingly, the potential of hydrogen oxidation potential seems to be more widespread among SOB than previously expected. It has to be confirmed, whether large colorless SOB use hydrogen as an alternative energy source.

Homologous genes for heterodisulfide reductases (*hdr*) were found and are supposedly involved in energy metabolism as intensively studied in methanogens (Thauer *et al.*, 2008) and sulfate-reducing *Deltaproteobacteria* (Haveman *et al.*, 2003; Zhang *et al.*, 2006; Strittmatter *et al.*, 2009). Methanogens use Hdr in a complex with a coupled methyl viologen-reducing hydrogenase (Mvh) to reduce a coenzyme during methanogenesis (Thauer *et al.*, 2008). We found the same Mvh was only found in "*Ca*. T. nelsonii", so a complex similar to methanogens and sulfate-reducing *Deltaproteobacteria* might be formed in large SOB. Interestingly, the gene displayed best blast hits to *Geobacter* spp. of 34 to 48% and showed a similar operon organization (Fig. S2). Its function in *Geobacter* spp. is so far not known (Coppi, 2005). The up-regulation of the Hdr in the sulfur-oxidizing endosymbiont "*Ca.* Endoriftia persephone" under sulfur-rich conditions (Markert *et al.*, 2007) suggested an involvement in sulfur oxidation. It could be active in the reverse form of a dithiol-cycle proposed for sulfate-reducing bacteria (Strittmatter *et al.*, 2009), helping to activate the stored elemental sulfur (Dahl *et al.*, 2008).

The enzyme Hdr*A* is flavin-based and could be coupled to the flavin-based membrane complex Rnf that is also detected in the genome of "*Ca*. T. nelsonii". Together, they could serve a flavin-based electron bifurcation for energy conservation (FBEB) (Table 2) that was recently proposed in addition to substrate and oxidative phosphorylation in anaerobic bacteria and methanogens (Buckel and Thauer, 2013). For a detailed description of the Mvh operon see SI.

Intracellular storage

It is well documented that large colorless SOB store several organic and inorganic compounds as granules in the periplasm, in the cytoplasm or dissolved in the central vacuole. We found a full set of genes for the uptake of inorganic phosphate and the production of polyphosphate, in all analyzed large, colorless SOB. The production of organic storage compounds in the form of polyhydroxybutyrate (PHB) were only found in *Beggiatoa alba* B18LD and *Beggiatoa* sp. strain 35Flor, which also encoded for the glyoxylate bypass to use acetate as an additional carbon source. (Fig. 1 and Table 2 and S7). Further details are described in the SI.

Conclusion

Thiomargarita species occur globally (Salman *et al.*, 2013) and are involved in biogeochemical cycles that are important for ecosystem functions. Despite their conspicuous size and general sulfur-oxidizing characteristics little is known about their genetic potential. Here, we represent the genomic features of a single cell of "*Ca.* Thiomargarita nelsonii" and investigated its potential for chemolithotrophy, carbon assimilation, energy metabolism and storage of nutrients. Also, we compared it to genomes of other *Beggiatoaceae* and some more distantly related organisms.

The genomic comparison of "*Ca*. T. nelsonii" to the other large colorless SOB showed that they share a large number of metabolic capabilities such as the complete TCA cycle and glycolysis, carbon fixation via the CBB-cycle, energy conservation via the oxidative phosphorylation, sulfide oxidation, polyphosphate syntheses, potential hydrogen oxidation, and Na^+-translocating membrane complexes (Table 2). The occurrence of two carbon fixation pathways and versatile energy metabolisms under oxic and anoxic conditions reflects their adaptation to live under rapidly changing conditions. Moreover "*Ca*. T. nelsonii" genome mirrors a potential survival strategy, which was newly proposed as the energy conserving metabolisms FBEB. This metabolic feature could be relevant in organisms exposed to long-term sulfidic conditions in the environment.

High sequence identities of genes from SOB to those in filamentous cyanobacteria has been demonstrated (Mußmann *et al.*, 2007; MacGregor *et al.*, 2013b) and are confirmed for "*Ca*. T. Nelsonii" in this study. This strongly supports early and extensive horizontal gene transfer between ancestors of these groups as a natural coexistence of cyanobacteria and *Thiomargarita* spp. has so far not been reported.

The here presented genome of a representative cell of the species "*Ca* T. nelsonii" is the first insight into the genome of the genus *Thiomargarita*, which harbors the largest free-living bacteria known. The hypothesized metabolic potential of "*Ca* T. nelsonii" offer a possibility for hypothesis-driven ecophysiological experiments and for cultivation approaches for large colorless SOB.

References

Aziz, R. K., Bartels, D., Best, A. A., DeJongh, M., Disz, T., Edwards, R. A., Formsma, K., Gerdes, S., Glass, E. M., Kubal, M., *et al.* (2008). The RAST server: rapid annotations using subsystems technology. *BMC Genomics* 9, 75.

Badger, M. R., and Bek, E. J. (2008). Multiple Rubisco forms in *Proteobacteria*: Their functional significance in relation to CO_2 acquisition by the CBB cycle. *J. Exp. Bot.* 59, 1525–1541.

Bailey, J. V., Salman, V., Rouse, G. W., Schulz-Vogt, H. N., Levin, L. A., and Orphan, V. J. (2011). Dimorphism in methane seep-dwelling ecotypes of the largest known bacteria. *ISME J.* 5, 1926–1935.

Bauwe, H., Hagemann, M., Kern, R., and Timm, S. (2012). Photorespiration has a dual origin and manifold links to central metabolism. *Curr. Opin. Plant Biol.* 15, 269–275.

Bennett, S. (2004). Solexa Ltd. *Pharmacogenomics* 5, 433–438.

Blainey, P. C., Mosier, A. C., Potanina, A., Francis, C. A., and Quake, S. R. (2011). Genome of a low-salinity ammonia-oxidizing archaeon determined by single-cell and metagenomic analysis. *PLoS ONE* 6, e16626.

Brock, J., Rhiel, E., Beutler, M., Salman, V., and Schulz-Vogt, H. N. (2012). Unusual polyphosphate inclusions observed in a marine *Beggiatoa* strain. *Antonie Van Leeuwenhoek* 101, 347–357.

Brock, J., and Schulz-Vogt, H. N. (2011). Sulfide induces phosphate release from polyphosphate in cultures of a marine *Beggiatoa* strain. *ISME J.* 5, 497–506.

Brüchert, V., Jørgensen, B. B., Neumann, K., Riechmann, D., Schlösser, M., and Schulz, H. (2003). Regulation of bacterial sulfate reduction and hydrogen sulfide fluxes in the central Namibian coastal upwelling zone. *Geochim. Cosmochim. Acta* 67, 4505–4518.

Buckel, W., and Thauer, R. K. (2013). Energy conservation via electron bifurcating ferredoxin reduction and proton/Na^+ translocating ferredoxin oxidation. *Biochim. Biophys. Acta BBA - Bioenerg.* 1827, 94–113.

Coppi, M. V. (2005). The hydrogenases of *Geobacter sulfurreducens*: A comparative genomic perspective. *Microbiology* 151, 1239–1254.

Dahl, C., Friedrich, C., and Kletzin, A. (2008). "Sulfur oxidation in prokaryotes," in *eLS* (John Wiley & Sons, Ltd)

Dayhoff, M. O., Schwartz, R., and Orcutt, B. C. (1978). "A model of Evolutionary Change in Proteins," in *In: Atlas of protein sequences and structure*.

Delcher, A. L., Bratke, K. A., Powers, E. C., and Salzberg, S. L. (2007). Identifying bacterial genes and endosymbiont DNA with Glimmer. *Bioinformatics* 23, 673–679.

Dyrløv Bendtsen, J., Nielsen, H., von Heijne, G., and Brunak, S. (2004). Improved prediction of signal peptides: SignalP 3.0. *J. Mol. Biol.* 340, 783–795.

Fossing, H., Gallardo, V. A., Jørgensen, B. B., Huttel, M., Nielsen, L. P., Schulz, H., Canfield, D. E., Forster, S., Glud, R. N., Gundersen, J. K., *et al.* (1995). Concentration and transport of nitrate by the mat-forming sulphur bacterium *Thioploca*. *Nature* 374, 713–715.

Garcia-Pichel, F., Mechling, M., and Castenholz, R. W. (1994). Diel migrations of microorganisms within a benthic, hypersaline mat community. *Appl. Environ. Microbiol.* 60, 1500–1511.

Girnth, A.-C., Grünke, S., Lichtschlag, A., Felden, J., Knittel, K., Wenzhöfer, F., de Beer, D., and Boetius, A. (2011). A novel, mat-forming *Thiomargarita* population associated with a sulfidic fluid flow from a deep-sea mud volcano. *Environ. Microbiol.* 13, 495–505.

Gnerre, S., MacCallum, I., Przybylski, D., Ribeiro, F. J., Burton, J. N., Walker, B. J., Sharpe, T., Hall, G., Shea, T. P., Sykes, S., *et al.* (2011). High-quality draft assemblies of mammalian genomes from massively parallel sequence data. *Proc. Natl. Acad. Sci.* 108, 1513-1518.

Grabovich, M. Y., Patritskaya, V. Y., Muntyan, M. S., and Dubinina, G. A. (2001). Lithoautotrophic growth of the freshwater strain *Beggiatoa* D-402 and energy conservation in a homogeneous culture under microoxic conditions. *FEMS Microbiol. Lett.* 204, 341–345.

Grünke, S., Felden, J., Lichtschlag, A., Girnth, A.-C., De Beer, D., Wenzhöfer, F., and Boetius, A. (2011). Niche differentiation among mat-forming, sulfide-oxidizing bacteria at cold seeps of the Nile Deep Sea Fan (Eastern Mediterranean Sea). *Geobiology* 9, 330–348.

Haveman, S. A., Brunelle, V., Voordouw, J. K., Voordouw, G., Heidelberg, J. F., and Rabus, R. (2003). Gene expression analysis of energy metabolism mutants of *Desulfovibrio vulgaris* Hildenborough indicates an important role for alcohol dehydrogenase. *J. Bacteriol.* 185, 4345–4353.

Hongoh, Y., Sharma, V. K., Prakash, T., Noda, S., Taylor, T. D., Kudo, T., Sakaki, Y., Toyoda, A., Hattori, M., and Ohkuma, M. (2008). Complete genome of the uncultured Termite Group 1 bacteria in a single host protist cell. *Proc. Natl. Acad. Sci.* 105, 5555–5560.

Hügler, M., and Sievert, S. M. (2011). Beyond the Calvin Cycle: Autotrophic carbon fixation in the ocean. *Annu. Rev. Mar. Sci.* 3, 261–289.

Jannasch, H. W., Nelson, D. C., and Wirsen, C. O. (1989). Massive natural occurrence of unusually large bacteria (*Beggiatoa* sp.) at a hydrothermal deep-sea vent site. *Nature* 342, 834–836.

Jogler, C., Wanner, G., Kolinko, S., Niebler, M., Amann, R., Petersen, N., Kube, M., Reinhardt, R., and Schüler, D. (2011). Conservation of proteobacterial magnetosome genes and structures in an uncultivated member of the deep-branching *Nitrospira* phylum. *Proc. Natl. Acad. Sci.* 108, 1134 –1139.

Jørgensen, B. B. (1977). Distribution of colorless sulfur bacteria (*Beggiatoa* spp.) in a coastal marine sediment. *Mar. Biol.* 41, 19–28.

Jørgensen, B. B., and Gallardo, V. A. (1999). *Thioploca* spp.: filamentous sulfur bacteria with nitrate vacuoles. *FEMS Microbiol. Ecol.* 28, 301–313.

Jørgensen, B. B., and Nelson, D. C. (2004). Sulfide oxidation in marine sediments: Geochemistry meets microbiology. *Geol. Soc. Am. Spec. Pap.* 379, 63–81.

Jørgensen, B. B., and Revsbech, N. P. (1983). Colorless sulfur bacteria, *Beggiatoa* spp. and *Thiovulum* spp., in O_2 and H_2S microgradients. *Appl. Environ. Microbiol.* 45, 1261–1270.

Kalanetra, K. M., Joye, S. B., Sunseri, N. R., and Nelson, D. C. (2005). Novel vacuolate sulfur bacteria from the Gulf of Mexico reproduce by reductive division in three dimensions. *Environ. Microbiol.* 7, 1451–1460.

Kanehisa, M., and Goto, S. (2000). KEGG: Kyoto Encyclopedia of Genes and Genomes. *Nucleic Acids Res.* 28, 27–30.

Kehr, J.-C., Gatte Picchi, D., and Dittmann, E. (2011). Natural product biosyntheses in cyanobacteria: A treasure trove of unique enzymes. *Beilstein J. Org. Chem.* 7, 1622–1635.

Kleiner, M., Petersen, J. M., and Dubilier, N. (2012a). Convergent and divergent evolution of metabolism in sulfur-oxidizing symbionts and the role of horizontal gene transfer. *Curr. Opin. Microbiol.* 15, 621–631.

Kleiner, M., Wentrup, C., Lott, C., Teeling, H., Wetzel, S., Young, J., Chang, Y.-J., Shah, M., VerBerkmoes, N. C., Zarzycki, J., *et al.* (2012b). Metaproteomics of a gutless marine

worm and its symbiotic microbial community reveal unusual pathways for carbon and energy use. *Proc. Natl. Acad. Sci.* 109, E1173-E1182

Krogh, A., Larsson, B., von Heijne, G., and Sonnhammer, E. L. . (2001). Predicting transmembrane protein topology with a hidden markov model: Application to complete genomes. *J. Mol. Biol.* 305, 567–580.

Lagesen, K., Hallin, P., Rødland, E. A., Stærfeldt, H.-H., Rognes, T., and Ussery, D. W. (2007). RNAmmer: Consistent and rapid annotation of ribosomal RNA genes. *Nucleic Acids Res.* 35, 3100–3108.

Larkin, J. M., and Strohl, W. R. (1983). *Beggiatoa*, *Thiothrix*, and *Thioploca*. *Annu. Rev. Microbiol.* 37, 341–367.

Lasken, R. S. (2012). Genomic sequencing of uncultured microorganisms from single cells. *Nat. Rev. Microbiol.* 10, 631–640.

Lowe, T. M., and Eddy, S. R. (1997). tRNAscan-SE: A program for improved detection of transfer RNA genes in genomic sequence. *Nucleic Acids Res.* 25, 0955–964.

Ludwig, W., Strunk, O., Westram, R., Richter, L., Meier, H., Yadhukumar, Buchner, A., Lai, T., Steppi, S., Jobb, G., *et al.* (2004). ARB: a software environment for sequence data. *Nucl Acids Res* 32, 1363–1371.

MacGregor, B. J., Biddle, J. F., Siebert, J. R., Staunton, E., Hegg, E. L., Matthysse, A. G., and Teske, A. (2013a). Why orange Guaymas Basin *Beggiatoa* spp. are orange: Single-filament-genome-enabled identification of an abundant octaheme cytochrome with hydroxylamine oxidase, hydrazine oxidase, and nitrite reductase activities. *Appl. Environ. Microbiol.* 79, 1183–1190.

MacGregor, B. J., Biddle, J. F., and Teske, A. (2013b). Mobile elements in a single-filament orange Guaymas Basin *Beggiatoa* ("*Candidatus* Maribeggiatoa") sp. draft genome: Evidence for genetic exchange with cyanobacteria. *Appl. Environ. Microbiol.* 79, 3974–3985.

Markert, S., Arndt, C., Felbeck, H., Becher, D., Sievert, S. M., Hügler, M., Albrecht, D., Robidart, J., Bench, S., Feldman, R. A., *et al.* (2007). Physiological proteomics of the uncultured endosymbiont of *Riftia pachyptila*. *Science* 315, 247–250.

Markowitz, V. M., Chen, I.-M. A., Palaniappan, K., Chu, K., Szeto, E., Grechkin, Y., Ratner, A., Jacob, B., Huang, J., Williams, P., *et al.* (2012). IMG: The integrated microbial genomes database and comparative analysis system. *Nucleic Acids Res.* 40, D115–D122.

Mattison, R. G., Abbiati, M., Dando, P. R., Fitzsimons, M. F., Pratt, S. M., Southward, A. J., and Southward, E. C. (1998). Chemoautotrophic microbial mats in submarine caves with hydrothermal sulphidic springs at Cape Palinuro, Italy. *Microb. Ecol.* 35, 58–71.

McHatton, S. C., Barry, J. P., Jannasch, H. W., and Nelson, D. C. (1996). High nitrate concentrations in vacuolate, autotrophic marine *Beggiatoa* spp. *Appl. Environ. Microbiol.* 62, 954–958.

Meyer, F., Goesmann, A., McHardy, A. C., Bartels, D., Bekel, T., Clausen, J., Kalinowski, J., Linke, B., Rupp, O., Giegerich, R., *et al.* (2003). GenDB - An open source genome annotation system for prokaryote genomes. *Nucleic Acids Res.* 31, 2187–2195.

Mezzino, M. J., Strohl, W. R., and Larkin, J. M. (1984). Characterization of *Beggiatoa alba*. *Arch. Microbiol.* 137, 139–144.

Moreno-Vivián, C., Cabello, P., Martínez-Luque, M., Blasco, R., and Castillo, F. (1999). Prokaryotic nitrate reduction: Molecular properties and functional distinction among bacterial nitrate reductases. *J. Bacteriol.* 181, 6573–6584.

Morozkina, E. V., and Zvyagilskaya, R. A. (2007). Nitrate reductases: Structure, functions, and effect of stress factors. *Biochem. Mosc.* 72, 1151–1160.

Mußmann, M., Hu, F. Z., Richter, M., de Beer, D., Preisler, A., Jørgensen, B. B., Huntemann, M., Glöckner, F. O., Amann, R., Koopman, W. J. H., *et al.* (2007). Insights into the

genome of large sulfur bacteria revealed by analysis of single filaments. *PLoS Biol* 5, e230.

Nelson, D. C., and Castenholz, R. W. (1982). Light responses of *Beggiatoa*. *Arch. Microbiol.* 131, 146–155.

Nelson, D. C., and Castenholz, R. W. (1981a). Organic nutrition of *Beggiatoa* sp. *J. Bacteriol.* 147, 236–247.

Nelson, D. C., and Castenholz, R. W. (1981b). Use of reduced sulfur compounds by *Beggiatoa* sp. *J. Bacteriol.* 147, 140–154.

Nelson, D. C., and Jannasch, H. W. (1983). Chemoautotrophic growth of a marine *Beggiatoa* in sulfide-gradient cultures. *Arch. Microbiol.* 136, 262–269.

Nelson, D. C., Jørgensen, B. B., and Revsbech, N. P. (1986a). Growth pattern and yield of a chemoautotrophic *Beggiatoa* sp. in oxygen-sulfide microgradients. *Appl. Environ. Microbiol.* 52, 225–233.

Nelson, D. C., Revsbech, N. P., and Jørgensen, B. B. (1986b). Microoxic-anoxic niche of *Beggiatoa* spp.: Microelectrode survey of marine and freshwater strains. *Appl. Environ. Microbiol.* 52, 161–168.

Nelson, D. C., Waterbury, J. B., and Jannasch, H. W. (1982). Nitrogen fixation and nitrate utilization by marine and freshwater *Beggiatoa*. *Arch. Microbiol.* 133, 172–177.

Noguchi, H., Park, J., and Takagi, T. (2006). MetaGene: Prokaryotic gene finding from environmental genome shotgun sequences. *Nucleic Acids Res.* 34, 5623–5630.

Otte, S., Kuenen, J. G., Nielsen, L. P., Paerl, H. W., Zopfi, J., Schulz, H. N., Teske, A., Strotmann, B., Gallardo, V. A., and Jørgensen, B. B. (1999). Nitrogen, carbon, and sulfur metabolism in natural *Thioploca* samples. *Appl Env. Microbiol* 65, 3148–3157.

Petersen, J. M., Zielinski, F. U., Pape, T., Seifert, R., Moraru, C., Amann, R., Hourdez, S., Girguis, P. R., Wankel, S. D., Barbe, V., *et al.* (2011). Hydrogen is an energy source for hydrothermal vent symbioses. *Nature* 476, 176–180.

Preisler, A., de Beer, D., Lichtschlag, A., Lavik, G., Boetius, A., and Jørgensen, B. B. (2007). Biological and chemical sulfide oxidation in a *Beggiatoa* inhabited marine sediment. *ISME J.* 1, 341.

Quast, C. (2006). MicHanThi – design and implementation of a system for the prediction of gene functions in genome annotation projects. Master thesis.

Quast, C., Pruesse, E., Yilmaz, P., Gerken, J., Schweer, T., Yarza, P., Peplies, J., and Glockner, F. O. (2012). The SILVA ribosomal RNA gene database project: Improved data processing and web-based tools. *Nucleic Acids Res.* 41, D590–D596.

Ramaswamy, K. S., Carrasco, C. D., Fatma, T., and Golden, J. W. (1997). Cell-type specificity of the *Anabaena fdxN*-element rearrangement requires *xisH* and *xisI*. *Mol. Microbiol.* 23, 1241–1249.

Reshetnikov, A. S., Rozova, O. N., Khmelenina, V. N., Mustakhimov, I. I., Beschastny, A. P., Murrell, J. C., and Trotsenko, Y. A. (2008). Characterization of the pyrophosphate-dependent 6-phosphofructokinase from *Methylococcus capsulatus* Bath. *FEMS Microbiol. Lett.* 288, 202–210.

Richter, M., Lombardot, T., Kostadinov, I., Kottmann, R., Duhaime, M. B., Peplies, J., and Glöckner, F. O. (2008). JCoast - A biologist-centric software tool for data mining and comparison of prokaryotic (meta)genomes. *BMC Bioinformatics* 9, 177.

Salman, V., Amann, R., Girnth, A.-C., Polerecky, L., Bailey, J. V., Høgslund, S., Jessen, G., Pantoja, S., and Schulz-Vogt, H. N. (2011). A single-cell sequencing approach to the classification of large, vacuolated sulfur bacteria. *Syst. Appl. Microbiol.* 34, 243–259.

Salman, V., Amann, R., Shub, D. A., and Schulz-Vogt, H. N. (2012). Multiple self-splicing introns in the 16S rRNA genes of giant sulfur bacteria. *Proc. Natl. Acad. Sci.* 109, 4203–4208.

Salman, V., Bailey, J. V., and Teske, A. (2013). Phylogenetic and morphologic complexity of giant sulphur bacteria. *Antonie Van Leeuwenhoek*, 104, 169-186.

Sayama, M., Risgaard-Petersen, N., Nielsen, L. P., Fossing, H., and Christensen, P. B. (2005). Impact of bacterial NO_3^- transport on sediment biogeochemistry. *Appl. Environ. Microbiol.* 71, 7575–7577.

Schulz, H. N. (2006). "The genus *Thiomargarita*," in *The Prokaryotes*, eds. M. D. P. Dr, S. Falkow, E. Rosenberg, K.-H. Schleifer, and E. Stackebrandt (Springer New York), 1156–1163.

Schulz, H. N., and de Beer, D. (2002). Uptake rates of oxygen and sulfide measured with individual *Thiomargarita namibiensis* cells by using microelectrodes. *Appl. Environ. Microbiol.* 68, 5746–5749.

Schulz, H. N., Brinkhoff, T., Ferdelman, T. G., Mariné, M. H., Teske, A., and Jørgensen, B. B. (1999). Dense populations of a giant sulfur bacterium in Namibian shelf sediments. *Science* 284, 493–495.

Schulz, H. N., and Schulz, H. D. (2005). Large sulfur bacteria and the formation of phosphorite. *Science* 307, 416–418.

Schwedt, A., Kreutzmann, A.-C., Polerecky, L., and Schulz-Vogt, H. N. (2012). Sulfur respiration in a marine chemolithoautotrophic *Beggiatoa* Strain. *Front. Microbiol.* 2, 276

Siegl, A., Kamke, J., Hochmuth, T., Piel, J., Richter, M., Liang, C., Dandekar, T., and Hentschel, U. (2011). Single-cell genomics reveals the lifestyle of *Poribacteria*, a candidate phylum symbiotically associated with marine sponges. *ISME J.* 5, 61–70.

Stepanova, I. Y., Eprintsev, A. T., Falaleeva, M. I., Parfenova, N. V., Grabovich, M. Y., Patritskaya, V. Y., and Dubinina, G. A. (2002). Dependence of malate dehydrogenase structure on the type of metabolism in freshwater filamentous colorless sulfur bacteria of the genus *Beggiatoa*. *Microbiology* 71, 377–382.

Strittmatter, A. W., Liesegang, H., Rabus, R., Decker, I., Amann, J., Andres, S., Henne, A., Fricke, W. F., Martinez-Arias, R., Bartels, D., *et al.* (2009). Genome sequence of *Desulfobacterium autotrophicum* HRM2, a marine sulfate reducer oxidizing organic carbon completely to carbon dioxide. *Environ. Microbiol.* 11, 1038–1055.

Strohl, W. R., Schmidt, T. M., Vinci, V. A., and Larkin, J. M. (1986). Electron transport and respiration in *Beggiatoa* and *Vitreoscilla*. *Arch. Microbiol.* 145, 71–75.

Sweerts, J.-P. R. A., Beer, D. D., Nielsen, L. P., Verdouw, H., den Heuvel, J. C. V., Cohen, Y., and Cappenberg, T. E. (1990). Denitrification by sulphur oxidizing *Beggiatoa* spp. mats on freshwater sediments. *Nature* 344, 762–763.

Tanaka, S., Lee, S.-O., Hamaoka, K., Kato, J., Takiguchi, N., Nakamura, K., Ohtake, H., and Kuroda, A. (2003). Strictly polyphosphate-dependent glucokinase in a polyphosphate-accumulating bacterium, *Microlunatus phosphovorus*. *J. Bacteriol.* 185, 5654–5656.

Teske, A., and Nelson, D. C. (2006). "The genera *Beggiatoa* and *Thioploca*," in *The Prokaryotes*, eds. M. D. P. Dr, S. Falkow, E. Rosenberg, K.-H. Schleifer, and E. Stackebrandt (Springer New York), 784–810

Thauer, R. K., Kaster, A.-K., Seedorf, H., Buckel, W., and Hedderich, R. (2008). Methanogenic archaea: Ecologically relevant differences in energy conservation. *Nat. Rev. Microbiol.* 6, 579–591.

Vargas, A., and Strohl, W. R. (1985). Utilization of nitrate by *Beggiatoa alba*. *Arch. Microbiol.* 142, 279–284.

Walsh, K., and Koshland, D. E. (1984). Determination of flux through the branch point of two metabolic cycles. The tricarboxylic acid cycle and the glyoxylate shunt. *J. Biol. Chem.* 259, 9646–9654.

Wood, A. P., Aurikko, J. P., and Kelly, D. P. (2004). A challenge for 21st century molecular biology and biochemistry: what are the causes of obligate autotrophy and methanotrophy? *FEMS Microbiol. Rev.* 28, 335–352.

Woyke, T., Tighe, D., Mavromatis, K., Clum, A., Copeland, A., Schackwitz, W., Lapidus, A., Wu, D., McCutcheon, J. P., McDonald, B. R., *et al.* (2010). One bacterial cell, one complete genome. *PLoS ONE* 5, e10314.

Woyke, T., Xie, G., Copeland, A., González, J. M., Han, C., Kiss, H., Saw, J. H., Senin, P., Yang, C., Chatterji, S., *et al.* (2009). Assembling the marine metagenome, one cell at a time. *PLoS ONE* 4, e5299.

Zerbino, D. R., and Birney, E. (2008). Velvet: Algorithms for de novo short read assembly using de Bruijn graphs. *Genome Res.* 18, 821–829.

Zhang, W., Gritsenko, M. A., Moore, R. J., Culley, D. E., Nie, L., Petritis, K., Strittmatter, E. F., Camp, D. G., Smith, R. D., and Brockman, F. J. (2006). A proteomic view of *Desulfovibrio vulgaris* metabolism as determined by liquid chromatography coupled with tandem mass spectrometry. *PROTEOMICS* 6, 4286–4299.

Zumft, W. G. (1997). Cell biology and molecular basis of denitrification. *Microbiol. Mol. Biol. Rev.* 61, 533–616.

Table 1: General genome feature of the investigated large, colorless SOB

genome feature	"*Candidatus* Thiomargarita nelsonii"	"*Candidatus* Isobeggiatoa divolgata"	orange *Beggiatoa* filament BOGUAY	*Beggiatoa* sp. 35Flor	*Beggiatoa alba* B18LD
nucleotides	5.3 Mb	7.6 Mb	4.8 Mb	4 Mb	4.3 Mb
contigs	3,613	6,769	822	284	21
ORF	7,596*	6,686	5,258	5,258	3,665
percentage coding	72	57	85	87	86
max. contig length	14 kb	19 kb	71 kb	138 kb	500 kb
tRNAs	23	45	46	37	46
GC content [%]	42	38.5	38,2	38,5	40
proteins of known function	3,486	3414	2962	2746	2867
conserved hypothetical proteins	967	1046	619	380	377
hypothetical proteins	3143	2226	1677	426	421
reference	this study	(Mußmann et al., 2007)	J. Craig Venter Institute	this study	DOE Joint Genome Institute

* likely overestimation due to high number of frame shifts

Table 2: Energy conservation and metabolic pathways in the investigated large, colorless SOB

	Large colorless sulfur-oxidizing bacteria				
Pathways	*Ca.* Thiomargarita nelsonii	*Ca.* Isobeggiatoa divolgata	orange *Beggiatoa* filament BOGUAY	*Beggiatoa* sp. 35Flor	*Beggiatoa alba* B18LD
sulfide oxidation	+	+	+	+	+
elmental sulfur oxidation via reverse DSR pathway	+	+	+	+	-?
sulfite oxidation	+	+	+	+	-
assimilatory sulfate reduction	?	-	-	+	+
thiosulfate oxidation via SOX pathway	+	+	+	+	+
dissimilatory nitrate reduction to ammonium	+	- (potential via multiheme protein?)	- (potential via multiheme protein?)	-	+
assimilatory nitrate reduction to ammonium	+	-	-	-	+
denitrification	+	+	+	-	+
glycolysis	+	+	+	+	+
tricarboxylic acid cycle	+	+	+	+	+
glyoxylate bypass	-	-	-	+	+
polyhydroxybutyrate syntheses	-	-	-	+	+
carbon fixation via CBB-cycle	+	+	+	+	+
carbon fixation via reductive tricarboxylic acid cycle/acetly-CoA reduction	+/+	-/-	+/-	-/-	-/-
C2-cycle (glycolate cycle)	+				+
oxidative phosphorylation	+	+	+	+	+
flavin-based energy bifurcation	+	+	+	-	-
potential hydrogen oxidation	+	+	+	+	+
Na^+ -translocating membrane complex	+	+	+	+	+

+ complete set of genes for metabolic pathway encoded
-? no complete set of genes for pathway or pathway with alternative genes
- genes of pathway not found or not encoded

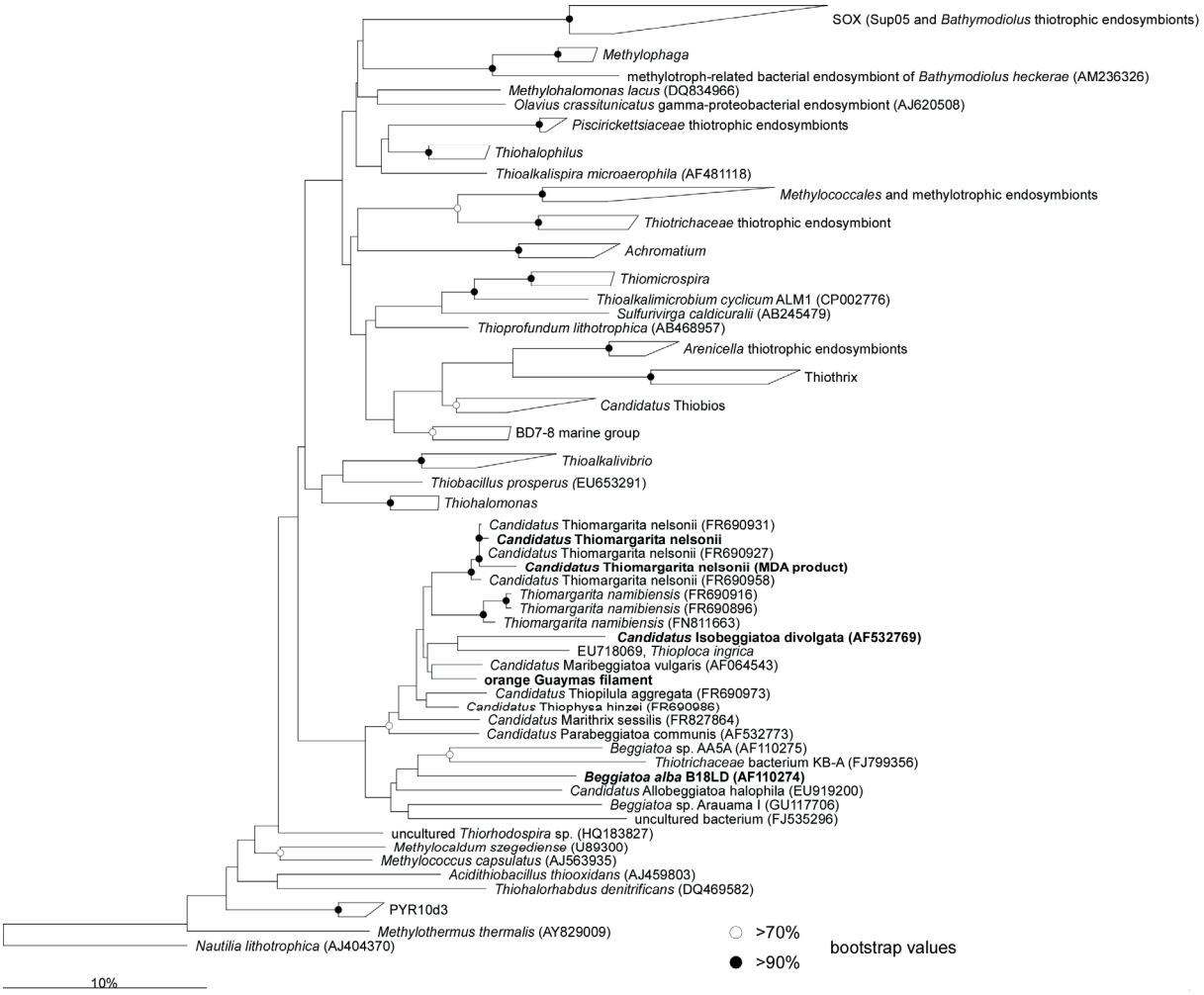

Figure 1: Phylogenetic tree of the 16S rRNA gene of sulfur and methane oxidizing *Gammaproteobacteria*. Sequences of investigated large, colorless SOB are shown in bold with the exception of *Beggiatoa* sp. 35Flor, where no 16S rRNA gene could be detected. Nucleotide sequences were imported into ARB and aligned with SINA aligner (Pruesse et al., 2012). Tree was calculated with RAxML implemented in ARB (1018 position used), a 50% position variability filter and the GTR substitution matrix. Bootstraps were calculated using 100 resampling's and bootstrap values are as shown in the legend. Scale bar represents 10% sequence divergence.

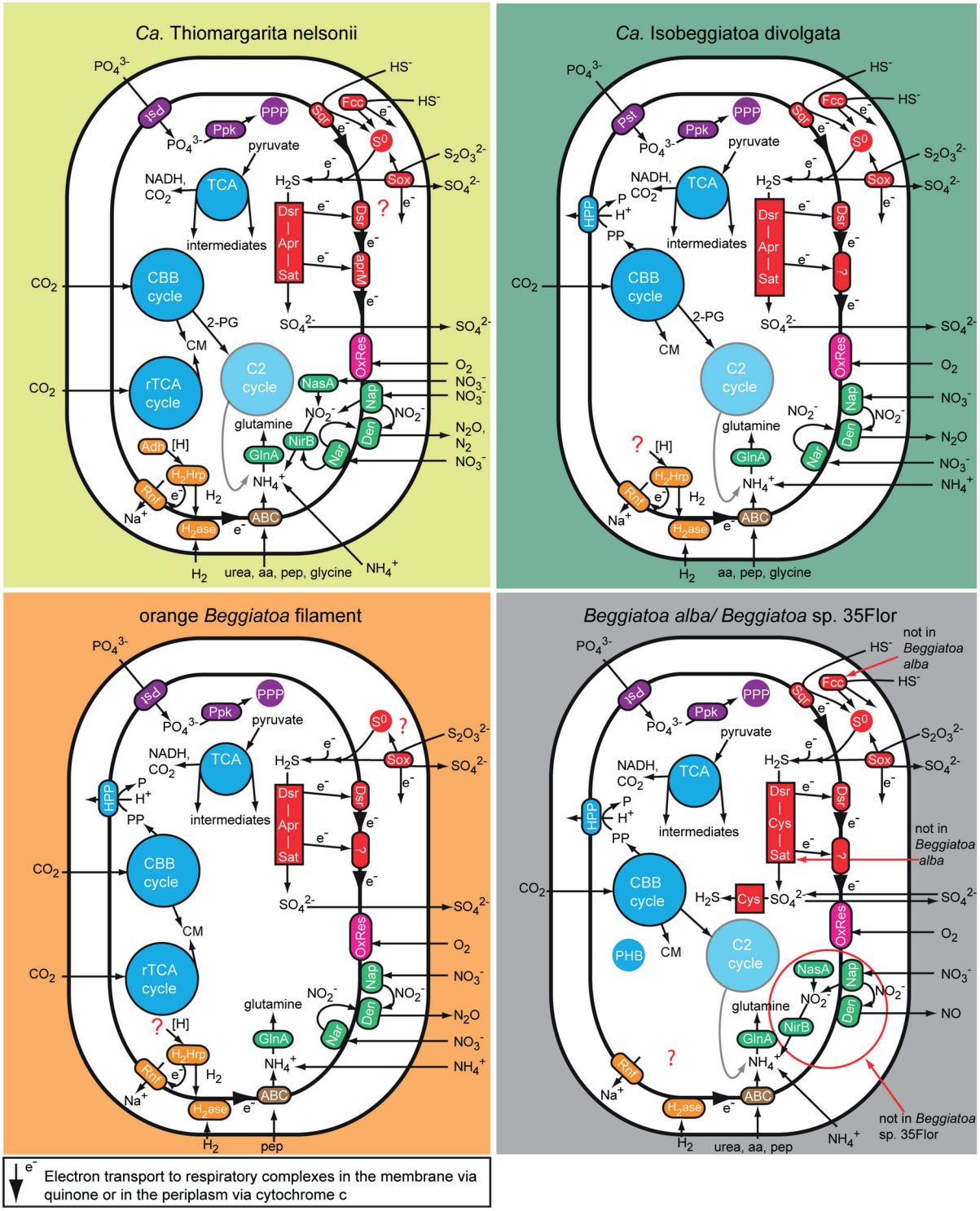

Figure 2: Comparison of C, N, S, P and energy pathways in the investigated large, colorless SOB based on the genomic information. Aa, amino acid; ABC, ABC transporter; Adh, alcohol dehydrogenase; Apr, APS reductase; CBB cycle, Calvin-Benson-Bashman cycle; C2 cycle, glyoxylate cycle; CM, cell material; Cys, 3' phosphoadenylylsulfate reductase; Den, denitrification proteins; Dsr, dissimilatory sulfite reductase and related proteins; Fcc, flavocyctochrome c; GlnA, Glutamine synthetase; H_2ase, uptake hydrogenase; H_2Hrp, methyl viologen-reducing hydrogenase:heterodisulfide reductase complex; HPP, proton translocating pyrophosphatase; Nar, membrane-bound respiratory nitrate reductase; Nap, periplasmatic respiratory nitrate reductase; NasA, assimilatory nitrate reductase; NirB, assimilatory and dissimilatory nitrite reductase; OxRes, oxygen respiration; pep, peptides; PHB,

polyhydroxybutyrate granule; PPP, polyphosphate granule; Ppk, polyphosphate kinase; Pst, phosphate transport system; Rnf, membrane-bound electron transport complex; rTCA, reductive tricarboxylic acid cycle; S^0, sulfur globoli; Sat, ATP sulfurylase; Sox, SOX enzyme complex; Sqr, sulfide quinone reductase; TCA, tricarboxylic acid cycle.

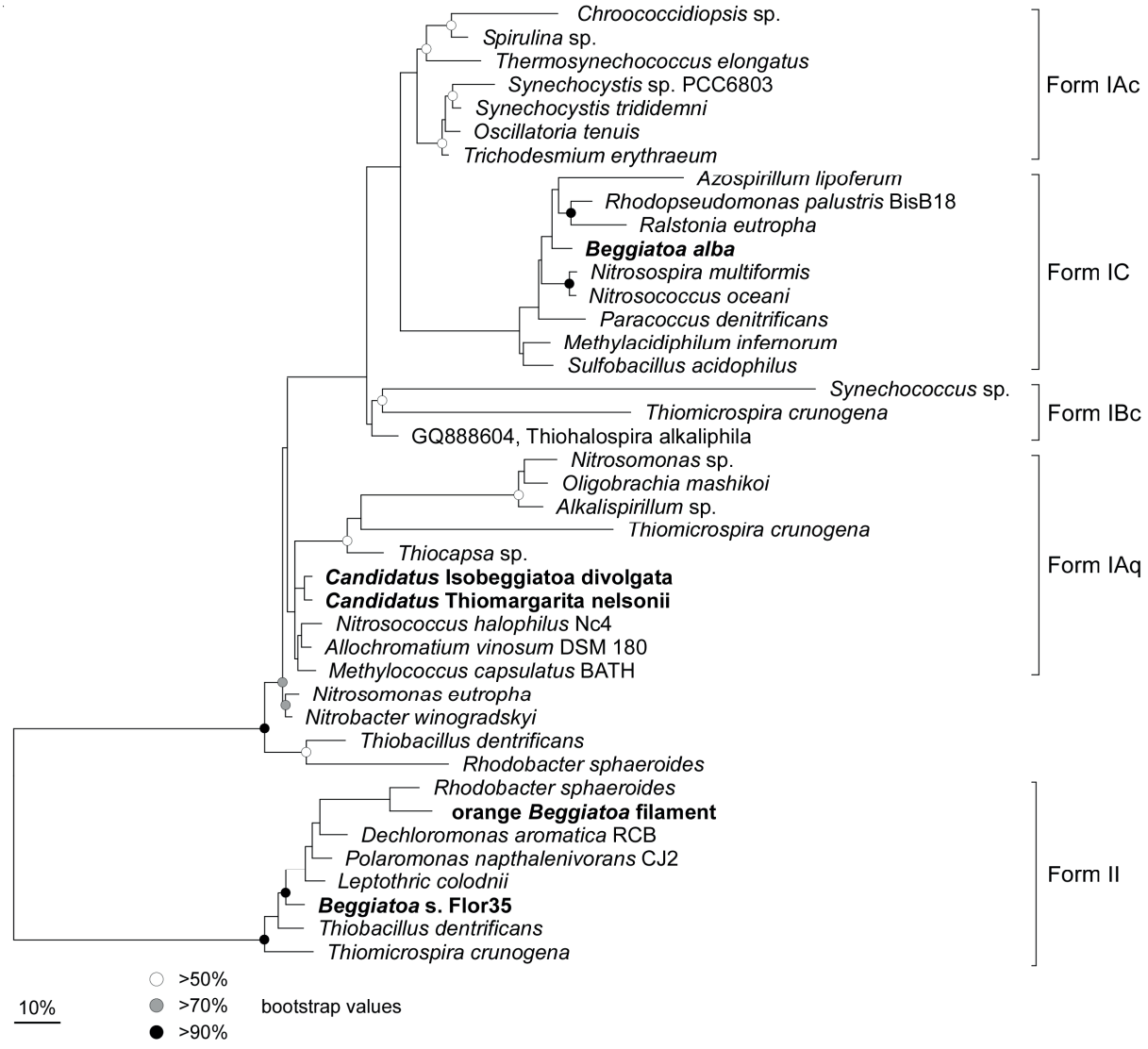

Figure 3: Phylogenetic tree of the large subunit from the protein ribulose-1,5-bisphosphate carboxylase/ oxygenase (RubisCO). The five investigated large, colorless SOB are shown in bold. Protein sequences were imported into ARB and aligned with integrated aligner. Tree was calculated with RAxML implemented in ARB (256 positions used). Bootstraps were calculated using 100 resampling's and bootstrap values are as shown in the legend. Scale bar represents 10% sequence divergence.

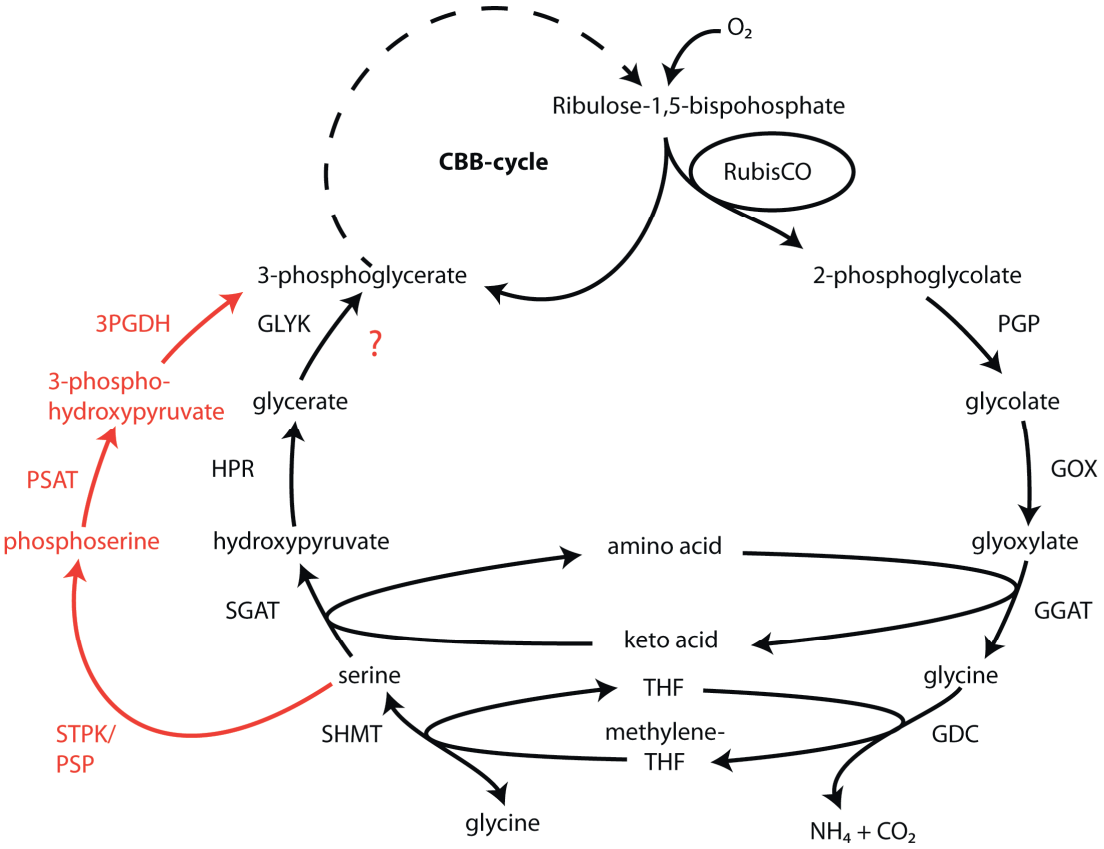

Figure 4: Glycolate cycle of the investigated large, colorless SOB with alternative phosphoserine shuttle of *Candidatus* Thiomargarita Nelsonii and *Candidatus* Isobeggiatoa divolgata (red) see also text. PGP= Phospoglycolate phosphatase, GOX= glycolate oxidase, GGAT= glutamate:glyoxylate aminotransferase, GDC= glycine decarboxylase, SHMT= serine hydroxymethyltransferase, SGAT= serine:glyoxlyate aminotransferase, HDR= hydroxypyruvate reductase, GLYK= glycerate kinase type III, STPK= serine threonine protein kinase, PSAT= phosphoserine aminotransferase, 3PGDH= 3-phosphoglycerate dehydrogenase.

Supporting Information

Material methods

Amplification of different genes for post-MDA testing

We amplified the 16S rRNA gene of the MDA product with different combinations of primers (Table S1). Furthermore, we amplified the functional marker gene adenylylsulfate reductase subunit A (*aprA*) involved in sulfite oxidation, the single copy gene (SCG) recombinase (*recA*) involved in DNA repair and the partial 23S rRNA gene intergenic spacer region (ITS) with specific primers (Table S1). Therefore 1 µl of different dilutions were used as template in a 20 µl PCR mix, containing 1 x PCR buffer (500 mM KCl, 100 mM Tris-HCl pH 8.3 at 25°C, 15 mM Mg^{2+}) (5 Prime, Hamburg, Germany), 0.2 mM of each deoxynucleoside (Roche, Basel, Schweiz), 0.5 µM of each primer (Biomers, Ulm, Deutschland), 0.3 mg ml^{-1} BSA (Fluka, Buchs, Schweiz) and 0.01 U $µl^{-1}$ *Taq*-polymerase (5 Prime, Hamburg, Germany). Primers were synthesized by Biomers (Ulm, Germany).The thermo cycler conditions were as followed: 94°C for 5 minutes (denaturation), followed by 30 cycles of 94°C for 1 minute (denaturation), temperatures see table S1 for 1.5 minutes (annealing) and 72°C for 1 minute (elongation). After the amplification PCR products were run on a 1% agarose gel together with a size marker and stained in an ethidium bromide bath.

Results and Discussion

Phylogenetic and functional gene amplification control of target DNA

Whole genome amplification using the sensitive MDA approach risks the amplification of non-target DNA from contaminating bacteria and free-DNA. To detect potentially contaminations during the MDA of "*Ca.* T. nelsonii" single cells we tested the MDA products with a PCR of the small subunit RNA. The 16S rRNA sequences in "*Ca.* T. nelsonii" is approximately 2350 nt in length and contains an intron of 855 nt (Salman *et al.*, 2012). This unique feature allowed us to discriminate against other bacterial 16S rRNA genes with length of approximately 1500 nt. We detected no contaminaition during the genome amplification. To further test the amplification of the whole genome, different PCRs were conducted to amplify the single copy gene (SCG) *recA* for the repair and recombination of DNA, the functional gene *aprA* for adenylylsulfate reductase alpha subunit, which is involved in the oxidation of reduced sulfur compounds and a partial intergenic transcribed spacer (ITS) region up/downstream of the 23S rRNA gene. Amplification of the SCG and the functional gene failed, which is a known problem for SCG of MDA-products of single cells (Raghunathan *et al.*, 2005). A reason might be the inaccessibility of the target region by the hyperbranched MDA-product, which could be also true for the functional gene. Another explanation might be that the primers were not matching the target site. Nevertheless, we successfully amplified an ITS/partial 23S rRNA gene sequence with specific primers for "*Ca.* T. nelsonii" species of the cylindrical cell morphotype (Salman *et al.*, 2011, 2012) that confirmed the success of the whole genome amplification.

Gene organization of nitrogen metabolism

The membrane-bound dissimilatory nitrate reductase (*nar*) of "*Ca*. T. nelsonii" was located on a contig in a complete *narGHJI* operon that is known for other *Gammaproteobacteria* (Table S2) (Moreno-Vivián *et al.*, 1999). The same operon was found in the genome of the orange *Beggiatoa* filament BOGUAY and "*Ca.* I. divolgata", while it was distributed over different contigs in the latter (Table S2) (Mußmann *et al.*, 2007). The marine *Beggiatoa* sp. strain 35Flor and the freshwater strain *B. alba* B18LD missed genes for the membrane-bound nitrate reductase (Table S2). "*Ca.* T. nelsonii" also encoded for a second set of the *narGH* nitrate reductase, similar as in "*Ca.* I. divolgata" and the orange BOGUAY filament (Table S2). Furthermore, "*Ca.* T. nelsonii"and "*Ca.* I. divolgata" contained nitrate/nitrite antiporter (*narK*) potentially involved in the accumulation of nitrate in the

central vacuole (Beutler *et al.*, 2012). The detected genes for the periplasmic dissimilatory nitrate reductase (*napABCGH*) (Morozkina and Zvyagilskaya, 2007) of the "*Ca.* T. nelsonii" genome were located on different contigs, while only *napA* and *napG* (THI153 and THI153_0) laid on one contig. Both genes were found twice in the genome, but at different locations (THI1149 → *napA* and THI485_1 → *napG*). All other large, colorless SOB with the exception of *Beggiatoa* sp. strain 35Flor contained genes for the same periplasmatic nitrate reductase, although the ferredoxin-type protein *napH* are missed and the ferredoxin-type protein *napG* only occurs in *B. alba* B18LD (Table S2). The assimilatory nitrate reductase (*nasA*) was identified in the genome of "*Ca.* T. nelsonii", and *B. alba* B18LD (Fig. 1 and Table S2). In the almost closed *B. alba* B18LD genome the gene is located next to the NAD(P)H-dependent nitrite reductase *nirBD*. This nitrite reductase is known to be involved in the assimilatory (Malm *et al.*, 2009) and dissimilatory nitrite reduction (Zumft, 1997). The "*Ca.* T. nelsonii" genome also encoded for the nitrite reductase large subunit (*nirB*), but missed the small subunit (*nirD*), which might be located on the yet not sequenced part of the genome. If "*Ca.* T. nelsonii" encodes for the full set of the *nirBD* gene besides the *narGHIJ* and *napABCGH* operon, a dissimilatory nitrate reduction to ammonia would be possible. DNRA is likely to occur in *B. alba* B18LD with *nirBD* and *napABCGH* and were shown in earlier studies with *B. alba* (Vargas and Strohl, 1985). The marine *Beggiatoa* genomes did not encode for nitrite reductases involved in DNRA, but a isolated and purified multiheme cytochrome of the orange *Beggiatoa* filament BOGUAY showed nitrite reductase-function (MacGregor *et al.*, 2013) maybe involved in DNRA. The same cytochrome was found in "*Ca.* I. divolgata" (MacGregor *et al.*, 2013), while it has not been detected in *Beggiatoa* sp. strain 35Flor (Fig. 1 and Table S2).

For a potential denitrification the genomes of "*Ca.* T. nelsonii" and "*Ca.* I. divolgata" contained an almost complete *nirSCFDLGHJEN* operon of the nitrite reductase that only missed some heme biosynthesis involved enzymes ("*Ca.* T. nelsonii" → *nirHE* and "*Ca.* I. divolgata" → *nirEN*; Table S2). This operon is known to occur in the denitrifying bacterium *Pseudomonas aeroginosa* (Bedzyk *et al.*, 1999) and together with the periplasmatic nitrate reductase *napABCGH* indicating the potential for denitrification in "*Ca.* T. nelsonii" and "*Ca.* I. divolgata". Furthermore, both genomes and the orange *Beggiatoa* filament BOGUAY genome encoded for a membrane-bound nitric oxide reductase complex *norBC*, and *norQDEF* (Table S2). *NorE* was only found in "*Ca.* T. nelsonii", while *norF* was not encoded by any genome. In "*Ca.* T. nelsonii" one contig (THI459) was organized in the order *norQEB* and *norQ* was flanked by two hypothetical membrane proteins, which are potentially involved

as anchor proteins. On another contig (THI692) a second *norQB* gene was identified. The *norQDEF*-complex analyzed in denitrifiying microorganisms have been shown to have regulatory effects, while nitrate and nitrite reduction was reduced by knockout of *norQ*. However, *norE* have similarities to cytochrome oxidase subunit III and knockouts effectively reduce nitric oxide reductase activity (Baker *et al.*, 1998). Besides the Nor-complex "*Ca.* T. nelsonii", *B. alba* B18LD and *Beggiatoa* sp. strain 35Flor also coantained genes encoding for a cyanide-sensitive nitric oxide dioxygenase (Table S2), which produces nitrate and has similar structures to flavohemoglobin from *Escherichia coli*. This enzyme appears to be ancient in the superfamily of hemoglobins (Gardner *et al.*, 1998) and a potential function in large colorless SOB is unclear.

Gene organization of sulfur oxidation pathways

Besides sulfide oxidation genes, we further found genes for the oxidation of the internal stored zerovalent sulfur encoded by the reductive dissimilatory sulfite reductase (rDSR) pathway. In the genome of "*Ca.* T. nelsonii" only some genes were found, which encoded for homologs of the operon *dsrABEFHCMKLJOPNRS* (Dahl *et al.*, 2008). We found *dsrB*, *dsrE*, *dsrC*, *dsrR*, *dsrS*, and contigs with *dsrMK* and *dsrKL* genes, so functionality in "*Ca.* T. nelsonii" is unclear (Fig.2 and Table S3). Nevertheless, a complete operon was found in the genomes *Beggiatoa* sp. strain 35Flor and the orange *Beggiatoa* filament BOGUAY, as well as larger contigs with parts of the operon in "*Ca.* I. divolgata" (Fig. 2 and Table S3).

The produced sulfite of the rDSR pathway is oxidized indirect by the AMP-dependent oxidation, which is catalyzed by the cytoplasmic adenosine-5´-phosphosulfate (APS) reductase and the ATP sulfurylase via substrate level phosphorylation to produce sulfate (Hagen and Nelson, 1997; Dahl *et al.*, 2008). A gene encoding a partial alpha subunit of the APS reductase (*aprA*) and a gene encoding for the ATP sulfurylase (*sat*) were detected on the genome of "*Ca*. T. nelsonii". A full set of *aprAB* and *sat* genes were found in "*Ca.* I. divolgata" and *Beggiatoa* sp. strain 35Flor, so a complete set of genes in "*Ca.* T. nelsonii" can be assumed. Furhtermore, genes for the assimilatory sulfate reduction (*cysCDNHIJ*) (Neumann *et al.*, 2000) together with an sulfate permease ABC transpoter (*cysAWT*) for sulfur assimilation were encoded on the *B. alba* B18LD genome (Fig. 2 and Table S3). It lacks genes for the dissimilatory sulfite oxidation (*aprAB* and *sat*) and had only a few detected genes (*dsrCEFHMKJ*) of the rDSR pathway (Table S3). The latter genes might be a relict of an obligate chemolithotrophic lifestyle. *Beggiatoa* sp. strain 35Flor also have genes for the assimilatory sulfate reduction via a high affinity sulfate permease tansporter (SuIP), a sulfate

adenylytransferase (*sat*), an adenylylsulfate (APS) kinase (*cysC*), a phosphor-adenylylsulfate (PAPS) reductase (*cysH*), and a ferredoxin sulfite reductase (*sir*) (Table S3) that produce hydrogen sulfide. This is incorporated in cysteine under a heterotrophic lifestyle. The complete oxidation of sulfur to sulfate might by occurr under chemolithotrophic conditions by the rDSR pathway and *sat*, while the dissimilatory phospho-adenylylsulfate reductase (*aprAB*) was missed. We also found genes involved in thiosulfate oxidation by the SOX pathway (Dahl *et al.*, 2008). The genes *soxBY*, were encoded on the genomes of "*Ca.* T. nelsonii", "*Ca.* I. divolgata, *Beggiatoa* sp. strain 35Flor and the orange *Beggiatoa* filament BOGUAY. Another gene on the genome of "*Ca*. T. nelsonii" involved in thiosulfate utilization was a thiosulfate sulfurtransferase (rhodanese) known from the thiosulfate disproportionation pathway (Table S3). Rhodaneses are assumed to be responsible for cyanide detoxification (Cipollone *et al.*, 2006), but can be involved in sulfur oxidation of chemolithautotrophic microorganisms as it converts thiosulfate to sulfite (Anantharaman *et al.*, 2013; Sheik *et al.*, 2013). A detailed description of the sulfur oxidation in *Beggiatoaceae* will be published elsewhere (see section in PhD thesis of A. Kreutzmann)

Carbon metabolism

Glycolysis

Besides the mentioned polyphosphate glucokinase (*ppgk*), "*Ca.* I. divolgata" also contained an ATP-glucokinase. This enzyme was detected in *B. alba* B18LD and *Beggiatoa* sp. 35Flor that lacks the polyphosphate-dependent form. The polyphosphate-dependent type of this enzyme is speculated to be an ancient form out of which the ATP-dependent type has been evolved (Tanaka *et al.*, 2003). The occurrence of polyphosphate-dependent enzymes supports the observation that *Thiomargarita* species and *Beggiatoa* sp. strain 35Flor produce polyphosphate and store it internal in granula (Schulz and Schulz, 2005; Brock *et al.*, 2012). A difference of "*Ca.* T. nelsonii" to all other investigated large, colorless SOB was the coding for a class I aldolase (Table S4), which is a typical enzyme to be found in animals and plants and have only rarely been detected in microorganisms.

All genomes encoded genes for converting the produced pyruvate to acetyl-CoA and shuttle it into the tricarboxylic acid cycle, with the exception of the orange *Beggiatoa* filament BOGUAY that missed one component (*aceF/pdhC*) of the multienzyme pyruvate dehydrogenase complex (Table S3). Further support for carbohydrate utilization was the detection of multiple gene copies for saccharide ABC transporter systems (data not shown). It

is not clear why these organisms don't grow on carbohydrates as sole carbon and energy source.

Pyrophosphatase coupled to carbon fixation

In endosymbiontic sulfur oxidizer and methanotrophic bacteria a coupling between the pyrophosphate-dependent 6-phosphofructokinase that produces pyrophosphate and a membrane-bound proton-tanslocating pyrophosphatase for energy conservation have been proposed (Reshetnikov *et al.*, 2008; Kleiner *et al.*, 2012b). Unlike these microorganisms large, colorless SOB did not encode for a proton-translocating pyrophosphatase in close proximity to the genome region of the pyrophosphate-dependent 6-phosphofructokinase (Kleiner *et al.*, 2012b). Nevertheless, we found at least one proton-translocating pyrophosphatase on the genomes of all large, colorless SOB with the exception of "*Ca.* T. nelsonii", which might be still together function in an energy saving alternative of the CBB-cycle (Kleiner *et al.*, 2012a).

C2-cycle and alternative phosphoserine shuttle

Most of the large, colorless SOB live in oxygen depleted habitats, so the formation of 2-phosphoglycolate (2-PG) by the oxygenase activity of the RubisCO that acts inhibitory for CO_2 fixation (Bauwe *et al.*, 2012), might play a minor role. Nevertheless, an active 2-PG metabolism (C2-cycle) to convert 2-PG and shuffle it back into the calvin cycle, has been demonstrated for unicellular cyanobacterium *Synechocystis* sp. strain PCC 6803 (Eisenhut *et al.*, 2008). This cycle is well known as photorespiratory by higher plants and believed to be evolutionary obtained by the endosymbiosis of a cyanobacterial ancestor (Kern *et al.*, 2013). Other earlier observations in the serine biosynthesis pathway of the methanotrophic *Methylococcus capsulatus* (Bath), proposed a similar pathway to the C2-cycle of higher plants (Taylor *et al.*, 1981; Ward *et al.*, 2004). Moreover, accumulation of glycolate under high O_2 concentration have been attributed to a chemorespiratory in chemoautotrophic bacteria similar to photorespiratory in plants, algae and cyanobacteria (Bowien and Schlegel, 1981). Hence, an active oxygenase activity of the RubisCO from chemoautotrophic bacteria can be expected.

The genome of "*Ca.* T. nelsonii" encoded for an almost complete set of genes, which is involved in the C2-cycle (Fig. 4), with key enzymes such as 2-phosphoglycolate phosphatase (*gph*), glycolate oxidase (*glcDEF*) and hydroxypyruvate reductase (*ttuD*) (Table S4). It is most likely that the RubisCO of "*Ca*. T. nelsonii" produce 2-PG under oxic conditions. However, the genome lacked a glycerate kinase of the class III (GLYK) (Table S4), which is essential to produce D-3-phosphogylcerate (3-PG) that is shuffled back into the

CBB-cycle. The produced organic carbon is not lost for the cells and an inhibition of the CBB-cycle by accumulation of 2-PG is prevented. Homolog genes were found in all other large, colorless SOB, with the exception of the orange *Beggiatoa* filament BOGUAY, which lacks a glycolate oxidase (Table S4). Besides this *B. alba* B18LD, *Beggiatoa* sp. strain Flor36 and the orange *Beggiatoa* filament BOGUAY did not encode for a serine-pyruvate aminotransferase, which converts serine and glyoxylate to hydroxypyruvate and glycine. Nevertheless, they encoded for aminotransferases class V that belong to the same subfamily as serine-pyruvate aminotransferases. This subfamily has same mechanistic features and high sequence identities.

Strikingly, all genomes also contained multiple copies of serine/ threonine kinase (STPK), which are involved in the phosphorylation of serine and play an important role in the signal transduction (Pereira *et al.*, 2011). If the produced serine in the C2-cycle can be phosphorylated by STPK, phosphoserine can be further converted by the gene phosphoserine aminotransferases (*serC*) producing 3-phospho-hydroxypyruvate. Another possible enzyme for the phosphorylation of serine is a phosphoserine phosphatase (*serB*). The produced 3-phospho-hydroxypyruvate by *serC* can be converted directly to 3-phospho-D-glycerate by the D-3-phosphoglycerate dehydrogenase (*serA*). Indeed the genomes of "*Ca.* T. nelsonii", "*Ca.* I. divolgata" and *B. alba* B18LD contained homologous genes for these enzymes, while "*Ca.* I. divolgata" lacked *serB*, whereas *B. alba* B18LD lacked *serA*. So it is possible, that they uses an alternative pathway to shuffle back the produced serine in the C2-cycle and therefore do not need a glycerate kinase (Fig. 4 and Table S4). While they still have the hydroxypyruvate reductase it is not clear, whether the incompleteness of the genomes led to no detection of the necessary glycerate kinase type III. Only recently it has been proved that a mutant of the cyanobacterium *Synchocystis* sp. strain PCC 6803, which has an inactivation in the same serine/ threonine kinase (STPK) that occur in large, colorless SOB, is impaired in growing under low inorganic carbon conditions (Laurent *et al.*, 2008). This behavior could be induced by a higher oxygenase activity of the RubisCO and therefore a higher production of 2-PG inhibiting the CBB-cycle. While *Synchocystis* sp. Strain PCC 6803 is know to express all genes involved in the C2-cycle (Eisenhut *et al.*, 2008) the genome also have a full set of the proposed alternative pathway via STPK, *serC* and *serA* (Fig. 4) (Kaneko *et al.*, 1996). Perhaps cyanobacteria and large, colorless SOB use the alternative pathways to convert 2-PG under specific environmental conditions. Physiological experiments are necessary to elucidate the occurrence and usage of the alternative pathway (phosphoserine shuttle).

Reductive tricarboxylic acid cycle with acetyl-CoA reduction

Besides the key enzyme citrate lyase in "*Ca.* T. nelsonii" and the orange *Beggiatoa* filament BOGUAY, we found unique genes for the rTCA such as 2-oxoglutarate:ferredoxin oxidoreductase (*korAB*) and the gene of the fumarate reductase large subunit (*frdA*). These genes were encoded on the genomes of "*Ca.* T. nelsonii", "*Ca.* I. divolgata" and orange *Beggiatoa* filament BOGUAY. The "*Ca.* T. nelsonii" genome also carried genes that further converts the produced acetyl-CoA of the ATP citrate lyase to fix two more molecules CO_2 (Evans *et al.*, 1966) (Table S4). The genes involved in this fixation are pyruvate:ferredoxin oxidoreductase (*porABGD*), phosphoenolpyruvate synthase (*ppsA*), and ATP-dependent phosphenolpyruvate carboxykinase (*pckA*). The latter have been demonstrated to occur in anaerobic green sulfur bacteria (Tang *et al.*, 2010). Besides "*Ca.* T. nelsonii" only the orange *Beggiatoa* filament BOGUAY had the same set of genes, and also encoded for a citrate lyase (Table S4), while a functional rTCA in "*Ca.* I. divolgata" is unclear due to the lack of ATP citrate lyase.

Variation in the genes of oxidative phosphorylation

Non-photosynthetic SOB are known to couple the oxidation of inorganic sulfur compounds or organic carbon (e.g. acetate) with the electron transport of oxidative phosphorylation to produce a proton motive force for energy production in the form of ATP. This has been shown for freshwater and marine *Beggiatoa* strains (Strohl *et al.*, 1986; Prince *et al.*, 1988).

Genes for all five complexes of the respiratory chain have been found in the genome of "*Ca.* T. nelsonii" and all other large, colorless SOB (Table S5). They shared similar enzymes for the four complexes. All genomes encoded for the NADH dehydrogenase I (*nouABCDEFGHIJKLMN*), which are organized in several operons, with the exception of "*Ca*. T. nelsonii", which missed the genes *nouABC* and *Beggiatoa* sp. strain 35Flor that missed the gene *nouE* (Table S5). The membrane-associated succinate dehydrogenase complex II (*sdhABCD*) were found in all genomes, while homologs for the membrane anchor (*sdhD*) could not been detected in "*Ca.* T. nelsonii" and the orange *Beggiatoa* filament BOGUAY. The third complex were encoded by genes for the ubiquinol-cytochrome c reductase and showed a similar operon (*petABC*) in all genomes, with exception of "*Ca.* I. divolgata" where the *petC* gene was located on a different contig than *petAB* genes (Table S5). Several different complexes IV were found in the genomes, while the cytochrome c oxidase cbb3-type (*ccoNOQP*) is found in all genomes (Table S5), we only detected the cytochrome c

oxidase aa3-type (*coxCBA*) in the genomes of "*Ca.* T. nelsonii" and "*Ca.* I. divolgata" (Table S5). This was unexpected since the activity of a cytochrome c oxidase aa3-type has been reported for the freshwater strain *Beggiatoa leptomitiformis* D-402 (Muntyan *et al.*, 2005). In the genome of *B. alba* B18LD and the orange *Beggiatoa* filament BOGUAY we found a third complex, a cytochrome d ubiquinol oxidase (*cydAB*) (Table S5). The different cytochrome c oxidases have been proven to be adapted to specific oxygen concentrations (Muntyan *et al.*, 2005). All genomes encoded for F-type ATPase (*atpCDGAHFEB*), while we only found homolog genes for a second V-type ATPase (*ntpABCDEFGHIK*) in all marine SOB (Table S5). Both ATPase are known to transfer protons and sodium ions from the periplasm into the cytoplasma and produce ATP (Mulkidjanian *et al.*, 2007). The V-type ATPase which is a vacuolar ATPase has been demonstrated to be involved in energy conservation over the vacuole membrane with nitrate as electron acceptor in "*Ca.* Allobeggiatoa" (Beutler *et al.*, 2012).

Flavin-based electron bifurcation (FBEB)

Heterodisulfide reductase has been detected in genomes of methanogens, methanotrophs and sulfate-reducing bacteria, which are microorganisms that sometimes live under energy limiting conditions. Physiological experiments have shown that the coding genes are involved in energy metabolism. In methanogens without cytochromes they build up multi-enzyme complexes, which consist of a heterodisulfide reductase subunit *hdrABC* coupled to a methyl viologen-reducing hydrogenase *mvhADG*-complex. This complex reduce the coenzyme M/coenzyme B complex (CoM-S-S-CoB) in the methanogenesis (Thauer *et al.*, 2008). However, the complex also exist in methanotrophic archaea (ANME) mediating the anaerobic oxidation of methane (AOM) and are proposed to oxidize the CoM-SH and CoB-SH in the reverse methanogenesis or could also be coupled to sulfate reduction (Meyerdierks *et al.*, 2005). Moreover, the same complex is present in deltaproteobacterial sulfate- and metal-reducing bacteria (Haveman *et al.*, 2003; Methé *et al.*, 2003).

In the geonome of "*Ca.* T. nelsonii" heterodisulfide reductases genes (*hdrDEF*) were detected which have high sequence identity values to *Geobacter spp*. and are organized in a similar operon (Fig. S2 and Table S6). *HdrDE* genes are known from methanogens with cytochromes, where this membrane-bound enzymes together with a hydrogenase (*vhoACG*) reduce the CoM-S-S-CoB complex similar to methanogens without cytochrome (Thauer *et al.*, 2008). Unusual none of the two enzymes showed transmembrane domains, but both had two typical iron-sulfur binding sites ($CX_2CX_2CX_3C$) and a heme binding site (CX_2CH) on the

hdrE. This pattern is similar to the sequences of *Geobacter* spp. genes (Childers *et al.*, 2002; Methé *et al.*, 2003; Aklujkar *et al.*, 2010) (data not shown). The function of the *hdrF* gen that encodes for a heterodisulfide oxidoreductase with a NAD(P)H subunit is unclear. The same sequence identity and operon structure to *Geobacter* spp. of the *hdrDEF* genes was also found in the genome of the orange *Beggiatoa* filament BOGUAY, while upstream of the complex a methyl viologen-reducing hydrogenase delta subunit (*mvhD*) together with two genes that encoded for the heterodisulfide reductase alpha subunit (*hdrA*) were located (Fig. S2 and Table S6). Interestingly, upstream of the *hdrA* genes a fumarate reductase/succinate dehydrogenase (*fdrA*/ *sdhA*) was located, which might be a coupling to membrane-bound electron transport. The latter was also found in the genome of "*Ca.* T. nelsonii" (Fig. 4).

The *mvh* of "*Ca.* T. nelsonii" was organized in an operon, which resembled again sequence idetnitiy and operon structure appearing in the genomes of *Geobacter* spp., (Childers *et al.*, 2002; Methé *et al.*, 2003; Aklujkar *et al.*, 2010). This could be caused by horizontal gene transfer of metabolic islands, as shown in sulfate-reducing bacteria (SRB) (Mußmann *et al.*, 2005). The operon did not encode for *hdr*-like genes like in SRB (Fig. S3) (Strittmatter *et al.*, 2009), which indicates a decoupling of the heterodisulfide reductases and hydrogenases in large, colorless SOB. The function of such an decoupled complex in SOB is unclear, but there are evidence that the heterodisulfide reductase are involved in sulfur oxidation, while they were up-regulated in the proteom of the sulfur oxidizing endosymbiont "*Ca.* Endoriftia persephone" under sulfur-rich conditions (Markert *et al.*, 2007). If the Hdr still form a complex with Mvh like in sulfate reducers, they could be involved in sulfide oxidation via a reverse form of the proposed dithiol-cycle in sulfate reducers (Strittmatter *et al.*, 2009).

The FAD-containing iron-sulfur protein *hdrA* is of special interest. It was proposed to use ferredoxin as electron acceptor and can be coupled to a ferredoxin-oxidizing Na^+-translocating membrane complex in a so called flavin-based electron bifurcation (FBEB) for energy conservation under anaerobic conditions (Buckel and Thauer, 2013). Strikingly, all genomes of the large, colorless SOB have genes for a full RnfABCDGE-complex which oxidizes ferredoxin and reduce NAD^+ (Biegel *et al.*, 2011) (Fig. S4 and Table S5). Therefore a FBEB process could be used by "*Ca.* T. nelsonii" under long-term anoxic conditions in sulfidic waters or during migration of "*Ca.* I. divolgata" and the orange *Beggiatoa* filament BOGUAY into deeper anoxic sediment layers, when their internal electron acceptor nitrate is used up.

The genome of "*Ca.* T. nelsonii" also contained other periplasmic hydrogenase involved in energy metabolism. The periplasmic-located iron-dependent hydrogenase (*hydAB*) was found in SRB and are up-regulated during ethanol oxidation in *Desulovibrio vulgaris* Hildenborough (Haveman *et al.*, 2003). In SRB they are proposed to be involved in hydrogen cycling between the cytoplasma and periplasma, whereby the alcohol dehydrogenase (*adh*) transfer hydrogen to the Hdr:Mvh-complex which produces dihydrogen. Dihydrogen is further transferred by a yet unidentified membrane complex directly to the periplasmic hydrogenase *hydAB* converting it back to protons, which produces a proton motive force (Haveman *et al.*, 2003). Thus a coupling of FBEB and hydrogen cycling would result in the higher proton/Na^+ ion motive force (Fig. S4). Interestingly, we also found an ORF (THI1260_0) encoding for an *adh* in the genome of "*Ca*. T. nelsonii", so an alcohol oxidation coupled to FBEB might be possible. Homologs for both *hydAB* and *adh* genes are not found in any other genome of the large, colorless SOB (Fig. S3 and Table S5).

Intracellular storage compounds

Large, colorless SOB are known to feature different storage capacities for organic and inorganic compounds such as sulfur, phosphorous, nitrate, and polyhydroxyalkanoates. If cells are large enough and have a central vacuole, they highly accumulate nitrate (Fossing *et al.*, 1995; McHatton *et al.*, 1996; Schulz *et al.*, 1999).

In the two genomes "*Ca.* T. nelsonii" and "*Ca.* I. divolgata" we found nitrate/nitrite transporters, cytochrome c oxidases, v-type ATPases, and cytochrome c, that could be involved in energy conservation via a proton motive force over the vacuole membrane like in "*Ca.* Allobeggiatoa" (Beutler *et al.*, 2012).

In all analyzed genomes we found phosphate specific transporter (*pst*) of the *pstSCABphoU* operon, which together with the polyphosphate synthesizing enzyme polyphosphate kinase (*ppk*) are part of the well described Pho-regulon (Vershinina and Znamenskaya, 2002) (Fig. 1 and Table S7). The inorganic phosphate uptake by the ATP-dependent Pst of the cytoplasmic membrane are transcriptional regulated by the two-component system *phoR-phoB*. The *phoB* that transcriptionally regulates the phosphate regulon could only be detected in the orange *Beggiatoa* filament BOGUAY, while the phosphor sensor regulon protein *phoR* were found in all other investigated genomes (Table S7). The genomes of "*Ca.* T. nelsonii", "*Ca.* I. divolgata" and the orange *Beggiatoa* filament BOGUAY also contained homologous genes to an outer membrane porine O and P (*phoE*) specific for uptake of orthophosphate and polyphosphate, respectively (Vershinina and

Znamenskaya, 2002) (Table S7). All of these genes are highly up regulated in microorganisms under phosphate limiting conditions, and are responsible for inorganic phosphate accumulation (Vershinina and Znamenskaya, 2002). The accumulation and storeage of polyphosphate in *T. namibiensis* and *Beggiatoa* sp. strain 35Flor was visualized by granules in their periplasma (Schulz and Schulz, 2005; Brock and Schulz-Vogt, 2011).

Besides the storage and accumulation of inorganic compounds, *Beggiatoa* store polyhydroxyalkanotes (PHA) in granules in their periplasma, most often in the form of polyhydroxybutyrate (PHB) (Pringsheim, 1964; Strohl and Larkin, 1978). Genes involved in the synthesis of polyhydroxybutyrate (PHB) were only found in the genomes of *B. alba* B18LD and *Beggiatoa* sp. strain 35Flor that also have the glyoxylate bypass to use acetate as a carbon source (Fig. 1 and Table S7).

Supporting Tables:

Table S1: Oligonucleotides used in this study

name	sequence 3'-5'	target gene	annealing T [°C]	Position[a]	combination	expected product size [bp]	reference
GM3F	AGA GTT TGA TCM TGG C	16S rRNA	48	8 - 23	GM4R	2350	(Muyzer *et al.*, 1995)
GM4R	TAC CTT GTT ACG ACT T	16S rRNA	48	1492 - 1507	GM3F	2350	(Muyzer *et al.*, 1995)
					1099R	1280	
GM5F	CCT ACG GGA GGC AGC AG	16S rRNA	55	341 - 357	907RM	550	(Muyzer *et al.*, 1995)
1099F	GYA ACG AGC GCA ACC C	16S rRNA	50	1099 - 1114	GM4R	400	(Wilmotte *et al.*, 1993)
907RM	CCG TCA ATT CMT TTG AGT TT	16S rRNA	55	907 - 927	GM5F	550	(Muyzer *et al.*, 1995)
recA_F	TNG ARA THT AYG GIC CIG ART C	*recA*[b]	55	-	recA_R	560	(Dale *et al.*, 2003)
recA_R	ACN ACY TTN ACI CGI GTY TCR CT	*recA*[b]	55	-	recA_F	560	(Dale *et al.*, 2003)
AprA-1-FW	TGG CAG ATC ATG ATY MAY GG	*aprA*[c]	50	1236 – 1256[d]	AprA-5-RV	400	(Meyer and Kuever, 2007)
AprA-5-RV	GCG CCA ACY GGR CCR TA	*aprA*[c]	50	1615 – 1631[d]	AprA-1-FW	400	(Meyer and Kuever, 2007)
ITS350F	AAT TAG GAA GCT GAT GTA AA	ITS		-	Gam42aR	1200	(Salman, 2011)
Gam42aR	GCC TTC CCA CAT CGT TTC C	23S rRNA		1027 - 1043	ITS350F	1200	(Manz *et al.*, 1992)

[a] corresponding nucleotide positions of the 16S rRNA of *Escherichia coli* according to (Brosius *et al.*, 1978)
[b] *recA* - recombinase protein involved in DNA repair, single copy gene
[c] *aprA* – dissimilatory adenosine-5'-phosposulfate reductase, involved in sulfite oxidation
[d] corresponding nucleotide positions of the aprBA operon of *Desulfovibrio vulgaris* subsp. *vulgaris* strain Hildenborough (GenBank accession no. Z69372).
[e] ITS – intergenic spacer region between 16S rRNA and 23S rRNA

Table S2: Nitrogen metabolism of *Candidatus* Thiomargarita nelsonii compared to other large, colorless SOB

product	gene	locus	E.C.	contig	AA	truncated	full	other large, colorless SOB	comment
Membrane-bound cytoplasmic nitrate reductase									
nitrate reductase, alpha subunit	*narG*	THI2233_0 THI39_2	1.7.99.4	THI2233 THI39	261 31	+ 		BOGUAY_0051 BOGUAY_0489 BGP_0139 BGP_3372 BGP_5024	
nitrate reductase, beta subunit	*narH*	THI39_1 THI713_1	1.7.99.4	THI39 THI713	497 394	+ +	+ 	BOGUAY_0490 BOGUAY_0049 BGP_4035 BGP_4784	
nitrate reductase, delta subunit	*narJ*	THI39	1.7.99.4	THI39	173		+	BOGUAY_0491 BGP_4033	molybdenum cofactor assembly chaperone
nitrate reductase, gamma subunit	*narI*	THI21821642981 THI3912301888	1.7.99.4	THI2182 THI39	213 75	+ +		BA07_32 BOGUAY_0492 BOGUAY_1505 BGP_2700	
nitrate reductase-like protein	*narX*	THI762_2 THI922_0	1.7.99.4	THI762 THI922	259 552	+ +		BOGUAY_0048 BOGUY_0146	
nitrate/ nitrite transporter	*narK*	THI3014□f2		THI3014	204	+		BGP_3802	
Periplasmic nitrate reductase									
nitrate reductase, periplasmatic, large subunit	*napA*	THI153 THI1149	1.7.99.4	THI153 THI1149	835 417	+ +	+ 	BA14_107 BOGUAY_0671 BGP_1198	
nitrate reductase, small subunit	*napB*	THI28521118749	1.7.99.4	THI2852	38	+		BA14_110 BOGUAY_0672 BGP_1425	

product	gene	locus	E.C.	contig	AA	truncated	full	other large, colorless SOB	comment
nitrate reductase cytochrome c-type protein	*napC*	THI214_0	1.7.99.4	THI214	222		+	BA14_111 BOGUAY_3233 BGP_1197 FLOR_01446	
nitrate reductase, ferredoxin-type potein	*napH*	THI25_1	1.7.99.4	THI25	315	+			
nitrate reductase, ferredoxin-type potein	*napG*	THI153_0 THI485_1	1.7.99.4	THI153 THI485	254 247		+	BA14_108	
nitrate reductase, periplasmatic	*napD*		1.7.99.4					BA14_106 BGP_1199	
nitrate reductase, ferredoxin-type potein	*napF*		1.7.99.4					BA14_105 BOGUAY_5179 BGP_1200	
nitrate reductase, large subunit	*nasA*	THI2051	1.7.99.4	THI2051	285	+		BA07_47	assimilatory nitrate reduction to ammonia
Cytoplasmic assimilatory/ dissimilatory nitrite reductase									
nitrite reductase, NAD(P)H large subunit	*nirB*	THI1112_0 THI111216991119 THI1573112241393	1.7.1.4	THI1112 THI1573	216 232 407	+		BA07_49	dissimilatory nitrate reduction to ammonia as well as assimilatory
nitrite reductase, NAD(P)H small subunit	*nirD*		1.7.1.4					BA07_48	dissimilatory nitrate reduction to ammonia as well as assimilatory

product	gene	locus	E.C.	contig	AA	truncated	full	other large, colorless SOB	comment
nitrite reductase, ferredoxin	*nirA*		1.7.7.1					FLOR_00816	dissimilatory nitrate reduction to ammonia as well as assimilatory
Periplasmic disimilatory nitrite reductase									
nitrite reductase cytochrome cd1	*nirS*	THI245_1	1.7.2.1 1.7.99.1	THI245	591		+	BGP_1272 BOGUAY_2967	involved in denitrification
nitrite reductase, cytochrome c55X	*nirC*	THI245_0	1.7.2.1 1.7.99.1	THI245	107	+		BGP_1371	
nitrite reductase, cytochrome cd1	*nirF*	THI24519191429 THI303211221068	1.7.2.1 1.7.99.1	THI245 THI3032	305 39	+		BGP_1372	
nitrite reductase heme biosynthesis G protein	*nirG*	THI471_3	1.7.2.1 1.7.99.1	THI471	147		+	BGP_1275	
nitrite reductase heme biosynthesis H protein	*nirH*		1.7.2.1 1.7.99.1					BGP_4270	
nitrite reductase heme biosynthesis J protein	*nirJ*	THI2061_0	1.7.2.1 1.7.99.1	THI2061	261		+	BGP_3921 BGP_4010	
nitrite reductase heme biosynthesis E protein	*nirE*		1.7.2.1 1.7.99.1						
nitrite reductase heme biosynthesis N protein	*nirN*	THI762_0	1.7.2.1 1.7.99.1	THI762	94	+			
Membrane-bound nitric oxide reductase									
nitric oxide reductase	*norB*	THI459_4 THI692_1	1.7.99.7	THI459 THI692	111		+	BOGUAY_0863 BGP_3622 BGP_5178	
nitric oxide reductase	*norC*	THI166412121441	1.7.99.7	THI1664	69	+		BOGUAY_0144 BOGUAY_4015 BGP_5602	

product	gene	locus	E.C.	contig	AA	truncated	full	other large, colorless SOB	comment
nitric oxide activation protein	*norQ*	THI459_1 THI69217431595	1.7.99.7	THI459 THI692	267 246	+	+	BA08_50 BGP_2171 BGP_2329 FLOR_01410 FLOR_02605	
nitric oxide activation protein	*norD*	THI217_1 THI806_0	1.7.99.7	THI127 THI806	644 537		+	BA16_151 BGP_5686 FLOR_00559 FLOR_00821	
nitric oxide activation protein	*norE*	THI459_3	1.7.99.7	THI459	192		+		
Periplasmic nitrous oxide reductase									
nitrous oxide reductase	*nosZ*	THI2864|f2	1.7.99.6	THI2864	218	+			
nitrous oxide reductase accesor protein	*nosD*	THI485_0	1.7.99.6	THI485	406		+		
Other genes involved in nitrogen metabolism									
nitric oxide dioxygenase	*hmp*	THI2464_0 THI353514351023 THI438_2	1.14.12.17	THI2464 THI3535 THI438	194 144 149	+ +		BA06_78 FLOR_02537	
glutamine synthetase	*glnA*	THI10531707618	6.3.1.2	THI1053	234	+		BA02_247 BA17_158 BGP_4113 BGP_4114 BOGUAY_0161 FLOR_03203	
ammonium transporter	*amt*	THI670_1		THI670	136			BA16_117 BA16_118 BOGUAY_3555 BGP1735 FLOR_02001 FLOR_02712	

Table S3: Sulfur metabolism of *Candidatus* Thiomargarita nelsonii compared to other large, colorless SOB

product	gene	locus	E.C.	contig	AA	truncated	full	other large, colorless SOB	comment
Sulfide oxidation									
sufide:quinone oxidoreductase	*sqr*	THI190_0	1.8.5.4	THI190	373		+	BA07_67 BA16_158 BGP_0667 BOGUAY_0181 BOGUAY_2390 FLOR_01938	
flavocytochrome c sulfide dehydrogenase, cytochrome c subunit	*fccA*	THI1301_0 THI36_7 THI712_2	1.8.2.3	THI1301 THI36 THI712	218 165 198	+	+	BGP_4977 BOGUAY_2852 BOGUAY_3988 FLOR_01512	
flavocytochrome c sulfide dehydrogenase, flavoprotein subunit	*fccB*	THI35_6 THI454_0 THI526_0 THI143717651827	1.8.2.3	THI35 THI454 THI526 THI1437	425 210 217 254	+	+	BGB_0124 BGP_4976 BOGUAY_2853 BOGUAY_3987 FLOR_01513	
Sulfur oxidation via reverse dissimilatory sulfite reduction									
dissimilatory sulfite reductase, alpha subunit	*dsrA*		1.8.99.1					BGP_6219 BGP_6220 BGP_6501 BOGUAY_1511 FLOR_02859 FLOR_01613	
dissimilatory sulfite reductase, beta subunit	*dsrB*	THI1794_0	1.8.99.1	THI1794	209	+		BGP_4858 BOGUAY_1510 FLOR_02585	
dissimilatory sulfite reductase, gamma subunit	*dsrC*/ *dsrC*-like	THI1718_0 THI348_2 THI40_4 THI2578139828	1.8.99.1	THI1718 THI348 THI40 THI2578	110 117 114 131	+		BA07_33 BGP_1169 BOGUAY_1506 FLOR_02854	dsr-like protein no ORFs of dsrC gene

product	gene	locus	E.C.	contig	AA	truncated	full	other large, colorless SOB	comment
	dsrE	THI3100487597478 THI33331369909		THI3100 THI3333	36 138	+		BA07_36 BGP_6597 BOGUAY_1509 FLOR_02857	
	dsrF							BA07_35 BGP_1172 BOGUAY_1508 FLOR_02856	
	dsrH							BA07_34 BGP_1170 BOGUAY_1507 FLOR_02855	
	dsrM	THI21821642981		THI2182	213	+		BA07_32 BGP_0409 BOGUAY_1505 FLOR_02853	
	dsrK	THI2182652907892 THI1139_0		THI2182 THI1139	84 44	+		BA01 (orf243_glimmer3) BGP_4599 BOGUAY_1504 FLOR_02852	
	dsrL	THI1139_2		THI1139	238	+		BGP_4600 BOGUAY3227 FLOR_02849	
	dsrJ							BA01 (orf244_glimmer3) BGP_4601 BOGUAY_1503 FLOR_02848	
	dsrO							BGP_4603 BGP_4604 BOGUAY_1503 FLOR_02847	

product	gene	locus	E.C.	contig	AA	truncated	full	other large, colorless SOB	comment
	dsrP							BGP_4605 BOGUAY_1500 FLOR_02846	
	dsrN							BGP_5248 FLOR_00351	
	dsrS	THI220_0		THI220	138	+		BGP_1012 FLOR_02633	
	dsrR							BGP_1732 FLOR_00352	
Sulfite oxidation									
APS reductase, alpha subunit	*aprA*	THI29_0	1.8.99.2	THI29	104	+		BGP_5623 BGP_5624 BOGUAY_2553	
APS reductase, beta subunit	*aprB*		1.8.99.2					BGP_5858 BOGUAY_2554	
sulfate adenylyltransferase	*sat*	THI2760_1 THI29375596391540	2.7.7.4	THI2760 THI2937	35 26	+		BGP_6163 BOGUAY_2370 FLOR_01554	
alkaline serine protease	*aprM*	THI3143□r1	3.4.21.-	THI3143	195	+			
SOX system									
SOX enzyme complex, subunit B	*soxB*	THI13761462477		THI1376	186			BGP_2304 BOGUAY_1092 FLOR_02744	thiosulfate oxidation
SOX enzyme complex, subunit Y	*soxY*	THI32931297475		THI3293	98			BA14_48 BGP_4779 BOGUAY_0115 FLOR_02368	thiosulfate oxidation
SOX enzyme complex, subunit AX	*soxAX*							BA17_207 BGP_5667 FLOR_03004	thiosulfate oxidation

product	gene	locus	E.C.	contig	AA	truncated	full	other large, colorless SOB	comment
SOX enzyme complex, subunit Z	*soxZ*							BA02_173 BA16_10 BA14_49 BGP_4779 BGP_4778 BOGUAY_0116 FLOR_02369	thiosulfate oxidation
Thiosulfate disproportionation									
thiosulfate sulfurtransferase, rhodanese	*tst*	THI213_0 THI29621557562	2.8.1.1	THI213 THI2962	186 184	+		BA02_312 BA09_105 BGP_3637 BOGUAY_2819 BOGUAY_1655	
Sulfate uptake system and assimilatory sulfate reduction									
sulfate permease, high affinity transporter	SuIP	THI276_2 THI335610454655		THI276 THI3356	80 146	+		BOGUAY_3672 BGP_2594 BGP_3542 FLOR_00582	
sulfate transporter, periplasmic binding protein	*sbp*							BA19_56 FLOR_01671	
sulfate ABC transporter, ATPase subunit	*cysA*							BA19_59 FLOR_00092	
sulfate ABC transporter, permease protein	*cysW*							BA19_58	
sulfate ABC transporter, permease protein	*cysT*							BA19_57	
adenylylsulfate kinase	*cysC*	THI1582_0	2.7.1.25	THI1582	+			BA02_231 BOGUAY_3365 FLOR_01349	
sulfate adenylyltransferase, large subunit	*cysN*		2.7.7.4					BA05_102	

product	gene	locus	E.C.	contig	AA	truncated	full	other large, colorless SOB	comment
sulfate adenylyltransferase, small subunit	*cysD*		2.7.7.4					BA05_101	
putative 3´-adenylylsulfate reductase	*cysH*		1.8.4.8					BA01 (orf301_glimmer3) FLOR_03186	
sulfite reductase, NADPH flavoprotein subunit	*cysJ*		1.8.1.2					BA06_137	
sulfite reductase, NADPH hemeprotein subunit	*cysI*		1.8.1.2					BA06_138 FLOR_03184	

Table S4: Carbon metabolism and carbon fixation in *Candidatus* Thiomargarita nelsonii compared to other large, colorless SOB

product	gene	locus	E.C.	contig	AA	truncated	full	other large, colorless SOB	comment
Glycolysis									
glucokinase	*glk*		2.7.1.2					BA19_147 BGP_0972 FLOR_02979	
polyphosphate glucokinase	*ppgk*	THI122_0	2.7.1.63	THI122	120	+		BGP_0205 BOGUAY_0012	
glucose-6-phosphate isomerase	*pgi*		5.1.3.9					BA07_114 BOGUAY_0259 BGP_3455 FLOR_03544 FLOR_03085	
6-phosphofructokinase, pyrophosphate dependent	*pfk*	THI71517826	2.7.1.11	THI715	259	+		BA15_115 BOGUAY_3135 BOGUAY_1318 BGP_4425 FLOR_02042	
bisphosphate aldolase A	*fbaA*		4.1.2.13					BA05_255 BOGUAY_1000 BGP_5969 FLOR_00835	
bisphosphate aldolase B	*fbaB*	THI3055|r2	4.1.2.13	THI3055	200	+			
glyceraldehyde-3-phosphate dehydrogenase	*gap*	THI10719461625106 1	1.2.1.12	THI1071	225	+		BA06_20 BOGIAY_2720 BGP_2190 BGP4586 FLOR_03217	

product	gene	locus	E.C.	contig	AA	truncated	full	other large, colorless SOB	comment
phosphoglycerate kinase	*pgk*	THI399_0 THI60216681202	2.7.2.3	THI399 THI602	138 221	+		BA02_240 BOGUAY_0998 BOGUAY_0999 BGP_4102 FLOR_00204	
phosphoglycerate mutase	*gpmA*	THI305_0	5.4.2.1	THI305	248		+	BA08_57 BA09_158 BA17_114 BOGUAY_1652 BOGUAY_0714 BGP_0770 BGP_0964 BGP_2533 FLOR_00744 FLOR_01466 FLOR_02612	
enolase	*eno*	THI17581197300 THI3523□r2	4.2.1.11	THI1758 THI3523	64 171	+		BA09_212 BOGUAY_3393 FLOR_02427	
pyruvate kinase	*pyk*	THI399_1	2.7.1.40	THI399	478		+	BA05_256 BGP_5856 FLOR_00836	
pyruvate dehydrogenase E1 component	*aceE*	THI1750_1 THI409125921151	1.2.4.1	THI1750 THI409	50 863	+	+	BA05_52 BGP2645 FLOR_02028	
dihydrolipoamide acetyltransferase E2 component	*aceF/ pdhC*	THI624_0	2.3.1.12	THI624	357	+		BA05_51 BGP_2646 FLOR_02029	
pyruvate dehydrogenase E1 component, alpha subunit	*pdhA*	THI32651477104	1.2.4.1	THI3265	158	+		BOGUAY_4507 BOGUAY_4468 BOGUAY_4738 BGP_1305	

product	gene	locus	E.C.	contig	AA	truncated	full	other large, colorless SOB	comment
pyruvate dehydrogenase E1 component, beta subunit	*pdhB*	THI3214⍰r2	1.2.4.1	THI3214	190	+		BOGUAY_4506 BOGUAY_4469 BGP_1304	
dihydrolipoamide dehydrogenase	*pdhD*	THI488_0 THI25811705778	1.8.1.4	THI488 THI2581	471 234			BA01 (orf126_glimmer3) BA17_328 BOGUAY_0563 BOGUAY_0328 BGP_0643 BGP_0644 BGP_4455 FLOR_01022 FLOR_03223	
Tricarboxylic acid cycle									
citrate synthase (type I and II)	*gltA*	THI2494 | f3	2.3.3.1	THI2494	255	+		BOGUAY_4141 (typeI) BGP_3693 (type II) BGP4913 (type II) FLOR02625 (type II) BA15_114 (type II)	
aconitate hydratase I and II	*acnA/ acnB*	THI85121501027 (acnB)	4.2.1.3	contig00002	715	+		BA05_79 (acnB) BA18_22 (acnA) BOGUAY_3060 (acnB) BGP4006 (acnB) FLOR_01010 (acnB) FLOR_02559 (acnA)	
isocitrate dehydrogenase	*icd*	THI78_3	1.1.1.42	THI78	227	+		BA09_306 BOGUAY_2441 FLOR_01072	
2-oxoglutarate dehydrogenase E1	*sucA*	THI521_4 THI1836 | r2 THI3420 | r1	1.2.4.2	THI521 THI1836 THI3402	213 360 178	+		BA17_326 BGP_4352 FLOR_01020	
dihydrolipoyl succinyl transferase E2	*sucB*	THI477_0	2.3.1.61	THi477	266	+		BA17_327 BGP_4350 FLOR_01021 FLOR_02029	

product	gene	locus	E.C.	contig	AA	truncated	full	other large, colorless SOB	comment
dihydrolipoyl dehydrogenase E3	*lpd*	THI488_0 THI25811705778	1.8.1.4	THI488 THI2681	471 234		+	BA01(orf126_glimmer3) BA17_328 BOGUAY_0563 BOGUAY_0328 BGP_0644 FLOR_01022	
succinyl-CoA synthetase, beta subunit	*sucC*	THI32_9	6.2.1.5	THI2418	283	+		BA06_38 BGP_0418 BOGUAY_1109 FLOR_00929	
Succinyl_CoA synthetase, alpha subunit	*sucD*	THI20821353706	6.2.1.5	THI2082	116	+		BA06_39 BGP_0419 BOGUAY_1109 FLOR_00930	
succinate dehydrogenase, flavoprotein subunit	*sdhA*	THI1107_1 THI1196_1 THI28471211210	1.3.5.1	THI1107 THI1196 THI2847	219 353 69	+		BA12_129 BOGUAY_0963 BGP_0843 BGP_0844 BGP_2544 FLOR_03153	
succinate dehydrogenaseiron-sulfur subunit	*sdhB*	THI1107_0 THI11071158159014 31	1.3.5.1	THI1107	128 143	+		BA12_130 BOGUAY_0707 BGP_1918 BGP_3026 BGP_5022 FLOR_03154	
succinate dehydrogenase, cytochrome b556 subunit	*sdhC*	THI39_4	1.3.5.1	THI39	293	+		BA12_127 BOGUAY_4609 BGP_2542 BGP_3027 BGP_3589 BGP_1067 FLOR_03151	

product	gene	locus	E.C.	contig	AA	truncated	full	other large, colorless SOB	comment
succinate dehydrogenase, membrane anchor	*sdhD*		1.3.5.1					BA12_128 BGP_2543 FLOR_03152	
fumarate hydratase	*fumAB*	THI146_2	4.2.1.2	THI146	505		+	BA05_146 BOGUAY_1148 BGP_4244 FLOR_02976	
malate dehydrogenase	*mdh*	THI497_0	1.1.1.37	THI497	325		+	BA17_325 BOGUAY_0329 FLOR_03183	
Reductive ricarbolxyic acid cycle									
ATP-citrate lyase	*aclA*	THI447_1	2.3.8.8	THI447	422		+	BOGUAY_3507 BOGUAY_3508	
citryl-CoA lyase, alpha subunit	*citF*								
citryl-CoA lyase, beta subunit	*citE*							BA09_64 FLOR_02468	
fumarate reductase, flavocytochrome C	*frdA*	THI1517_0 THI940_0	1.33.9.1	THI1517 THI940	140 433	+		BOGUAY_3541 BGP_2143	
fumarate reductase, iron-sulfur protein	*frdB*		1.33.9.1						
2-oxoglutarate:ferredoxin oxidoreductase, alpha subunit	*korA*	THI1378_0	1.2.7.3	THI1378	377		+	BOGUAY_1065 BGP_0270	
2-oxoglutarate:ferredoxin oxidoreductase, beta subunit	*korB*	THI2163	1.2.7.3	THI2163	191		+	BOGUAY_1064	
2-oxoglutarate:ferredoxin oxidoreductase, gamma subunit	*korG*								
2-oxoglutarate:ferredoxin oxidoreductase, delta subunit	*korD*								

product	gene	locus	E.C.	contig	AA	truncated	full	other large, colorless SOB	comment
pyruvate:ferredoxin oxidoreductase, alpha subunit	*porA*	THI187_1 THI413_1 THI670_0	1.2.7.1	THI187 THI413 THI670	753 388 309	+	+	BOGUAY_4121 FLOR_00935 BGP_3761	
pyruvate:ferredoxin oxidoreductase, beta subunit	*porB*	THI413159326321152	1.2.7.1	THI413	345		+	BGP_5558	
pyruvate:ferredoxin oxidoreductase, gamma subunit	*porG*	THI187_0	1.2.7.1	THI187	118	+		BOGUAY_4123 BGP_2254 FLOR_00934	
pyruvate:ferredoxin oxidoreductase, delta subunit	*porD*	THI413_0	1.2.7.1	THI413	131	+		BOGUAY_4122	
pyruvate flavodoxin/ ferredoxin oxidoreductase	*porACDB ("nifJ")*	THI109_1 THI2670_1 THI789_0 THI02487_	1.2.7.	THI109 THI2670 THI789 THI0248 7	126 2	+		BOGUAY_0108 BOGUAY_2919	
acetyl-CoA syntethase	*acs*	THI962_0	6.2.1.1	THI962	223	+		BA01 (orf249_glimmer3) BGP_6368 FLOR_00817	
pyruvate phosphate dikinase	*ppdK*	THI223716111301 THI2650467231739	2.7.9.1	THI2237 THI2650	202 225	+		BGP _3309 BGP_3310 FLOR_02175 BOGUAY_5237	
phosphoenolpyruvate synthase	*ppsA*	THI00(orf12_glimmer3) THI2983 | r3 THI843 | f1	2.7.9.2	THI00 THI2983 THI843	281	+		BA19_245 FLOR_02068	
phosphoenolpyruvate carboxylase /ATP or GTP dependent cabroxykinase	*pckA/ pckG/ ppc*	THI252814771862 (pckA ATP)	4.1.1.31/ 4.1.1.32/ 4.1.1.49	THI2528	158	+		FLOR_01047 (pckA ATP) BA05_178 (pckA ATP) BGP_5540 (pckA ATP) BGP_2644 (pckG GTP) BA16_192 (ppc) FLOR_00831 (ppc)	

product	gene	locus	E.C.	contig	AA	truncated	full	other large, colorless SOB	comment
Calvin-Benson-Bassham cycle									
ribulose bisphosphate carboxylase large chain, form I	*rbcL*	THI237_1 THI20331953763 THI177814111609*	4.1.1.39	THI237 THI2033 THI1778				BA02_42 BGP_3377	
ribulose bisphosphate carboxylase large chain, form II	*rbcM*		4.1.1.39					BOGUAY_1665 FLOR01412	
ribulose bisphosphate carboxylase small subunit	*rbcS*	THI237112239	4.1.1.39	THI237		+		BA02_41 BGP_3376	
phosphoglycerate kinase	*pgk*	THI399_0 THI60216681202	2.7.2.3	THI399 THI6021	138 221	+		BA02_240 BOGUAY_0998 BOGUAY_0999 BGP_4102 FLOR_4102	
glyceraldehyde-3-phosphate dehydrogenase	*gapA*	THI10719461625106 1	1.2.1.12	THI1071	225		+	BA06_20 BOGUAY_2720 BGP_2190 BGP_4586 FLOR_03217	
bisphosphate aldolase A	*fbaA*		4.1.2.13					BA05_255 BOGUAY_1000 BGP_5969 FLOR_00835	
bisphosphate aldolase B	*fbaB*	THI3055|r2	4.1.2.13	THI3055	200	+			
fructose-1,6-bisphosphatase	*fbp*							BA01 (orf112_glimmer3) FLOR_00141	
transketolase	*tkt*	THI1071_0 THI1325_0 THI1325_1	2.2.1.1	THI1071 THI1325	280 112 106	+		BA06_18 BGP_0483 BGP_2087 BGP_2695 BOGUAY_2721 FLOR_02879	

product	gene	locus	E.C.	contig	AA	truncated	full	other large, colorless SOB	comment
pyrphosphate dependent 6-phosphofructokinase	*ppi-pfk*	THI71517826	2.7.1.90	THI715	259	+		BA15_115 BOGUAY_3135 BOGUAY_1318 BGP_4425 FLOR_02042	
ribose-5-phosphatisomerase	*cbbI*		5.3.1.6					BA19_78 BOGUAY_3213 BGP_5744 FLOR00803	
phosphoribulokinase	*prkA*	THI1792_1	2.7.1.19	THI1792	250	+		BA01 (orf143_glimmer3) Boguay_2689 BGP_2255 FLOR_02126	
C2 cycle (glycolate cycle)									
phosphoglycolate phosphatase	*gph*	THI2179_0 THI772_0 THI34371209832	3.1.3.18	THI2179 THI772 THI3437	216 109 68	+		BA05_44 BA06_120 BA12_109 BOGUAY_4193 BOGUAY_0641 BOGUAY_0964 BGP_2114 BGP_4813 BGP_5647 FLOR_02636 FLOR_02818	
glycolate oxidase	*glcD*	THI156_0 THI943163417831370 THI1470?r1	1.1.3.15	THI156 THI943 THI1470	441 49 429	+		BA05_108 BGP_2712 FLOR_03339 FLOR_03342	
glycolate oxidase, FAD-binding subunit	*glcE*	THI156_1	1.1.3.15	THI156	347	+		BA02_4 BGP_4161 FLOR_02865	

product	gene	locus	E.C.	contig	AA	truncated	full	other large, colorless SOB	comment
glycolate oxidase, iron-sulfur subunit	*glcF*	THI676_0 THI1442_1 THI206018701508	1.1.3.16	THI676 THI1442 THI2060	537 212 289	+		BA02_05 BA17_179 BGP_4162 FLOR_01250	
glutamate-glyoxylate aminotransferase	GGAT	THI15311054124861 7	2.6.1.	THI1531	64			BA05_185 BA06_131 BOGUAY_1325 BGP_1896 BGP_1897 FLOR_00764 FLOR_02517	
glycine cleavage system, glycine dehydrogenase, P-protein	*gcvPB*	THI981_1 (gcvB)	1.4.4.2	THI981	456		+	BA16_23 BOGUAY_1468 BOGUAY_3307 BGP_1733 BGP_1734 BGP_6215 FLOR_02629 FLOR_03006 FLOR_02133	
glycine cleavage system, aminomethyltransferase, T-protein	*gcvT*	THI2312_0 THI2956 r3	2.1.2.10	THI2312 _0 THI2956	243	+		BA01 (orf347_glimmer3) BA19_184 BOGUAY_3309 BGP_1517 FLOR_01593 FLOR_02629	
glycine cleavage system, dihydrolipoyl dehydrogenase, L-protein	*lpd*	THI488_0 THI25811705778	1.8.1.4	THI488 THI2581 THI2643	471 234 216		+	BA01 (orf126_glimmer3 BA17_328 BOGUAY_0563 BOGUAY_0328 BGP_0644 FLOR_01022	

product	gene	locus	E.C.	contig	AA	truncated	full	other large, colorless SOB	comment
glycine cleavage system, H-protein	*gcvH*		1.4.4.2					BA01 (orf348_glimmer3) BOGUAY_3308 BGP_5185 FLOR_01150	
glycine cleavage transcriptional repressor	*gcvR*							BA02_98 FLOR_01593	
serine/ glycine hydroxymethyltransferase	*glyA*	THI1694_0 THI543_1	2.1.2.1	THI1694 THI543	341 152	+		BA01 (orf287_glimmer3) BOGUAY_1680 BGP_4519 FLOR_00302	
serine-glyoxylate aminotransferase	SGAT	THI942_0	2.6.1.51	THI942	107	+		BGP_3194 BGP_5274	
serine/ threonine protein kinase	STPK	THI1128_1 THI1189_0 THI1198_0 THI1807_0 THI19_0 THI265_2 THI593115341060	2.7.11.1	THI1128 THI1189 THI1198 THI1807 THI19 THI265 THI593	216 395 477 113 550 380 510	+		BA02_66 BA02_251 BGP_3584 BGP_4568 FLOR_01423 FLOR_03350 FLOR_03427	we detected much more genes encoding for STPK, which are not shown here
phosphoserine phosphatase	*serB*	THI312915871681	3.1.3.3	THI3129	194	+		BA05_75	bifunctional enzyme with EC 2.7.11.1
phosphoserine aminotransferase	*serC*	THI1309113551637	2.6.1.52	THI309	450	+		BA07_58 BOGUAY_0357 BGP_2880 BGP_2994 FLOR_03048	
D-3-phosphoglycerate dehydrogenase	*serA*	THI1288_0 THI371_2 THI61_1	1.1.1.95	THI1288 THI371 THI61	255 127 304	+		BGP_2879 BGP_5532	

product	gene	locus	E.C.	contig	AA	truncated	full	other large, colorless SOB	comment
glycerate dehydrogenase	*dhg*	THI36517661676	1.1.1.29	THI365	254	+			same function as hydroxy-pyruvate reductase
hydroxypyruvate reductase	*ttuD*	THI752_0	1.1.1.81	THI752	212	+		BGP_3955 FLOR_01443 BOGUAY_4043	
glycerate kinase	GLCK		2.7.1.31					BA02_212	

Table S5: Oxidative phosphorylation of *Candidatus* Thiomargarita nelsonii compared to other large, colorless SOB

product	gene	locus	E.C.	contig	AA	truncated	full	other large, colorless SOB	function
Complex I									
NADH dehydrogenase, subunit A	*nouA*		1.6.5.3					BA09_275 BGP_0197 BOGUAY_1243 FLOR_00620	
NADH dehydrogenase, subunit B	*nouB*		1.6.5.3					BA09_276 BGP_0198 BGP_0509 BOGUAY_1242 FLOR_00621	
NADH dehydrogenase, subunit C	*nouC*		1.6.5.3					BA09_277 BGP_0508 BOGUAY_1236 FLOR_00622	
NADH dehydrogenase, subunit D, iron-sulfur protein	*nouD*	THI927110718071451	1.6.5.3	THI927	232	+		BA09_278 BGP_0004 BGP_4191 BOGUAY_1234 FLOR_01604 FLOR_02881	
NADH dehydrogenase, subunit E, FMN	*nouE*	THI793_1	1.6.5.3	THI793	165		+	BA09_279 BGP_0171 BOGUAY_1225	
NADH dehydrogenase, subunit F, FMN	*nouF*	THI1749_0 THI288113681845 THI79316221977345	1.6.5.3	THI1749 THI2881 THI1793	276 121 117	+		BA09_280 BA06_69 BGP_5079 BGP_0263 BOGUAY_1100 BOGUAY_2594 FLOR_01601 FLOR_01761 FLOR_00941	

product	gene	locus	E.C.	contig	AA	truncated	full	other large, colorless SOB	function
NADH dehydrogenase, subunit G, FMN	*nouG*	THI20207410051172 THI381_2	1.6.5.3	THI2020 THI381	309 395	 +		BA09_281 BGP_2702 BOGUAY_3220	
NADH dehydrogenase, subunit H, membrane complex	*nouH*	THI1116_1 THI1494_0	1.6.5.3	THI1116 THI1494	304 333		 +	BA09_282 BGP_1810 BGP_1811 BGP_1812 BGP_5679 BOGUAY_3219 BOGUAY_1731 FLOR_02882	
NADH dehydrogenase, subunit H, iron-sulfur protein	*nouI*	THI14941245476	1.6.5.3	THI1494	80	+		BA09_283 BGP_1809 BOGUAY_3218 FLOR_02883	
NADH dehydrogenase, subunit J, membrane complex	*nouJ*	THI136113621552	1.6.5.3	THI1361	119	+		BA09_285 BGP_0811 BOGUAY_3216 FLOR_02885	
NADH dehydrogenase, subunit K, membrane complex	*nouK*	THI231313541257 THI1361_0	1.6.5.3	THI2313 THI1361	117 144	 +		BA09_286 BGP_0509 BGP_0810 BOGUAY_3215 FLOR_02886	
NADH dehydrogenase, subunit L, membrane complex	*nouL*	THI1972_0 THI356_1	1.6.5.3	THI1972 THI356	223 376	 +		BA09_287 BGP_5518 BGP_5519 BOGUAY_4484 FLOR_02887	
NADH dehydrogenase, subunit M, membrane complex	*nouM*	THI356_0	1.6.5.3	THI356	505	+		BA09_288 BGP_4202 BOGUAY_1496 BOGUAY_2740 FLOR_02888	

product	gene	locus	E.C.	contig	AA	truncated	full	other large, colorless SOB	function
NADH dehydrogenase, subunit N, membrane complex	*nouN*	THI315_0 THI627_1	1.6.5.3	THI315 THI627	50 328	+		BA09_289 BGP_3173 BGP_3174 BGP_5502 BGP_6044 BOGUAY_3866 BOGUAY_2982 BOGUAY_0688 FLOR_02893	
NAD-dependent epimerase/ dehydratase		THI924_0 THI525_0	1.6.5.3	THI924 THI525	329 157	+		BA17-32 BGP_0215 BGP_1167 BGP_1168 BGP_1982 BGP_3469 BOGUAY_2206 BOGUAY_4092 FLOR_01345 FLOR_03013	
Complex II									
succinate dehydrogenase, flavoprotein subunit	*sdhA*	THI1196_1 THI28471211210 THI1517_0	1.3.5.1	THI1196 THI2847 THI1517	353 69 140	+		BA12_129 BOGUAY_0963 BOGUAY_3541 BGP_0843 BGP_0844 BGP_2143 BGP_2544 FLOR_03153	
succinate dehydrogenase, iron-sulfur subunit	*sdhB*	THI1107_0 THI1107115815901431	1.3.5.1	THI1107	128 143	+		BA12_130 BOGUAY_0707 BGP_1918 BGP_3026 BGP_5022 FLOR_03154	

product	gene	locus	E.C.	contig	AA	truncated	full	other large, colorless SOB	function
succinate dehydrogenase, cytochrome b556 subunit	*sdhC*	THI39_4	1.3.5.1	THI39	293	+		BA12_127 BOGUAY_4609 BGP_2542 BGP_3027 BGP_3589 BGP_1067 FLOR_03151	
succinate dehydrogenase/ fumarate reductase, membrane anchor	*sdhD*		1.3.5.1					BA12_128 BGP_2543 FLOR_03152	
Complex III									
ubiquinol-cytochrome c reductase, iron-sulfur subunit	*petA*	THI736_1	1.10.2.2	THI736				BA01_14 BGP_0838 BOGUAY_0396 FLOR_00183	
ubiquinol-cytochrome c reductase, cytochrome b subunit	*petB*	THI736_0	1.10.2.2	THI736	408		+	BA01 (orf15_glimmer3) BGP_0839 BGP_5122 BOGUAY_0395 FLOR_00184	
ubiquinol-cytochrome c reductase, cytochrome c1 subunit	*petC*	THI471_0 THI7361431872	1.10.2.2	THI471 THI736	100 142	+		BA01 (orf16_glimmer3) BGP_6663 BOGUAY_0394 FLOR_00185	
Complex IV									
cyotchrome c oxidase cbb3-type, subunit I	*CcoN*	THI267_0 THI97913441283	1.9.3.1	THI267 THI979	132 113	+		BA01 (orf210_glimmer3) BGP_2112 BOGUAY_3546 FLOR_00924	
cyotchrome c oxidase cbb3-type, subunit II	*CcoO*	THI267_1	1.9.3.1	THI267	205		+	BA01 (orf211_glimmer3) BGP_3209 BOGUAY_3547 FLOR_00573 FLOR_00923	

product	gene	locus	E.C.	contig	AA	truncated	full	other large, colorless SOB	function
cyotchrome c oxidase cbb3-type, subunit IV	CcoQ	THI267_2	1.9.3.1	THI267	53		+	BA01 (orf212_glimmer3) BGP_3208 BOGUAY_3548 FLOR_00572	
cyotchrome c oxidase cbb3-type, subunit III	CcoP	THI267_3	1.9.3.1	THI267	301		+	BA01 (orf213_glimmer3) BGP_3207 BOGUAY_3549 FLOR_00571	
cyotchrome c oxidase accessory protein	CcoG	THI267_4	1.9.3.1	THI267	229	+			
cytochrome d ubiquinol oxidase, subunit I	cydA		1.10.3.-					BA19_83 BOGUAY_1879 BOGUAY_0143	
cytochrome d ubiquinol oxidase, subunit II	cydB		1.10.3.-					BA19_82 BOGUAY_1880	
protoheme IX farnesyltransferase	cyoE	THI45_3	2.5.1.	THI45		+		BGP_2365	
cytochrome c oxidase, aa3 type, subunit III	coxC	THI195312791821	1.9.3.1	THI1953	92	+		BGP_2863	
cytochrome c oxidase, aa3 type, subunit II	coxB	THI2043_0	1.9.3.1	THI2043	260	+		BGP_2865	
cytochrome c oxidase, aa3 type, subunit I	coxA	TH509_0	1.9.3.1	THI509	263	+		BGP_2866	
cytochrome c oxidase synthesis factor	SCO							BGP_2864	
Complex V									
V-type ATP (sodium) synthase subunit A	atpA/ ntpA	THI363_0	3.6.3.14/ 3.6.1.15	THI363	593		+	BGP_4884 BOGUAY_2821 FLOR_01562	
V-type ATP (sodium) synthase subunit A	atpB/ ntpB		3.6.3.14/ 3.6.1.15					BGP_3881 BOGUAY_2662 FLOR_01509	

product	gene	locus	E.C.	contig	AA	truncated	full	other large, colorless SOB	function
V-type ATP (sodium) synthase subunit C	atpC/ ntpC	THI361_2	3.6.3.14/ 3.6.1.15	THI361	328	+		BGP_0940 BOGUAY_2136 BOGUAY_2457 FLOR_00138	
V-type (sodium) ATP synthase subunit D	atpD/ ntpD	THI1004_1	3.6.3.14/ 3.6.1.15	THI1004	210		+	BGP_3601 BOGUAY_1958 BOGUAY_1959 BOGUAY_2137 FLOR_02619	
V-type (sodium) ATP synthase subunit E	atpE/ ntpE	THI363_1	3.6.3.14/ 3.6.1.15	THI363	140	+		BOGUAY_2822 FLOR_01561	
V-type (sodium) ATP synthase subunit E	atpF/ ntpF	THI1439_0	3.6.3.14/ 3.6.1.15	THI1439	106	+			
V-type (sodium) ATP synthase subunit H	atpH/ ntpH	THI361_3	3.6.3.14/ 3.6.1.15	THI361	124	+			
V-type (sodium) ATP synthase subunit I	atpI/ ntpI		3.6.3.14/ 3.6.1.15					BGP_1588 BOGUAY_0078 BOGUAY_3163 FLOR_00139	
V-type (sodium) ATP synthase subunit K	atpK/ ntpK	THI1439_1	3.6.3.14/ 3.6.1.15	THI1439	92	+		BGP_2819 BOGUAY_2663 FLOR_00638	
F-type ATP synthase, subunit epsilon	atpC	THI35561418215	3.6.3.14	THI3556	138	+		BA17_293 BGP_2403 FLOR_00765 FLOR_00766	
F-type ATP synthase, subunit beta	atpD	THI1201_0	3.6.3.14	THI1201	458		+	BA17_294 BGP_2491 FLOR_00767	
F-type ATP synthase, subunit gamma	atpG	THI208_3	3.6.3.14	THI208	283		+	BA17_295 BGP_2492 BGP_1963 BOGUAY_1279 FLOR_00768	

product	gene	locus	E.C.	contig	AA	truncated	full	other large, colorless SOB	function
F-type ATP synthase, subunit gamma	atpA		3.6.3.14					BA17_296 BGP_0784 BOGUAY_3168 FLOR_01115	
F-type ATP synthase, subunit delta	atpH		3.6.3.14					BA17_297 BGP_0785 BOGUAY_3167 FLOR_01114	
F-type ATP synthase, subunit beta	atpF		3.6.3.14					BA17_298 BGP_0786 BOGUAY_3166 FLOR_01113	
F-type ATP synthase, chain C	atpE		3.6.3.14					BA17_300 BGP_0787 BOGUAY_3165 FLOR_01112	
F-type ATP synthase,chain A	atpB		3.6.3.14					BA17_300 BGP_0788 BGP_0789 BOGUAY_3164 FLOR_01111 FLOR_02054	
F-type ATP synthase,?	atp?		3.6.3.14					BGP_0790 BOGUAY_3163	
polyphosphate kinase	ppk	THI45_0	2.7.4.1	THI45	654			BA01 (orf27_glimmer3) BGP_5434 BOGUAY_0085 FLOR_02687	
membrane-bound proton translocating pyrophosphatase/ inorganic pyrophosphatase	hppA/ ppa/ LHPP		3.6.1.1					BA01 (orf50_glimmer3) BA02 (orf419_glimmer3) BA01 (orf223_glimmer) BGP_2409 BOGUAY_430 FLOR_00254 FLOR_00748 FLOR_01358	

Table S6: Additional energy metabolism of *Candidatus* Thiomargarita nelsonii compared to other large, colorless SOB

product	gene	locus	E.C.	contig	AA	truncated	full	other large, colorless SOB	comment
Heterodisulfide reductase									
heterodisulfide reductase, subunit A	*hdrA*	THI1755_0 THI94014081436 THI141793213291590	1.8.98.1	THI1755 THI940 THI1417	249 135 131	+ 		BOGUAY_3539 BOGUAY_3540 BOGUAY_2741 BGP_0252 BGP_0253	
heterodisulfide reductase, subunit B	*hdrB*		1.8.98.1					BGP_2617	
heterodisulfide reductase, subunit C	*hdrC*	THI846_1	1.8.98.1	THI846	213	+		BGP_2616	
heterodisulfide oxidoreductase, iron-sulfur cluster-binding subunit D	*hdrD*	THI303_0 THI58_	1.8.98.1	THI303 THI58	309 302	 	 +	BA05_133 BOGUAY_3538	
heterodisulfide oxidoreductase, iron-sulfur cluster-binding subunit E	*hdrE*	THI303_1	1.8.98.1	THI303	368		+	BOGUAY_3536	
heterodisulfide reductase, cytochrome reductase subunit	*hdrF*	THI30323473009988	1.8.98.1	THI303	220	+		BOGUAY_3535	
Methyl viologen-reducing hydrogemas									
methyl viologen-reducing hydrogenase, delt subunit	*mvhD*	THI8461340616	1.12.99.	THI846	112		+	BOGUAY_3538	
methyl viologen-reducing hydrogenase-associated ferredoxin	*mvhF*	THI43_3	1.12.99.	THI43	245	+			
nickel-dependent methyl viologen-reducing hydrogenase, large subunit	*mvhA*	THI43_4 THI175580411251660	1.12.99.	THI43 THI1755	471 106	 	 +	BA05_132 BGP_0253	

product	gene	locus	E.C.	contig	AA	truncated	full	other large, colorless SOB	comment
nickel-dependent methyl viologen-reducing hydrogenase, small subunit	*mvhG*	THI43_5	1.12.99.	THI43	313		+		functional similar to F420 non reducing-hydrogenase
methyl viologen-reducing hydrogenase maturation protease	*mvhP*	THI43_7	1.12.99.	THI43					
Na^+-translocating membrane complex									
electron transport complex, subunit A	*rnfA*	THI1445_0		THI1445	191		+	BA01 (orf340_glimmer3) BA09_372 BOGUAY_2644 BOGUAY_0446 BGP_4894 BGP_4895 FLOR_00005 FLOR_00042	
electron transport complex, subunit B, ferredoxin subunit	*rnfB*	THI1789_0 THI11991215885		THI1789 THI1199	298 70		+	BA01 (orf339_glimmer3) BA09_373 BOGUAY_1961 BOGUAY_0445 BGP_5165 FLOR_00004 FLOR_01801	
electron transport complex, subunit C, flavin subunit	*rnfC*	THI1294_0 THI571_1		THI1294 THI571	289 484	+ 	+ 	BA01 (orf338_glimmer3) BA07_22 BA09_374 BOGUAY_0327 BOGUAY_0444 BGP_1887 FLOR_00003 FLOR_03168	

product	gene	locus	E.C.	contig	AA	truncated	full	other large, colorless SOB	comment
electron transport complex, subunit D	*rnfD*	THI1238_0 THI1019_0 THI856_1		THI1238 THI1019 THI856	300 239 344	+ + +		BA01 (orf337_glimmer3) BA09_375 BOGUAY_4422 BOGUAY_2718 BGP_2194 BGP_2824 FLOR_00109 FLOR_02202	
electron transport complex, subunit G	*rnfG*	THI2459_0		THI2549	207		+	BA01 (orf336_glimmer3) BA09_376 BOGUAY_1747 BOGUAY_2719 BGP_5931 BGP_6563 FLOR_00108 FLOR_02203	
electron transport complex, subunit E	*rnfE*	THI331745553225		THI3317	168	+		BA01 (orf335_glimmer3) BA09_218 BOGUAY_2233 BOGUAY_2643 FLOR_00471 FLOR_02204	
hypothetical protein	*rnfH*							BOGUAY_1193	
Uptake hydrogenase									
respiratory membrane-bound hydrogen uptake [Ni,Fe] hydrogenase, small subunit	*hupS*	THI8271464146 THI18711751500	1.12.99.6	THI827 THI187	153 57	+ +		BA02_59 BA05_135 BOGUAY_1709 BOGUAY_0684 FLOR_00588 FLOR_02642	

product	gene	locus	E.C.	contig	AA	truncated	full	other large, colorless SOB	comment
respiratory membrane-bound hydrogen uptake [Ni,Fe] hydrogenase, large subunit	*hupL*	THI368_2 THI58_3 THI1400_1	1.12.99.6	THI368 THI58 THI1400	592 219 256	+	+	BA02_58 BA05_132 BOGUAY_4411 FLOR_00363 FLOR_02641	
[Ni,Fe] hydrogenase 1b-type cytochrome	*hupC*		1.12.99.6					BA02_57 FLOR_02639	
[Ni,Fe] hydrogenase maturation protein	*hupD*		3.4.24.-					BA02_280 BOGUAY_2760 FLOR_03012	
[Ni,Fe] hydrogenase expression protein	*hupH*							BA07_105 FLOR_00978	
Other hydrogenases and maturation proteins									
NAD (P) transhydrogenase, alpha subunit	*pntA*	THI20533979841684 THI1715_0	1.6.1.2	THI2053 THI1715	159 282	+		BA19_120 BA19_121 BOGUAY_3230 BGP_1955 BGP_5439 FLOR_01451 FLOR_01452	
NAD (P) transhydrogenase, beta subunit	*pntB*	THI268917081244 THI171512431286	1.6.1.2	THI2689 THI1715	235 80	+		BA19_122 BOGUAY_3228 BOGUAY_3229 FLOR_01453	
hydrogenase nickel insertion protein, cytochrome alpha chain	*hypA*							BA05_135 BA14_43 BA17_362 BOGUAY_1790 FLOR_00762	maturation of hydrogenase
hydrogenase acessory protein	*hypB*							BA01 (orf69_glimmer3) BOGUAY_1512 FLOR_00958 FLOR_02868	maturation of hydrogenase

product	gene	locus	E.C.	contig	AA	truncated	full	other large, colorless SOB	comment
hydrogenase assembly protein	*hypC*							BA14_42 BOGUAY_1791 FLOR_00763	maturation of hydrogenase
hydrogenase expression/ formation protein	*hypD*							BA02_307 BOGUAY_1513 BOGUAY_3052 FLOR_03072	maturation of hydrogenase
hydrogenase expression/ formation protein	*hypE*							BA14_122 BOGUAY_3356 FLOR_01477 FLOR_03103	maturation of hydrogenase
hydrogenase maturation protein	*hypF*	THI648_4		THI648	74	+		BA01 (orf45_glimmer3) FLOR_02743	maturation of hydrogenase
hydrogenase 4 membrane component	*hyfE*							BA02_301	membrane complex
hydrogenase 4 component F	*hyfF*							BA02_354	membrane complex
hydrogenase 4	*hyfB*							BA12_29	membrane complex
hydrogenase 4	*hyfG*							BA15_42	membrane complex
iron-dependent hydrogenase, alpha subunit	*hydA*	THI12341744405	1.12.1.2	THI1234	247	+		BA17_361 FLOR_00048	
iron -dependent hydrogenase, beta subunit	*hydB*	THI25911671469	1.12.1.2	THI2591	222	+		BA17_359	
iron -dependent hydrogenase, delta subunit	*hydD*							BA17_362 FLOR_00047	
iron -dependent hydrogenase, gamma subunit	*hydG*							BA17_358	

Table S7: Intracellular storage of *Candidatus* Thiomargarita nelsonii compared to other large, colorless SOB

product	gene	locus	E.C.	contig	AA	truncated	full	other large, colorless SOB	function
Polyphosphate storage system									
phosphate ABC transporter, inner membrane subunit	*pstA*	THI1009_1	3.6.3.27	THI1009	236	+		BA04_28 BA16_208 BGP_3522 BOGUAY_3725 FLOR_00686	
phosphate ABC transporter, ATP binding subunit	*pstB*	THI466_3	3.6.3.27	THI466	285		+	BA04_29 BGP_2125 BOGUAY_3724 FLOR_00687	
phosphate ABC transporter, inner membrane component	*pstC*	THI273_2	3.6.3.27	THI273	506	+		BA04_27 BGP_3523 BOGUAY_3726 FLOR_00685	
phosphate ABC transporter, periplasmatic phosphate-binding protein	*pstS*		3.6.3.27					BA12_62 BGP_3525 BOGUAY_ 3729 BOGUAY_ 3728 FLOR_02873 FLOR_01348	
phosphate ABC transporter, phosphat binding protein	*pstD*		3.6.3.27					BA10_71	
phosphate regulon sensor protein	*phoR*	THI1120_1		THI1120	421	+		BA02_323 BOGUAY_4336	
phsophate transport system regulator protein	*phoU*	THI46622302531967		THI466	99	+		BA04_30 BGP_1356 BOGUAY_3723 FLOR_02932 FLOR_00688	

product	gene	locus	E.C.	contig	AA	truncated	full	other large, colorless SOB	function
phosphate stravation-inducible protein	*phoH*							FLOR_03136	
phosphate regulon transcriptional regulatory	*phoB*							BOGUAY_4337	
phosphate-selective porin O and P	*phoE*	THI1278_0 THI711_1		THI1278 THI711	387 391		+	BGP_4216 BGP_0268 BGP_0269 BOGUAY_2057	
polyphosphate kinase	*ppk*	THI45_0	2.7.4.1	THI45	654			BA01 (orf27_glimmer3) BGP_5434 BOGUAY_0085 FLOR_02687	
Polyhydroxyalkanoate/ -butyrate storage system									
polyphosphate:AMP phosphotransferase	*pap*	THI191911041837	2.7.4.-					BA10_37 BOGUAY_0604 FLOR_02303	
acetyl-CoA acetyltransferase	*phaA/ phbA*	THI234_0	2.3.1.9	THI_234	370		+	BA05_42 BA17_147 FLOR_00713	
acetoacetyl-CoA reductase	*phaB/ phbB*		1.1.1.36					BA17_145 BGP_0317 BOGUAY_0874 FLOR_00822	
poly-beta hydroxybutyrate polymerase/ poly(R)-hydroxyalkanoate acid synthase, class I	*phaC*		2.3.1-					BA02_82 BA06_09 BA19_224 BA02 (orf427_glimmer3) FLOR_01645 FLOR_03182 FLOR_03197	
poly(R)-hydroxyalaknoic acid synthase, class III	*phaE*							BA08_131 FLOR_01646	

product	gene	locus	E.C.	contig	AA	truncated	full	other large, colorless SOB	function
poly(3-hydroxybutyrate) depolymerase	*phaZ*							BA09_314 BA09_315 FLOR_03285	
putative regulator of polymer accumulation	*phaR*							BA07_146 BGP_4849 FLOR_00714	

Suuporting Figures

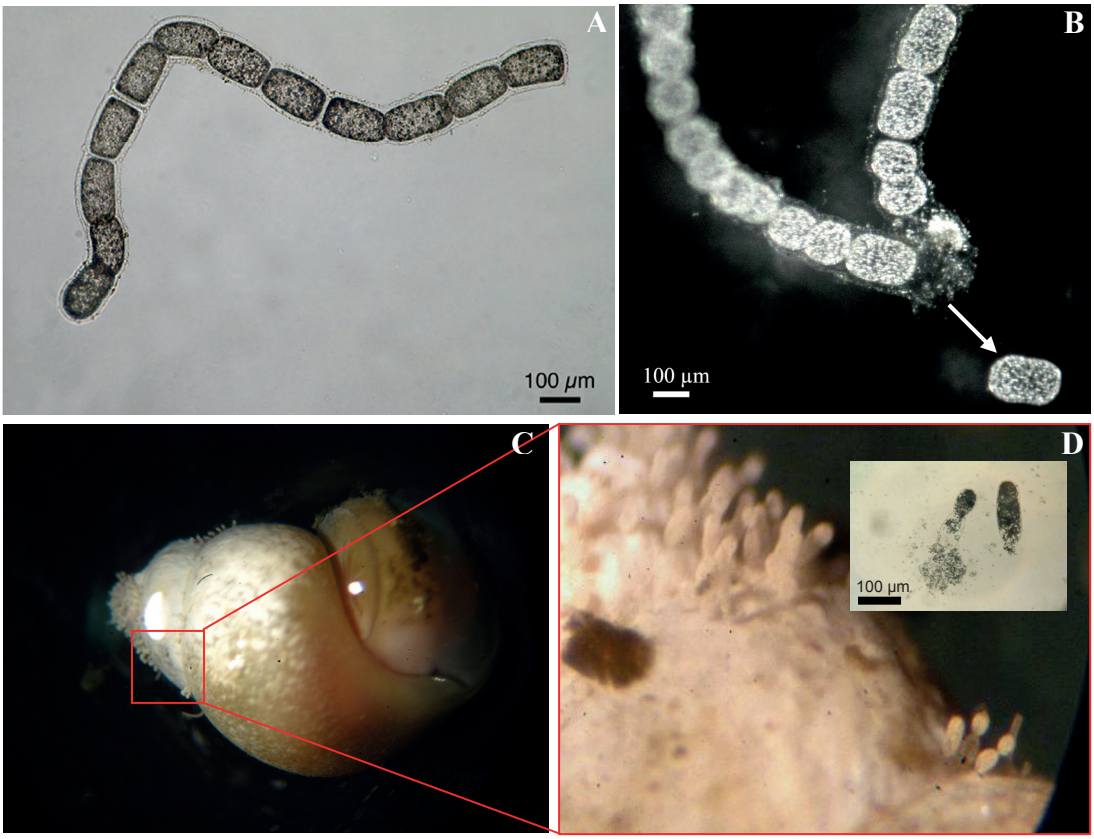

Figure S1: *Candidatus* Thiomargarita nelsonii chain-forming morphotype with cylindrical cells (A and B). Arrow indicates a cell that was manually seperated from the surrounding mucus sheath (B). Snail with attached *Candidatus* Thiomargarita nelsonii cells of the sessile single cell-morphotype from the Guaymas Basin (C). Detail of C with inlet showing a micrograph of unattached single cells (D).

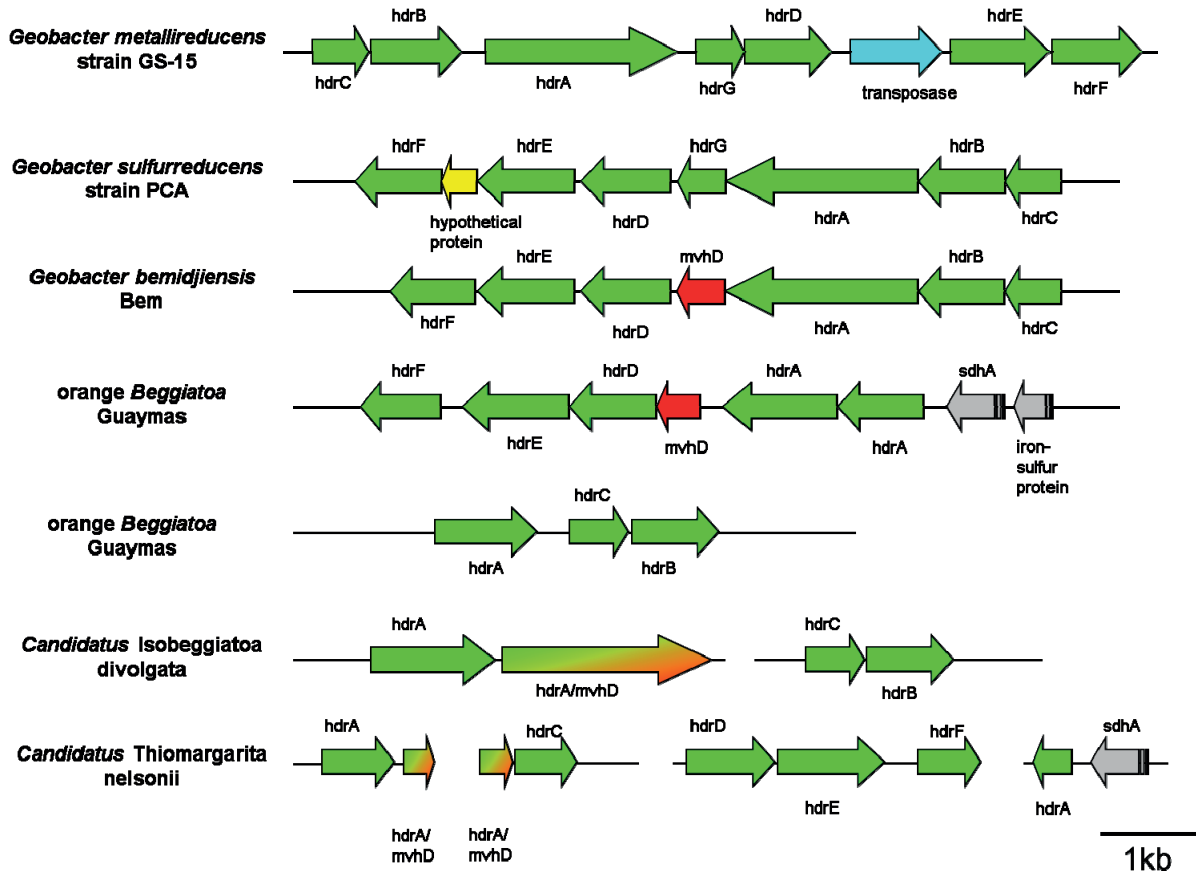

Figure S2: Genomic organization of the heterodisulfide reductases (*hdr*) operon. *Hdr* are shown in green, fusion genes between *hdr* and the methyl viologen-reducing hydrogenase (*mvh*) are shown in green-red, while separated *mvhD*are shown in red. Hypothetical proteins are shown in yellow, mobile elements in the form of transposases are shown in light blue and protein with other functionsare shown in gray. SdhA stands for the succinate dehydrogenase/ fumarate reductase subunit A, which is a membrane-located complex of the oxidative phosphorylation and tricarboxylic acid cycle. The organization of the *Geobacter* spezies are published elsewhere (Childers *et al.*, 2002; Methé *et al.*, 2003; Aklujkar *et al.*, 2010)

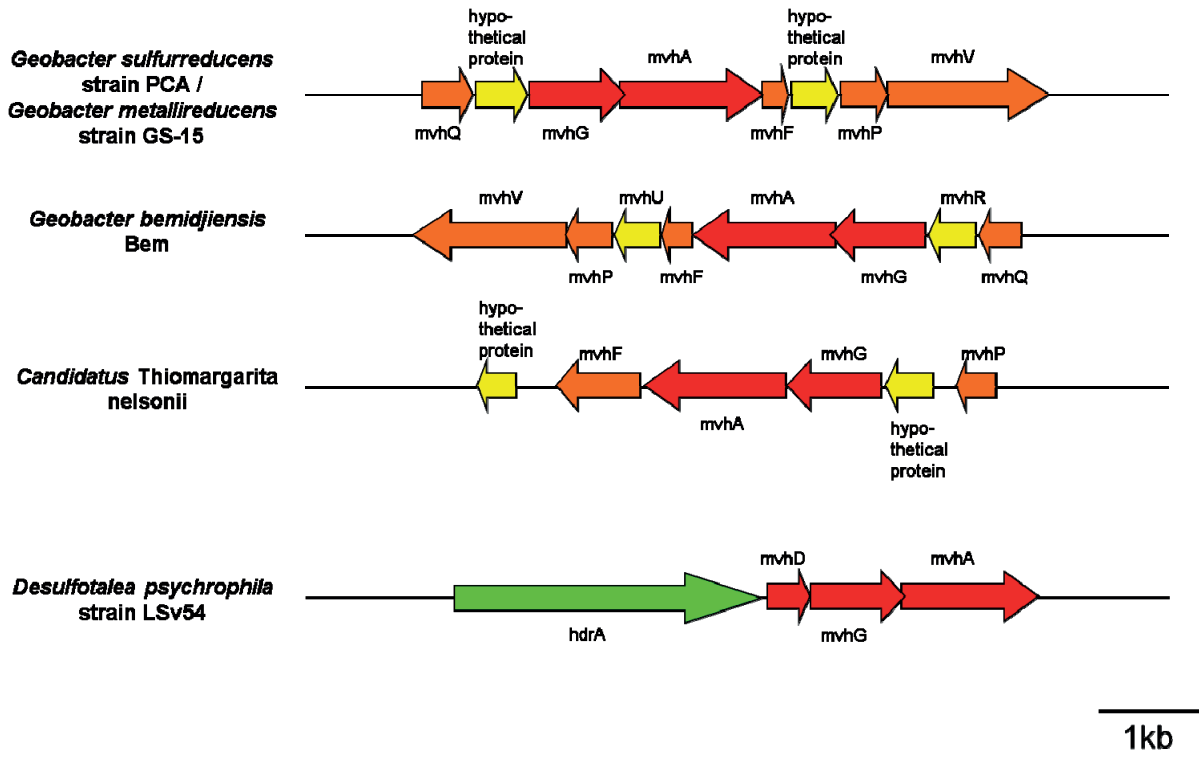

Figure S3: Genomic organization of the methyl viologen-reducing hydrogenase (*mvh*) operon. *Mvh* are shown in red, *mvh* associated and regulating genes are shown in orange, and heterodisulfide reductases (*hdr*) are shown in green. Hypothetical proteins a**r**e shown in yellow. The organization of the *Geobacter* spezies and the sulfate-reducer Desulfotalea psychrophila strain LSv54 are published elsewhere (Childers *et al.*, 2002; Methé *et al.*, 2003; Aklujkar *et al.*, 2010; Rabus *et al.*, 2004).

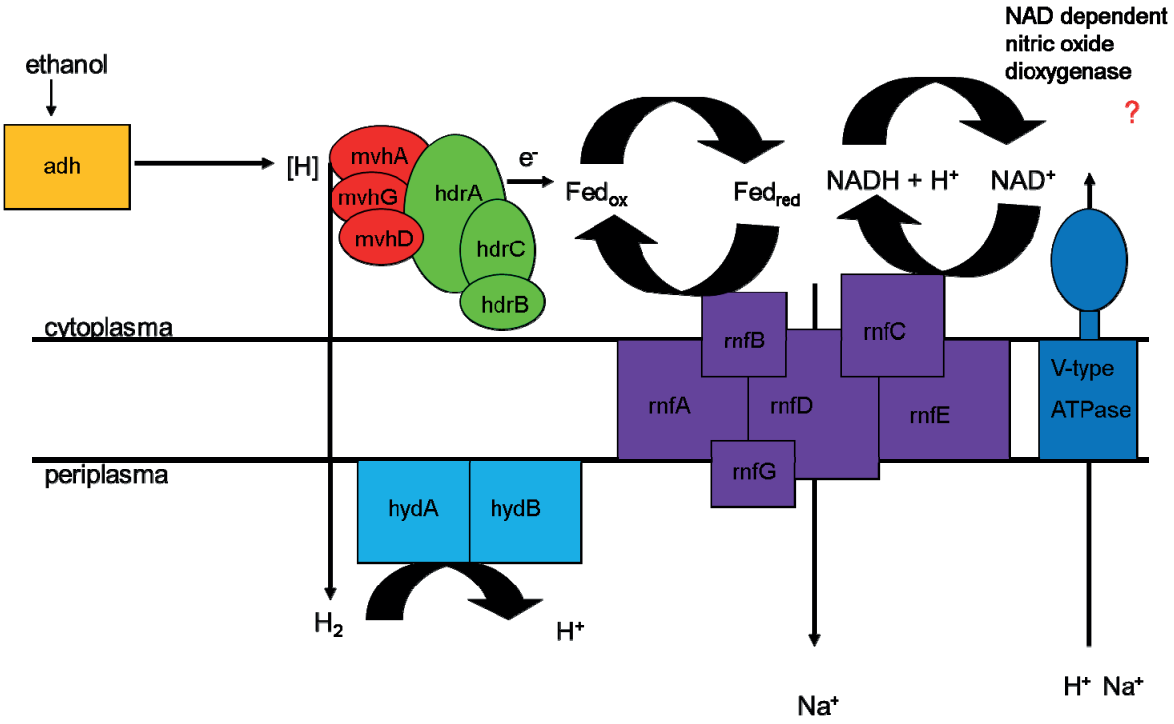

Figure S4: Flavin-based eletron bifurcation coupled to ethanol oxidation. Adh, alcohol dehydrogenase; hdr, heterdisulfide reductase; hyd, periplasmatic hydrogenase; mvh, methyl viologen-reducing hydrogenase; rnf, membrane-bound electron transport complex

References

Aklujkar, M., Young, N. D., Holmes, D., Chavan, M., Risso, C., Kiss, H. E., Han, C. S., Land, M. L., and Lovley, D. R. (2010). The genome of *Geobacter bemidjiensis*, exemplar for the subsurface clade of *Geobacter* species that predominate in Fe(III)-reducing subsurface environments. *BMC Genomics* 11, 490.

Anantharaman, K., Breier, J. A., Sheik, C. S., and Dick, G. J. (2013). Evidence for hydrogen oxidation and metabolic plasticity in widespread deep-sea sulfur-oxidizing bacteria. *Proc. Natl. Acad. Sci.* 110, 330–335.

Baker, S. C., Ferguson, S. J., Ludwig, B., Page, M. D., Richter, O.-M. H., and Spanning, R. J. M. van (1998). Molecular genetics of the genus *Paracoccus*: Metabolically versatile bacteria with bioenergetic flexibility. *Microbiol. Mol. Biol. Rev.* 62, 1046–1078.

Bauwe, H., Hagemann, M., Kern, R., and Timm, S. (2012). Photorespiration has a dual origin and manifold links to central metabolism. *Curr. Opin. Plant Biol.* 15, 269–275.

Bedzyk, L., Wang, T., and Ye, R. W. (1999). The periplasmic nitrate reductase in *Pseudomonas* sp. strain G-179 catalyzes the first step of denitrification. *J. Bacteriol.* 181, 2802–2806.

Beutler, M., Milucka, J., Hinck, S., Schreiber, F., Brock, J., Mußmann, M., Schulz-Vogt, H. N., and de Beer, D. (2012). Vacuolar respiration of nitrate coupled to energy conservation in filamentous *Beggiatoaceae*. *Environ. Microbiol.* 14, 2911–2919.

Biegel, E., Schmidt, S., González, J. M., and Müller, V. (2011). Biochemistry, evolution and physiological function of the Rnf complex, a novel ion-motive electron transport complex in prokaryotes. *Cell. Mol. Life Sci.* 68, 613–634.

Bowien, B., and Schlegel, H. G. (1981). Physiology and biochemistry of aerobic hydrogen-oxidizing bacteria. *Annu. Rev. Microbiol.* 35, 405–452.

Brock, J., Rhiel, E., Beutler, M., Salman, V., and Schulz-Vogt, H. N. (2012). Unusual polyphosphate inclusions observed in a marine *Beggiatoa* strain. *Antonie Van Leeuwenhoek* 101, 347–357.

Brock, J., and Schulz-Vogt, H. N. (2011). Sulfide induces phosphate release from polyphosphate in cultures of a marine *Beggiatoa* strain. *ISME J.* 5, 497–506.

Brosius, J., Palmer, M. L., Kennedy, P. J., and Noller, H. F. (1978). Complete nucleotide sequence of a 16S ribosomal RNA gene from *Escherichia coli*. *Proc. Natl. Acad. Sci.* 75, 4801–4805.

Buckel, W., and Thauer, R. K. (2013). Energy conservation via electron bifurcating ferredoxin reduction and proton/Na^+ translocating ferredoxin oxidation. *Biochim. Biophys. Acta BBA - Bioenerg.* 1827, 94–113.

Childers, S. E., Ciufo, S., and Lovley, D. R. (2002). *Geobacter metallireducens* accesses insoluble Fe(III) oxide by chemotaxis. *Nature* 416, 767–769.

Cipollone, R., Ascenzi, P., Frangipani, E., and Visca, P. (2006). Cyanide detoxification by recombinant bacterial rhodanese. *Chemosphere* 63, 942–949.

Dahl, C., Friedrich, C., and Kletzin, A. (2008). "Sulfur oxidation in prokaryotes," in *eLS* (John Wiley & Sons, Ltd).

Dale, C., Wang, B., Moran, N., and Ochman, H. (2003). Loss of DNA recombinational repair enzymes in the initial stages of genome degeneration. *Mol. Biol. Evol.* 20, 1188–1194.

Eisenhut, M., Ruth, W., Haimovich, M., Bauwe, H., Kaplan, A., and Hagemann, M. (2008). The photorespiratory glycolate metabolism is essential for *Cyanobacteria* and might have been conveyed endosymbiontically to plants. *Proc. Natl. Acad. Sci.* 105, 17199–17204.

Evans, M. C., Buchanan, B. B., and Arnon, D. I. (1966). A new ferredoxin-dependent carbon reduction cycle in a photosynthetic bacterium. *Proc. Natl. Acad. Sci.* 55, 928–934.

Fossing, H., Gallardo, V. A., Jørgensen, B. B., Huttel, M., Nielsen, L. P., Schulz, H., Canfield, D. E., Forster, S., Glud, R. N., Gundersen, J. K., *et al.* (1995). Concentration and transport of nitrate by the mat-forming sulphur bacterium *Thioploca*. *Nature* 374, 713–715.

Gardner, P. R., Gardner, A. M., Martin, L. A., and Salzman, A. L. (1998). Nitric oxide dioxygenase: An enzymic function for flavohemoglobin. *Proc. Natl. Acad. Sci.* 95, 10378–10383.

Hagen, K. D., and Nelson, D. C. (1997). Use of reduced sulfur compounds by *Beggiatoa* spp.: Enzymology and physiology of marine and freshwater strains in homogeneous and gradient cultures. *Appl. Environ. Microbiol.* 63, 3957–3964.

Haveman, S. A., Brunelle, V., Voordouw, J. K., Voordouw, G., Heidelberg, J. F., and Rabus, R. (2003). Gene expression analysis of energy metabolism mutants of *Desulfovibrio vulgaris* Hildenborough indicates an important role for alcohol dehydrogenase. *J. Bacteriol.* 185, 4345–4353.

Kaneko, T., Sato, S., Kotani, H., Tanaka, A., Asamizu, E., Nakamura, Y., Miyajima, N., Hirosawa, M., Sugiura, M., Sasamoto, S., *et al.* (1996). Sequence analysis of the genome of the unicellular cyanobacterium *Synechocystis* sp. strain PCC6803. II. Sequence determination of the entire genome and assignment of potential protein-coding regions. *DNA Res.* 3, 109–136.

Kern, R., Eisenhut, M., Bauwe, H., Weber, A. P. M., and Hagemann, M. (2013). Does the *Cyanophora paradoxa* genome revise our view on the evolution of photorespiratory enzymes? *Plant Biol.* 15, 759–768.

Kleiner, M., Petersen, J. M., and Dubilier, N. (2012a). Convergent and divergent evolution of metabolism in sulfur-oxidizing symbionts and the role of horizontal gene transfer. *Curr. Opin. Microbiol.* 15, 621–631.

Kleiner, M., Wentrup, C., Lott, C., Teeling, H., Wetzel, S., Young, J., Chang, Y.-J., Shah, M., VerBerkmoes, N. C., Zarzycki, J., *et al.* (2012b). Metaproteomics of a gutless marine worm and its symbiotic microbial community reveal unusual pathways for carbon and energy use. *Proc. Natl. Acad. Sci.* 109, E1173-E1182.

Laurent, S., Jang, J., Janicki, A., Zhang, C.-C., and Bédu, S. (2008). Inactivation of *spkD*, encoding a Ser/Thr kinase, affects the pool of the TCA cycle metabolites in *Synechocystis* sp. strain PCC 6803. *Microbiology* 154, 2161–2167.

MacGregor, B. J., Biddle, J. F., Siebert, J. R., Staunton, E., Hegg, E. L., Matthysse, A. G., and Teske, A. (2013). Why orange Guaymas Basin *Beggiatoa* spp. are orange: Single-filament-genome-enabled identification of an abundant octaheme cytochrome with hydroxylamine oxidase, hydrazine oxidase, and nitrite reductase activities. *Appl. Environ. Microbiol.* 79, 1183–1190.

Malm, S., Tiffert, Y., Micklinghoff, J., Schultze, S., Joost, I., Weber, I., Horst, S., Ackermann, B., Schmidt, M., Wohlleben, W., *et al.* (2009). The roles of the nitrate reductase NarGHJI, the nitrite reductase NirBD and the response regulator GlnR in nitrate assimilation of *Mycobacterium tuberculosis*. *Microbiology* 155, 1332–1339.

Manz, W., Amann, R., Ludwig, W., Wagner, M., and Schleifer, K.-H. (1992). Phylogenetic oligodeoxynucleotide probes for the major subclasses of Proteobacteria: Problems and solutions. *Syst. Appl. Microbiol.* 15, 593–600.

Markert, S., Arndt, C., Felbeck, H., Becher, D., Sievert, S. M., Hügler, M., Albrecht, D., Robidart, J., Bench, S., Feldman, R. A., *et al.* (2007). Physiological proteomics of the uncultured endosymbiont of *Riftia pachyptila*. *Science* 315, 247–250.

McHatton, S. C., Barry, J. P., Jannasch, H. W., and Nelson, D. C. (1996). High nitrate concentrations in vacuolate, autotrophic marine *Beggiatoa* spp. *Appl. Environ. Microbiol.* 62, 954–958.

Methé, B. A., Nelson, K. E., Eisen, J. A., Paulsen, I. T., Nelson, W., Heidelberg, J. F., Wu, D., Wu, M., Ward, N., Beanan, M. J., *et al.* (2003). Genome of *Geobacter sulfurreducens*: Metal reduction in subsurface environments. *Science* 302, 1967–1969.

Meyer, B., and Kuever, J. (2007). Molecular analysis of the diversity of sulfate-reducing and sulfur-oxidizing prokaryotes in the Environment, Using aprA as functional marker gene. *Appl. Environ. Microbiol.* 73, 7664–7679.

Meyerdierks, A., Kube, M., Lombardot, T., Knittel, K., Bauer, M., Glöckner, F. O., Reinhardt, R., and Amann, R. (2005). Insights into the genomes of archaea mediating the anaerobic oxidation of methane. *Environ. Microbiol.* 7, 1937–1951.

Moreno-Vivián, C., Cabello, P., Martínez-Luque, M., Blasco, R., and Castillo, F. (1999). Prokaryotic nitrate reduction: Molecular properties and functional distinction among bacterial nitrate reductases. *J. Bacteriol.* 181, 6573–6584.

Morozkina, E. V., and Zvyagilskaya, R. A. (2007). Nitrate reductases: Structure, functions, and effect of stress factors. *Biochem. Mosc.* 72, 1151–1160.

Mulkidjanian, A. Y., Makarova, K. S., Galperin, M. Y., and Koonin, E. V. (2007). Inventing the dynamo machine: The evolution of the F-type and V-type ATPases. *Nat. Rev. Microbiol.* 5, 892–899.

Muntyan, M. S., Grabovich, M. Y., Patritskaya, V. Y., and Dubinina, G. A. (2005). Regulation of metabolic and electron transport pathways in the freshwater bacterium *Beggiatoa leptomitiformis* D-402. *Microbiology* 74, 388–394.

Mußmann, M., Hu, F. Z., Richter, M., de Beer, D., Preisler, A., Jørgensen, B. B., Huntemann, M., Glöckner, F. O., Amann, R., Koopman, W. J. H., *et al.* (2007). Insights into the genome of large sulfur bacteria revealed by analysis of single filaments. *PLoS Biol.* 5, e230.

Mußmann, M., Richter, M., Lombardot, T., Meyerdierks, A., Kuever, J., Kube, M., Glöckner, F. O., and Amann, R. (2005). Clustered genes related to sulfate respiration in uncultured prokaryotes support the theory of their concomitant horizontal transfer. *J. Bacteriol.* 187, 7126–7137.

Muyzer, G., Teske, A., Wirsen, C., and Jannasch, H. (1995). Phylogenetic relationships of Thiomicrospira species and their identification in deep-sea hydrothermal vent samples by denaturing gradient gel electrophoresis of 16S rDNA fragments. *Arch. Microbiol.* 164, 165–172.

Neumann, S., Wynen, A., Trüper, H. G., and Dahl, C. (2000). Characterization of the cys gene locus from *Allochromatium vinosum* indicates an unusual sulfate assimilation pathway. *Mol. Biol. Rep.* 27, 27–33.

Pereira, S. F. F., Goss, L., and Dworkin, J. (2011). Eukaryote-like serine/threonine kinases and phosphatases in bacteria. *Microbiol. Mol. Biol. Rev.* 75, 192–212.

Prince, R. C., Stokley, K. E., Haith, C. E., and Jannasch, H. W. (1988). The cytochromes of a marine *Beggiatoa*. *Arch. Microbiol.* 150, 193–196.

Pringsheim, E. G. (1964). Heterotrophism and species concepts in *Beggiatoa*. *Am. J. Bot.* 51, 898–913.

Rabus, R., Ruepp, A., Frickey, T., Rattei, T., Fartmann, B., Stark, M., Bauer, M., Zibat, A., Lombardot, T., Becker, I., *et al.* (2004). The genome of *Desulfotalea psychrophila*, a sulfate-reducing bacterium from permanently cold Arctic sediments. *Environ. Microbiol.* 6, 887–902.

Raghunathan, A., Jr, H. R. F., Bornarth, C. J., Song, W., Driscoll, M., and Lasken, R. S. (2005). Genomic DNA amplification from a single bacterium. *Appl. Environ. Microbiol.* 71, 3342–3347.

Reshetnikov, A. S., Rozova, O. N., Khmelenina, V. N., Mustakhimov, I. I., Beschastny, A. P., Murrell, J. C., and Trotsenko, Y. A. (2008). Characterization of the pyrophosphate-

dependent 6-phosphofructokinase from *Methylococcus capsulatus* Bath. *FEMS Microbiol. Lett.* 288, 202–210.

Salman, V. (2011). Diversity studies and molecular analyses with single cells and filaments of large, colorless sulfur bacteria. PhD thesis

Salman, V., Amann, R., Girnth, A.-C., Polerecky, L., Bailey, J. V., Høgslund, S., Jessen, G., Pantoja, S., and Schulz-Vogt, H. N. (2011). A single-cell sequencing approach to the classification of large, vacuolated sulfur bacteria. *Syst. Appl. Microbiol.* 34, 243–259.

Salman, V., Amann, R., Shub, D. A., and Schulz-Vogt, H. N. (2012). Multiple self-splicing introns in the 16S rRNA genes of giant sulfur bacteria. *Proc. Natl. Acad. Sci.* 109, 4203–4208.

Schulz, H. N., Brinkhoff, T., Ferdelman, T. G., Mariné, M. H., Teske, A., and Jørgensen, B. B. (1999). Dense Populations of a Giant Sulfur Bacterium in Namibian Shelf Sediments. *Science* 284, 493–495.

Schulz, H. N., and Schulz, H. D. (2005). Large Sulfur Bacteria and the Formation of Phosphorite. *Science* 307, 416–418.

Sheik, C. S., Jain, S., and Dick, G. J. (2013). Metabolic flexibility of enigmatic SAR324 revealed through metagenomics and metatranscriptomics. *Environ. Microbiol.*, [DOI: 10.1111/1462-2920.12165] (2013/10/09).

Strittmatter, A. W., Liesegang, H., Rabus, R., Decker, I., Amann, J., Andres, S., Henne, A., Fricke, W. F., Martinez-Arias, R., Bartels, D., *et al.* (2009). Genome sequence of *Desulfobacterium autotrophicum* HRM2, a marine sulfate reducer oxidizing organic carbon completely to carbon dioxide. *Environ. Microbiol.* 11, 1038–1055.

Strohl, W. R., and Larkin, J. M. (1978). Enumeration, isolation, and characterization of *Beggiatoa* from freshwater sediments. *Appl. Environ. Microbiol.* 36, 755–770.

Strohl, W. R., Schmidt, T. M., Vinci, V. A., and Larkin, J. M. (1986). Electron transport and respiration in *Beggiatoa* and *Vitreoscilla*. *Arch. Microbiol.* 145, 71–75.

Tanaka, S., Lee, S.-O., Hamaoka, K., Kato, J., Takiguchi, N., Nakamura, K., Ohtake, H., and Kuroda, A. (2003). Strictly polyphosphate-dependent glucokinase in a polyphosphate-accumulating bacterium, *Microlunatus phosphovorus*. *J. Bacteriol.* 185, 5654–5656.

Tang, K.-H., Feng, X., Zhuang, W.-Q., Alvarez-Cohen, L., Blankenship, R. E., and Tang, Y. J. (2010). Carbon flow of Heliobacteria is related more to *Clostridia* than to the Green Sulfur Bacteria. *J. Biol. Chem.* 285, 35104–35112.

Taylor, S. C., Dalton, H., and Dow, C. S. (1981). Ribulose-1,5-bisphosphate carboxylase/oxygenase and carbon assimilation in *Methylococcus capsulatus* (Bath). *J. Gen. Microbiol.* 122, 89–94.

Thauer, R. K., Kaster, A.-K., Seedorf, H., Buckel, W., and Hedderich, R. (2008). Methanogenic archaea: Ecologically relevant differences in energy conservation. *Nat. Rev. Microbiol.* 6, 579–591.

Vargas, A., and Strohl, W. R. (1985). Utilization of nitrate by *Beggiatoa alba*. *Arch. Microbiol.* 142, 279–284.

Vershinina, O. A., and Znamenskaya, L. V. (2002). The Pho regulons of bacteria. *Microbiology* 71, 497–511.

Ward, N., Larsen, Ø., Sakwa, J., Bruseth, L., Khouri, H., Durkin, A. S., Dimitrov, G., Jiang, L., Scanlan, D., Kang, K. H., *et al.* (2004). Genomic insights into methanotrophy: The complete genome sequence of *Methylococcus capsulatus* (Bath). *PLoS Biol* 2, e303.

Wilmotte, A., Van der Auwera, G., and De Wachter, R. (1993). Structure of the 16S ribosomal RNA of the thermophilic cyanobacterium *Chlorogloeopsis* HTF ("*Mastigocladus laminosus* HTF") strain PCC7518, and phylogenetic analysis. *FEBS Lett.* 317, 96–100.

Zumft, W. G. (1997). Cell biology and molecular basis of denitrification. *Microbiol. Mol. Biol. Rev.* 61, 533–616.

ChapterV

Synopsis

This part of my thesis summarizes the major achievements of the publications and discusses them in a broader view. Moreover I present results of additional experiments, which are related to the topics of the individual publications. Nevertheless, this part does not replace the discussion of the three publications.

1. Niche differentiation of aerobic and anaerobic ammonia-oxidizing microorganisms in the Guaymas Basin sediment

Hydrothermal vent systems are highly dynamic ecosystems with a broad range of energy sources mostly in the form of inorganic compounds that are used by chemosynthetic microbial communities. Nitrification, the aerobic oxidation of ammonia to nitrite and further to nitrate has only been scarcely studied in hydrothermal vent systems, although indications for this metabolism are found in the literature (Bourbonnais *et al.*, 2012; McHatton *et al.*, 1996). Before I started my thesis there were only two studies published that investigated the ammonia oxidation at hydrothermal systems, namely in the hydrothermal plume (Lam *et al.*, 2004, 2008). Besides that, one study targeted anammox in chimneys and mussel beds (Byrne *et al.*, 2008).

The nitrification rates up to 74 - 605 µmol N l^{-1} mat d^{-1} that we measured with two independent methods in sulfur-oxidizing *Beggiatoa* mats of the Guaymas Basin (Chapter II) are the highest rates that were so far reported for deep-sea ecosystems. This suggests that the process is likely ecologically relevant for the benthic zones in the Guaymas Basin and might also occur in *Beggiatoa* mats such as coastal sediments or cold seeps (Jørgensen, 1977; Kalanetra *et al.*, 2005; Kalanetra and Nelson, 2010; Grünke *et al.*, 2011). Moreover, out of five investigated gene libraries (340 clones), two from *Beggiatoa* mats and one from hydrothermal sediment showed the highest microdiversity of the ammonia monooxygenase subunit A (amoA) that were found. Most likely this reflects different niches due to steep thermal and chemical gradients in the system. Especially the *Beggiatoa* mats create microenvironments of oxic, suboxic and anoxic conditions (van Gemerden, 1993). The *Beggiatoa* microecosystems of Guaymas Basin did not show a higher diversity than bare hydrothermal sediments based on *amoA* genes (Chapter II). However, mats of SOB in general are associated with specific bacterial communities (Mills *et al.*, 2004; Prokopenko *et al.*, 2006, 2013). A specific association of functionally different groups would explain the high beta diversity (species/ OTU turnover between sampling sites) that was observed between different *Beggiatoa* mats of the system (Meyer *et al.*, 2013).

Any attempt to detect a possible contribution to ammonium oxidation by anammox bacteria in the *Beggiatoa* mats failed, although these bacteria have been shown to be associated with the closely related SOB *Thioploca* (Prokopenko *et al.*, 2006, 2013). Functional genes, such as the nitrite reductase (*nirS*) specific for *Scalindua* spp. (Lam *et al.*, 2009), or specific anammox bacterial 16S rRNA genes could not be amplified from that mats, although relatively high numbers of the corresponding phylum *Plantomycetes* (approx. 8%) were detected by FISH (Winkel, 2009). Stable isotope pairing incubations with ^{15}N-ammonium and ^{14}N-nitrite showed very low anammox rates, which were often below the detection limit (data not shown).

Hence, all analyses pointed towards nitrification as an important process in mats of large SOB. Moreover, AOA seemed to be the key nitrifying microorganisms that always outnumbered AOB by up to 100-fold (Chapter II), as shown for other ecosystems (Leininger *et al.*, 2006; Wuchter *et al.*, 2006; Beman *et al.*, 2008; Mußmann *et al.*, 2011). High nitrification rates in sulfidic (up to 1 mM) environments such as the *Beggiatoa* mats (McKay *et al.*, 2012) might be due to lower sulfide sensitivity of AOA compared to AOB. The latter are already inhibited by less than 10 µM sulfide concentrations (Sears *et al.*, 2004). Contrastingly, many AOA tolerate higher sulfide concentrations of up to 100-500 µM (Caffrey *et al.*, 2007). However, in upper parts of the mats and the overlaying water column with low sulfide concentration (Fig. 13) AOB might still oxidize ammonium at high rates. This was shown by inhibition experiments that suggested niches for both AOA and AOB in *Beggiatoa* mats. Allylthiourea (ATU) at used concentrations of 100 µM only partially inhibits AOA (approximately 70%), while it completely inhibits AOB (Santoro and Casciotti, 2011). One *Beggiatoa* mat showed a full inhibition of the nitrification that pointed towards AOB-driven nitrification, while a second *Beggiatoa* mat were only partial inhibited. The inhibited mat still showed 39% of the ATU-free mat that might be due to AOA.

Marine AOA are inhibited by ammonium concentrations (≥ 2 mM) (Martens-Habbena *et al.*, 2009), which were exceeded in the *Beggiatoa* mat (up to 5 mM; Chapter II). A higher tolerance has only been reported for AOA members of the thaumarchaeotal group I.1b that still perform ammonia oxidation at levels of up to 10-20 mM (Tourna *et al.*, 2011; Jung *et al.*, 2011). The adaptation to high ammonium concentrations could be unique for AOA of sediment-hosted hydrothermal systems in contrast to other marine AOA. Usually AOB tolerate much higher ammonium levels (50 to 1000 mM) (Koops and Pommerening-Röser, 2005) and would have been expected to dominate over AOA under the concentrations that are found in the *Beggiatoa* mats and hydrothermal sediments of the Guaymas Basin. Therefore,

other factors such as the adaptation to low oxygen (Lam *et al.*, 2007, 2009) or the mentioned tolerance for higher sulfide levels could favor AOA in sediment-hosted hydrothermal

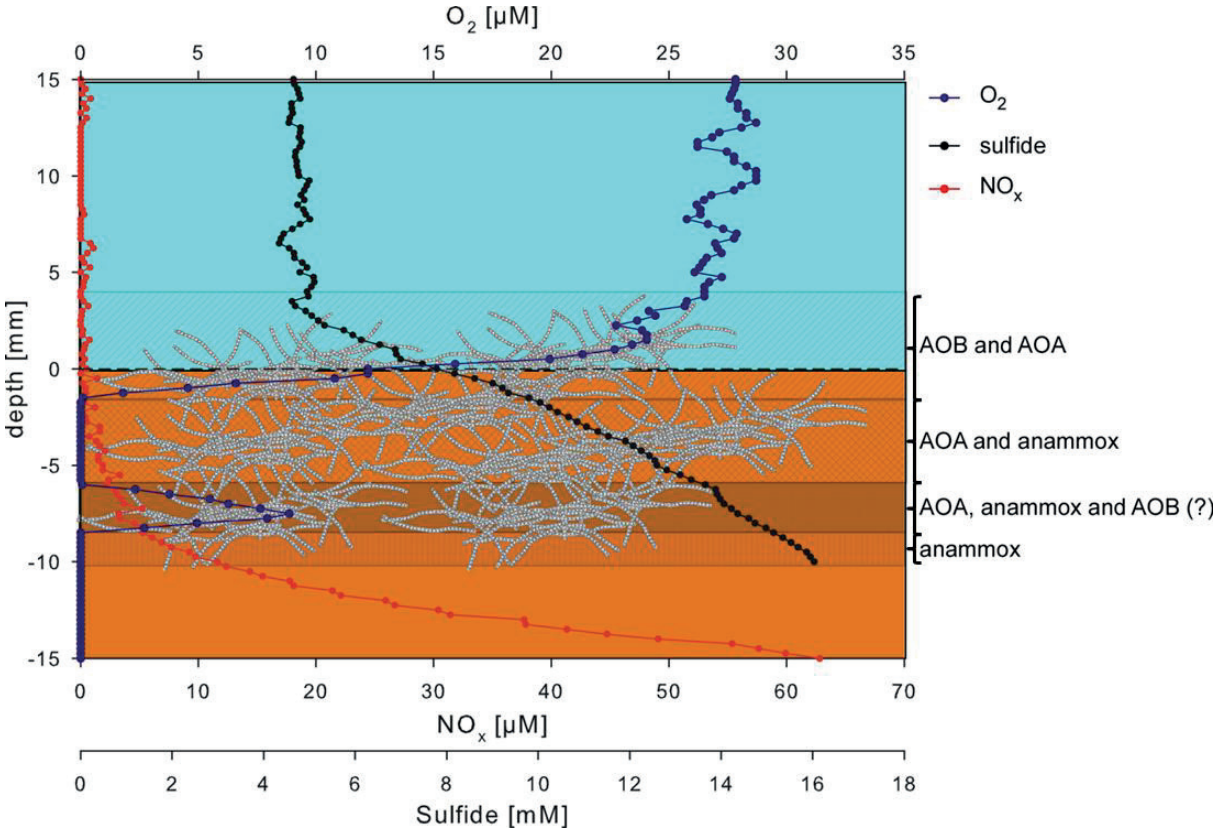

Figure 13: Model of the distribution of ammonia-oxidizing microorganisms in *Beggiatoa* mats. The different horizontal bars represent different niches based on sulfide and oxygen concentrations. Microsensor profiles are those from sample BM1 see Chapter II.

systems. Inhibition experiments suggested niches for both AOA and AOB in *Beggiatoa* mats. Allylthiourea (ATU) at used concentrations of 100 µM only partially inhibits AOA (approximately 70%), while it completely inhibits AOB. One *Beggiatoa* mat showed a full inhibition of the nitrification that pointed towards AOB-driven nitrification, while a second *Beggiatoa* mat were only partial inhibited. The inhibited mat still showed 39% of the ATU-free mat that might be due to AOA.

The model in Figure 13 demonstrates the possible location of AOA, AOB and anammox bacteria in the *Beggiatoa* mat that are influenced by the steep gradients of sulfide and oxygen.

2. Microbe-microbe interactions

In our study (Chapter II) we found indications that nitrifying communities are associated with *Beggiatoa* mats and provide them with nitrate as electron acceptor. Nitrate is internally stored by *Beggiatoa* and other related, large SOB such as *Thioploca* and *Thiomargarita* (Chapter

IV). The nitrate concentration in the vacuole is elevated by up to 20,000-fold compared to ambient seawater (Fossing *et al.*, 1995; McHatton *et al.*, 1996) and is respired via the DNRA under anoxic conditions (Chapter IV) (Sayama *et al.*, 2005; Preisler *et al.*, 2007). The release of ammonia by *Beggiatoa* and the re-oxidation of ammonia to nitrate could facilitate an internal cycling of nitrogen within the *Beggiatoa* mats (Chapter II, Figure 6). However, the extent of nitrogen recycling is unclear, since nitrate was permanently available in the water column (approx. 20 µM) and ammonium concentrations of the diffuse fluids were high. Optionally, large SOB may respire their internal nitrate pool via denitrification (Chapter IV), which would yield more energy than DNRA (Jørgensen and Nelson, 2004), but would result in an N-loss for the system. It is generally assumed that large SOB rather perform DNRA (Jørgensen and Nelson, 2004; Sayama *et al.*, 2005; Preisler *et al.*, 2007), however, genetic (Mußmann *et al.*, 2007; MacGregor *et al.*, 2013) and biogeochemical (Mußmann *et al.*, 2007) evidence pointed at a denitrification potential of large SOB. Moreover, the genome comparison of the large SOB in my thesis, showed genes for both pathways (Chapter IV) in most of the analyzed large SOB. Yet, it is not clear if they can use both pathways and under what conditions DNRA or denitrification would be active. Future studies should therefore consider thermodynamic calculations of both pathways under *in situ* conditions in combination with tracer experiments and enzyme activity measurements to clarify pathways of nitrate respiration in large SOB.

The association of AOA with *Beggiatoa* shown by CARD-FISH (Chapter II) supported an interaction between these two microorganisms and a possible coupling of the nitrogen and sulfur cycle. In contrast, AOB were less often found to be associated with filaments and occurred more often as single cells. Most of the *Beggiatoa* filaments with AOA attached to the surface had a narrow diameter of 5-10 µm. An examination of the larger filaments was not possible due to high background fluorescence. Even for narrow filaments without a central vacuole it would be beneficial to be constantly supplied with nitrate during migration between the oxic and sulfidic layers of the sediment. The larger filaments with a central vacuole would also have an advantage from an interaction with AOA. When internally stored nitrate is used up in suboxic layers of the sediment, AOA and unidentified nitrite-oxidizing bacteria (NOB) could provide SOB with additional nitrate under these oxygen limited conditions. Thus, both nitrifiers could provide nitrate to the *Beggiatoa* filaments via nitrification under suboxic conditions. AOA are known to be ideally adapted to suboxic conditions, since they are found in similar conditions of oxygen minimum zones (Lam *et al.*, 2007, 2009; Molina and Farías, 2009). Furthermore, temporal flushes of oxygen into the mat (Chapter II) (Gundersen *et al.*,

1992) create temporary oxic conditions, while the amount of oxygen might be to little for the larger SOB to oxidize sulfide. The input of oxygen into the mat could also create niches for AOB that are more adapted to higher oxygen concentrations. By attaching to gliding SOB AOA/AOB would benefit from becoming mobile, thus e.g. not getting buried by sedimentation events. Moreover, SOB may lower locally high sulfide concentrations that might otherwise inhibit nitrification. Furthermore, AOA could be transported into layers with higher ammonium supply (Magenheim and Gieskes, 1992), since they tolerate more sulfide than AOB (Caffrey *et al.*, 2007; Erguder *et al.*, 2009). Astonishingly, in an attempt to enrich AOA from marine sediments co-cultured SOB oxidized thiosulfate and depleted oxygen that favored growth of AOA (Park *et al.*, 2010). Such an association further points towards an interaction of AOA and SOB that might live in a kind of syntrophy. Possible NOB that are necessary to convert the toxic nitrite into nitrate were not found. Interestingly, a recent metagenomic study of nitrogen-driven microbial communities in underwater caves assigned genes for the nitrate/nitrite oxidoreductase (key enzyme for nitrite oxidation) to *Thaumarchaeota* (Tetu *et al.*, 2013). One could speculate that besides known bacterial NO also archaeal NO exist in nature that has similar physiological adaptations like AOA.

While the nitrification in mats of large SOB in hydrothermal systems could be identified as an important process driven by AOA, AOB and yet not clear identified NO, it remains open how specific such an association is. It might also be that *Beggiatoa* filaments only serve as a substrate for attachment of nitrifying microorganisms. The filamentous mats offer a better surface for attachments than sediments and with their mobility helps to perfectly position the nitrifying into the ammonium-rich fluids However, observed ammonium profiles under *Beggiatoa* mats of cold seeps (Boetius and Suess, 2004; Joye *et al.*, 2004), hypersaline mats (Hinck *et al.*, 2007) and coastal marine environments (Sayama, 2001) showed high concentrations that might point to similar association. Moreover, archaeal populations associated with *Beggiatoa* mats are often phylogenetically related to the group I.1a of the *Thaumarchaetoa* (Mills *et al.*, 2004; Lösekann *et al.*, 2007; Crépeau *et al.*, 2011). So I propose that a close relation of AOA and SOB is not only found in hydrothermal systems but is rather typical for marine sediments with steep sulfide gradients and high ammonium concentrations. Mat formation might be influenced by the combination of high sulfide concentrations and elevated ammonium concentrations that supports an active nitrifying community.

Future studies should target microbial interactions with combinations of biogeochemical rate measurements, specific inhibition of AOB or AOA and an identification of corresponding

microorganisms with culture-independent methods. A more direct approach is to study the incorporation of stable isotope labeled substrates into *Beggiatoa* populations by nanoSIMS combined and to see an incorporation of $15NO_3^-$ into their vacuoles.

Furthermore it should be investigated if nitrification also occurs in sediment-free MOR systems, with low ammonium concentrations (5-30 µM) in the fluids (Chapter III).

3. Ammonia-oxidizing archaea in a rock-hosted hydrothermal vent system

In Menez Gwen measured ammonium concentrations were low ranging from 5-29 µM, whereas seawater concentrations were three times higher 67 µM. Nevertheless, these concentrations are still sufficient for ammonia oxidation by archaea (Martens-Habbena *et al.*, 2009). Amplification and sequencing of 16S rRNA genes in the fluids showed potential AOA of the Marine Group I (MGI) *Thaumarchaeota*, which often correlate with archaeal *amoA* gene copy numbers (Wuchter *et al*., 2006; Mincer *et al*., 2007) . Therefore, we wanted to test if nitrification in particular ammonia oxidation is more widespread in hydrothermal systems than previously assumed. To investigate potential ammonia oxidation in the diffuse fluids of the rock-hosted Menez Gwen vent field, I used two different approaches. One approach was to amend retrieved fluids with ammonium chloride (final concentration 3 mM). Enrichments were grown at 4°C and room temperature. Unfortunately, none of the enrichments showed growth or production of nitrate. One possibility might be that the ammonia concentration was too high, as the initial isolation of a marine AOA were achieved with a three times lower concentration of 1 mM (Könneke *et al.*, 2005). Another reason might be that AOA have to be isolated in co-culture with other organisms that keep oxygen levels low (Park *et al.*, 2010). Further investigations to isolate AOA should use additional carbon substrates, since there are several indications that some AOA might be heterotrophs and only facultatively use inorganic carbon (Agogué *et al.*, 2008; Tourna *et al.*, 2011; Mußmann *et al.*, 2011; Xu *et al.*, 2012; French *et al.*, 2012) (see also section 6 this chapter). In the second approach I extracted DNA from fluids and amplified the archaeal *amoA*. The gene library showed a similar diversity to that of the bottom water from the Guaymas Basin with minimum sequence identity of 83%, while most of the sequences (71.4%) fell into one operational taxonomic unit (OTU; >98% sequence identity; Fig. 14).

Surprisingly, almost all of the retrieved sequences (>99%) from all hydrothermal compartments (including sequences from the Guaymas Basin) were not closely related (78-96% sequence identity) to the only cultivated AOA "*Nitrosopumilus maritimus"* of the

thaumarchaeotal group I.1a (Könneke *et al.*, 2005), which suggests a high diversity of *amoA*. This high diversity (minimum 68% sequences identity) is further confirmed by a manually aligned and curated non-redundant *amoA* database (18,250 sequences; 08.09.2013) covering a huge spectrum of different ecosystems (see Appendix).

The preliminary analysis of AOA in rock-hosted systems indicated an ammonia-oxidizing community that might be active and involved in nitrification. Theses ammonia-limited systems needs further investigations to clarify the contribution of AOA to the nitrogen and carbon cycle.

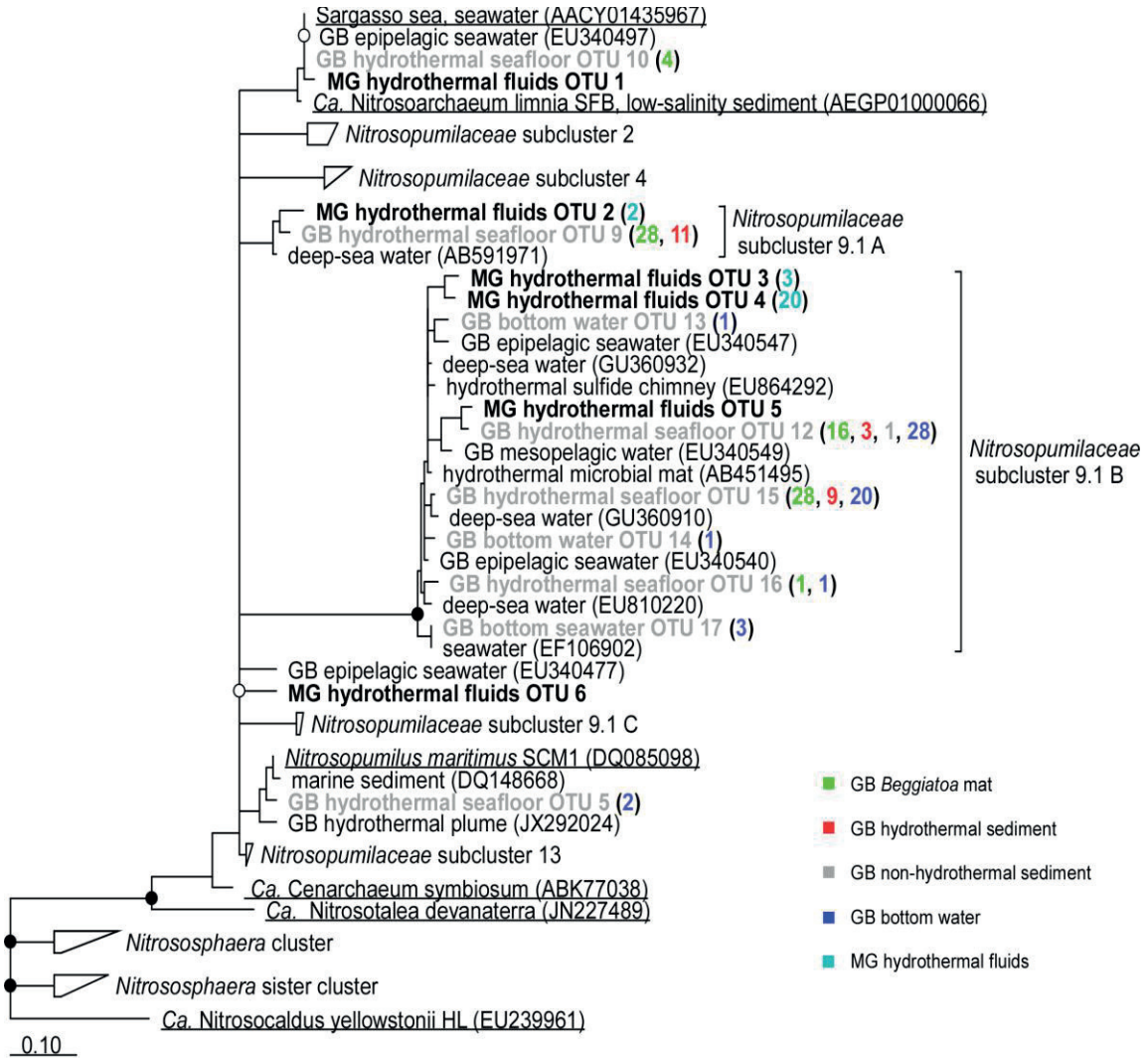

Figure 14: Consensus tree of archaeal AmoA sequences from compartments in the hydrothermal systems of the Guaymas Basin and Menez Gwen. Open circles indicate >70% bootstrap support, closed circles indicate >90% bootstrap support (maximum likelihood). Scale bar corresponds to 10% sequence divergence.

4. Acetate-assimilating microbial populations in rock-hosted hydrothermal systems

The carbon cycle at hydrothermal vent systems is mostly influenced by chemolithotrophic processes, however, the consumption of produced organic compounds by heterotrophic or

mixotrophic microorganisms is also important and yet not well understood (Karl, 1995). Therefore I investigated acetate utilization in diffuse fluids from two geographically distant hydrothermal vent systems. In diffuse fluids with different temperatures (4°C-72°C), nanoSIMS combined with CARD-FISH identified distinct gammaproteobacterial and epsilonproteobacterial populations that assimilated acetate. The 289 analyzed cells showed enrichment of up 15% ^{13}C. In addition to acetate, ammonium was used as a general marker to target active cells, since ammonium is known to be the preferred nitrogen source for heterotrophic bacteria over other more oxidized nitrogen species such as nitrate (Kirchman and Wheeler, 1998). Individual cells showed up to 60% ^{15}N-enrichment. In the fluids from Menez Gwen we observed different assimilation patterns in the epsilonproteobacterial-dominated population that showed potential subpopulations. One of the subpopulations had low ^{13}C and high ^{15}N assimilation rates with average C:N ratio of 1:7.2. It is not clear why this subpopulation accumulated much more ammonium than other epsilonproteobacteria, since ammonium concentrations in the background (~ 7 µM) were equal to that amended in the experiments (10 µM). Thus ammonium should not be a limitation factor in the system. However, it might be that the active growth on an ideal substrate also stimulated the uptake of inorganic nitrogen sources and that they stored ammonium in the cells, which is known for other bacteria (Schmidt *et al.*, 2004). The other subpopulation showed a 1:2.7 C:N ratio and an almost linear relation between the two incorporated substrates (Chapter III). Here, cells with high incorporation of ^{13}C and ^{15}N might have divided several times and therefore showed an higher enrichment in the daughter cells, whereas cells that have not divided often show lower assimilation rates. The C:N ratio of both subpopulations showed that they incorporate more ^{13}C than ^{15}N, which have to be interpreted with caution, since only one carbon atom of the acetate was labeled. The increase in cell numbers in experiments with acetate also showed that they oxidize acetate, thus a large amount of the labeled ^{13}C should have been released as $^{13}CO_2$.

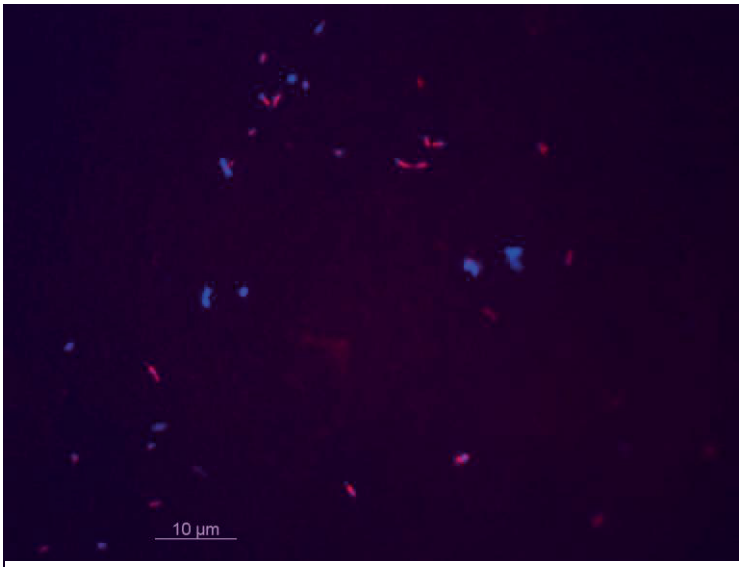

Figure 15: Nile red staining of Nautiliaceae cells after acetate assimilation. Red signals shows polyhydroxyalkanote inclusions, while blue signals shows DAPI counterstaining.

Some of novel identified Menez Gwen-specific *Nautiliaceae* cells (NautMG-group) showed high ^{13}C incorporation. Therefore we tested for storage compounds. In these NautMG cells polyhydroxyalkanoate (PHA) granules could be detected by nile red staining (Spiekermann *et al.*, 1999). Often the nile red signal did not appear in the typical dot like shape expected for PHAs (Fig. 15). This might be a methodological problem since the concentration of nile red often has to be optimized for samples. However, due to positive staining of some NautMG cells it can be assumed that part of the acetate is not oxidized or used as carbon source but stored as PHA.

The novel *Nautiliaceae* clade is the first report for an aerobic chemoorganoheterotrophic member of this family. All previously described *Nautiliaceae* live under anaerobic to microaerobic conditions and a few strains of the genus *Nautilia* are known to use organic compounds as additional carbon and energy sources (Campbell *et al.*, 2006). So far no member of the family has been described that can use organic compounds as energy sources under aerobic conditions (Campbell *et al.*, 2006; Sievert and Vetriani, 2012).

In contrast to the MAR system, *Gammaproteobacteria* dominated the active acetate assimilating community in the experiments with cold (4°C) to warm (37°C) fluids of the back-arc system, Manus Basin (Chapter III). This difference in active heterotrophic communities could be temperature-dependent, while *Gammaproteobacteria* in hydrothermal systems are often found in temperature ranges between 30-40°C, *Nautiliaceae* prefer higher temperatures of 37-60°C (Sievert and Vetriani, 2012). The acetate-assimilating *Gammaproteobacteria* were closely related to known heterotrophic groups such as *Marinobacter*, *Alteromonas*, and *Acinetobacter*. Sequences related to *Marinobacter* dominated the 37°C and were exclusively found in one replicate which showed the highest uptake in the bulk measurements of ^{13}C and ^{15}N. Unexpectedly, no sequences related to *Marinobacter* were found in the source fluids sample, which showed that the population was so low abundant that the sequencing coverage of our pyrosequencing approach was not enough to detect the population. Nevertheless, they strongly increased in only 8-12 h, which showed a perfect adaptation to a heterotrophic lifestyle. Interestingly, all detected *Gammaproteobacteria,* which included *Alcanivorax* related sequences of the Menez Gwen fluids, showed highest similarities to known hydrocarbon-degrading microorganisms. In a recent attempt to cultivate hydrothermal vent microorganisms and screen for new alkane degrading enzymes, Betrand and colleagues isolated one *Marinobacter* strain and two *Alcanivorax* strains (Bertrand *et al.*, 2013) closely related to the sequence from our incubations. It is not clear whether high concentrations of hydrocarbon exist in hydrothermal

systems. Furthermore, the detected groups of possible hydrocarbon degraders seem to be globally important and highly adapted to different environmental conditions (Head *et al.*, 2006; Yakimov *et al.*, 2007; Gutierrez *et al.*, 2013). The exact niche of heterotrophic microorganisms in hydrothermal system is still unclear.

The rapid response to acetate suggests a pre-adaptation of the microbial populations in rock-hosted hydrothermal vent systems. There are several potential sources in the system and acetate has measured in different hydrothermal systems (Martens, 1990; Zeng and Liu, 2000; Lang *et al.*, 2010). An abiotic formation via serpentinization and Fischer-Tropsch-type reaction has been predicted (Shock, 1992; McCollom and Seewald, 2003, 2006), although an exact confirmation of abiotic origin is difficult (Lang *et al.*, 2010). Another possibility could be the formation of acetate via thermal degradation of organic matter deposits in flanks of mid-oceanic ridges. The last possible source of acetate is via biological formation. Marc Lever and colleagues (Lever *et al.*, 2010) showed the formation of acetate via acetogenesis in subseafloor sediments of a hydrothermal system. A possible formation is also expected to occur in the subsurface of rock-hosted hydrothermal systems (M. Lever, personal communication). Another biological source of acetate in hydrothermal systems are mussels such as *Bathymodilus* spp. which produce acetate as a waste product (Pimenov *et al.*, 2002). This biologically produced acetate could be a major source, due to the high biomass of mussel populations in these systems (Desbruyères *et al.*, 2001). The ideal niche for the *Nautiliaceae* would be under the mussel bed since steep temperatures gradients form layers with temperatures of 40-60°C (Perner *et al.*, 2010) that is the optimal temperature range of most *Nautiliaceae* (Campbell *et al.*, 2006). In these zones they would have a constant supply with organic waste products from the mussel and high temperatures for an optimal growth. Instead *Gammaproteobacteria* would prefer a more moderate temperature and could grow between vent fauna patches as biofilms. It has to be considered that temperature is only one factor that could influence the composition of the heterotrophic communities. Other chemical and physical parameters such as pH, concentrations of sulfide or metals might be as relevant. The exact niche of these heterotrophs in natural systems is unclear. Further experiments with different carbon sources or temperature gradient experiments from the same source fluid could help to elucidate influencing factors.

5. Other heterotrophic populations

During the cruise at the Menez Gwen vent field I collected diffuse fluids and concentrated the microbes in the fluids by a cell trap. These cells, which were conserved in glycerol (19%) or betaine (4%), were used for enrichments.

In an attempt to enrich the NautMG-group glycerol-stored cells were inoculated into artificial seawater, which was amended with i) acetate and formate; ii) acetate and thiosulfate or iii) thiosulfate. In all three approaches we observed fast growth in the first 24 hours at *in situ* temperatures of 55°C. An analysis with epsilon- and gammaproteobacterial-specific probes gave no signals, whereas SYBR green staining showed uniform, small coccid cells with 0.5 µm in diameter for cetate and formate as well as for acetate and thiosulfate incubations (Fig. 16 A and B). Thiosulfate alone yielded different cell-morphologies (Fig.16 C). Amplification of bacterial 16S rRNA genes failed, whereas we were able to gain an

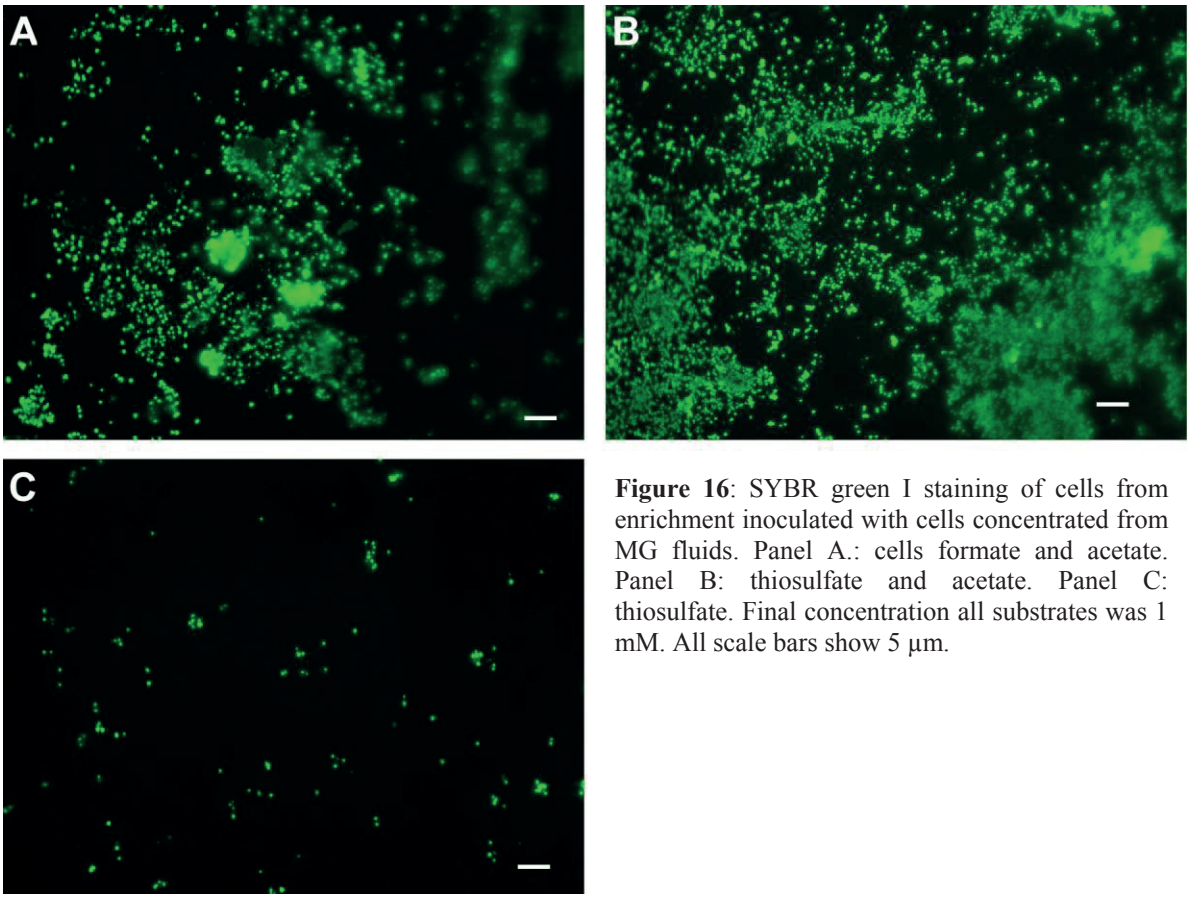

Figure 16: SYBR green I staining of cells from enrichment inoculated with cells concentrated from MG fluids. Panel A.: cells formate and acetate. Panel B: thiosulfate and acetate. Panel C: thiosulfate. Final concentration all substrates was 1 mM. All scale bars show 5 µm.

archaeal 16S rRNA gene product. Thus, *Archaea* that made up to 5% in the source fluid (D. Meier, personal communication) seemed to be highly enriched in these growth experiments. Pyrotag-sequencing of 16S rRNA genes showed an enrichment of MGI-thaumarchaeote (77% of all amplicons) in the acetate and thiosulfate enrichment, while the acetate and formiate enrichment were dominated by *Thermoplasmatales* of the *Euryarchaeota* (70% of all amplicons) (Fig. 17).

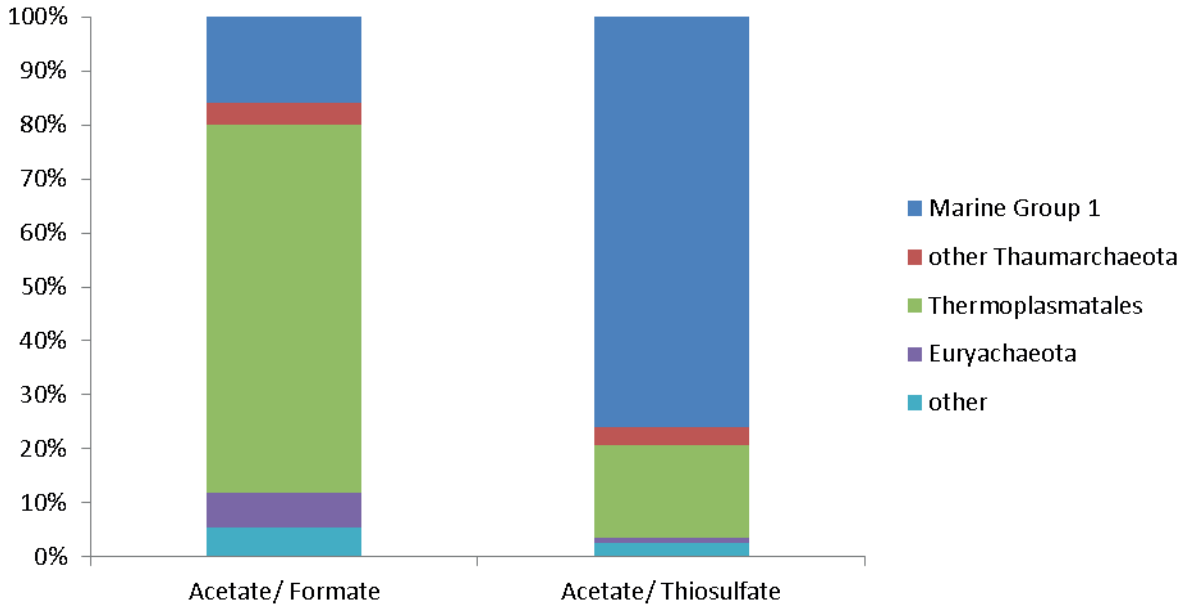

Figure 17: Archaeal 16S rRNA gene amplicons of 454 pyrosequencing from the enrichment. Acetate/ Formate library (n=1567 sequences) and Acetate/ Thiosulfate (n=6715 sequences)

Surprisingly, no heterotrophic MGI-thaumarchaeote has been isolated till today. MGI might also use organic compounds as carbon sources, since CO_2 fixation rates do not correlate with ammonia oxidation rates (Agogué *et al.*, 2008). The media also contained 0.5 mM ammonium that would be sufficient to fuel an ammonium oxidation with organic carbon instead of inorganic carbon. Furthermore, MGI are not known to grow under thermophilic conditions, although *amoA* genes have been amplified from hydrothermal altered sediment (Wang *et al.*, 2009; Nunoura *et al.*, 2010). FISH experiments have to confirm an enrichment of *Archaea*.

6. Final remarks and outlook

In my thesis I provide new insights into two microbial processes that have only rarely been studied in hydrothermal vent systems. Active nitrification was detected in a sediment-hosted hydrothermal system and might be more widespread in hydrothermal systems than previously assumed. Moreover, an association between nitrifying communities and large SOB might be found in other sediment-related systems. With the help of whole genome sequencing, it might be possible to understand the pathways of inorganic nitrogen sources and the intermediates that shuffled between functionally different groups like AOA, AOB, anammox bacteria and SOB. New syntrophic relationships between the latter have already be confirmed (Prokopenko *et al.*, 2006, 2013). Nitrification in rock-hosted systems has not yet been shown,

but significant ammonia concentrations and detection of archaeal *amoA* genes suggest that ammonia oxidation also occurs in these hydrothermal systems. However, the preliminary results of a possible heterotrophic AOA group that might use acetate as carbon source is of great interest for carbon and nitrogen cycling in deep-sea waters and hydrothermal systems. The enrichment with concentrated cells have to be repeated to isolate a heterotrophic MGI *Thaumarchaeota* and study its physiology. Moreover, by sequencing the genome of this group we would have genetic information of this successful group in the deep-sea.

The combination of nanoSIMS, deep-pyrosequencing and CARD-FISH analyses helped me to confirm the existents of a novel group within the *Nautiliaceae* of the *Epsilonproteobacteria* that live chemoorganoheterotrophically under aerobic, thermophilic conditions. However, until now it is not clear whether they can use additional energy sources, what their exact ecological niche is, if they are also found in other systems and how they contribute to the carbon cycle in hydrothermal vent ecosystems. A more detailed local screening in hydrothermal systems such as Menez Gwen and a global screening in other hydrothermal systemsshould be performed. Another possibility to study such a specific group would be to sequence single cell genomes and metagenomes, which gives insight in their metabolic potential.

In the field of microbial ecology sequencing of single cell genomes has developed rapidly due to lower costs. This leads to a deeper insight in the genetic potential of uncultured microorganisms and might help to define conditions that allow us to isolate these microorganisms. However, single cell genomics alone can only raise new hypotheses of metabolic pathways that have to be tested with pure cultures. Often microorganisms only grow in natural and laboratory conditions in co-culture with other microorganisms. Therefore, it is important to step away from pure culture approaches and to study microbial populations under controlled conditions of continuous cultures such as chemostats that allow investigating the physiology of uncultured microorganisms refusing to grow in pure cultures.

8. Reference

Agogué, H., Brink, M., Dinasquet, J., and Herndl, G. J. (2008). Major gradients in putatively nitrifying and non-nitrifying *Archaea* in the deep North Atlantic. *Nature* 456, 788–791.

Beman, J. M., Popp, B. N., and Francis, C. A. (2008). Molecular and biogeochemical evidence for ammonia oxidation by marine *Crenarchaeota* in the Gulf of California. *ISME J* 2, 429–441.

Bertrand, E. M., Keddis, R., Groves, J. T., Vetriani, C., and Austin, R. N. (2013). Identity and mechanisms of alkane-oxidizing metalloenzymes from deep-sea hydrothermal vents. *Front. Microbiol. Chem.* 4, 109.

Boetius, A., and Suess, E. (2004). Hydrate Ridge: A natural laboratory for the study of microbial life fueled by methane from near-surface gas hydrates. *Chem. Geol.* 205, 291–310.

Bourbonnais, A., Lehmann, M. F., Butterfield, D. A., and Juniper, S. K. (2012). Subseafloor nitrogen transformations in diffuse hydrothermal vent fluids of the Juan de Fuca Ridge evidenced by the isotopic composition of nitrate and ammonium. *Geochem. Geophys. Geosystems* 13, Q02T01.

Byrne, N., Strous, M., Crepeau, V., Kartal, B., Birrien, J.-L., Schmid, M., Lesongeur, F., Schouten, S., Jaeschke, A., Jetten, M., *et al.* (2008). Presence and activity of anaerobic ammonium-oxidizing bacteria at deep-sea hydrothermal vents. *ISME J* 3, 117–123.

Caffrey, J. M., Bano, N., Kalanetra, K., and Hollibaugh, J. T. (2007). Ammonia oxidation and ammonia-oxidizing bacteria and archaea from estuaries with differing histories of hypoxia. *ISME J* 1, 660–662.

Campbell, B. J., Engel, A. S., Porter, M. L., and Takai, K. (2006). The versatile ε-proteobacteria: key players in sulphidic habitats. *Nat. Rev. Microbiol.* 4, 458–468.

Crépeau, V., Cambon Bonavita, M.-A., Lesongeur, F., Randrianalivelo, H., Sarradin, P.-M., Sarrazin, J., and Godfroy, A. (2011). Diversity and function in microbial mats from the Lucky Strike hydrothermal vent field. *FEMS Microbiol. Ecol.* 76, 524–540.

Desbruyères, D., Biscoito, M., Caprais, J.-C., Colaço, A., Comtet, T., Crassous, P., Fouquet, Y., Khripounoff, A., Le Bris, N., Olu, K., *et al.* (2001). Variations in deep-sea hydrothermal vent communities on the Mid-Atlantic Ridge near the Azores plateau. *Deep Sea Res. Part Ocean. Res. Pap.* 48, 1325–1346.

Erguder, T. H., Boon, N., Wittebolle, L., Marzorati, M., and Verstraete, W. (2009). Environmental factors shaping the ecological niches of ammonia-oxidizing archaea. *FEMS Microbiol. Rev.* 33, 855–869.

Fossing, H., Gallardo, V. A., Jørgensen, B. B., Huttel, M., Nielsen, L. P., Schulz, H., Canfield, D. E., Forster, S., Glud, R. N., Gundersen, J. K., *et al.* (1995). Concentration and transport of nitrate by the mat-forming sulphur bacterium *Thioploca*. *Nature* 374, 713–715.

French, E., Kozlowski, J. A., Mukherjee, M., Bullerjahn, G., and Bollmann, A. (2012). Ecophysiological Characterization of ammonia-oxidizing archaea and bacteria from freshwater. *Appl. Environ. Microbiol.* 78, 5773–5780.

Van Gemerden, H. (1993). Microbial mats: A joint venture. *Mar. Geol.* 113, 3–25.

Grünke, S., Felden, J., Lichtschlag, A., Girnth, A.-C., De Beer, D., Wenzhöfer, F., and Boetius, A. (2011). Niche differentiation among mat-forming, sulfide-oxidizing bacteria at cold seeps of the Nile Deep Sea Fan (Eastern Mediterranean Sea). *Geobiology* 9, 330–348.

Gundersen, J. K., Jørgensen, B. B., Larsen, E., and Jannasch, H. W. (1992). Mats of giant sulphur bacteria on deep-sea sediments due to fluctuating hydrothermal flow. *Nature* 360, 454–456.

Gutierrez, T., Singleton, D. R., Berry, D., Yang, T., Aitken, M. D., and Teske, A. (2013). Hydrocarbon-degrading bacteria enriched by the Deepwater Horizon oil spill identified by cultivation and DNA-SIP. *ISME J.* (DOI: 10.1038/ismej.2013.98) (131013)

Head, I. M., Jones, D. M., and Röling, W. F. M. (2006). Marine microorganisms make a meal of oil. *Nat. Rev. Microbiol.* 4, 173–182.

Hinck, S., Neu, T. R., Lavik, G., Mußmann, M., de Beer, D., and Jonkers, H. M. (2007). Physiological adaptation of a nitrate-Storing *Beggiatoa* sp. to diel cycling in a phototrophic hypersaline mat. *Appl Env. Microbiol* 73, 7013–7022.

Jørgensen, B. B. (1977). Distribution of colorless sulfur bacteria (*Beggiatoa* spp.) in a coastal marine sediment. *Mar. Biol.* 41, 19–28.

Jørgensen, B. B., and Nelson, D. C. (2004). Sulfide oxidation in marine sediments: Geochemistry meets microbiology. *Geol. Soc. Am. Spec. Pap.* 379, 63–81.

Joye, S. B., Boetius, A., Orcutt, B. N., Montoya, J. P., Schulz, H. N., Erickson, M. J., and Lugo, S. K. (2004). The anaerobic oxidation of methane and sulfate reduction in sediments from Gulf of Mexico cold seeps. *Chem. Geol.* 205, 219–238.

Jung, M.-Y., Park, S.-J., Min, D., Kim, J.-S., Rijpstra, W. I. C., Sinninghe Damsté, J. S., Kim, G.-J., Madsen, E. L., and Rhee, S.-K. (2011). Enrichment and characterization of an autotrophic ammonia-oxidizing archaeon of mesophilic crenarchaeal group I.1a from an agricultural soil. *Appl. Environ. Microbiol.* 77, 8635–8647.

Kalanetra, K. M., Joye, S. B., Sunseri, N. R., and Nelson, D. C. (2005). Novel vacuolate sulfur bacteria from the Gulf of Mexico reproduce by reductive division in three dimensions. *Environ. Microbiol.* 7, 1451–1460.

Kalanetra, K. M., and Nelson, D. C. (2010). Vacuolate-attached filaments: highly productive *Ridgeia piscesae* epibionts at the Juan de Fuca hydrothermal vents. *Mar. Biol.* 157, 791–800.

Karl, D. M. (1995). "Ecology of free-living, hydrothermal vent microbial communities," in *Microbiology of Deep-Sea Hydrothermal Vents*, ed. D. M. Karl (CRC Press).

Kirchman, D. L., and Wheeler, P. A. (1998). Uptake of ammonium and nitrate by heterotrophic bacteria and phytoplankton in the sub-Arctic Pacific. *Deep Sea Res. Part Ocean. Res. Pap.* 45, 347–365.

Könneke, M., Bernhard, A. E., de la Torre, J. R., Walker, C. B., Waterbury, J. B., and Stahl, D. A. (2005). Isolation of an autotrophic ammonia-oxidizing marine archaeon. *Nature* 437, 543–546.

Koops, H.-P., and Pommerening-Röser, A. (2005). "The Lithoautotrophic Ammonia-Oxidizing Bacteria," in *Bergey's Manual® of Systematic Bacteriology*, eds. D. J. Brenner, N. R. Krieg, J. T. Staley, and G. M. G. Sc.D (Springer US), 141–147.

Lam, P., Cowen, J. P., and Jones, R. D. (2004). Autotrophic ammonia oxidation in a deep-sea hydrothermal plume. *FEMS Microbiol. Ecol.* 47, 191–206.

Lam, P., Cowen, J. P., Popp, B. N., and Jones, R. D. (2008). Microbial ammonia oxidation and enhanced nitrogen cycling in the Endeavour hydrothermal plume. *Geochim. Cosmochim. Acta* 72, 2268–2286.

Lam, P., Jensen, M. M., Lavik, G., McGinnis, D. F., Müller, B., Schubert, C. J., Amann, R., Thamdrup, B., and Kuypers, M. M. M. (2007). Linking crenarchaeal and bacterial nitrification to anammox in the Black Sea. *Proc. Natl. Acad. Sci.* 104, 7104–7109.

Lam, P., Lavik, G., Jensen, M. M., van de Vossenberg, J., Schmid, M., Woebken, D., Gutierrez, D., Amann, R., Jetten, M. S. M., and Kuypers, M. M. M. (2009). Revising the nitrogen cycle in the Peruvian oxygen minimum zone. *Proc. Natl. Acad. Sci.* 106, 4752–4757.

Lang, S. Q., Butterfield, D. A., Schulte, M., Kelley, D. S., and Lilley, M. D. (2010). Elevated concentrations of formate, acetate and dissolved organic carbon found at the Lost City hydrothermal field. *Geochim. Cosmochim. Acta* 74, 941–952.

Leininger, S., Urich, T., Schloter, M., Schwark, L., Qi, J., Nicol, G. W., Prosser, J. I., Schuster, S. C., and Schleper, C. (2006). Archaea predominate among ammonia-oxidizing prokaryotes in soils. *Nature* 442, 806–809.

Lever, M., Heuer, V., Morono, Y., Masui, N., Schmidt, F., Alperin, M., Inagaki, F., Hinrichs, K.-U., and Teske, A. (2010). Acetogenesis in deep subseafloor sediments of the Juan

de Fuca Ridge Flank: A synthesis of geochemical, thermodynamic, and gene-based evidence. *Geomicrobiol. J.* 27, 183–211.

Lösekann, T., Knittel, K., Nadalig, T., Fuchs, B., Niemann, H., Boetius, A., and Amann, R. (2007). Diversity and abundance of aerobic and anaerobic methane oxidizers at the Haakon Mosby Mud Volcano, Barents Sea. *Appl Env. Microbiol* 73, 3348–3362.

MacGregor, B. J., Biddle, J. F., Harbort, C., Matthysse, A. G., and Teske, A. (2013). Sulfide oxidation, nitrate respiration, carbon acquisition, and electron transport pathways suggested by the draft genome of a single orange Guaymas Basin *Beggiatoa* (*Cand*. Maribeggiatoa) sp. filament. *Mar. Genomics*. (DOI: 10.1016/j.margen.2013.08.001) (131013)

Magenheim, A. J., and Gieskes, J. M. (1992). Hydrothermal discharge and alteration in near-surface sediments from the Guaymas Basin, Gulf of California. *Geochim. Cosmochim. Acta* 56, 2329–2338.

Martens, C. S. (1990). Generation of short chain acid anions in hydrothermally altered sediments of the Guaymas Basin, Gulf of California. *Appl. Geochem.* 5, 71–76.

Martens-Habbena, W., Berube, P. M., Urakawa, H., de la Torre, J. R., and Stahl, D. A. (2009). Ammonia oxidation kinetics determine niche separation of nitrifying *Archaea* and *Bacteria*. *Nature* 461, 976–979.

McCollom, T. M., and Seewald, J. S. (2006). Carbon isotope composition of organic compounds produced by abiotic synthesis under hydrothermal conditions. *Earth Planet. Sci. Lett.* 243, 74–84.

McCollom, T. M., and Seewald, J. S. (2003). Experimental constraints on the hydrothermal reactivity of organic acids and acid anions: I. Formic acid and formate. *Geochim. Cosmochim. Acta* 67, 3625–3644.

McHatton, S. C., Barry, J. P., Jannasch, H. W., and Nelson, D. C. (1996). High nitrate concentrations in vacuolate, autotrophic marine *Beggiatoa* spp. *Appl. Environ. Microbiol.* 62, 954–958.

McKay, L. J., MacGregor, B. J., Biddle, J. F., Albert, D. B., Mendlovitz, H. P., Hoer, D. R., Lipp, J. S., Lloyd, K. G., and Teske, A. P. (2012). Spatial heterogeneity and underlying geochemistry of phylogenetically diverse orange and white *Beggiatoa* mats in Guaymas Basin hydrothermal sediments. *Deep Sea Res. Part Ocean. Res. Pap.* 67, 21–31.

Meyer, J. L., Akerman, N. H., Proskurowski, G., and Huber, J. A. (2013). Microbiological characterization of post-eruption “snowblower” vents at Axial Seamount, Juan de Fuca Ridge. *Front. Extreme Microbiol.* 4, 153.

Mills, H. J., Martinez, R. J., Story, S., and Sobecky, P. A. (2004). Identification of members of the metabolically active microbial populations associated with *Beggiatoa* species mat communities from Gulf of Mexico cold-seep sediments. *Appl. Environ. Microbiol.* 70, 5447–5458.

Mincer, T. J., Church, M. J., Taylor, L. T., Preston, C., Karl, D. M., and DeLong, E. F. (2007). Quantitative distribution of presumptive archaeal and bacterial nitrifiers in Monterey Bay and the North Pacific Subtropical Gyre. *Environ. Microbiol.* 9, 1162–1175.

Molina, V. and Farís, L. (2009).Aerobic ammonium oxidation in the oxycline and oxygen minimum zone of the eastern tropical South Pacific off northern Chile (~20°S). Deep Sea Res. Part II Top. Stud. Ocean. 56, 1032-1041.

Mußmann, M., Brito, I., Pitcher, A., Sinninghe Damsté, J. S., Hatzenpichler, R., Richter, A., Nielsen, J. L., Nielsen, P. H., Müller, A., Daims, H., *et al.* (2011). Thaumarchaeotes abundant in refinery nitrifying sludges express *amoA* but are not obligate autotrophic ammonia oxidizers. *Proc. Natl. Acad. Sci.* 108, 16771-16776.

Mußmann, M., Hu, F. Z., Richter, M., de Beer, D., Preisler, A., Jørgensen, B. B., Huntemann, M., Glöckner, F. O., Amann, R., Koopman, W. J. H., *et al.* (2007). Insights into the genome of large sulfur bacteria revealed by analysis of single filaments. *PLoS Biol* 5, e230.

Nunoura, T., Oida, H., Nakaseama, M., Kosaka, A., Ohkubo, S. B., Kikuchi, T., Kazama, H., Hosoi-Tanabe, S., Nakamura, K., Kinoshita, M., *et al.* (2010). Archaeal diversity and distribution along thermal and geochemical gradients in hydrothermal sediments at the Yonaguni Knoll IV hydrothermal field in the Southern Okinawa Trough. *Appl Env. Microbiol* 76, 1198–1211.

Park, B.-J., Park, S.-J., Yoon, D.-N., Schouten, S., Sinninghe Damste, J. S., and Rhee, S.-K. (2010). Cultivation of autotrophic ammonia-oxidizing archaea from marine sediments in coculture with sulfur-oxidizing bacteria. *Appl Env. Microbiol* 76, 7575–7587.

Perner, M., Petersen, J. M., Zielinski, F., Gennerich, H.-H., and Seifert, R. (2010). Geochemical constraints on the diversity and activity of H_2-oxidizing microorganisms in diffuse hydrothermal fluids from a basalt- and an ultramafic-hosted vent. *FEMS Microbiol. Ecol.* 74, 55–71.

Pimenov, N. V., Kalyuzhnaya, M. G., Khmelenina, V. N., Mityushina, L. L., and Trotsenko, Y. A. (2002). Utilization of methane and carbon dioxide by symbiotrophic bacteria in gills of *Mytilidae* (*Bathymodiolus*) from the Rainbow and Logachev hydrothermal fields on the Mid-Atlantic Ridge. *Microbiology* 71, 587–594.

Preisler, A., de Beer, D., Lichtschlag, A., Lavik, G., Boetius, A., and Jørgensen, B. B. (2007). Biological and chemical sulfide oxidation in a *Beggiatoa* inhabited marine sediment. *ISME J.* 1, 341.

Prokopenko, M. G., Hammond, D. E., Berelson, W. M., Bernhard, J. M., Stott, L., and Douglas, R. (2006). Nitrogen cycling in the sediments of Santa Barbara basin and Eastern Subtropical North Pacific: Nitrogen isotopes, diagenesis and possible chemosymbiosis between two lithotrophs (*Thioploca* and Anammox)--"riding on a glider." *Earth Planet. Sci. Lett.* 242, 186–204.

Prokopenko, M. G., Hirst, M. B., De Brabandere, L., Lawrence, D. J. P., Berelson, W. M., Granger, J., Chang, B. X., Dawson, S., Crane Iii, E. J., Chong, L., *et al.* (2013). Nitrogen losses in anoxic marine sediments driven by *Thioploca*-anammox bacterial consortia. *Nature* 500, 194–198.

Santoro, A. E., and Casciotti, K. L. (2011). Enrichment and characterization of ammonia-oxidizing archaea from the open ocean: phylogeny, physiology and stable isotope fractionation. *ISME J.* 5, 1796–1808.

Sayama, M. (2001). Presence of Nitrate-Accumulating Sulfur Bacteria and Their Influence on Nitrogen cycling in a shallow coastal marine sediment. *Appl. Environ. Microbiol.* 67, 3481–3487.

Sayama, M., Risgaard-Petersen, N., Nielsen, L. P., Fossing, H., and Christensen, P. B. (2005). Impact of bacterial NO_3^- transport on sediment biogeochemistry. *Appl. Environ. Microbiol.* 71, 7575–7577.

Schmidt, I., Look, C., Bock, E., and Jetten, M. S. M. (2004). Ammonium and hydroxylamine uptake and accumulation in *Nitrosomonas*. *Microbiology* 150, 1405–1412.

Sears, K., Alleman, J. E., Barnard, J. L., and Oleszkiewicz, J. A. (2004). Impacts of reduced sulfur components on active and resting ammonia oxidizers. *J. Ind. Microbiol. Biotechnol.* 31, 369–378.

Shock, E. L. (1992). Chapter 5 Chemical environments of submarine hydrothermal systems. *Orig. Life Evol. Biosph.* 22, 67–107.

Sievert, S., and Vetriani, C. (2012). Chemoautotrophy at deep-sea vents: Past, present, and future. *Oceanography* 25, 218–233.

Spiekermann, P., Rehm, B. H. A., Kalscheuer, R., Baumeister, D., and Steinbüchel, A. (1999). A sensitive, viable-colony staining method using Nile red for direct screening of bacteria that accumulate polyhydroxyalkanoic acids and other lipid storage compounds. *Arch. Microbiol.* 171, 73–80.

Tetu, S. G., Breakwell, K., Elbourne, L. D. H., Holmes, A. J., Gillings, M. R., and Paulsen, I. T. (2013). Life in the dark: metagenomic evidence that a microbial slime community is driven by inorganic nitrogen metabolism. *ISME J.* 7, 1227-1236

Tourna, M., Stieglmeier, M., Spang, A., Könneke, M., Schintlmeister, A., Urich, T., Engel, M., Schloter, M., Wagner, M., Richter, A., *et al.* (2011). *Nitrososphaera viennensis*, an ammonia oxidizing archaeon from soil. *Proc. Natl. Acad. Sci.* 108, 8420-8425

Wang, S., Xiao, X., Jiang, L., Peng, X., Zhou, H., Meng, J., and Wang, F. (2009). Diversity and abundance of ammonia-oxidizing archaea in hydrothermal vent chimneys of the Juan de Fuca Ridge. *Appl Env. Microbiol* 75, 4216–4220.

Winkel, M. (2009). Nitrifizierende Mikroorganismen in hydrothermalen Systemen des Guaymas Becken. Diploma

Wuchter, C., Abbas, B., Coolen, M. J. L., Herfort, L., van Bleijswijk, J., Timmers, P., Strous, M., Teira, E., Herndl, G. J., Middelburg, J. J., *et al.* (2006). Archaeal nitrification in the ocean. *Proc. Natl. Acad. Sci.* 103, 12317–12322.

Xu, M., Schnorr, J., Keibler, B., and Simon, H. M. (2012). Comparative analysis of 16S rRNA and *amoA* genes from archaea selected with organic and inorganic amendments in enrichment culture. *Appl. Environ. Microbiol.* 78, 2137–2146.

Yakimov, M. M., Timmis, K. N., and Golyshin, P. N. (2007). Obligate oil-degrading marine bacteria. *Curr. Opin. Biotechnol.* 18, 257–266.

Zeng, Y., and Liu, J. (2000). Short-chain carboxylates in fluid inclusions in minerals. *Appl. Geochem.* 15, 13–25.

Acknowledgements

First a special thanks to **Prof. Dr. Rud(i)olf Amann** for introducing me to the fantastic MolEcol group and for all the support over the last 4 years. Your enthusiastic way to explain the secrets of microbial ecology always motivated me. Also thanks for reviewing this thesis. I would like to thank **Dr. Marc Mußmann** for all his patience during this thesis and always believing in me. You helped me to think logically, write in a proper scientific language and work on three fascinating topics. I specially thank you for the opportunity to participate on the cruise to the Menez Gwen hydrothermal vent field, an unforgettable experience. At this point I would also like to thank the chief scientist, **Prof. Dr. Nicole Dubilier**, for the perfect organization and the nice working atmosphere during the weeks on board. **Prof. Dr. Wolfgang Bach** is acknowledged for willing to review this thesis and for the opportunity to use the REM in his department. Thanks to **Prof. Dr. Ulrich Fischer, Dr. Anke Meyerdierks and Dr. Gaute Lavik** for been part of my thesis committee.
I would also like to thank all the excellent students that have supported the work in the different projects, thanks to **Elizabeth K. Robertson, Maria Suciu, and Katrin Schmidt** for hours and hours in the lab.
A very special thanks goes to the best office mates you can think of. **Silke** and **Nicole** without your knowledge with every problem regarding molecular techniques and an open ear for personal problems this thesis would have not the same quality. **Emil** words can not tell how much I have to thank you. You not even helped with discussing literally every topic in all parts of life, but also improved this thesis by proofreading the important parts. I am looking forward for our first shared project. Thanks also to my long-time companions **Anna** and **Sven**, finally we reach (or have reached) the end of our academic carriers. **Anna, Janis** and **Petra** I thank you for proofreading parts of this thesis and helping to improve the understanding and layout.
Thanks also to all my other MPI colleagues, **Cecilia and Jörg** (best bench mates), **Andreas E**., **Regina, Lars, Dennis F., Dimitri, Jill, Bernhard** (thanks for your motivation), **Christian B. and Christian L.** (I will never forget our mid-night "Brötchen Platten", thanks for all the special support), **Christiane** (MarMic mum), **Stefan D.**, **Marion, Mina, Harald** (thanks for all the wonderful discussions and bringing me save to my hotel in Seattle), **Manuel** (thanks for numerous nanoSIMS sessions and wonderful discussions of genetic pathways), **Amandine, Adrien, Judith Z.** (thanks for willing to join my committee)**, Michael** (thanks for always finding time to help me with bioinformatic problems), **Elmar, Christian Q., Jost, Andreas K.** (thanks for nanoSIMS support), **Stefan T.** (the best "Onion"), **Verena** (SOB queen), **Anne-Christin**, **Kathleen**, **Thomas H., Thomas W., Judith N.**, **Mari, Viola, Phillipp** and my favorite Mensa group **Alban, Christina, Gunther, Gerd and Daphne.**

I like to thank **my parents** for all the support during my studies, without you I would be not the same person. A very special thanks goes to **Jenny** (my angel), who gave birth to our beautiful child's **Rahel and Joshua** and did a unbelievable job during the final phase of this thesis. Thank you so much you believed in me and have dealt perfectly with all my moods after short nights. I love you.

Table S2: Nitrogen metabolism of *Candidatus* Thiomargarita nelsonii compared to other large, colorless SOB

product	gene	locus	E.C.	contig	AA	truncated	full	other large, colorless SOB	comment
Membrane-bound cytoplasmic nitrate reductase									
nitrate reductase, alpha subunit	*narG*	THI2233_0 THI39_2	1.7.99.4	THI2233 THI39	261 31	+ 		BOGUAY_0051 BOGUAY_0489 BGP_0139 BGP_3372 BGP_5024	
nitrate reductase, beta subunit	*narH*	THI39_1 THI713_1	1.7.99.4	THI39 THI713	497 394	+ +	+ 	BOGUAY_0490 BOGUAY_0049 BGP_4035 BGP_4784	
nitrate reductase, delta subunit	*narJ*	THI39	1.7.99.4	THI39	173		+	BOGUAY_0491 BGP_4033	molybdenum cofactor assembly chaperone
nitrate reductase, gamma subunit	*narI*	THI21821642981 THI3912301888	1.7.99.4	THI2182 THI39	213 75	+ +		BA07_32 BOGUAY_0492 BOGUAY_1505 BGP_2700	
nitrate reductase-like protein	*narX*	THI762_2 THI922_0	1.7.99.4	THI762 THI922	259 552	+ +		BOGUAY_0048 BOGUY_0146	
nitrate/ nitrite transporter	*narK*	THI3014□f2		THI3014	204	+		BGP_3802	
Periplasmic nitrate reductase									
nitrate reductase, periplasmatic, large subunit	*napA*	THI153 THI1149	1.7.99.4	THI153 THI1149	835 417	+ +	+ 	BA14_107 BOGUAY_0671 BGP_1198	
nitrate reductase, small subunit	*napB*	THI28521118749	1.7.99.4	THI2852	38	+		BA14_110 BOGUAY_0672 BGP_1425	

product	gene	locus	E.C.	contig	AA	truncated	full	other large, colorless SOB	comment
nitrate reductase cytochrome c-type protein	*napC*	THI214_0	1.7.99.4	THI214	222		+	BA14_111 BOGUAY_3233 BGP_1197 FLOR_01446	
nitrate reductase, ferredoxin-type potein	*napH*	THI25_1	1.7.99.4	THI25	315	+			
nitrate reductase, ferredoxin-type potein	*napG*	THI153_0 THI485_1	1.7.99.4	THI153 THI485	254 247		+	BA14_108	
nitrate reductase, periplasmatic	*napD*		1.7.99.4					BA14_106 BGP_1199	
nitrate reductase, ferredoxin-type potein	*napF*		1.7.99.4					BA14_105 BOGUAY_5179 BGP_1200	
nitrate reductase, large subunit	*nasA*	THI2051	1.7.99.4	THI2051	285	+		BA07_47	assimilatory nitrate reduction to ammonia
Cytoplasmic assimilatory/ dissimilatory nitrite reductase									
nitrite reductase, NAD(P)H large subunit	*nirB*	THI1112_0 THI111216991119 THI1573112241393	1.7.1.4	THI1112 THI1573	216 232 407	+		BA07_49	dissimilatory nitrate reduction to ammonia as well as assimilatory
nitrite reductase, NAD(P)H small subunit	*nirD*		1.7.1.4					BA07_48	dissimilatory nitrate reduction to ammonia as well as assimilatory

product	gene	locus	E.C.	contig	AA	truncated	full	other large, colorless SOB	comment
nitrite reductase, ferredoxin	*nirA*		1.7.7.1					FLOR_00816	dissimilatory nitrate reduction to ammonia as well as assimilatory
Periplasmic disimilatory nitrite reductase									
nitrite reductase cytochrome cd1	*nirS*	THI245_1	1.7.2.1 1.7.99.1	THI245	591		+	BGP_1272 BOGUAY_2967	involved in denitrification
nitrite reductase, cytochrome c55X	*nirC*	THI245_0	1.7.2.1 1.7.99.1	THI245	107	+		BGP_1371	
nitrite reductase, cytochrome cd1	*nirF*	THI24519191429 THI303211221068	1.7.2.1 1.7.99.1	THI245 THI3032	305 39	+		BGP_1372	
nitrite reductase heme biosynthesis G protein	*nirG*	THI471_3	1.7.2.1 1.7.99.1	THI471	147		+	BGP_1275	
nitrite reductase heme biosynthesis H protein	*nirH*		1.7.2.1 1.7.99.1					BGP_4270	
nitrite reductase heme biosynthesis J protein	*nirJ*	THI2061_0	1.7.2.1 1.7.99.1	THI2061	261		+	BGP_3921 BGP_4010	
nitrite reductase heme biosynthesis E protein	*nirE*		1.7.2.1 1.7.99.1						
nitrite reductase heme biosynthesis N protein	*nirN*	THI762_0	1.7.2.1 1.7.99.1	THI762	94	+			
Membrane-bound nitric oxide reductase									
nitric oxide reductase	*norB*	THI459_4 THI692_1	1.7.99.7	THI459 THI692	111		+	BOGUAY_0863 BGP_3622 BGP_5178	
nitric oxide reductase	*norC*	THI166412121441	1.7.99.7	THI1664	69	+		BOGUAY_0144 BOGUAY_4015 BGP_5602	

product	gene	locus	E.C.	contig	AA	truncated	full	other large, colorless SOB	comment
nitric oxide activation protein	*norQ*	THI459_1 THI69217431595	1.7.99.7	THI459 THI692	267 246	+	+	BA08_50 BGP_2171 BGP_2329 FLOR_01410 FLOR_02605	
nitric oxide activation protein	*norD*	THI217_1 THI806_0	1.7.99.7	THI127 THI806	644 537		+	BA16_151 BGP_5686 FLOR_00559 FLOR_00821	
nitric oxide activation protein	*norE*	THI459_3	1.7.99.7	THI459	192		+		
Periplasmic nitrous oxide reductase									
nitrous oxide reductase	*nosZ*	THI2864|f2	1.7.99.6	THI2864	218	+			
nitrous oxide reductase accesor protein	*nosD*	THI485_0	1.7.99.6	THI485	406		+		
Other genes involved in nitrogen metabolism									
nitric oxide dioxygenase	*hmp*	THI2464_0 THI353514351023 THI438_2	1.14.12.17	THI2464 THI3535 THI438	194 144 149	+		BA06_78 FLOR_02537	
glutamine synthetase	*glnA*	THI10531707618	6.3.1.2	THI1053	234	+		BA02_247 BA17_158 BGP_4113 BGP_4114 BOGUAY_0161 FLOR_03203	
ammonium transporter	*amt*	THI670_1		THI670	136			BA16_117 BA16_118 BOGUAY_3555 BGP1735 FLOR_02001 FLOR_02712	

Table S3: Sulfur metabolism of *Candidatus* Thiomargarita nelsonii compared to other large, colorless SOB

product	gene	locus	E.C.	contig	AA	truncated	full	other large, colorless SOB	comment
Sulfide oxidation									
sufide:quinone oxidoreductase	sqr	THI190_0	1.8.5.4	THI190	373		+	BA07_67 BA16_158 BGP_0667 BOGUAY_0181 BOGUAY_2390 FLOR_01938	
flavocytochrome c sulfide dehydrogenase, cytochrome c subunit	fccA	THI1301_0 THI36_7 THI712_2	1.8.2.3	THI1301 THI36 THI712	218 165 198	+	+	BGP_4977 BOGUAY_2852 BOGUAY_3988 FLOR_01512	
flavocytochrome c sulfide dehydrogenase, flavoprotein subunit	fccB	THI35_6 THI454_0 THI526_0 THI143717651827	1.8.2.3	THI35 THI454 THI526 THI1437	425 210 217 254	+	+	BGB_0124 BGP_4976 BOGUAY_2853 BOGUAY_3987 FLOR_01513	
Sulfur oxidation via reverse dissimilatory sulfite reduction									
dissimilatory sulfite reductase, alpha subunit	dsrA		1.8.99.1					BGP_6219 BGP_6220 BGP_6501 BOGUAY_1511 FLOR_02859 FLOR_01613	
dissimilatory sulfite reductase, beta subunit	dsrB	THI1794_0	1.8.99.1	THI1794	209	+		BGP_4858 BOGUAY_1510 FLOR_02585	
dissimilatory sulfite reductase, gamma subunit	dsrC/ dsrC-like	THI1718_0 THI348_2 THI40_4 THI2578139828	1.8.99.1	THI1718 THI348 THI40 THI2578	110 117 114 131	+		BA07_33 BGP_1169 BOGUAY_1506 FLOR_02854	dsr-like protein no ORFs of dsrC gene

product	gene	locus	E.C.	contig	AA	truncated	full	other large, colorless SOB	comment
	dsrE	THI3100487597478 THI33331369909		THI3100 THI3333	36 138	+ 		BA07_36 BGP_6597 BOGUAY_1509 FLOR_02857	
	dsrF							BA07_35 BGP_1172 BOGUAY_1508 FLOR_02856	
	dsrH							BA07_34 BGP_1170 BOGUAY_1507 FLOR_02855	
	dsrM	THI21821642981		THI2182	213	+		BA07_32 BGP_0409 BOGUAY_1505 FLOR_02853	
	dsrK	THI2182652907892 THI1139_0		THI2182 THI1139	84 44	+ +		BA01 (orf243_glimmer3) BGP_4599 BOGUAY_1504 FLOR_02852	
	dsrL	THI1139_2		THI1139	238	+		BGP_4600 BOGUAY3227 FLOR_02849	
	dsrJ							BA01 (orf244_glimmer3) BGP_4601 BOGUAY_1503 FLOR_02848	
	dsrO							BGP_4603 BGP_4604 BOGUAY_1503 FLOR_02847	

product	gene	locus	E.C.	contig	AA	truncated	full	other large, colorless SOB	comment
	dsrP							BGP_4605 BOGUAY_1500 FLOR_02846	
	dsrN							BGP_5248 FLOR_00351	
	dsrS	THI220_0		THI220	138	+		BGP_1012 FLOR_02633	
	dsrR							BGP_1732 FLOR_00352	
Sulfite oxidation									
APS reductase, alpha subunit	aprA	THI29_0	1.8.99.2	THI29	104	+		BGP_5623 BGP_5624 BOGUAY_2553	
APS reductase, beta subunit	aprB		1.8.99.2					BGP_5858 BOGUAY_2554	
sulfate adenylyltransferase	sat	THI2760_1 THI293755963915 40	2.7.7.4	THI2760 THI2937	35 26	+		BGP_6163 BOGUAY_2370 FLOR_01554	
alkaline serine protease	aprM	THI3143|r1	3.4.21.-	THI3143	195	+			
SOX system									
SOX enzyme complex, subunit B	soxB	THI13761462477		THI1376	186			BGP_2304 BOGUAY_1092 FLOR_02744	thiosulfate oxidation
SOX enzyme complex, subunit Y	soxY	THI32931297475		THI3293	98			BA14_48 BGP_4779 BOGUAY_0115 FLOR_02368	thiosulfate oxidation
SOX enzyme complex, subunit AX	soxAX							BA17_207 BGP_5667 FLOR_03004	thiosulfate oxidation

product	gene	locus	E.C.	contig	AA	truncated	full	other large, colorless SOB	comment
SOX enzyme complex, subunit Z	soxZ							BA02_173 BA16_10 BA14_49 BGP_4779 BGP_4778 BOGUAY_0116 FLOR_02369	thiosulfate oxidation
Thiosulfate disproportionation									
thiosulfate sulfurtransferase, rhodanese	tst	THI213_0 THI29621557562	2.8.1.1	THI213 THI2962	186 184	+		BA02_312 BA09_105 BGP_3637 BOGUAY_2819 BOGUAY_1655	
Sulfate uptake system and assimilatory sulfate reduction									
sulfate permease, high affinity transporter	SulP	THI276_2 THI335610454655		THI276 THI3356	80 146	+		BOGUAY_3672 BGP_2594 BGP_3542 FLOR_00582	
sulfate transporter, periplasmic binding protein	sbp							BA19_56 FLOR_01671	
sulfate ABC transporter, ATPase subunit	cysA							BA19_59 FLOR_00092	
sulfate ABC transporter, permease protein	cysW							BA19_58	
sulfate ABC transporter, permease protein	cysT							BA19_57	
adenylylsulfate kinase	cysC	THI1582_0	2.7.1.25	THI1582	+			BA02_231 BOGUAY_3365 FLOR_01349	
sulfate adenylyltransferase, large subunit	cysN		2.7.7.4					BA05_102	

product	gene	locus	E.C.	contig	AA	truncated	full	other large, colorless SOB	comment
sulfate adenylyltransferase, small subunit	cysD		2.7.7.4					BA05_101	
putative 3´phospho-adenylylsulfate reductase	cysH		1.8.4.8					BA01 (orf301_glimmer3) FLOR_03186	
sulfite reductase, NADPH flavoprotein subunit	cysJ		1.8.1.2					BA06_137	
sulfite reductase, NADPH hemeprotein subunit	cysI		1.8.1.2					BA06_138	
sulfite reductase, ferredoxin	sir		1.8.7.1					FLOR_03184	

Table S4: Carbon metabolism and carbon fixation in *Candidatus* Thiomargarita nelsonii compared to other large, colorless SOB

product	gene	locus	E.C.	contig	AA	truncated	full	other large, colorless SOB	comment
Glycolysis									
glucokinase	*glk*		2.7.1.2					BA19_147 BGP_0972 FLOR_02979	
polyphosphate glucokinase	*ppgk*	THI122_0	2.7.1.63	THI122	120	+		BGP_0205 BOGUAY_0012	
glucose-6-phosphate isomerase	*pgi*		5.1.3.9					BA07_114 BOGUAY_0259 BGP_3455 FLOR_03544 FLOR_03085	
6-phosphofructokinase, pyrophosphate dependent	*pfk*	THI71517826	2.7.1.11	THI715	259	+		BA15_115 BOGUAY_3135 BOGUAY_1318 BGP_4425 FLOR_02042	
bisphosphate aldolase A	*fbaA*		4.1.2.13					BA05_255 BOGUAY_1000 BGP_5969 FLOR_00835	
bisphosphate aldolase B	*fbaB*	THI3055|r2	4.1.2.13	THI3055	200	+			
glyceraldehyde-3-phosphate dehydrogenase	*gap*	THI10719461625106 1	1.2.1.12	THI1071	225	+		BA06_20 BOGIAY_2720 BGP_2190 BGP4586 FLOR_03217	

product	gene	locus	E.C.	contig	AA	truncated	full	other large, colorless SOB	comment
phosphoglycerate kinase	*pgk*	THI399_0 THI60216681202	2.7.2.3	THI399 THI602	138 221	+		BA02_240 BOGUAY_0998 BOGUAY_0999 BGP_4102 FLOR_00204	
phosphoglycerate mutase	*gpmA*	THI305_0	5.4.2.1	THI305	248		+	BA08_57 BA09_158 BA17_114 BOGUAY_1652 BOGUAY_0714 BGP_0770 BGP_0964 BGP_2533 FLOR_00744 FLOR_01466 FLOR_02612	
enolase	*eno*	THI17581197300 THI3523□r2	4.2.1.11	THI1758 THI3523	64 171	+		BA09_212 BOGUAY_3393 FLOR_02427	
pyruvate kinase	*pyk*	THI399_1	2.7.1.40	THI399	478		+	BA05_256 BGP_5856 FLOR_00836	
pyruvate dehydrogenase E1 component	*aceE*	THI1750_1 THI409125921151	1.2.4.1	THI1750 THI409	50 863	+	+	BA05_52 BGP2645 FLOR_02028	
dihydrolipoamide acetyltransferase E2 component	*aceF/ pdhC*	THI624_0	2.3.1.12	THI624	357	+		BA05_51 BGP_2646 FLOR_02029	
pyruvate dehydrogenase E1 component, alpha subunit	*pdhA*	THI32651477104	1.2.4.1	THI3265	158	+		BOGUAY_4507 BOGUAY_4468 BOGUAY_4738 BGP_1305	

product	gene	locus	E.C.	contig	AA	truncated	full	other large, colorless SOB	comment
pyruvate dehydrogenase E1 component, beta subunit	*pdhB*	THI3214⍰r2	1.2.4.1	THI3214	190	+		BOGUAY_4506 BOGUAY_4469 BGP_1304	
dihydrolipoamide dehydrogenase	*pdhD*	THI488_0 THI25811705778	1.8.1.4	THI488 THI2581	471 234			BA01 (orf126_glimmer3) BA17_328 BOGUAY_0563 BOGUAY_0328 BGP_0643 BGP_0644 BGP_4455 FLOR_01022 FLOR_03223	
Tricarboxylic acid cycle									
citrate synthase (type I and II)	*gltA*	THI2494 | f3	2.3.3.1	THI2494	255	+		BOGUAY_4141 (typeI) BGP_3693 (type II) BGP4913 (type II) FLOR02625 (type II) BA15_114 (type II)	
aconitate hydratase I and II	*acnA/ acnB*	THI85121501027 (acnB)	4.2.1.3	contig00002	715	+		BA05_79 (acnB) BA18_22 (acnA) BOGUAY_3060 (acnB) BGP4006 (acnB) FLOR_01010 (acnB) FLOR_02559 (acnA)	
isocitrate dehydrogenase	*icd*	THI78_3	1.1.1.42	THI78	227	+		BA09_306 BOGUAY_2441 FLOR_01072	
2-oxoglutarate dehydrogenase E1	*sucA*	THI521_4 THI1836 | r2 THI3420 | r1	1.2.4.2	THI521 THI1836 THI3402	213 360 178	+		BA17_326 BGP_4352 FLOR_01020	
dihydrolipoyl succinyl transferase E2	*sucB*	THI477_0	2.3.1.61	THi477	266	+		BA17_327 BGP_4350 FLOR_01021 FLOR_02029	

product	gene	locus	E.C.	contig	AA	truncated	full	other large, colorless SOB	comment
dihydrolipoyl dehydrogenase E3	*lpd*	THI488_0 THI25811705778	1.8.1.4	THI488 THI2681	471 234		+	BA01(orf126_glimmer3) BA17_328 BOGUAY_0563 BOGUAY_0328 BGP_0644 FLOR_01022	
succinyl-CoA synthetase, beta subunit	*sucC*	THI32_9	6.2.1.5	THI2418	283	+		BA06_38 BGP_0418 BOGUAY_1109 FLOR_00929	
Succinyl_CoA synthetase, alpha subunit	*sucD*	THI20821353706	6.2.1.5	THI2082	116	+		BA06_39 BGP_0419 BOGUAY_1109 FLOR_00930	
succinate dehydrogenase, flavoprotein subunit	*sdhA*	THI1107_1 THI1196_1 THI28471211210	1.3.5.1	THI1107 THI1196 THI2847	219 353 69	+		BA12_129 BOGUAY_0963 BGP_0843 BGP_0844 BGP_2544 FLOR_03153	
succinate dehydrogenaseiron-sulfur subunit	*sdhB*	THI1107_0 THI11071158159014 31	1.3.5.1	THI1107	128 143	+		BA12_130 BOGUAY_0707 BGP_1918 BGP_3026 BGP_5022 FLOR_03154	
succinate dehydrogenase, cytochrome b556 subunit	*sdhC*	THI39_4	1.3.5.1	THI39	293	+		BA12_127 BOGUAY_4609 BGP_2542 BGP_3027 BGP_3589 BGP_1067 FLOR_03151	

product	gene	locus	E.C.	contig	AA	truncated	full	other large, colorless SOB	comment
succinate dehydrogenase, membrane anchor	*sdhD*		1.3.5.1					BA12_128 BGP_2543 FLOR_03152	
fumarate hydratase	*fumAB*	THI146_2	4.2.1.2	THI146	505		+	BA05_146 BOGUAY_1148 BGP_4244 FLOR_02976	
malate dehydrogenase	*mdh*	THI497_0	1.1.1.37	THI497	325		+	BA17_325 BOGUAY_0329 FLOR_03183	
Reductive ricarbolxyic acid cycle									
ATP-citrate lyase	*aclA*	THI447_1	2.3.8.8	THI447	422		+	BOGUAY_3507 BOGUAY_3508	
citryl-CoA lyase, alpha subunit	*citF*								
citryl-CoA lyase, beta subunit	*citE*							BA09_64 FLOR_02468	
fumarate reductase, flavocytochrome C	*frdA*	THI1517_0 THI940_0	1.33.9.1	THI1517 THI940	140 433	+		BOGUAY_3541 BGP_2143	
fumarate reductase, iron-sulfur protein	*frdB*		1.33.9.1						
2-oxoglutarate:ferredoxin oxidoreductase, alpha subunit	*korA*	THI1378_0	1.2.7.3	THI1378	377		+	BOGUAY_1065 BGP_0270	
2-oxoglutarate:ferredoxin oxidoreductase, beta subunit	*korB*	THI2163	1.2.7.3	THI2163	191		+	BOGUAY_1064	
2-oxoglutarate:ferredoxin oxidoreductase, gamma subunit	*korG*								
2-oxoglutarate:ferredoxin oxidoreductase, delta subunit	*korD*								

product	gene	locus	E.C.	contig	AA	truncated	full	other large, colorless SOB	comment
pyruvate:ferredoxin oxidoreductase, alpha subunit	*porA*	THI187_1 THI413_1 THI670_0	1.2.7.1	THI187 THI413 THI670	753 388 309	+	+	BOGUAY_4121 FLOR_00935 BGP_3761	
pyruvate:ferredoxin oxidoreductase, beta subunit	*porB*	THI413159326321152	1.2.7.1	THI413	345		+	BGP_5558	
pyruvate:ferredoxin oxidoreductase, gamma subunit	*porG*	THI187_0	1.2.7.1	THI187	118	+		BOGUAY_4123 BGP_2254 FLOR_00934	
pyruvate:ferredoxin oxidoreductase, delta subunit	*porD*	THI413_0	1.2.7.1	THI413	131	+		BOGUAY_4122	
pyruvate flavodoxin/ ferredoxin oxidoreductase	*porACDB ("nifJ")*	THI109_1 THI2670_1 THI789_0 THI02487_	1.2.7.	THI109 THI2670 THI789 THI02487	126 2	+		BOGUAY_0108 BOGUAY_2919	
acetyl-CoA syntethase	*acs*	THI962_0	6.2.1.1	THI962	223	+		BA01 (orf249_glimmer3) BGP_6368 FLOR_00817	
pyruvate phosphate dikinase	*ppdK*	THI223716111301 THI2650467231739	2.7.9.1	THI2237 THI2650	202 225	+		BGP _3309 BGP_3310 FLOR_02175 BOGUAY_5237	
phosphoenolpyruvate synthase	*ppsA*	THI00(orf12_glimmer3) THI2983 | r3 THI843 | f1	2.7.9.2	THI00 THI2983 THI843	281	+		BA19_245 FLOR_02068	
phosphoenolpyruvate carboxylase /ATP or GTP dependent cabroxykinase	*pckA/ pckG/ ppc*	THI252814771862 (pckA ATP)	4.1.1.31/ 4.1.1.32/ 4.1.1.49	THI2528	158	+		FLOR_01047 (pckA ATP) BA05_178 (pckA ATP) BGP_5540 (pckA ATP) BGP_2644 (pckG GTP) BA16_192 (ppc) FLOR_00831 (ppc)	

product	gene	locus	E.C.	contig	AA	truncated	full	other large, colorless SOB	comment
Calvin-Benson-Bassham cycle									
ribulose bisphosphate carboxylase large chain, form I	*rbcL*	THI237_1 THI20331953763 THI177814111609*	4.1.1.39	THI237 THI2033 THI1778				BA02_42 BGP_3377	
ribulose bisphosphate carboxylase large chain, form II	*rbcM*		4.1.1.39					BOGUAY_1665 FLOR01412	
ribulose bisphosphate carboxylase small subunit	*rbcS*	THI237112239	4.1.1.39	THI237		+		BA02_41 BGP_3376	
phosphoglycerate kinase	*pgk*	THI399_0 THI60216681202	2.7.2.3	THI399 THI6021	138 221	+		BA02_240 BOGUAY_0998 BOGUAY_0999 BGP_4102 FLOR_4102	
glyceraldehyde-3-phosphate dehydrogenase	*gapA*	THI10719461625106 1	1.2.1.12	THI1071	225		+	BA06_20 BOGUAY_2720 BGP_2190 BGP_4586 FLOR_03217	
bisphosphate aldolase A	*fbaA*		4.1.2.13					BA05_255 BOGUAY_1000 BGP_5969 FLOR_00835	
bisphosphate aldolase B	*fbaB*	THI3055|r2	4.1.2.13	THI3055	200	+			
fructose-1,6-bisphosphatase	*fbp*							BA01 (orf112_glimmer3) FLOR_00141	
transketolase	*tkt*	THI1071_0 THI1325_0 THI1325_1	2.2.1.1	THI1071 THI1325	280 112 106	+		BA06_18 BGP_0483 BGP_2087 BGP_2695 BOGUAY_2721 FLOR_02879	

product	gene	locus	E.C.	contig	AA	truncated	full	other large, colorless SOB	comment
pyrphosphate dependent 6-phosphofructokinase	*ppi-pfk*	THI71517826	2.7.1.90	THI715	259	+		BA15_115 BOGUAY_3135 BOGUAY_1318 BGP_4425 FLOR_02042	
ribose-5-phosphatisomerase	*cbbI*		5.3.1.6					BA19_78 BOGUAY_3213 BGP_5744 FLOR00803	
phosphoribulokinase	*prkA*	THI1792_1	2.7.1.19	THI1792	250	+		BA01 (orf143_glimmer3) Boguay_2689 BGP_2255 FLOR_02126	
C2 cycle (glycolate cycle)									
phosphoglycolate phosphatase	*gph*	THI2179_0 THI772_0 THI34371209832	3.1.3.18	THI2179 THI772 THI3437	216 109 68	+		BA05_44 BA06_120 BA12_109 BOGUAY_4193 BOGUAY_0641 BOGUAY_0964 BGP_2114 BGP_4813 BGP_5647 FLOR_02636 FLOR_02818	
glycolate oxidase	*glcD*	THI156_0 THI943163417831370 THI1470?r1	1.1.3.15	THI156 THI943 THI1470	441 49 429	+		BA05_108 BGP_2712 FLOR_03339 FLOR_03342	
glycolate oxidase, FAD-binding subunit	*glcE*	THI156_1	1.1.3.15	THI156	347	+		BA02_4 BGP_4161 FLOR_02865	

product	gene	locus	E.C.	contig	AA	truncated	full	other large, colorless SOB	comment
glycolate oxidase, iron-sulfur subunit	*glcF*	THI676_0 THI1442_1 THI206018701508	1.1.3.16	THI676 THI1442 THI2060	537 212 289	+		BA02_05 BA17_179 BGP_4162 FLOR_01250	
glutamate-glyoxylate aminotransferase	GGAT	THI15311054124861 7	2.6.1.	THI1531	64			BA05_185 BA06_131 BOGUAY_1325 BGP_1896 BGP_1897 FLOR_00764 FLOR_02517	
glycine cleavage system, glycine dehydrogenase, P-protein	*gcvPB*	THI981_1 (gcvB)	1.4.4.2	THI981	456		+	BA16_23 BOGUAY_1468 BOGUAY_3307 BGP_1733 BGP_1734 BGP_6215 FLOR_02629 FLOR_03006 FLOR_02133	
glycine cleavage system, aminomethyltransferase, T-protein	*gcvT*	THI2312_0 THI2956 r3	2.1.2.10	THI2312_0 THI2956	243	+		BA01 (orf347_glimmer3) BA19_184 BOGUAY_3309 BGP_1517 FLOR_01593 FLOR_02629	
glycine cleavage system, dihydrolipoyl dehydrogenase, L-protein	*lpd*	THI488_0 THI25811705778	1.8.1.4	THI488 THI2581 THI2643	471 234 216		+	BA01 (orf126_glimmer3 BA17_328 BOGUAY_0563 BOGUAY_0328 BGP_0644 FLOR_01022	

product	gene	locus	E.C.	contig	AA	truncated	full	other large, colorless SOB	comment
glycine cleavage system, H-protein	*gcvH*		1.4.4.2					BA01 (orf348_glimmer3) BOGUAY_3308 BGP_5185 FLOR_01150	
glycine cleavage transcriptional repressor	*gcvR*							BA02_98 FLOR_01593	
serine/ glycine hydroxymethyltransferase	*glyA*	THI1694_0 THI543_1	2.1.2.1	THI1694 THI543	341 152	+		BA01 (orf287_glimmer3) BOGUAY_1680 BGP_4519 FLOR_00302	
serine-glyoxylate aminotransferase	SGAT	THI942_0	2.6.1.51	THI942	107	+		BGP_3194 BGP_5274	
serine/ threonine protein kinase	STPK	THI1128_1 THI1189_0 THI1198_0 THI1807_0 THI19_0 THI265_2 THI593115341060	2.7.11.1	THI1128 THI1189 THI1198 THI1807 THI19 THI265 THI593	216 395 477 113 550 380 510	+		BA02_66 BA02_251 BGP_3584 BGP_4568 FLOR_01423 FLOR_03350 FLOR_03427	we detected much more genes encoding for STPK, which are not shown here
phosphoserine phosphatase	*serB*	THI312915871681	3.1.3.3	THI3129	194	+		BA05_75	bifunctional enzyme with EC 2.7.11.1
phosphoserine aminotransferase	*serC*	THI1309113551637	2.6.1.52	THI309	450	+		BA07_58 BOGUAY_0357 BGP_2880 BGP_2994 FLOR_03048	
D-3-phosphoglycerate dehydrogenase	*serA*	THI1288_0 THI371_2 THI61_1	1.1.1.95	THI1288 THI371 THI61	255 127 304	+		BGP_2879 BGP_5532	

product	gene	locus	E.C.	contig	AA	truncated	full	other large, colorless SOB	comment
glycerate dehydrogenase	*dhg*	THI36517661676	1.1.1.29	THI365	254	+			same function as hydroxy-pyruvate reductase
hydroxypyruvate reductase	*ttuD*	THI752_0	1.1.1.81	THI752	212	+		BGP_3955 FLOR_01443 BOGUAY_4043	
glycerate kinase	GLCK		2.7.1.31					BA02_212	

Table S5: Oxidative phosphorylation of *Candidatus* Thiomargarita nelsonii compared to other large, colorless SOB

product	gene	locus	E.C.	contig	AA	truncated	full	other large, colorless SOB	function
Complex I									
NADH dehydrogenase, subunit A	*nouA*		1.6.5.3					BA09_275 BGP_0197 BOGUAY_1243 FLOR_00620	
NADH dehydrogenase, subunit B	*nouB*		1.6.5.3					BA09_276 BGP_0198 BGP_0509 BOGUAY_1242 FLOR_00621	
NADH dehydrogenase, subunit C	*nouC*		1.6.5.3					BA09_277 BGP_0508 BOGUAY_1236 FLOR_00622	
NADH dehydrogenase, subunit D, iron-sulfur protein	*nouD*	THI927110718071451	1.6.5.3	THI927	232	+		BA09_278 BGP_0004 BGP_4191 BOGUAY_1234 FLOR_01604 FLOR_02881	
NADH dehydrogenase, subunit E, FMN	*nouE*	THI793_1	1.6.5.3	THI793	165		+	BA09_279 BGP_0171 BOGUAY_1225	
NADH dehydrogenase, subunit F, FMN	*nouF*	THI1749_0 THI288113681845 THI79316221977345	1.6.5.3	THI1749 THI2881 THI1793	276 121 117	+		BA09_280 BA06_69 BGP_5079 BGP_0263 BOGUAY_1100 BOGUAY_2594 FLOR_01601 FLOR_01761 FLOR_00941	

product	gene	locus	E.C.	contig	AA	truncated	full	other large, colorless SOB	function
NADH dehydrogenase, subunit G, FMN	*nouG*	THI20207410051172 THI381_2	1.6.5.3	THI2020 THI381	309 395	 +		BA09_281 BGP_2702 BOGUAY_3220	
NADH dehydrogenase, subunit H, membrane complex	*nouH*	THI1116_1 THI1494_0	1.6.5.3	THI1116 THI1494	304 333		 +	BA09_282 BGP_1810 BGP_1811 BGP_1812 BGP_5679 BOGUAY_3219 BOGUAY_1731 FLOR_02882	
NADH dehydrogenase, subunit H, iron-sulfur protein	*nouI*	THI14941245476	1.6.5.3	THI1494	80	+		BA09_283 BGP_1809 BOGUAY_3218 FLOR_02883	
NADH dehydrogenase, subunit J, membrane complex	*nouJ*	THI136113621552	1.6.5.3	THI1361	119	+		BA09_285 BGP_0811 BOGUAY_3216 FLOR_02885	
NADH dehydrogenase, subunit K, membrane complex	*nouK*	THI231313541257 THI1361_0	1.6.5.3	THI2313 THI1361	117 144	 +		BA09_286 BGP_0509 BGP_0810 BOGUAY_3215 FLOR_02886	
NADH dehydrogenase, subunit L, membrane complex	*nouL*	THI1972_0 THI356_1	1.6.5.3	THI1972 THI356	223 376	 +		BA09_287 BGP_5518 BGP_5519 BOGUAY_4484 FLOR_02887	
NADH dehydrogenase, subunit M, membrane complex	*nouM*	THI356_0	1.6.5.3	THI356	505	+		BA09_288 BGP_4202 BOGUAY_1496 BOGUAY_2740 FLOR_02888	

product	gene	locus	E.C.	contig	AA	truncated	full	other large, colorless SOB	function
NADH dehydrogenase, subunit N, membrane complex	*nouN*	THI315_0 THI627_1	1.6.5.3	THI315 THI627	50 328	+		BA09_289 BGP_3173 BGP_3174 BGP_5502 BGP_6044 BOGUAY_3866 BOGUAY_2982 BOGUAY_0688 FLOR_02893	
NAD-dependent epimerase/ dehydratase		THI924_0 THI525_0	1.6.5.3	THI924 THI525	329 157	+		BA17-32 BGP_0215 BGP_1167 BGP_1168 BGP_1982 BGP_3469 BOGUAY_2206 BOGUAY_4092 FLOR_01345 FLOR_03013	
Complex II									
succinate dehydrogenase, flavoprotein subunit	*sdhA*	THI1196_1 THI28471211210 THI1517_0	1.3.5.1	THI1196 THI2847 THI1517	353 69 140	+		BA12_129 BOGUAY_0963 BOGUAY_3541 BGP_0843 BGP_0844 BGP_2143 BGP_2544 FLOR_03153	
succinate dehydrogenase, iron-sulfur subunit	*sdhB*	THI1107_0 THI1107115815901431	1.3.5.1	THI1107	128 143	+		BA12_130 BOGUAY_0707 BGP_1918 BGP_3026 BGP_5022 FLOR_03154	

product	gene	locus	E.C.	contig	AA	truncated	full	other large, colorless SOB	function
succinate dehydrogenase, cytochrome b556 subunit	*sdhC*	THI39_4	1.3.5.1	THI39	293	+		BA12_127 BOGUAY_4609 BGP_2542 BGP_3027 BGP_3589 BGP_1067 FLOR_03151	
succinate dehydrogenase/ fumarate reductase, membrane anchor	*sdhD*		1.3.5.1					BA12_128 BGP_2543 FLOR_03152	
Complex III									
ubiquinol-cytochrome c reductase, iron-sulfur subunit	*petA*	THI736_1	1.10.2.2	THI736				BA01_14 BGP_0838 BOGUAY_0396 FLOR_00183	
ubiquinol-cytochrome c reductase, cytochrome b subunit	*petB*	THI736_0	1.10.2.2	THI736	408		+	BA01 (orf15_glimmer3) BGP_0839 BGP_5122 BOGUAY_0395 FLOR_00184	
ubiquinol-cytochrome c reductase, cytochrome c1 subunit	*petC*	THI471_0 THI7361431872	1.10.2.2	THI471 THI736	100 142	+		BA01 (orf16_glimmer3) BGP_6663 BOGUAY_0394 FLOR_00185	
Complex IV									
cyotchrome c oxidase cbb3-type, subunit I	*CcoN*	THI267_0 THI97913441283	1.9.3.1	THI267 THI979	132 113	+		BA01 (orf210_glimmer3) BGP_2112 BOGUAY_3546 FLOR_00924	
cyotchrome c oxidase cbb3-type, subunit II	*CcoO*	THI267_1	1.9.3.1	THI267	205		+	BA01 (orf211_glimmer3) BGP_3209 BOGUAY_3547 FLOR_00573 FLOR_00923	

product	gene	locus	E.C.	contig	AA	truncated	full	other large, colorless SOB	function
cyotchrome c oxidase cbb3-type, subunit IV	CcoQ	THI267_2	1.9.3.1	THI267	53		+	BA01 (orf212_glimmer3) BGP_3208 BOGUAY_3548 FLOR_00572	
cyotchrome c oxidase cbb3-type, subunit III	CcoP	THI267_3	1.9.3.1	THI267	301		+	BA01 (orf213_glimmer3) BGP_3207 BOGUAY_3549 FLOR_00571	
cyotchrome c oxidase accessory protein	CcoG	THI267_4	1.9.3.1	THI267	229	+			
cytochrome d ubiquinol oxidase, subunit I	cydA		1.10.3.-					BA19_83 BOGUAY_1879 BOGUAY_0143	
cytochrome d ubiquinol oxidase, subunit II	cydB		1.10.3.-					BA19_82 BOGUAY_1880	
protoheme IX farnesyltransferase	cyoE	THI45_3	2.5.1.	THI45		+		BGP_2365	
cytochrome c oxidase, aa3 type, subunit III	coxC	THI195312791821	1.9.3.1	THI1953	92	+		BGP_2863	
cytochrome c oxidase, aa3 type, subunit II	coxB	THI2043_0	1.9.3.1	THI2043	260	+		BGP_2865	
cytochrome c oxidase, aa3 type, subunit I	coxA	TH509_0	1.9.3.1	THI509	263	+		BGP_2866	
cytochrome c oxidase synthesis factor	SCO							BGP_2864	
Complex V									
V-type ATP (sodium) synthase subunit A	atpA/ ntpA	THI363_0	3.6.3.14/ 3.6.1.15	THI363	593		+	BGP_4884 BOGUAY_2821 FLOR_01562	
V-type ATP (sodium) synthase subunit A	atpB/ ntpB		3.6.3.14/ 3.6.1.15					BGP_3881 BOGUAY_2662 FLOR_01509	

product	gene	locus	E.C.	contig	AA	truncated	full	other large, colorless SOB	function
V-type ATP (sodium) synthase subunit C	atpC/ ntpC	THI361_2	3.6.3.14/ 3.6.1.15	THI361	328	+		BGP_0940 BOGUAY_2136 BOGUAY_2457 FLOR_00138	
V-type (sodium) ATP synthase subunit D	atpD/ ntpD	THI1004_1	3.6.3.14/ 3.6.1.15	THI1004	210		+	BGP_3601 BOGUAY_1958 BOGUAY_1959 BOGUAY_2137 FLOR_02619	
V-type (sodium) ATP synthase subunit E	atpE/ ntpE	THI363_1	3.6.3.14/ 3.6.1.15	THI363	140	+		BOGUAY_2822 FLOR_01561	
V-type (sodium) ATP synthase subunit E	atpF/ ntpF	THI1439_0	3.6.3.14/ 3.6.1.15	THI1439	106	+			
V-type (sodium) ATP synthase subunit H	atpH/ ntpH	THI361_3	3.6.3.14/ 3.6.1.15	THI361	124	+			
V-type (sodium) ATP synthase subunit I	atpI/ ntpI		3.6.3.14/ 3.6.1.15					BGP_1588 BOGUAY_0078 BOGUAY_3163 FLOR_00139	
V-type (sodium) ATP synthase subunit K	atpK/ ntpK	THI1439_1	3.6.3.14/ 3.6.1.15	THI1439	92	+		BGP_2819 BOGUAY_2663 FLOR_00638	
F-type ATP synthase, subunit epsilon	atpC	THI35561418215	3.6.3.14	THI3556	138	+		BA17_293 BGP_2403 FLOR_00765 FLOR_00766	
F-type ATP synthase, subunit beta	atpD	THI1201_0	3.6.3.14	THI1201	458		+	BA17_294 BGP_2491 FLOR_00767	
F-type ATP synthase, subunit gamma	atpG	THI208_3	3.6.3.14	THI208	283		+	BA17_295 BGP_2492 BGP_1963 BOGUAY_1279 FLOR_00768	

product	gene	locus	E.C.	contig	AA	truncated	full	other large, colorless SOB	function
F-type ATP synthase, subunit gamma	atpA		3.6.3.14					BA17_296 BGP_0784 BOGUAY_3168 FLOR_01115	
F-type ATP synthase, subunit delta	atpH		3.6.3.14					BA17_297 BGP_0785 BOGUAY_3167 FLOR_01114	
F-type ATP synthase, subunit beta	atpF		3.6.3.14					BA17_298 BGP_0786 BOGUAY_3166 FLOR_01113	
F-type ATP synthase, chain C	atpE		3.6.3.14					BA17_300 BGP_0787 BOGUAY_3165 FLOR_01112	
F-type ATP synthase,chain A	atpB		3.6.3.14					BA17_300 BGP_0788 BGP_0789 BOGUAY_3164 FLOR_01111 FLOR_02054	
F-type ATP synthase,?	atp?		3.6.3.14					BGP_0790 BOGUAY_3163	
polyphosphate kinase	ppk	THI45_0	2.7.4.1	THI45	654			BA01 (orf27_glimmer3) BGP_5434 BOGUAY_0085 FLOR_02687	
membrane-bound proton translocating pyrophosphatase/ inorganic pyrophosphatase	hppA/ ppa/ LHPP		3.6.1.1					BA01 (orf50_glimmer3) BA02 (orf419_glimmer3) BA01 (orf223_glimmer) BGP_2409 BOGUAY_430 FLOR_00254 FLOR_00748 FLOR_01358	

Table S6: Additional energy metabolism of *Candidatus* Thiomargarita nelsonii compared to other large, colorless SOB

product	gene	locus	E.C.	contig	AA	truncated	full	other filamentous sulfur oxidizer	comment
Heterodisulfide reductase									
heterodisulfide reductase, subunit A	hdrA	THI1755_0 THI94014081436 THI141793213291590	1.8.98.1	THI1755 THI940 THI1417	249 135 131	+		BOGUAY_3539 BOGUAY_3540 BOGUAY_2741 BGP_0252 BGP_0253	
heterodisulfide reductase, subunit B	hdrB		1.8.98.1					BGP_2617	
heterodisulfide reductase, subunit C	hdrC	THI846_1	1.8.98.1	THI846	213	+		BGP_2616	
heterodisulfide oxidoreductase, iron-sulfur cluster-binding subunit D	hdrD	THI303_0 THI58_	1.8.98.1	THI303 THI58	309 302		+ +	BA05_133 BOGUAY_3538	
heterodisulfide oxidoreductase, iron-sulfur cluster-binding subunit E	hdrE	THI303_1	1.8.98.1	THI303	368		+	BOGUAY_3536	
heterodisulfide reductase, cytochrome reductase subunit	hdrF	THI30323473009988	1.8.98.1	THI303	220	+		BOGUAY_3535	
Methyl viologen-reducing hydrogemas									
methyl viologen-reducing hydrogenase, delt subunit	mvhD	THI8461340616	1.12.99.	THI846	112		+	BOGUAY_3538	
methyl viologen-reducing hydrogenase-associated ferredoxin	mvhF	THI43_3	1.12.99.	THI43	245	+			
nickel-dependent methyl viologen-reducing hydrogenase, large subunit	mvhA	THI43_4 THI175580411251660	1.12.99.	THI43 THI1755	471 106		+ +	BA05_132 BGP_0253	

product	gene	locus	E.C.	contig	AA	truncated	full	other filamentous sulfur oxidizer	comment
nickel-dependent methyl viologen-reducing hydrogenase, small subunit	mvh G	THI43_5	1.12.99.	THI43	313		+		functional similar to F420 non reducing-hydrogenase
methyl viologen-reducing hydrogenase maturation protease	mvhP	THI43_7	1.12.99.	THI43					
Na^+-translocating membrane complex									
electron transport complex, subunit A	rnfA	THI1445_0		THI1445	191		+	BA01 (orf340_glimmer3) BA09_372 BOGUAY_2644 BOGUAY_0446 BGP_4894 BGP_4895 FLOR_00005 FLOR_00042	
electron transport complex, subunit B, ferredoxin subunit	rnfB	THI1789_0 THI11991215885		THI1789 THI1199	298 70		+	BA01 (orf339_glimmer3) BA09_373 BOGUAY_1961 BOGUAY_0445 BGP_5165 FLOR_00004 FLOR_01801	

product	gene	locus	E.C.	contig	AA	truncated	full	other filamentous sulfur oxidizer	comment
electron transport complex, subunit C, flavin subunit	rnfC	THI1294_0 THI571_1		THI1294 THI571	289 484	 +	 +	BA01 (orf338_glimmer3) BA07_22 BA09_374 BOGUAY_0327 BOGUAY_0444 BGP_1887 FLOR_00003 FLOR_03168	
electron transport complex, subunit D	rnfD	THI1238_0 THI1019_0 THI856_1		THI1238 THI1019 THI856	300 239 344	 +	 	BA01 (orf337_glimmer3) BA09_375 BOGUAY_4422 BOGUAY_2718 BGP_2194 BGP_2824 FLOR_00109 FLOR_02202	
electron transport complex, subunit G	rnfG	THI2459_0		THI2549	207		+	BA01 (orf336_glimmer3) BA09_376 BOGUAY_1747 BOGUAY_2719 BGP_5931 BGP_6563 FLOR_00108 FLOR_02203	
electron transport complex, subunit E	rnfE	THI331745553225		THI3317	168	+		BA01 (orf335_glimmer3) BA09_218 BOGUAY_2233 BOGUAY_2643 FLOR_00471 FLOR_02204	
hypothetical protein	rnfH							BOGUAY_1193	

product	gene	locus	E.C.	contig	AA	truncated	full	other filamentous sulfur oxidizer	comment
Uptake hydrogenase									
respiratory membrane-bound hydrogen uptake [Ni,Fe] hydrogenase, small subunit	hupS	THI8271464146 THI18711751500	1.12.99.6	THI827 THI187	153 57	+		BA02_59 BA05_135 BOGUAY_1709 BOGUAY_0684 FLOR_00588 FLOR_02642	
respiratory membrane-bound hydrogen uptake [Ni,Fe] hydrogenase, large subunit	hupL	THI368_2 THI58_3 THI1400_1	1.12.99.6	THI368 THI58 THI1400	592 219 256	+	+	BA02_58 BA05_132 BOGUAY_4411 FLOR_00363 FLOR_02641	
[Ni,Fe] hydrogenase 1b-type cytochrome	hupC		1.12.99.6					BA02_57 FLOR_02639	
[Ni,Fe] hydrogenase maturation protein	hupD		3.4.24.-					BA02_280 BOGUAY_2760 FLOR_03012	
[Ni,Fe] hydrogenase expression protein	hupH							BA07_105 FLOR_00978	
Other hydrogenases and maturation proteins									
NAD (P) transhydrogenase, alpha subunit	pntA	THI20533979841684 THI1715_0	1.6.1.2	THI2053 THI1715	159 282	+		BA19_120 BA19_121 BOGUAY_3230 BGP_1955 BGP_5439 FLOR_01451 FLOR_01452	
NAD (P) transhydrogenase, beta subunit	pntB	THI268917081244 THI171512431286	1.6.1.2	THI2689 THI1715	235 80	+		BA19_122 BOGUAY_3228 BOGUAY_3229 FLOR_01453	

product	gene	locus	E.C.	contig	AA	truncated	full	other filamentous sulfur oxidizer	comment
hydrogenase nickel insertion protein, cytochrome alpha chain	hypA							BA05_135 BA14_43 BA17_362 BOGUAY_1790 FLOR_00762	maturation of hydrogenase
hydrogenase acessory protein	hypB							BA01 (orf69_glimmer3) BOGUAY_1512 FLOR_00958 FLOR_02868	maturation of hydrogenase
hydrogenase assembly protein	hypC							BA14_42 BOGUAY_1791 FLOR_00763	maturation of hydrogenase
hydrogenase expression/ formation protein	hypD							BA02_307 BOGUAY_1513 BOGUAY_3052 FLOR_03072	maturation of hydrogenase
hydrogenase expression/ formation protein	hypE							BA14_122 BOGUAY_3356 FLOR_01477 FLOR_03103	maturation of hydrogenase
hydrogenase maturation protein	hypF	THI648_4		THI648	74	+		BA01 (orf45_glimmer3) FLOR_02743	maturation of hydrogenase
hydrogenase 4 membrane component	hyfE							BA02_301	membrane complex
hydrogenase 4 component F	hyfF							BA02_354	membrane complex
hydrogenase 4	hyfB							BA12_29	membrane complex

Table S7: Intracellular storage of *Candidatus* Thiomargarita nelsonii compared to other large, colorless SOB

product	gene	locus	E.C.	contig	AA	truncated	full	other large, colorless SOB	function
Polyphosphate storage system									
phosphate ABC transporter, inner membrane subunit	*pstA*	THI1009_1	3.6.3.27	THI1009	236	+		BA04_28 BA16_208 BGP_3522 BOGUAY_3725 FLOR_00686	
phosphate ABC transporter, ATP binding subunit	*pstB*	THI466_3	3.6.3.27	THI466	285		+	BA04_29 BGP_2125 BOGUAY_3724 FLOR_00687	
phosphate ABC transporter, inner membrane component	*pstC*	THI273_2	3.6.3.27	THI273	506	+		BA04_27 BGP_3523 BOGUAY_3726 FLOR_00685	
phosphate ABC transporter, periplasmatic phosphate-binding protein	*pstS*		3.6.3.27					BA12_62 BGP_3525 BOGUAY_ 3729 BOGUAY_ 3728 FLOR_02873 FLOR_01348	
phosphate ABC transporter, phosphat binding protein	*pstD*		3.6.3.27					BA10_71	
phosphate regulon sensor protein	*phoR*	THI1120_1		THI1120	421	+		BA02_323 BOGUAY_4336	
phsophate transport system regulator protein	*phoU*	THI46622302531967		THI466	99	+		BA04_30 BGP_1356 BOGUAY_3723 FLOR_02932 FLOR_00688	

product	gene	locus	E.C.	contig	AA	truncated	full	other large, colorless SOB	function
phosphate stravation-inducible protein	*phoH*							FLOR_03136	
phosphate regulon transcriptional regulatory	*phoB*							BOGUAY_4337	
phosphate-selective porin O and P	*phoE*	THI1278_0 THI711_1		THI1278 THI711	387 391		+	BGP_4216 BGP_0268 BGP_0269 BOGUAY_2057	
polyphosphate kinase	*ppk*	THI45_0	2.7.4.1	THI45	654			BA01 (orf27_glimmer3) BGP_5434 BOGUAY_0085 FLOR_02687	
Polyhydroxyalkanoate/ -butyrate storage system									
polyphosphate:AMP phosphotransferase	*pap*	THI191911041837	2.7.4.-					BA10_37 BOGUAY_0604 FLOR_02303	
acetyl-CoA acetyltransferase	*phaA/ phbA*	THI234_0	2.3.1.9	THI_234	370		+	BA05_42 BA17_147 FLOR_00713	
acetoacetyl-CoA reductase	*phaB/ phbB*		1.1.1.36					BA17_145 BGP_0317 BOGUAY_0874 FLOR_00822	
poly-beta hydroxybutyrate polymerase/ poly(R)-hydroxyalkanoate acid synthase, class I	*phaC*		2.3.1-					BA02_82 BA06_09 BA19_224 BA02 (orf427_glimmer3) FLOR_01645 FLOR_03182 FLOR_03197	
poly(R)-hydroxyalaknoic acid synthase, class III	*phaE*							BA08_131 FLOR_01646	

product	gene	locus	E.C.	contig	AA	truncated	full	other large, colorless SOB	function
poly(3-hydroxybutyrate) depolymerase	*phaZ*							BA09_314 BA09_315 FLOR_03285	
putative regulator of polymer accumulation	*phaR*							BA07_146 BGP_4849 FLOR_00714	

Digital database

The digital version of the amoA database can be accessed by the intranet of “Max Planck Institute for Marine Microbiology” directory TUX/molecol_new/mwinkel_public.